Australian Government

BIOREGIONAL ASSESSMENTS

PROVIDING SCIENTIFIC WATER RESOURCE INFORMATION ASSOCIATED WITH COAL SEAM GAS AND LARGE COAL MINES

# Observations analysis, statistical analysis and interpolation for the Galilee subregion

## Product 2.1-2.2 for the Galilee subregion from the Lake Eyre Basin Bioregional Assessment

2018

A scientific collaboration between the Department of the Environment and Energy, Bureau of Meteorology, CSIRO and Geoscience Australia

## The Bioregional Assessment Programme

The Bioregional Assessment Programme is a transparent and accessible programme of baseline assessments that increase the available science for decision making associated with coal seam gas and large coal mines. A bioregional assessment is a scientific analysis of the ecology, hydrology, geology and hydrogeology of a bioregion with explicit assessment of the potential impacts of coal seam gas and large coal mining development on water resources. This Programme draws on the best available scientific information and knowledge from many sources, including government, industry and regional communities, to produce bioregional assessments that are independent, scientifically robust, and relevant and meaningful at a regional scale.

The Programme is funded by the Australian Government Department of the Environment and Energy. The Department of the Environment and Energy, Bureau of Meteorology, CSIRO and Geoscience Australia are collaborating to undertake bioregional assessments. For more information, visit http://www.bioregionalassessments.gov.au.

## Department of the Environment and Energy

The Australian Government Department of the Environment and Energy is strengthening the regulation of coal seam gas and large coal mining development by ensuring that future decisions are informed by substantially improved science and independent expert advice about the potential water-related impacts of those developments. For more information, visit https://www.environment.gov.au/water/coal-and-coal-seam-gas/office-of-water-science.

## Bureau of Meteorology

The Bureau of Meteorology is Australia's national weather, climate and water agency. Under the *Water Act 2007*, the Bureau is responsible for compiling and disseminating Australia's water information. The Bureau is committed to increasing access to water information to support informed decision making about the management of water resources. For more information, visit http://www.bom.gov.au/water/.

## CSIRO

Australia is founding its future on science and innovation. Its national science agency, CSIRO, is a powerhouse of ideas, technologies and skills for building prosperity, growth, health and sustainability. It serves governments, industries, business and communities across the nation. For more information, visit http://www.csiro.au.

## Geoscience Australia

Geoscience Australia is Australia's national geoscience agency and exists to apply geoscience to Australia's most important challenges. Geoscience Australia provides geoscientific advice and information to the Australian Government to support current priorities. These include contributing to responsible resource development; cleaner and low emission energy technologies; community safety; and improving marine planning and protection. The outcome of Geoscience Australia's work is an enhanced potential for the Australian community to obtain economic, social and environmental benefits through the application of first class research and information. For more information, visit http://www.ga.gov.au.

**ISBN-PDF 978-1-925315-26-4**

## Citation

Evans T, Kellett J, Ransley T, Harris-Pascal C, Radke B, Cassel R, Karim F, Hostetler S, Galinec V, Dehelean A, Caruana L and Kilgour P (2018) Observations analysis, statistical analysis and interpolation for the Galilee subregion. Product 2.1-2.2 for the Galilee subregion from the Lake Eyre Basin Bioregional Assessment. Department of the Environment and Energy, Bureau of Meteorology, CSIRO and Geoscience Australia, Australia. http://data.bioregionalassessments.gov.au/product/LEB/GAL/2.1-2.2.

Authorship is listed in relative order of contribution.

## Copyright



## Disclaimer



## Cover photograph

Artesian Spring Wetland at Doongmabulla Nature Refuge, Queensland, 2013

Credit: Jeremy Drimer, University of Queensland

Australian Government

Department of the Environment and Energy

Bureau of Meteorology

Geoscience Australia

CSIRO

v20180612

# Contents

# Figures

# Tables

# Contributors to the Technical Programme

The following individuals have contributed to the Technical Programme, the part of the Bioregional Assessment Programme that undertakes bioregional assessments.

| Role or team | Contributor(s) |
|---|---|
| Assistant Secretary | Department of the Environment and Energy: Matthew Whitfort |
| Programme Director | Department of the Environment and Energy: John Higgins, Anthony Swirepik |
| Technical Programme Director | Bureau of Meteorology: Julie Burke |
| Projects Director | CSIRO: David Post |
| Principal Science Advisor | Department of the Environment and Energy: Peter Baker |
| Science Directors | CSIRO: Brent Henderson<br>Geoscience Australia: Steven Lewis |
| Integration | Bureau of Meteorology: Richard Mount (Integration Leader)<br>CSIRO: Becky Schmidt |
| Programme management | Bureau of Meteorology: Louise Minty<br>CSIRO: Paul Bertsch, Warwick McDonald<br>Geoscience Australia: Stuart Minchin |
| Project Leaders | CSIRO: Alexander Herr, Kate Holland, Tim McVicar, David Rassam<br>Geoscience Australia: Tim Evans<br>Bureau of Meteorology: Natasha Herron |
| Assets and receptors | Bureau of Meteorology: Richard Mount (Discipline Leader)<br>Department of the Environment and Energy: Glenn Johnstone, Wasantha Perera, Jin Wang |
| Bioregional Assessment Information Platform | Bureau of Meteorology: Lakshmi Devanathan (Team Leader), Derek Chen, Trevor Christie-Taylor, Melita Dahl, Angus MacAulay, Christine Price, Paul Sheahan, Kellie Stuart<br>CSIRO: Peter Fitch, Ashley Sommer<br>Geoscience Australia: Neal Evans |
| Communications | Bureau of Meteorology: Jessica York<br>CSIRO: Clare Brandon<br>Department of the Environment and Energy: John Higgins, Miriam McMillan, Milica Milanja<br>Geoscience Australia: Aliesha Lavers |
| Coordination | Bureau of Meteorology: Brendan Moran, Eliane Prideaux, Sarah van Rooyen<br>CSIRO: Ruth Palmer<br>Department of the Environment and Energy: Anisa Coric, Lucy Elliott, James Hill, Andrew Stacey, David Thomas, Emily Turner |
| Ecology | CSIRO: Anthony O'Grady (Discipline Leader), Caroline Bruce, Tanya Doody, Brendan Ebner, Craig MacFarlane, Patrick Mitchell, Justine Murray, Chris Pavey, Jodie Pritchard, Nat Raisbeck-Brown, Ashley Sparrow |

| Role or team | Contributor(s) |
| --- | --- |
| Geology | CSIRO: Deepak Adhikary, Emanuelle Frery, Mike Gresham, Jane Hodgkinson, Zhejun Pan, Matthias Raiber, Regina Sander, Paul Wilkes<br>Geoscience Australia: Steven Lewis (Discipline Leader) |
| Geographic information systems | CSIRO: Jody Bruce, Debbie Crawford, Dennis Gonzales, Mike Gresham, Steve Marvanek, Arthur Read<br>Geoscience Australia: Adrian Dehelean |
| Groundwater modelling | CSIRO: Russell Crosbie (Discipline Leader), Tao Cui, Warrick Dawes, Lei Gao, Sreekanth Janardhanan, Luk Peeters, Praveen Kumar Rachakonda, Wolfgang Schmid, Saeed Torkzaban, Chris Turnadge, Andy Wilkins, Binzhong Zhou |
| Hydrogeology | Geoscience Australia: Tim Ransley (Discipline Leader), Chris Harris-Pascal, Jessica Northey, Emily Slatter |
| Information management | Bureau of Meteorology: Brendan Moran (Team Leader), Christine Panton<br>CSIRO: Qifeng Bai, Simon Cox, Phil Davies, Geoff Hodgson, Brad Lane, Ben Leighton, David Lemon, Trevor Pickett, Shane Seaton, Ramneek Singh, Matt Stenson<br>Geoscience Australia: Matti Peljo |
| Information model and impact analysis | Bureau of Meteorology: Carl Sudholz (Project Manager), Mark Dyall, Michael Lacey, Brett Madsen, Eliane Prideaux<br>Geoscience Australia: Trevor Tracey-Patte |
| Products | CSIRO: Becky Schmidt (Products Manager), Maryam Ahmad, Helen Beringen, Clare Brandon, Heinz Buettikofer, Sonja Chandler, Siobhan Duffy, Karin Hosking, Allison Johnston, Maryanne McKay, Linda Merrin, Sally Tetreault-Campbell, Catherine Ticehurst<br>Geoscience Australia: Penny Kilgour |
| Risk and uncertainty | CSIRO: Simon Barry (Discipline Leader), Jeffrey Dambacher, Rob Dunne, Jess Ford, Keith Hayes, Geoff Hosack, Adrien Ickowicz, Warren Jin, Dan Pagendam |
| Surface water hydrology | CSIRO: Neil Viney and Yongqiang Zhang (Discipline Leaders), Santosh Aryal, Mat Gilfedder, Fazlul Karim, Lingtao Li, Dave McJannet, Jorge Luis Peña-Arancibia, Tom Van Niel, Jai Vaze, Bill Wang, Ang Yang |

# Acknowledgements

This technical product was reviewed by several groups:

- Discipline Leaders: Steven Lewis (geology), Russell Crosbie (groundwater modelling), Jim Kellett (hydrogeology)
- Senior Science Leaders: David Post (Projects Director), Steven Lewis (Science Director, Geoscience Australia), Becky Schmidt (Products Manager)
- Technical Assurance Reference Group: Chaired by Peter Baker (Principal Science Advisor, Department of the Environment and Energy), this group comprises officials from the NSW, Queensland, South Australian and Victorian governments
- Independent reviewer: Peter Cook (NCGRT).

# Currency of scientific results

The modelling results contained in this product were completed in December 2015 using the best available data, models and approaches available at that time. The product content was completed in October 2017.

All products in the model-data analysis, impact and risk analysis, and outcome synthesis (see Figure 1) were published as a suite when completed.

# Introduction

The Independent Expert Scientific Committee on Coal Seam Gas and Large Coal Mining Development (IESC) was established to provide advice to the federal Minister for the Environment on potential water-related impacts of coal seam gas (CSG) and large coal mining developments (IESC, 2015).

Bioregional assessments (BAs) are one of the key mechanisms to assist the IESC in developing this advice so that it is based on best available science and independent expert knowledge. Importantly, technical products from BAs are also expected to be made available to the public, providing the opportunity for all other interested parties, including government regulators, industry, community and the general public, to draw from a single set of accessible information. A BA is a scientific analysis, providing a baseline level of information on the ecology, hydrology, geology and hydrogeology of a bioregion with explicit assessment of the potential impacts of CSG and coal mining development on water resources.

The IESC has been involved in the development of *Methodology for bioregional assessments of the impacts of coal seam gas and coal mining development on water resources* (the BA methodology; Barrett et al., 2013) and has endorsed it. The BA methodology specifies how BAs should be undertaken. Broadly, a BA comprises five components of activity, as illustrated in Figure 1. Each BA is different, due in part to regional differences, but also in response to the availability of data, information and fit-for-purpose models. Where differences occur, these are recorded, judgments exercised on what can be achieved, and an explicit record is made of the confidence in the scientific advice produced from the BA.

## The Bioregional Assessment Programme

The Bioregional Assessment Programme is a collaboration between the Department of the Environment and Energy, the Bureau of Meteorology, CSIRO and Geoscience Australia. Other technical expertise, such as from state governments or universities, is also drawn on as required. For example, natural resource management groups and catchment management authorities identify assets that the community values by providing the list of water-dependent assets, a key input.

The Technical Programme, part of the Bioregional Assessment Programme, has undertaken BAs for the following bioregions and subregions (see http://www.bioregionalassessments.gov.au/assessments for a map and further information):

- the Galilee, Cooper, Pedirka and Arckaringa subregions, within the Lake Eyre Basin bioregion
- the Maranoa-Balonne-Condamine, Gwydir, Namoi and Central West subregions, within the Northern Inland Catchments bioregion
- the Clarence-Moreton bioregion
- the Hunter and Gloucester subregions, within the Northern Sydney Basin bioregion

- the Sydney Basin bioregion
- the Gippsland Basin bioregion.

Technical products (described in a later section) will progressively be delivered throughout the Programme.

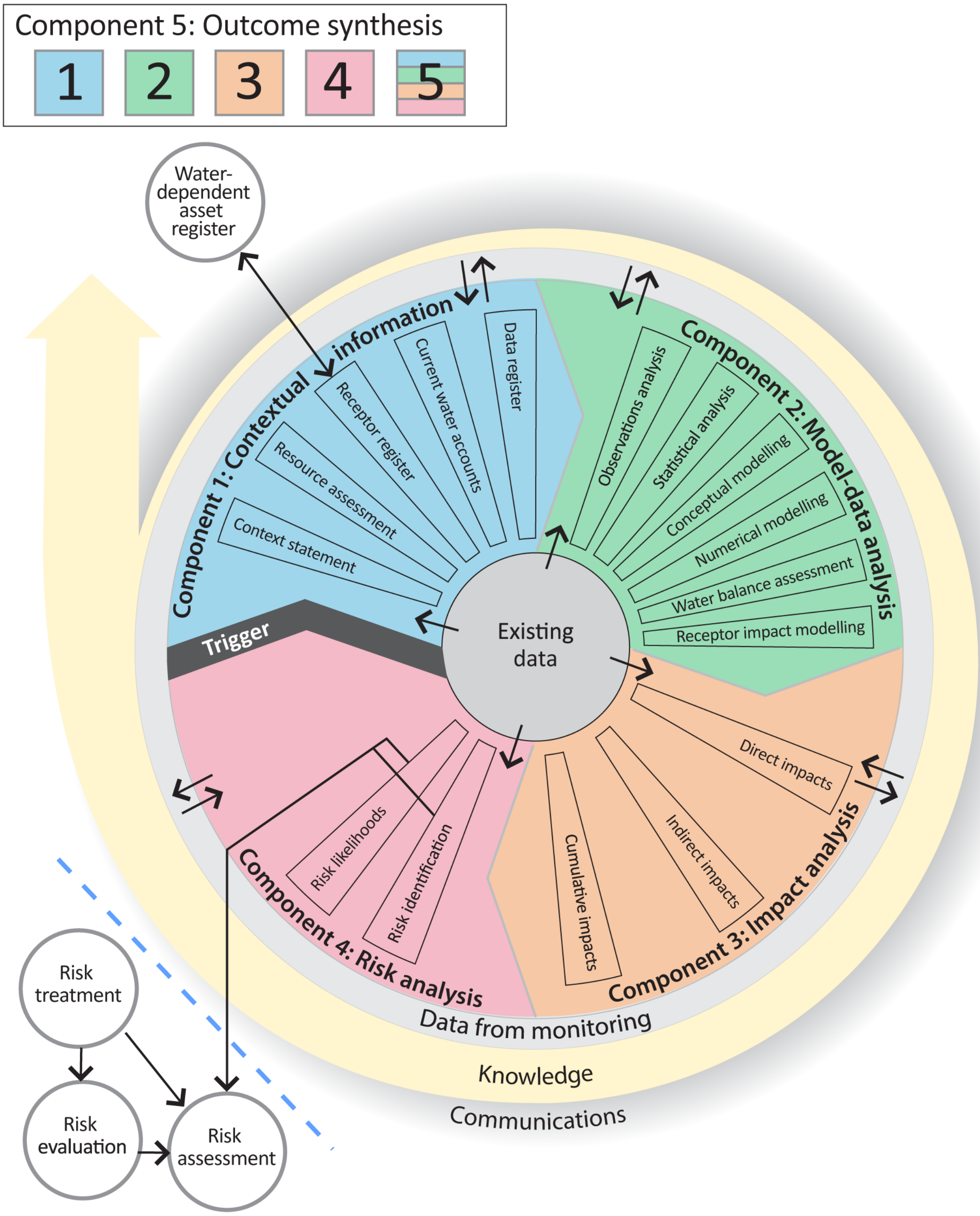


**Figure 1 Schematic diagram of the bioregional assessment methodology**

The methodology comprises five components, each delivering information into the bioregional assessment and building on prior components, thereby contributing to the accumulation of scientific knowledge. The small grey circles indicate activities external to the bioregional assessment. Risk identification and risk likelihoods are conducted within a bioregional assessment (as part of Component 4) and may contribute activities undertaken externally, such as risk evaluation, risk assessment and risk treatment. Source: Figure 1 in Barrett et al. (2013), © Commonwealth of Australia

# Methodologies

The overall scientific and intellectual basis of the BAs is provided in the BA methodology (Barrett et al., 2013). Additional guidance is required, however, about how to apply the BA methodology to a range of subregions and bioregions. To this end, the teams undertaking the BAs have developed and documented detailed scientific submethodologies (Table 1), in the first instance, to support the consistency of their work across the BAs and, secondly, to open the approach to scrutiny, criticism and improvement through review and publication. In some instances, methodologies applied in a particular BA may differ from what is documented in the submethodologies.

The relationship of the submethodologies to BA components and technical products is illustrated in Figure 2. While much scientific attention is given to assembling and transforming information, particularly through the development of the numerical, conceptual and receptor impact models, integration of the overall assessment is critical to achieving the aim of the BAs. To this end, each submethodology explains how it is related to other submethodologies and what inputs and outputs are required. They also define the technical products and provide guidance on the content to be included. When this full suite of submethodologies is implemented, a BA will result in a substantial body of collated and integrated information for a subregion or bioregion, including new information about the potential impacts of coal resource development on water and water-dependent assets.

**Table 1 Methodologies**

Each submethodology is available online at http://data.bioregionalassessments.gov.au/submethodology/XXX, where ‘XXX’ is replaced by the code in the first column. For example, the BA methodology is available at http://data.bioregionalassessments.gov.au/submethodology/bioregional-assessment-methodology and submethodology M02 is available at http://data.bioregionalassessments.gov.au/submethodology/M02. Submethodologies might be added in the future.

| Code | Proposed title | Summary of content |
|---|---|---|
| bioregional-assessment-methodology | *Methodology for bioregional assessments of the impacts of coal seam gas and coal mining development on water resources* | A high-level description of the scientific and intellectual basis for a consistent approach to all bioregional assessments |
| M02 | *Compiling water-dependent assets* | Describes the approach for determining water-dependent assets |
| M03 | *Assigning receptors to water-dependent assets* | Describes the approach for determining receptors associated with water-dependent assets |
| M04 | *Developing a coal resource development pathway* | Specifies the information that needs to be collected and reported about known coal and coal seam gas resources as well as current and potential resource developments |
| M05 | *Developing the conceptual model of causal pathways* | Describes the development of the conceptual model of causal pathways, which summarises how the ‘system’ operates and articulates the potential links between coal resource development and changes to surface water or groundwater |
| M06 | *Surface water modelling* | Describes the approach taken for surface water modelling |
| M07 | *Groundwater modelling* | Describes the approach taken for groundwater modelling |
| M08 | *Receptor impact modelling* | Describes how to develop receptor impact models for assessing potential impact to assets due to hydrological changes that might arise from coal resource development |
| M09 | *Propagating uncertainty through models* | Describes the approach to sensitivity analysis and quantification of uncertainty in the modelled hydrological changes that might occur in response to coal resource development |
| M10 | *Impacts and risks* | Describes the logical basis for analysing impact and risk |
| M11 | *Systematic analysis of water-related hazards associated with coal resource development* | Describes the process to identify potential water-related hazards from coal resource development |

## Technical products

The outputs of the BAs include a suite of technical products presenting information about the ecology, hydrology, hydrogeology and geology of a bioregion and the potential impacts of CSG and coal mining developments on water resources, both above and below ground. Importantly, these technical products are available to the public, providing the opportunity for all interested parties, including community, industry and government regulators, to draw from a single set of accessible information when considering CSG and large coal mining developments in a particular area.

The information included in the technical products is specified in the BA methodology. Figure 2 shows the relationship of the technical products to BA components and submethodologies. Table 2 lists the content provided in the technical products, with cross-references to the part of the BA methodology that specifies it. The red outlines in both Figure 2 and Table 2 indicate the information included in this technical product.

Technical products are delivered as reports (PDFs). Additional material is also provided, as specified by the BA methodology:

- unencumbered data syntheses and databases
- unencumbered tools, model code, procedures, routines and algorithms
- unencumbered forcing, boundary condition, parameter and initial condition datasets
- lineage of datasets (the origin of datasets and how they are changed as the BA progresses)
- gaps in data and modelling capability.

In this context, unencumbered material is material that can be published according to conditions in the licences or any applicable legislation. All reasonable efforts were made to provide all material under a Creative Commons Attribution 3.0 Australia Licence.

Technical products, and the additional material, are available online at http://www.bioregionalassessments.gov.au.

The Bureau of Meteorology archives a copy of all datasets used in the BAs. This archive includes datasets that are too large to be stored online and datasets that are encumbered. The community can request a copy of these archived data at http://www.bioregionalassessments.gov.au.

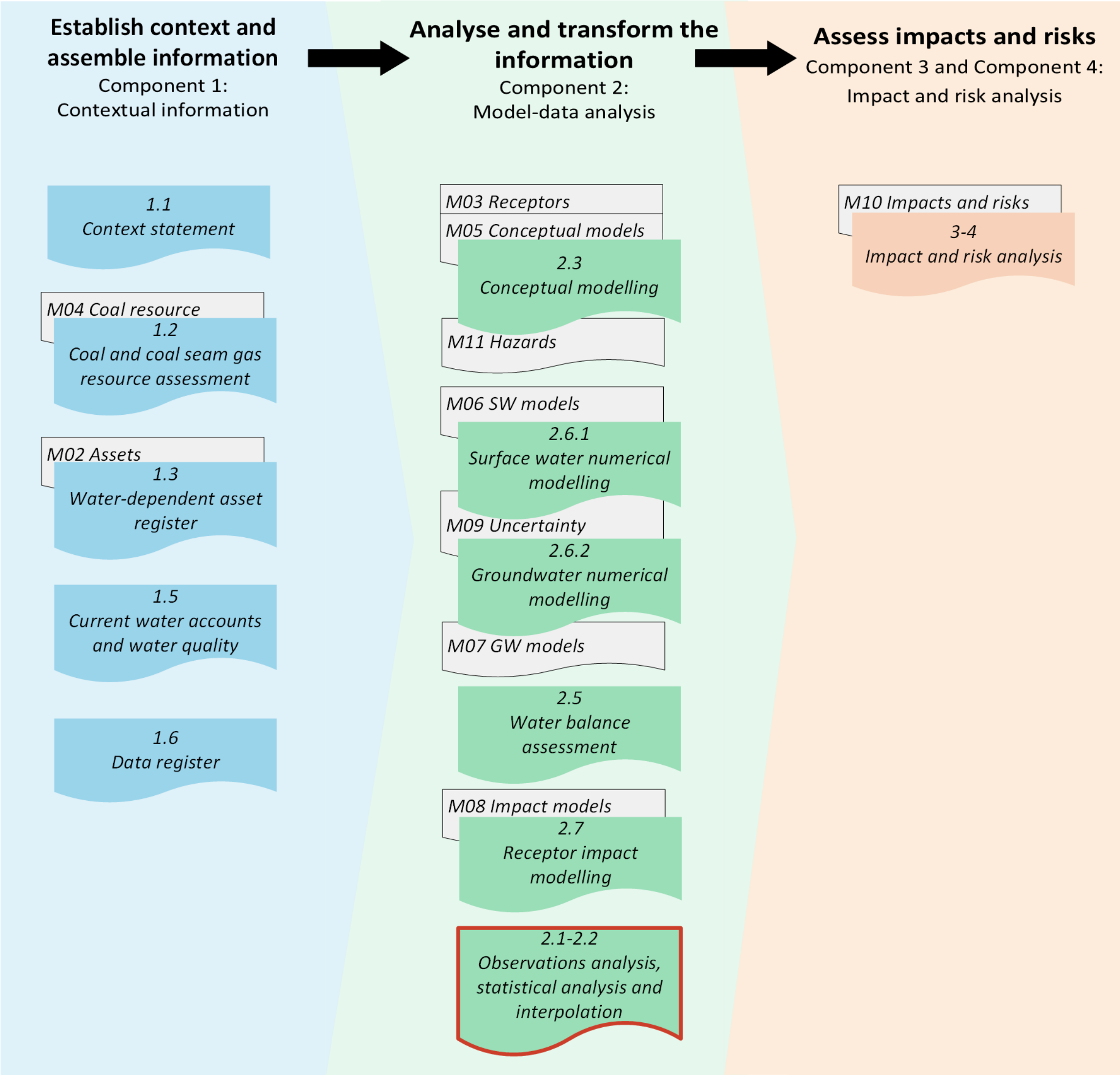


**Figure 2 Technical products and submethodologies associated with each component of a bioregional assessment**

In each component (Figure 1) of a bioregional assessment, a number of technical products (coloured boxes, see also Table 2) are potentially created, depending on the availability of data and models. The light grey boxes indicate submethodologies (Table 1) that specify the approach used for each technical product. The red outline indicates this technical product. The BA methodology (Barrett et al., 2013) specifies the overall approach.

**Table 2 Technical products delivered for the Galilee subregion**

For each subregion in the Lake Eyre Basin Bioregional Assessment, technical products are delivered online at http://www.bioregionalassessments.gov.au, as indicated in the 'Type' column[a]. Other products – such as datasets, metadata, data visualisation and factsheets – are provided online. There is no product 1.4. Originally this product was going to describe the receptor register and application of landscape classes as per Section 3.5 of the BA methodology, but this information is now included in product 2.3 (conceptual modelling) and used in product 2.6.1 (surface water numerical modelling) and product 2.6.2 (groundwater numerical modelling). There is no product 2.4. Originally this product was going to include two- and three-dimensional representations as per Section 4.2 of the BA methodology, but these are instead included in products such as product 2.3 (conceptual modelling), product 2.6.1 (surface water numerical modelling) and product 2.6.2 (groundwater numerical modelling).

| Component | Product code | Title | Section in the BA methodology[b] | Type[a] |
|---|---|---|---|---|
| Component 1: Contextual information for the Galilee subregion | 1.1 | Context statement | 2.5.1.1, 3.2 | PDF, HTML |
| | 1.2 | Coal and coal seam gas resource assessment | 2.5.1.2, 3.3 | PDF, HTML |
| | 1.3 | Description of the water-dependent asset register | 2.5.1.3, 3.4 | PDF, HTML, register |
| | 1.5 | Current water accounts and water quality | 2.5.1.5 | PDF, HTML |
| | 1.6 | Data register | 2.5.1.6 | Register |
| Component 2: Model-data analysis for the Galilee subregion | 2.1-2.2 | Observations analysis, statistical analysis and interpolation | 2.5.2.1, 2.5.2.2 | PDF, HTML |
| | 2.3 | Conceptual modelling | 2.5.2.3, 4.3 | PDF, HTML |
| | 2.5 | Water balance assessment | 2.5.2.4 | PDF, HTML |
| | 2.6.1 | Surface water numerical modelling | 4.4 | PDF, HTML |
| | 2.6.2 | Groundwater numerical modelling | 4.4 | PDF, HTML |
| | 2.7 | Receptor impact modelling | 2.5.2.6, 4.5 | PDF, HTML |
| Component 3 and Component 4: Impact and risk analysis for the Galilee subregion | 3-4 | Impact and risk analysis | 5.2.1, 2.5.4, 5.3 | PDF, HTML |
| Component 5: Outcome synthesis for the Galilee subregion | 5 | Outcome synthesis | 2.5.5 | PDF, HTML |

[a]The types of products are as follows:

- 'PDF' indicates a PDF document that is developed by the Lake Eyre Basin Bioregional Assessment using the structure, standards and format specified by the Programme.
- 'HTML' indicates the same content as in the PDF document, but delivered as webpages.
- 'Register' indicates controlled lists that are delivered using a variety of formats as appropriate.

[b]*Methodology for bioregional assessments of the impacts of coal seam gas and coal mining development on water resources* (Barrett et al., 2013)

## About this technical product

The following notes are relevant only for this technical product.

- All reasonable efforts were made to provide all material under a Creative Commons Attribution 3.0 Australia Licence.
- All maps created as part of this BA for inclusion in this product used the Albers equal area projection with a central meridian of 140.0° East for the Lake Eyre Basin bioregion and two standard parallels of –18.0° and –36.0°.
- Visit http://bioregionalassessments.gov.au to access metadata (including copyright, attribution and licensing information) for datasets cited or used to make figures in this product.
- In addition, the datasets are published online if they are unencumbered (able to be published according to conditions in the licence or any applicable legislation). The Bureau of Meteorology archives a copy of all datasets used in the BAs. This archive includes datasets that are too large to be stored online and datasets that are encumbered. The community can request a copy of these archived data at http://www.bioregionalassessments.gov.au.
- The citation details of datasets are correct to the best of the knowledge of the Bioregional Assessment Programme at the publication date of this product. Readers should use the hyperlinks provided to access the most up-to-date information about these data; where there are discrepancies, the information provided online should be considered correct. The dates used to identify Bioregional Assessment Source Datasets are the dataset's published date. Where the published date is not available, the last updated date or created date is used. For Bioregional Assessment Derived Datasets, the created date is used.

### *References*

Barrett DJ, Couch CA, Metcalfe DJ, Lytton L, Adhikary DP and Schmidt RK (2013) Methodology for bioregional assessments of the impacts of coal seam gas and coal mining development on water resources. A report prepared for the Independent Expert Scientific Committee on Coal Seam Gas and Large Coal Mining Development through the Department of the Environment. Department of the Environment, Australia. Viewed 12 June 2018, http://data.bioregionalassessments.gov.au/submethodology/bioregional-assessment-methodology.

IESC (2015) Information guidelines for the Independent Expert Scientific Committee advice on coal seam gas and large coal mining development proposals. Independent Expert Scientific Committee on Coal Seam Gas and Large Coal Mining Development, Australia. Viewed 12 June 2018, http://www.iesc.environment.gov.au/publications/information-guidelines-independent-expert-scientific-committee-advice-coal-seam-gas.

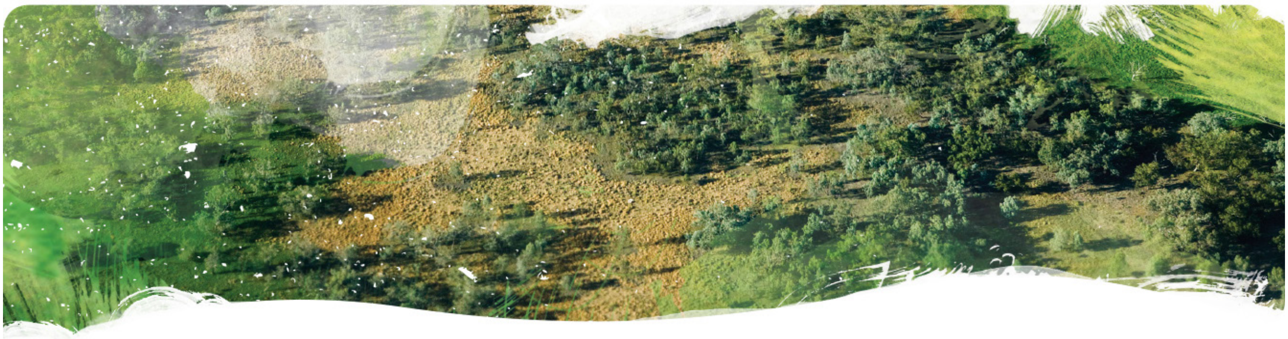

# 2.1 Observations analysis for the Galilee subregion

This product includes the observations analysis, statistical analysis and interpolation of datasets used in the bioregional assessment. Only those datasets required for product 2.6.1 (surface water numerical modelling), product 2.6.2 (groundwater numerical modelling) and product 2.3 (conceptual modelling) are covered.

The data are categorised according to the following disciplines:

- geography
- geology
- hydrogeology and groundwater quality
- surface water hydrology and water quality
- surface water – groundwater interactions.

The observations analysis includes an assessment of data errors and uncertainties; the spatial and temporal resolution of observations; and algorithms used in the development of derived datasets. It requires development – and reporting – of summary statistics that describe the datasets' nature, variation and uncertainty.

The statistical analysis and interpolation aims to develop a quantitative understanding of the Galilee subregion by analysing the observed data and – where required – interpolating into locations where data are sparse.

This product also provides advice on data gaps. More information on data gaps will be reported in later products.

This product concludes with a detailed description of water management for coal resource developments. Only that information required for numerical modelling (in product 2.6.1 (surface water numerical modelling) and product 2.6.2 (groundwater numerical modelling)) is included.

## 2.1.1 Geography


### *Summary*

The Galilee subregion encompasses a large area (248,000 km$^2$) and has sparse climatic data coverage. This section provides an analysis of the errors associated with the climate data used for the water balance modelling. To characterise errors of the input climate data, the long-term (from January 1980 to December 2009) monthly values of precipitation (P) and maximum ($T_{max}$) and minimum ($T_{min}$) temperatures were calculated along with root mean square error (RMSE) values for the same variables. Results showed relative errors of 84.7%, 1% and 3% in P, $T_{max}$, and $T_{min}$ respectively.


### *2.1.1.1 Observed data*

The basic geographic data for the Galilee subregion were reported in companion product 1.1 for the Galilee subregion (Evans et al., 2014).

### *2.1.1.2 Statistical analysis and interpolation*

All geographic data specific to the Galilee subregion were obtained from state or national datasets. This means no statistical analysis or interpolation was performed to generate any of the geographic datasets. However, to characterise errors of the input climate data used for the water balance modelling, some subregion-specific spatial analysis was performed. This is outlined in this section.

In addition to generating daily and monthly grids of meteorological variables (precipitation, maximum temperature, minimum temperature), the Bureau of Meteorology (Jones et al., 2009) also generate daily and monthly root mean square error (RMSE) grids of the same variables. RMSE is often used in comparisons of modelled values with observations; however, the daily and monthly RMSE grids provided by the Bureau of Meteorology are instead a combined measure of the observational error and geostatistical error. The latter is a function of the interpolation algorithm, density of isolated station observations and degree of spatial autocorrelation of the process(es) driving the spatial variance captured in the data being interpolated.

To characterise errors of the input climate data, the long-term (from January 1980 to December 2009) monthly mean values for precipitation (P), maximum temperature ($T_{max}$) and minimum temperature ($T_{min}$) were calculated. Also calculated were the long-term monthly RMSE mean values for the same variables for the same time period. Relative error, expressed as a percent, was calculated by dividing monthly RMSE mean grid by the monthly mean grids (i.e. RMSE grid/mean grid for each meteorological variable).

The spatially-averaged long-term monthly mean P for the Galilee subregion is 39.9 mm/month, and the associated P RMSE subregion mean is 30.7 mm/month (see Figure 3a and Figure 3b respectively). This results in a relative error of 84.7% in the input P grids (Figure 3c). The high relative error is due, in part, to P being a highly spatially variable process (it has low spatial autocorrelation).

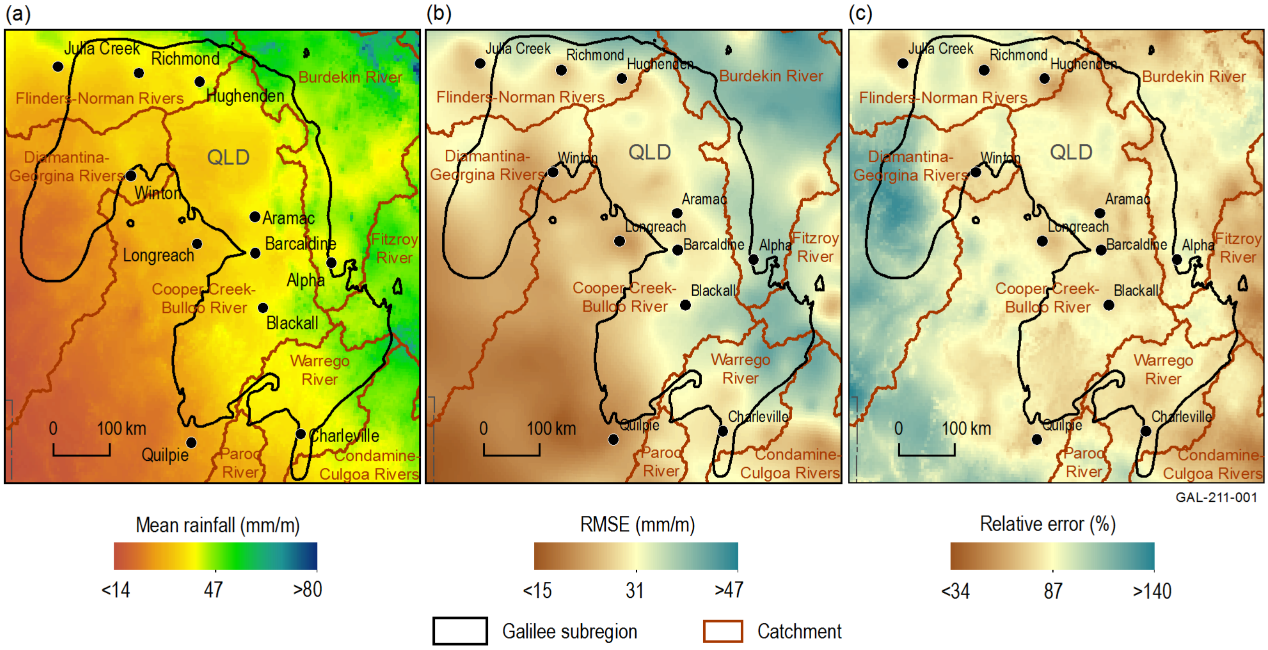


**Figure 3 Spatial variation of precipitation from 1980 to 2009**

(a) monthly mean precipitation (b) monthly mean root mean square error (RMSE) precipitation and (c) monthly mean precipitation relative error for the Galilee subregion and proximal surface water basins
Population centres are shown by black dots.
Data: Bioregional Assessment Programme (Dataset 1)

For air temperatures, a meteorological field that has higher spatial autocorrelation than P, regional distribution is governed by topography and distance from the ocean. The $T_{max}$ spatially-averaged long-term monthly mean is 30.7 °C for the Galilee subregion (Figure 4a). The associated RMSE is approximately 0.3 °C (Figure 4b), which leads to a relative error of approximately 1% for $T_{max}$ (Figure 4c). For $T_{min}$ in the Galilee subregion, there are similar spatial patterns, with the spatially-averaged long-term monthly mean being 15.9 °C (Figure 5a) and the associated RMSE being approximately 0.5 °C (Figure 5b), which leads to a relative error of about 3% for $T_{min}$ (Figure 5c).

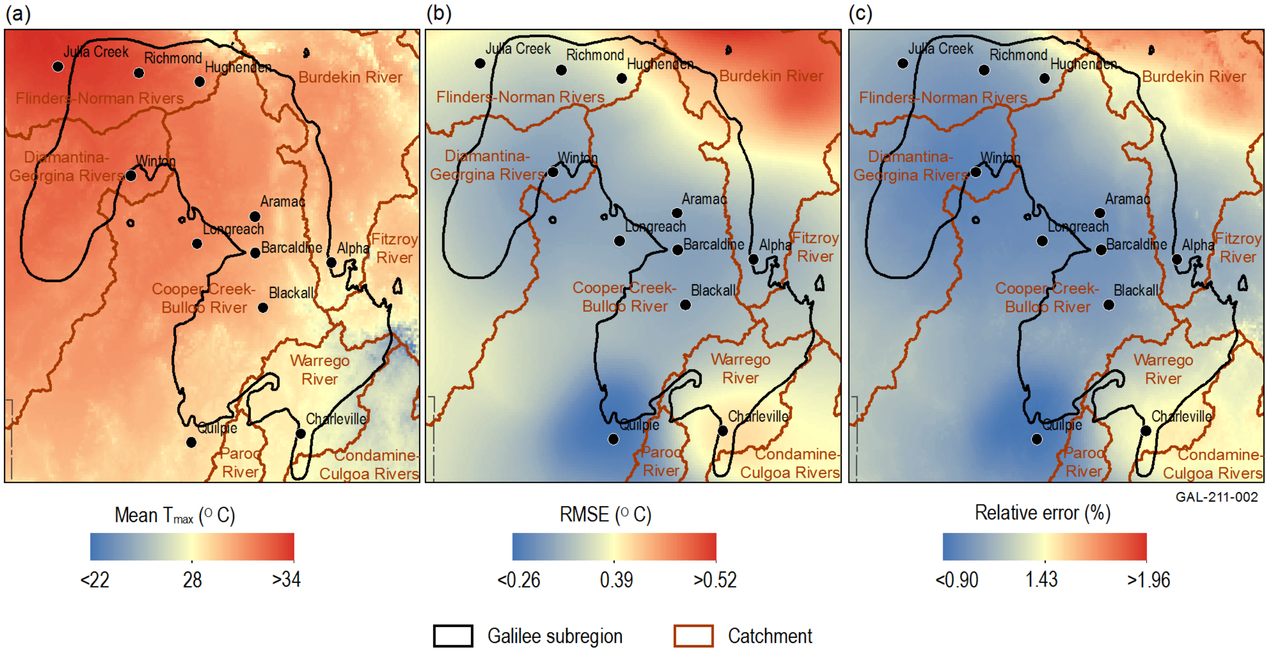


**Figure 4 Spatial variation of maximum air temperature ($T_{max}$) from 1980 to 2009**

(a) monthly mean $T_{max}$ (b) monthly mean root mean square error (RMSE) $T_{max}$ and (c) monthly mean $T_{max}$ relative error for the Galilee subregion and proximal surface water basins
Population centres are shown by black dots.
Data: Bioregional Assessment Programme (Dataset 1)

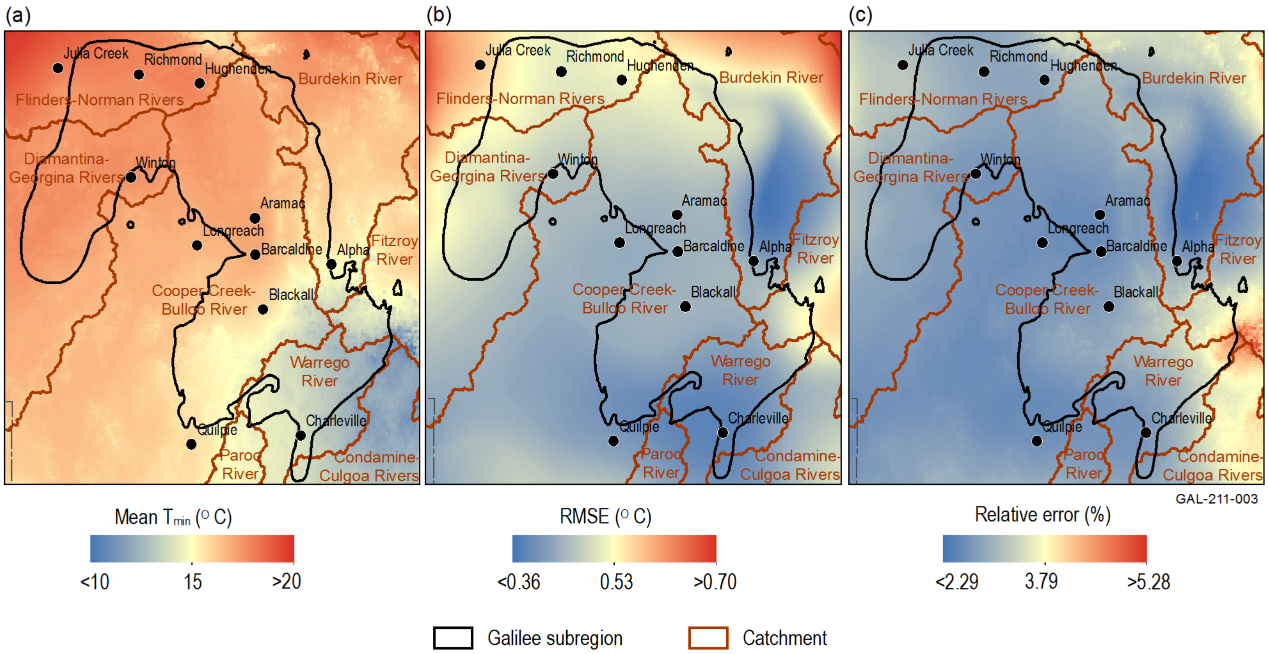


**Figure 5 Spatial variation of minimum air temperature ($T_{min}$) from 1980 to 2009**

(a) monthly mean $T_{min}$ (b) monthly mean root mean square error (RMSE) $T_{min}$ and (c) monthly mean $T_{min}$ relative error for the Galilee subregion and proximal surface water basins
Population centres are shown by black dots.
Data: Bioregional Assessment Programme (Dataset 1)

### 2.1.1.3 Gaps

The characterisation of input data errors suggests that having a denser network of official Bureau of Meteorology stations recording precipitation is essential for improved water-related modelling in the Galilee subregion.

Based on the coal resource development pathway, the coal resource development projects most likely to begin production in the next five to ten years all lie within the Belyando river basin, which comprises a part of the Burdekin river basin (see Section 2.5.2 in companion product 2.5 for the Galilee subregion (Karim et al., 2018)). Therefore if further climatic data were collected in the subregion, increasing the density of observations in the Burdekin river basin should be treated as a priority. As coal resource development continues, rain gauges installed by industry may represent an important addition to the existing network.

### References

Evans T, Tan KP, Magee J, Karim F, Sparrow A, Lewis S, Marshall S, Kellett J and Galinec V (2014) Context statement for the Galilee subregion. Product 1.1 from the Lake Eyre Basin Bioregional Assessment. Department of the Environment, Bureau of Meteorology, CSIRO and Geoscience Australia, Australia. Viewed 12 May 2016, http://data.bioregionalassessments.gov.au/product/LEB/GAL/1.1.

Jones DA, Wang W and Fawcett R (2009) High-quality spatial climate data-sets for Australia. Australian Meteorological and Oceanographic Journal 58(4), 233–248.

Karim F, Hostetler S and Evans T (2018) Water balance assessment for the Galilee subregion. Product 2.5 for the Galilee subregion from the Lake Eyre Basin Bioregional Assessment. Department of the Environment and Energy, Bureau of Meteorology, CSIRO and Geoscience Australia, Australia. http://data.bioregionalassessments.gov.au/product/LEB/GAL/2.5.

### Datasets

Dataset 1 Bioregional Assessment Programme (2015) BILO Climate Relative Error Grids V01. Bioregional Assessment Derived Dataset. Viewed 06 May 2016, http://data.bioregionalassessments.gov.au/dataset/c0c139f5-3648-4e0f-9acf-a884b7cc859b.

## 2.1.2 Geology


### *Summary*

The Galilee subregion covers an area of about 248,000 $km^2$ in central Queensland, and is defined by the known extent of the geological Galilee Basin which hosts important coal-bearing sequences that are in current demand for coal mining, coal seam gas production, and continued petroleum exploration. These coal seams are the focus of some 13 coal and 3 coal seam gas (CSG) projects that are targeting resources in the upper Permian coal measures. The Galilee Basin sequence is only exposed along its eastern margin in a tract of about 600 km long and up to 80 km wide, where the outcropping and near-surface sub-bituminous coal resources are present.

The geology of the Galilee subregion can stratigraphically be subdivided into three geological sequences, which from oldest to youngest are: Galilee Basin, Eromanga Basin, Cenozoic sediments and volcanics. Each sequence comprises a number of stratigraphic units.

The Galilee Basin, accumulated over a period from 323 to 238 million years ago (Upper Carboniferous to Middle Triassic), is largely buried by the Early Jurassic-Late Cretaceous Eromanga Basin and scattered Cenozoic deposits. The Galilee Basin surrounds three sides of the Maneroo Platform, which is comprised of rocks from part of geological basement for the Galilee subregion. The Galilee Basin has four main depocentres: the Koburra Trough, and Aramac, Lovelle and Powell depressions. Maximum thickness of the sequence is about 2800 m in the Koburra Trough.

The overlying Eromanga Basin sequence accumulated over the period 197 to 95 million years ago, from Early Jurassic to Late Cretaceous. Deposition initially took place in river, lake and swamp environments to produce an alternating series of sandstone aquifers and mudstone-siltstone aquitards. A marine incursion in the Early Cretaceous terminated this cyclicity with a very thick sequence of fine-grained marine sediments. With retreat of the sea, uplift and major erosion to the east, another very thick clastic sequence accumulated in estuarine and then continental conditions.

During the subsequent 60 million years to the present in the Cenozoic, subtle regional deformation created scattered small basins as well as extensive sheet-wash gravels from erosion of the uplifting Great Dividing Range.

A review of geological structures is included in this section to assist in understanding and interpreting features that are apparent in the geological model. Much of the existing information focuses on regional structures, there is much less information available on distribution and occurrence of smaller-scale (semi-regional to local) structures in the Galilee subregion.

Significant fault displacements in the Galilee-Eromanga sequence are present along the subregion margin against the Maneroo Platform, the Holberton-Cork-Wetherby structures in the Lovelle Depression and the Canaway Fault in the Powell Depression. These structures are

in or adjoin deeply buried depocentres where CSG may be of interest, but do not impinge on proposed coal mining areas on the eastern basin margin.

There is considerable variation in the quality and distribution of publicly available drillhole data across the Galilee subregion. Approximately 8% of all bores located in the Galilee subregion lacked drillhole depth information. Furthermore, most bores did not have stratigraphic data that could be used for modelling purposes.

From available data, CSG contents for the upper Permian coal measures tend to peak at their highest levels between 900 and 1200 m depth. CSG contents appear to drop off below 1300 m. Available gas isotope data suggest that CSG down to around 1400 m depth is primarily derived through biogenic (microbial) processes.

In the upper Permian coal measures, high average gas contents tend to occur in the central parts of the northern Galilee Basin, in the vicinity of CSG project areas. A zone of higher gas contents forms a north-east trending CSG fairway. Several faults in upper Permian coal measures also trend in the same direction as the CSG fairway, which suggests some structural control (faults) are influencing the distribution of CSG. It is likely that structures that affect the distribution of CSG may also influence potential groundwater flow in the upper Permian coal measures.

The geological model developed for the bioregional assessment (BA) for the Galilee subregion consists of a series of upper surfaces of stratigraphic sequences (presented as structure contours) and thickness (isopach) maps for each stratigraphic sequence. These were compiled to form a composite geological model of stratigraphic units in the Eromanga and Galilee basins. For Eromanga Basin stratigraphic units, the model layers were derived from the *Hydrogeological atlas of the Great Artesian Basin* (GAB Atlas; Ransley et al., 2015). For the Galilee Basin, geological model layers were developed as part of the BA for the Galilee subregion. Galilee Basin model layers define the upper surface of each of the units which are, in descending order: Moolayember Formation, Clematis Group, Rewan Group, upper Permian coal measures, Joe Joe Group and base of the Galilee Basin. These units represent a significant update on previous sub-surface regional geological mapping for the Galilee Basin.

The variable extent and thickness of individual stratigraphic units within the combined Galilee-Eromanga basin sequence indicate potential interconnectivity of aquifers between these two basins along the north-eastern margin of the Maneroo Platform, in the deeper south-westward extent in the Lovelle Depression, and in parts of the southern Galilee Basin.

The various Galilee Basin units are not evenly distributed across the basin. The Joe Joe Group shows considerable variation in thickness, which is consistent with it being deposited in areas of active subsidence (e.g. the Koburra Trough) during the early formative phases of the Galilee Basin. The upper Permian coal measures blanket much of the Joe Joe Group and are generally less than 160 m in thickness. The thickest parts of the coal measures coincide with the areas of interest of the most advanced proposals for coal exploitation along the eastern margin of the Galilee subregion. Where the overlying Rewan Group is present, its average thickness is 148 m. Erosion of the overlying Rewan Group, Clematis Group and Moolayember Formation has taken place in areas such as Barcaldine Ridge and around the western margin of the Galilee subregion. This has enabled upper Permian coal measures and Clematis Group to be in direct contact in places with the overlying Hutton Sandstone of the Eromanga Basin. These erosional windows may provide potential pathways for hydraulic connectivity between Galilee and Eromanga basins.

Further work may include: improved quality assurance/quality control of drillhole databases and, where possible, attainment of missing drillhole stratigraphic data; refinements to the regional stratigraphic correlations for upper Permian coal measures; and access to coal company drillhole data and geological mapping. Collectively this work would help to refine the conceptual geological model in particular in the vicinity of coal resource development proposals, identify finer-scaled structures in the Galilee subregion and improve the resolution of extent and thickness of stratigraphic units across the Galilee Basin. More detailed assessments of available two-dimensional seismic reflection and well log data may improve understanding of the distribution and variations in lithology and porosity for different stratigraphic units as well as provide further detail on the nature and distribution of geological structures in the subregion. This information could be incorporated into future iterations of the geological model, which would in turn improve the understanding of hydrogeology of the subregion.

### *2.1.2.1 Observed data*

#### 2.1.2.1.1 Overview

This product outlines the rationale for the development of a geological model of the Galilee subregion. It details the data used in its construction, and the known limitations of certainty to this data. The geological model is presented as maps of various sedimentary sequences, with the extent, regional orientation and thickness of each package defined sufficiently to generate a three-dimensional representation of the geology of the Galilee subregion.

Knowledge of the geological architecture of the Galilee subregion is essential as a framework for conceptualising the hydrogeology of the Galilee and Eromanga basins as well as providing a framework for surface water - interactions.

There are three main types of observed geological data available:

- drillhole data
- geophysical data
- geological maps and models.

#### 2.1.2.1.2 Drillhole data

Several sources of drillhole data and other related information were accessed for the BA for the Galilee subregion. These data are from three Queensland Department of Natural Resources and Mines (DNRM) sources:

- Queensland groundwater database
- Queensland Petroleum Exploration Database (QPED)

- well completion reports from the Queensland digital exploration reports (QDEX).

From publicly available bore data (Bureau of Meteorology, Dataset 1) in total some 7350 bores have been drilled in the Galilee subregion for groundwater, petroleum, CSG or stratigraphic purposes.

As of December 2013, there were 321 petroleum, CSG and stratigraphic wells in the Galilee subregion comprising some 202 wells for petroleum and CSG, and 119 stratigraphic drillholes (Figure 6 and Table 4). A slight increase in well density is evident in the southern Galilee subregion near the Gilmore gas field, and in the central portions of the northern Galilee Basin, which is the main area of focus for CSG exploration.

More information can be obtained for petroleum, CSG and stratigraphic wells from their original well completion reports. The Queensland groundwater database contains the most publicly available groundwater bore data. Government agencies drilled some regional coal exploration bores in the 1960s through to the 1970s.

As of July 2014, 7029 groundwater bores had been drilled in the Galilee subregion (Bureau of Meteorology, Dataset 1). Of these, 4712 were currently classed as operational in companion product 1.5 for the Galilee subregion (Evans et al., 2015). Figure 5 through to Figure 8 in companion product 1.5 for the Galilee subregion (Evans et al., 2015) show the distribution of operational groundwater bores in the Galilee subregion.

It is important to note that within the Galilee subregion, some 560 bores (approximately 8% of total) have no available depth information (Figure 7). The drillholes missing depth information are almost all groundwater bores. Figure 7 also highlights the considerable variation in bore depth, which is partially dependent on the original purpose of a bore. While some groundwater bores can be up to 1500 m deep, most groundwater bores (approximately 87%) are less than 500 m deep. Groundwater bores greater than 500 m in depth target deep artesian aquifers in the Eromanga Basin. Bores greater than 1500 m in depth are almost exclusively exploration wells that target petroleum reservoirs in the Galilee Basin or the underlying Adavale Basin. CSG wells target coal seams in the Galilee Basin and range in depth from approximately 600 to 1500 m.

Company groundwater monitoring bore data is available through the Queensland groundwater database. However, company drillhole data for mineral and coal exploration are not readily available in a digital format to the public. It is likely that hundreds, if not thousands, of coal resource appraisal bores have been drilled in the Galilee subregion. The majority of the bores drilled by industry cluster around the known coal resource project areas, in particular those projects located along the eastern margin of the Galilee subregion (Figure 6). It is likely that the incorporation of company coal drillhole data would significantly refine geological models for the subregion, in particular the modelled geological surfaces for the Galilee Basin. Such refinements would improve understanding of the geological architecture and potential connective pathways.

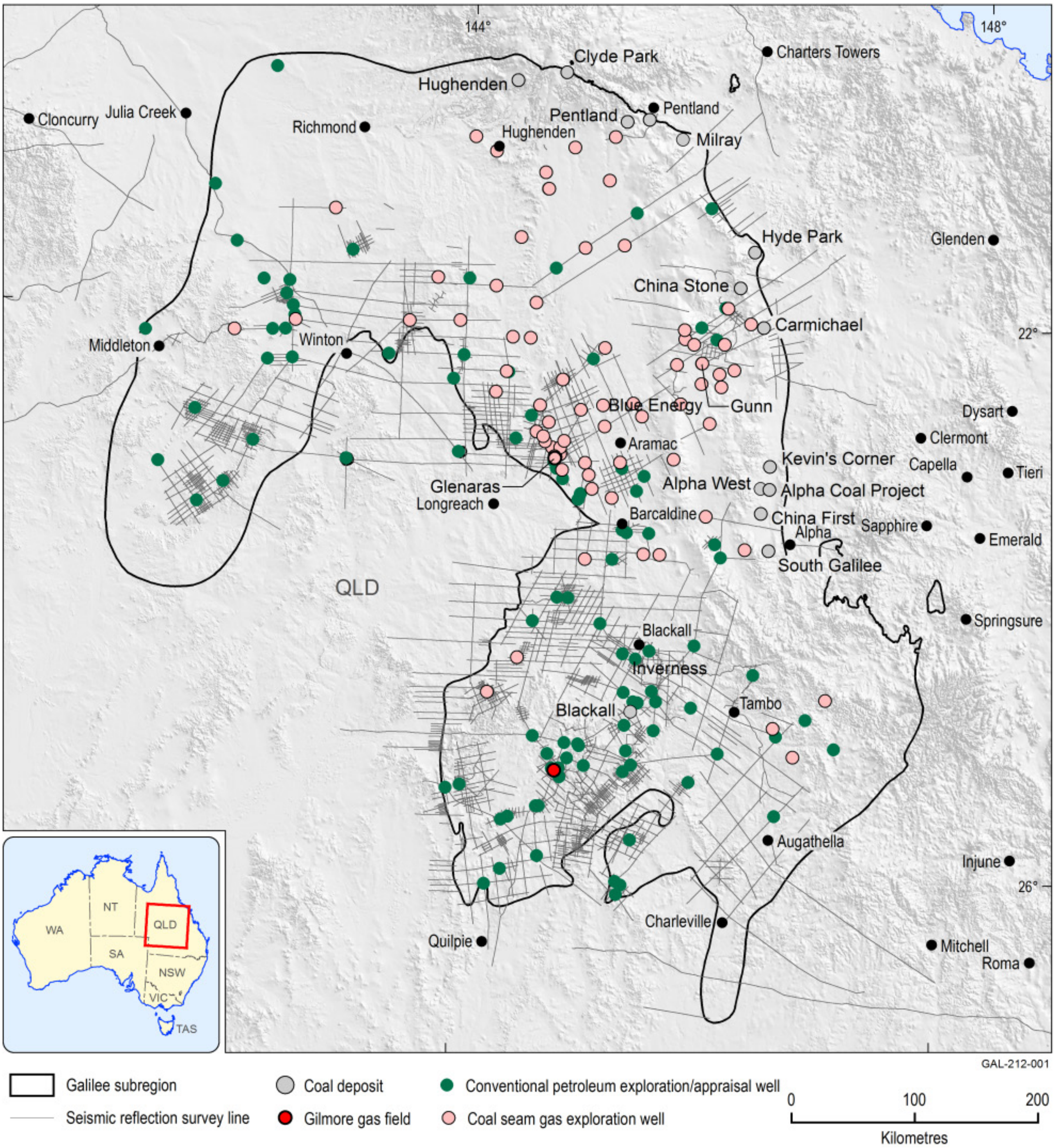


**Figure 6 Distribution of petroleum, stratigraphic coal seam gas wells, two-dimensional seismic reflection survey lines and locations of coal and CSG projects in the Galilee subregion**

Gilmore gas field is situated in the Adavale Basin, which underlies the Galilee Basin. This Gilmore gas field is a conventional gas field that is not associated with coal or CSG.
Data: Bureau of Meteorology (Dataset 1), Geological Survey of Queensland (Dataset 2), Bioregional Assessment Programme (Dataset 3, Dataset 4, Dataset 7), Queensland Department of Natural Resources and Mines (Dataset 5, Dataset 6)

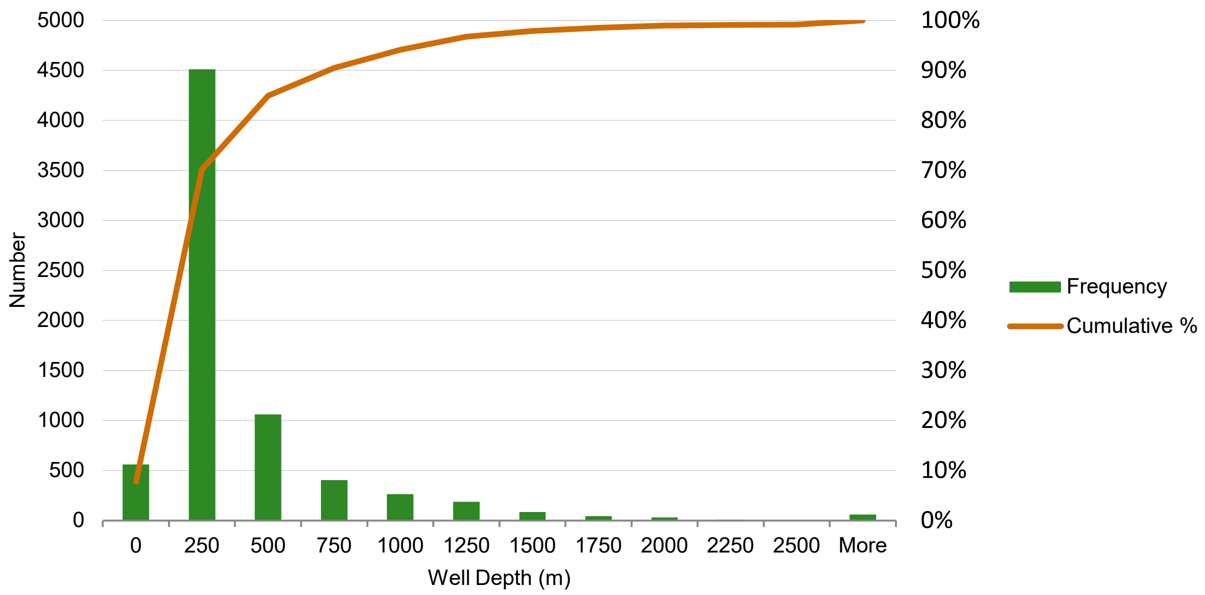


**Figure 7 Number of wells per depth interval and cumulative percentage of total number of bores in the Galilee subregion**

Data: Bioregional Assessment Programme (Dataset 8)

## 2.1.2.1.3 Geophysics

Numerous geophysical surveys have been undertaken in the Galilee subregion over the last 60 years. The regional geophysical datasets include ground-based gravity measurements, airborne aeromagnetics and radiometrics, and two-dimensional seismic reflection surveys.

### *2.1.2.1.3.1 Gravity and magnetics*

Airborne magnetics and radiometrics survey data and ground-based gravity measurements were obtained from the geophysics archive and data delivery system (GADDS; Geoscience Australia, 2015). Numerous surveys of varying quality, configuration and extent exist across the subregion, Relevant data from some of these surveys have been combined into a consistent framework on a continent-wide basis for Bouguer gravity (Geoscience Australia, 2015), aeromagnetics and radiometrics (Geoscience Australia, 2015). There will be no further discussion on radiometrics as this data type was not used as part of this iteration of the BA for the Galilee subregion. Radiometrics could be used in future studies to refine surface geological mapping, which may in turn be used to refine estimates of recharge to groundwater systems.

Gravity and magnetic potential field data provide a consistent regional coverage that can be used to delineate regional structural fabric, provide infill for gaps in other datasets, and help to substantiate interpretation between existing seismic lines and drillhole data. A composite image of gravity (in colour) and magnetics is shown in Figure 8. This combined data image can be used to help delineate the distribution and thickness of sedimentary cover, as well as changes in basement lithology and structure.

The Galilee subregion overlaps an area of active research on basement character and tectonics (e.g. Spampinato et al., 2015a, 2015b, 2015c). Subsequent movement along many pre-existing faults in geological basement (e.g. Cork Fault, Wetherby Structure, and Hulton-Rand Structure) have disrupted overlying Galilee and Eromanga basin sequences.

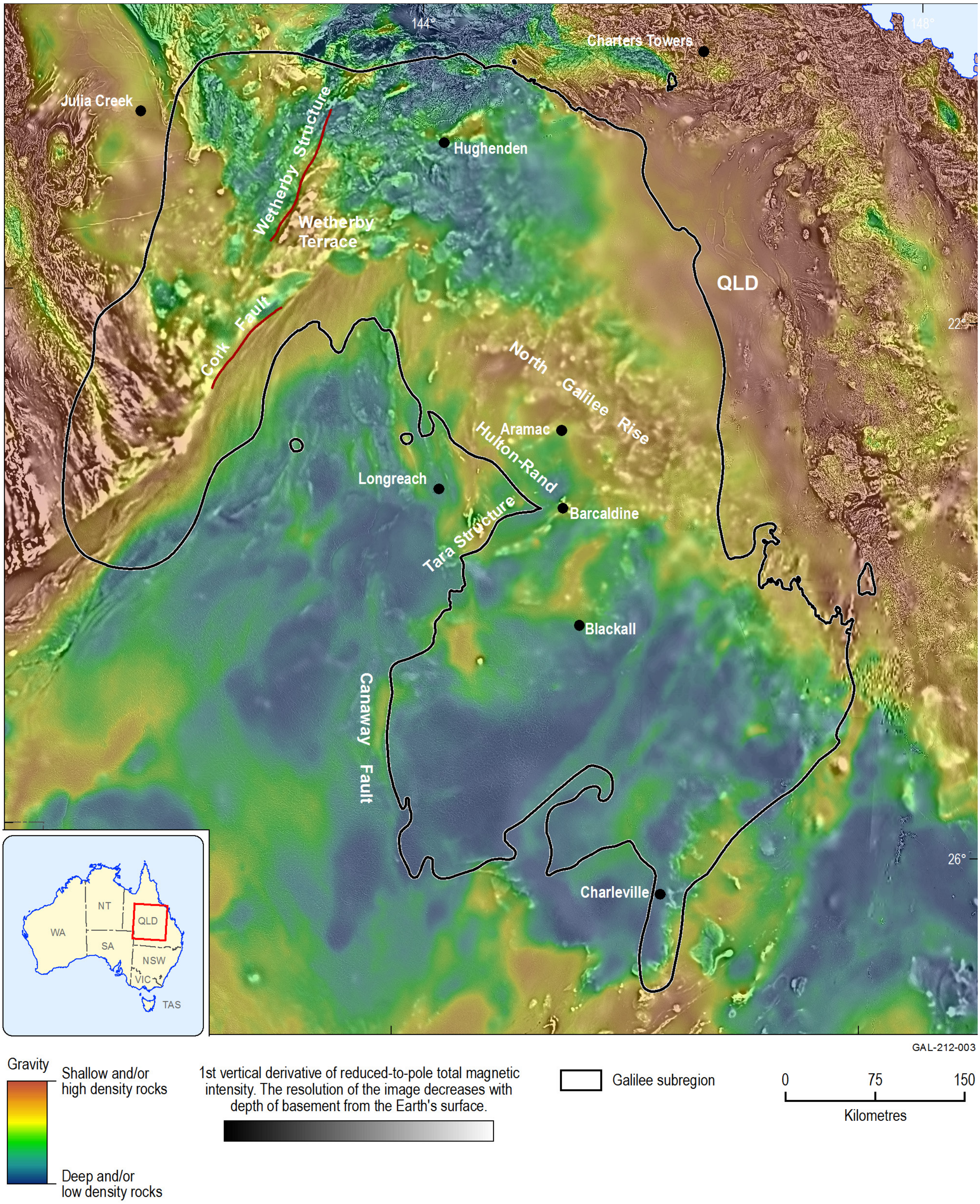


**Figure 8 Composite potential field (gravity and aeromagnetics) image for the Galilee subregion**

Structural trends in basement are indicated from composite potential field data. Gravity (in colour) indicates a combination of depth and density of basement. Magnetics (total magnetic intensity (TMI), reduced to pole and 1st vertical derivative) in sun-shaded monochrome highlights the structural character of the geological basement as well as its depth from surface.
Data: Geoscience Australia (Dataset 9), Bioregional Assessment Programme (Dataset 10)

#### *2.1.2.1.3.2 Seismic*

Seismic data can be used to extend and correlate stratigraphic surfaces between drillhole stratigraphic controls to provide a more regional coverage. Since the late 1950s, companies and government agencies have acquired two-dimensional seismic reflection survey data across the Galilee subregion. More recent seismic reflection surveys have been conducted as part of regional exploration programmes for CSG as well as deep crustal studies by Geoscience Australia. From the distribution of two-dimensional seismic reflection survey lines (Figure 6) it is apparent that the northern and eastern margins of the Galilee subregion have sparse to non-existent coverage. Marsh et al. (2008) reviewed available seismic and well data in the Galilee subregion as part of studies into the storage of carbon dioxide ($CO_2$). They found that although seismic coverage was relatively abundant in some areas of the Galilee subregion, much of the seismic data was not available in a readily usable format. Other issues include variable quality in resolution of the seismic and location data.

Existing publicly available seismic horizon mapping from reports (Queensland Department of Natural Resources and Mines, Dataset 6; Bioregional Assessment Programme, Dataset 7) was utilised in the development of the Galilee Basin geological surfaces and model (Section 2.1.2.2.4).

### 2.1.2.1.4 Geological maps and models

The surface geology of the Galilee subregion was systematically mapped during the 1960s and 1970s and resulted in a series of maps (Figure 10) being published at a scale of 1:250,000 (1 cm = 2.5 km). These maps defined the surface distribution of stratigraphic units, regional structures, bores and other features as well as incorporating information from geophysical surveys that existed at the time. Several surface geology datasets at smaller scales, for example 1:1,000,000 (1 cm = 10 km), are derived from the original 1:250,000 regional mapping. References for the 1:250,000 map sheets are detailed in Table 3.

Recently, more detailed larger-scale maps at a 1:100,000 scale (1 cm = 1 km) have been published for selected areas along the eastern margin of the Galilee subregion. There are notable discrepancies in the occurrence and distribution of Galilee Basin stratigraphic units at the different scales of geological mapping. For instance on the Mt Tutah 1:100,000 map sheet (DME, 2008) there occurs outcrop of Galilee Basin sedimentary rocks whereas some of these outcrop areas are not shown on the equivalent 1;250,000 map sheet (Buchanan 1;250,000 map sheet (Olgers, 1970)). Some of the implications of these discrepancies are further discussed in companion product 3-4 for the Galilee subregion (Lewis et al., 2018).

#### *2.1.2.1.4.1 Updated stratigraphic column*

Since the publication of the original stratigraphic column in companion product 1.1 for the Galilee subregion (Evans et al., 2014), new work has been published that refines the understanding of the stratigraphy in the subregion. The refinements as shown on Figure 9 include:

- addition of the Precipice Sandstone and Evergreen Formation. The recent publication of the GAB Atlas (Ransley et al., 2015) demonstrates that equivalents of these formations are present in the Lovelle and Powell depressions of the Galilee subregion
- minor refinements to the Cenozoic sections of the Galilee subregion stratigraphic column

- new uranium-lead zircon dates that pinpoint the age of deposition for the Edie Tuff Member to 294.8±0.08 Ma (Nicoll et al., 2015). These precise age dates, coupled with an improved understanding of biostratigraphy of the Aramac Coal Measures, have compressed the depositional time interval for lower Permian sequences in the Galilee Basin by some 8 to 10 million years.

Ongoing work as outlined in Nicoll et al. (2015) and Phillips et al. (2015, 2016) will further refine the Permian stratigraphy and geological understanding of the Galilee Basin. This may result in future updates to the Galilee subregion stratigraphic column.

#### *2.1.2.1.4.2 Existing geological models*

Several existing geological models have been used as a basis for the development of the Galilee subregion geological model.

Structure in basement has been modelled by de Vries et al. (2006) as a continent-wide OZ SEEBASE surface. While OZ SEEBASE addresses magnetic basement, which is itself subject to interpretation, it does offer a regional template for interpretation of basement depth and structure across the Galilee subregion that can be better constrained with use of more recent seismic and drillhole data.

The hydrostratigraphic architecture of the GAB has recently been defined by Ransley et al. (2015). Their approach categorises stratigraphic packages as regional aquifers and aquitards as a way to conceptually simplify the hydrogeological understanding of a myriad of lithostratigraphic units. For the Galilee subregion, the isopach maps of hydrostratigraphic units offer a basis for developing a consistent stratigraphic model of the Jurassic to Cenozoic sequence.

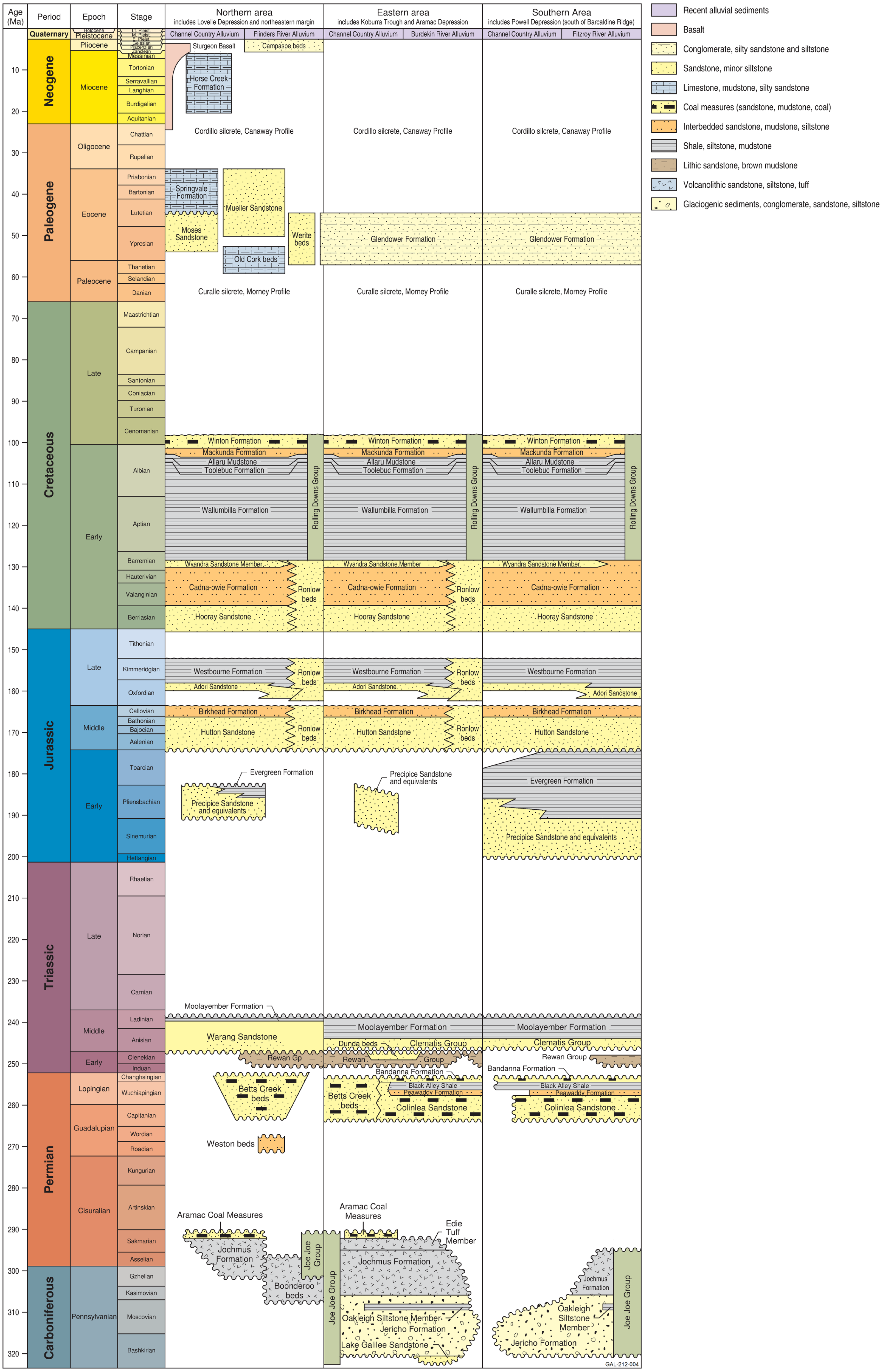


**Figure 9 Updated stratigraphic column for the Galilee subregion**

Updated stratigraphic column compiled from companion product 1.1 for the Galilee subregion (Evans et al., 2014) and McKellar and Henderson (2013)

This figure has been optimised for printing on A3 paper (297 mm x 420 mm).

#### 2.1.2.1.5 Geological uncertainty

The confidence in understanding subsurface geology in the Galilee subregion is primarily a function of density and quality of the acquired geophysics and drillhole data in combination with the surface geological mapping.

Each of the 1:250,000 geological maps (Figure 10) has an associated reliability diagram that outlines in general terms which areas of each map sheet were mapped in detail. Mapping with greater reliability usually equates to higher field traverse density and good air photo coverage. For this 1:250,000 mapping programme, on-ground geological mapping tended to focus on areas of pre-Cenozoic outcrop. Areas of lower reliability usually equate to those regions covered by Cenozoic sediments. The areas of significant Cenozoic cover can be ascertained from Figure 10. Further detail on the geology and relative uncertainty can be found in the geological notes (references outlined in Table 3) that accompany each 1:250,000 map sheet. Discrepancies in the surface geological mapping, such as those outlined in Section 2.1.2.1.4, would contribute to geological uncertainty, as surface geological mapping is a key input dataset to any geological modelling and conceptualisation.

##### *2.1.2.1.5.1 Drillhole data and uncertainty*

Available drillhole databases are largely archival in nature with data derived from a range of sources. The main types of data required from drillhole datasets to build various geological models for BAs are stratigraphic picks and bore location data. The discussion here will focus on these aspects.

In terms of the data, it is difficult to assess inherent uncertainty on a per bore basis. Data quality can vary considerably from bore to bore, and is partially dependent on: the original purpose for which the bore was drilled (e.g. groundwater, coal or petroleum); when the bore was drilled (data vintage); how the bore was drilled (drilling operations and type of drilling); the care with which data were collated and reported; the relative experience of the well site geologist and other personnel; and if other types of data collected during drilling of the bore can be used for comparison and to cross check results (e.g. downhole geophysics logs, biostratigraphy, lithological samples).

In general, stratigraphic and positioning data for petroleum, CSG and stratigraphic wells represent the higher quality datasets because usually a more methodical and consistent approach was taken in collecting multiple types of data from each well. There is also usually enough detailed information to corroborate the stratigraphic picks, which were derived from the various datasets (e.g. geophysical well logs, detailed lithology, biostratigraphy). If stratigraphic picks need to be re-interpreted then there is usually adequate data available from the bore in question to do so.

There is more variation in the quality of stratigraphic interpretations and bore positioning data with groundwater bores. Sometimes more care is taken in the collection of data from deeper (and more expensive) groundwater bores than those obtained from shallow pastoral bores. The locations of the shallow pastoral bores may not have been surveyed. Interpretation of their stratigraphy is commonly solely from drillers' logs, rather than from variety of data sources. However, the proportionately much greater number of groundwater bores available offers a better regional coverage if they can be integrated carefully with stratigraphic information from the more reliable deeper stratigraphic and exploration wells.

Data from coal resource appraisal bores are generally of good quality, as they have been collected in a methodical and composite approach. However, these data are commonly not available in the public domain and are therefore not readily available for use in this BA.

Adjoining resource companies may hold divergent views on stratigraphic interpretation and nomenclature. Examples of this problem are outlined in Section 2.1.2.2.5.3 (under 'Upper Permian coal measures'). Although this is not necessarily an issue for interpreted stratigraphy at a mine scale, such variance can become a significant issue when trying to correlate geological units on a regional scale.

Varying definitions for stratigraphic boundaries over time can also increase uncertainty in stratigraphic drillhole picks, which in turn can lead to less reliable geological models. For instance, in the Galilee Basin, the boundary between Triassic sequences such as the Rewan Group and the upper Permian coal measures can be difficult to pick subsurface from drillhole data (Phillips et al., 2015).

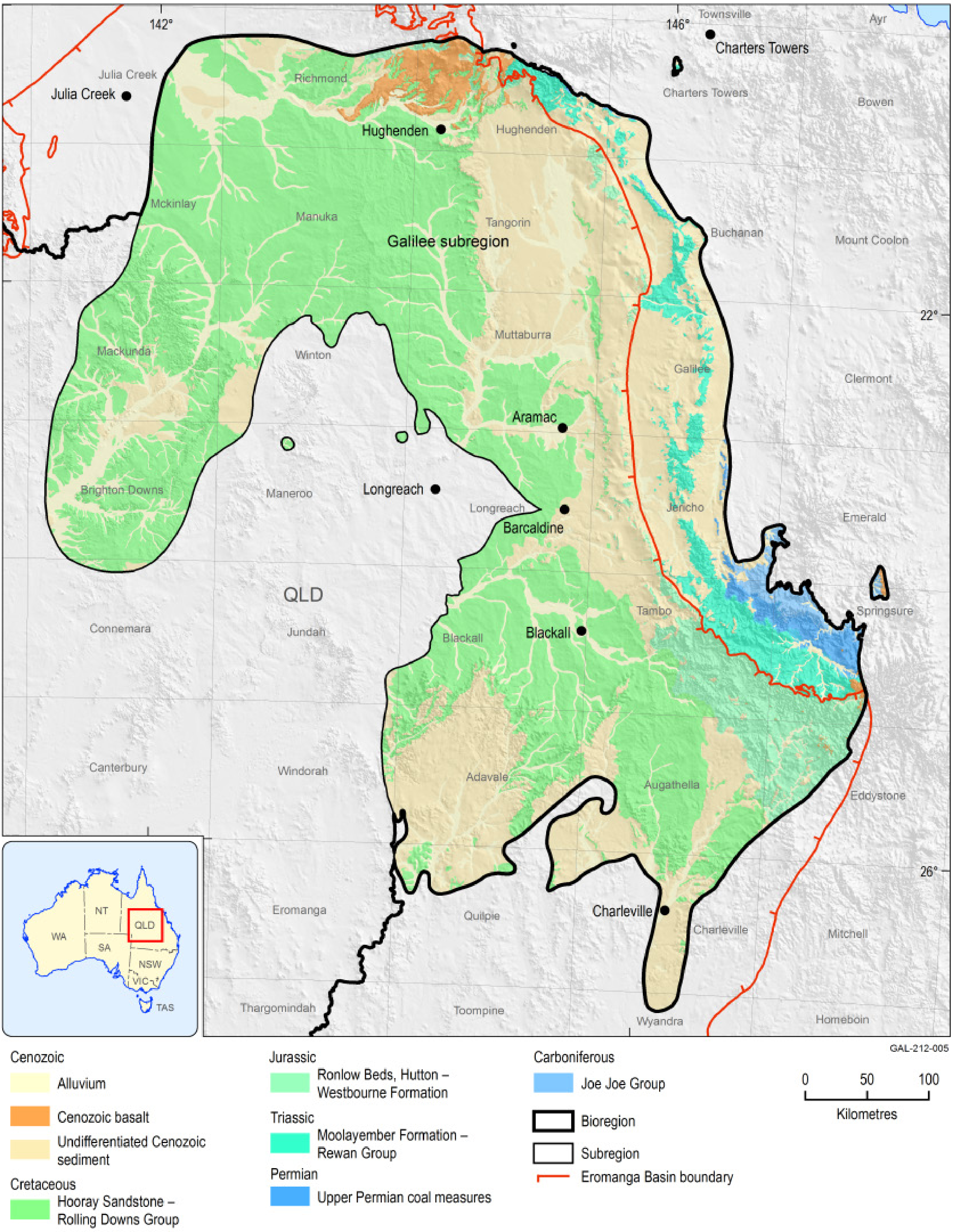


**Figure 10 Surface geology and 1:250,000 map sheet coverage in the Galilee subregion**

Data: Geoscience Australia (Dataset 11, Dataset 12)

**Table 3 References for 1:250,000 geological map sheets in the Galilee subregion**

| Map sheet name | Reference |
|---|---|
| Adavale | Galloway (1970a) |
| Augathella | Galloway (1970b) |
| Blackall | Casey (1971) |
| Brighton Downs | Jauncey (1962) |
| Buchanan | Olgers (1970) |
| Charleville | Senior (1971b) |
| Charters Towers | Clarke (1970) |
| Connemara | Senior (1969a) |
| Eddystone | Exon (1968) |
| Emerald | Olgers (1969) |
| Galilee | Vine (1972) |
| Hughenden | Vine (1974) |
| Jericho | Senior (1973) |
| Julia Creek | Vine (1962a) |
| Jundah | Senior (1969b) |
| Longreach | Vine (1970a) |
| Mackunda | Vine (1962b) |
| Maneroo | Jauncey (1965) |
| Manuka | Casey (1965a) |
| Mckinlay | Vine (1962c) |
| Muttaburra | Vine (1970b) |
| Quilpie | Senior (1971a) |
| Richmond | Vine (1970c) |
| Springsure | Mollan (1967) |
| Tambo | Exon (1970) |
| Tangorin | Casey (1969) |
| Windorah | Gregory (1969) |
| Winton | Casey (1965b) |

Data: Geoscience Australia (Dataset 11)

### *2.1.2.2 Statistical analysis and interpolation*

#### 2.1.2.2.1 Bore locations

The location of a bore and the height of a bore above a datum (usually the Australian Height Datum (AHD)) are crucial information for geological and hydrogeological modelling and interpretation. The accuracy of the bore location coordinates will vary depending on methods used to determine its location and the original purpose for the bore. Although not always the case, resource company drill data are usually more accurately located than groundwater bore data. Due to the expense of drilling and construction, the location of deep groundwater bores is usually better defined than the location of shallow groundwater bores. Bore location accuracy was not assessed as part of the BA.

Most groundwater bores in the Galilee subregion did not have elevation recorded in the database. Elevation data were calculated using the Geoscience Australia, 1-second Shuttle Radar Topography Mission (SRTM) digital elevation model (DEM) (Geoscience Australia, Dataset 19). The locations of most CSG and petroleum wells are formally surveyed, thus elevation data were available from well completion reports. Surveyed bore elevation data were utilised as part of the geological modelling process.

### 2.1.2.2.2 Stratigraphic data from drillholes

Useful stratigraphic information from borehole data includes downhole depths to the top of a stratigraphic interval and thickness of a stratigraphic interval in a bore. To estimate an interval thickness both depths to the top and base of the stratigraphic interval are required. Not all stratigraphic intervals are fully intersected, for instance a bore may be drilled until a target stratigraphic interval is reached.

Of the 7350 bores identified in Section 2.1.2.1.2, some 3301 bores (45%) have a stratigraphic record (Table 4). Of these, stratigraphic records from 2366 bores have data of suitable quality that could be potentially utilised for modelling.

Table 4 demonstrates that the majority of groundwater bores in the Galilee subregion are missing what is considered to be interpretable stratigraphic picks. Many stratigraphic picks from groundwater bores are of limited use due to the records missing from either one or both downhole depth intervals or alternatively the stratigraphic description is difficult to interpret. This is a reflection of the archival nature of the bore databases, as outlined in Section 2.1.2.1.5.1.

Petroleum, CSG and stratigraphic bores with missing stratigraphic picks are either old bores (pre-1970s) or recently drilled wells with data that are still classed as confidential.

Table 5 shows there is considerable variation in depths to top of various major stratigraphic units and thickness encountered by drillholes for major stratigraphic groups in the Galilee subregion. In general, the mean thickness approximates the 50th percentile for stratigraphic formations in the Eromanga Basin (Winton Formation down to the Ronlow beds). The exception is the Ronlow beds, which could be due to the small number of samples available. There is considerably more variation between median percentile and mean thickness for stratigraphic units assigned to the Galilee Basin (Moolayember Formation down to the Joe Joe Group). The difference between the 90th percentile of thickness and the maximum thickness demonstrates that the latter usually represents an extreme value. Extreme values may reflect poor stratigraphic picks (especially in the case of surficial sediments) or natural variation of units intercepted by sparse deeper drilling data. The lower units of the Galilee Basin sequence are known to infill extreme topography and the resultant high variability could readily account for such statistics. Table 5 also provides a summary of drillhole data available for various geological formations.

**Table 4 Number of bores and stratigraphic record data from bore databases for the Galilee subregion**

| Bore type | Number of bores in subregion | Number of bores with a stratigraphic record | Number of bores with an interpretable stratigraphic record | Number of bores that fully intersected a stratigraphic unit |
|---|---|---|---|---|
| Groundwater | 7029 | 3064 | 2133 | 576 |
| Petroleum, CSG, stratigraphic | 321 | 237 | 233 | 212 |
| **Total** | **7350** | **3301 (45%)**[a] | **2366 (32%)**[a] | **788 (11%)**[a] |

[a]percentage of total number of bores in Galilee subregion
CSG = coal seam gas
Data: Bioregional Assessment Programme (Dataset 8)

**Table 5 Statistics on bore intercepts for stratigraphic units in the Galilee subregion**

| Stratigraphic sequence | Stratigraphic unit | Bioregional Assessment unit | Number of bores fully intercepting a unit | Minimum depth below surface (m) | Maximum depth below surface (m) | Minimum thickness (m) | Maximum thickness (m) | Mean thickness (m) | 10th percentile of unit thickness (m) | 50th percentile of unit thickness (m) | 90th percentile of unit thickness (m) |
|---|---|---|---|---|---|---|---|---|---|---|---|
| Cenozoic | Alluvium | Cenozoic | 138 | 0 | na | 0 | 55 | 8 | 1 | 6 | 18 |
| Cenozoic | Cenozoic Sediments | Cenozoic | 85 | 0 | 6 | 2 | 90 | 25 | 7 | 23 | 37 |
| Eromanga Basin | Winton Formation | Winton-Mackunda | 94 | 0 | 149 | 5 | 681 | 269 | 63 | 267 | 480 |
| Eromanga Basin | Mackunda Formation | Winton-Mackunda | 119 | 0 | 713 | 5 | 341 | 107 | 34 | 107 | 170 |
| Eromanga Basin | na | Winton-Mackunda (all units) | 148 | 0 | 149 | 10 | 817 | 253 | 41 | 212 | 549 |
| Eromanga Basin | Allaru Mudstone | Rolling Downs Group aquitard | 236 | 0 | 844 | 2 | 388 | 158 | 26 | 165 | 273 |
| Eromanga Basin | Toolebuc Formation | Rolling Downs Group aquitard | 263 | 0 | 1050 | 1 | 70 | 14 | 4 | 10 | 27 |
| Eromanga Basin | Wallumbilla Formation | Rolling Downs Group aquitard | 385 | 0 | 1068 | 1 | 665 | 196 | 58 | 191 | 296 |
| Eromanga Basin | na | Rolling Downs Group aquitard (all units) | 402 | 0 | 844 | 1 | 597 | 292 | 77 | 284 | 488 |
| Eromanga Basin | Wyandra Sandstone Member | Cadna-owie – Hooray | 79 | 39 | 1314 | 2 | 52 | 18 | 6 | 16 | 31 |
| Eromanga Basin | Cadna-owie Formation | Cadna-owie – Hooray | 183 | 0 | 1366 | 5 | 208 | 56 | 19 | 48 | 94 |
| Eromanga Basin | Hooray Sandstone | Cadna-owie – Hooray | 246 | 0 | 1396 | 3 | 320 | 79 | 20 | 69 | 138 |
| Eromanga Basin | na | Cadna-owie – Hooray (all units) | 265 | 0 | 1351 | 5 | 419 | 116 | 34 | 103 | 206 |

| Stratigraphic sequence | Stratigraphic unit | Bioregional Assessment unit | Number of bores fully intercepting a unit | Minimum depth below surface (m) | Maximum depth below surface (m) | Minimum thickness (m) | Maximum thickness (m) | Mean thickness (m) | 10th percentile of unit thickness (m) | 50th percentile of unit thickness (m) | 90th percentile of unit thickness (m) |
|---|---|---|---|---|---|---|---|---|---|---|---|
| Eromanga Basin | Westbourne Formation | Injune Creek Group | 219 | 0 | 1526 | 3 | 214 | 82 | 27 | 89 | 128 |
| Eromanga Basin | Adori Sandstone | Injune Creek Group | 193 | 0 | 1624 | 5 | 137 | 31 | 12 | 25 | 62 |
| Eromanga Basin | Birkhead Formation | Injune Creek Group | 209 | 0 | 1657 | 2 | 275 | 89 | 36 | 80 | 151 |
| Eromanga Basin | na | Injune Creek Group (all units) | 233 | 0 | 1526 | 14 | 468 | 163 | 62 | 135 | 283 |
| Eromanga Basin | Hutton Sandstone | Hutton Sandstone | 175 | 0 | 1725 | 10 | 299 | 134 | 80 | 135 | 203 |
| Eromanga Basin | Ronlow beds | Ronlow beds | 9 | 0 | 402 | 47 | 225 | 124 | 66 | 97 | 220 |
| Eromanga Basin | na | Precipice–Evergreen | 74 | 0 | 1876 | 7 | 189 | 77 | 19 | 78 | 116 |
| Galilee Basin | Moolayember Formation | Moolayember Formation | 92 | 0 | 1685 | 8 | 717 | 175 | 17 | 122 | 409 |
| Galilee Basin | Clematis Group | Clematis Group | 97 | 0 | 1962 | 13 | 394 | 94 | 33 | 80 | 163 |
| Galilee Basin | Dunda beds | Rewan Group | 11 | 0 | 1079 | 12 | 223 | 83 | 50 | 71 | 124 |
| Galilee Basin | Rewan Group | Rewan Group | 82 | 0 | 1309 | 9 | 389 | 160 | 22 | 157 | 325 |
| Galilee Basin | na | Rewan Group (all units) | 83 | 0 | 1079 | 9 | 449 | 169 | 22 | 159 | 336 |
| Galilee Basin | Betts Creek beds | Upper Permian coal measures | 78 | 0 | 1634 | 15 | 215 | 131 | 76 | 137 | 175 |
| Galilee Basin | Bandanna Formation | Upper Permian coal measures | 58 | 0 | 2013 | 2 | 161 | 58 | 21 | 44 | 116 |
| Galilee Basin | Black Alley Shale | Upper Permian coal measures | 25 | 15 | 2033 | 11 | 96 | 41 | 22 | 38 | 58 |

| Stratigraphic sequence | Stratigraphic unit | Bioregional Assessment unit | Number of bores fully intercepting a unit | Minimum depth below surface (m) | Maximum depth below surface (m) | Minimum thickness (m) | Maximum thickness (m) | Mean thickness (m) | 10th percentile of unit thickness (m) | 50th percentile of unit thickness (m) | 90th percentile of unit thickness (m) |
|---|---|---|---|---|---|---|---|---|---|---|---|
| Galilee Basin | Peawaddy Formation | Upper Permian coal measures | 16 | 0 | 1366 | 14 | 198 | 63 | 24 | 45 | 121 |
| Galilee Basin | Colinlea Sandstone | Upper Permian coal measures | 39 | 0 | 1709 | 11 | 123 | 49 | 14 | 37 | 102 |
| Galilee Basin | | Upper Permian coal measures (all units) | 121 | 0 | 1634 | 5 | 282 | 124 | 63 | 129 | 180 |
| Galilee Basin | Aramac Coal Measures | Joe Joe Group | 48 | 490 | 1600 | 18 | 272 | 106 | 38 | 87 | 194 |
| Galilee Basin | Jochmus Formation | Joe Joe Group | 36 | 55 | 1872 | 17 | 1028 | 276 | 37 | 239 | 481 |
| Galilee Basin | Edie Tuff member | Joe Joe Group | 24 | 878 | 1499 | 4 | 214 | 53 | 13 | 29 | 124 |
| Galilee Basin | Jericho Formation | Joe Joe Group | 39 | 44 | 2091 | 53 | 730 | 305 | 125 | 226 | 598 |
| Galilee Basin | Oakleigh Siltstone member | Joe Joe Group | 11 | 492 | 2176 | 46 | 167 | 110 | 69 | 113 | 154 |
| Galilee Basin | Lake Galilee Sandstone | Joe Joe Group | 6 | 5 | 2734 | 20 | 287 | 185 | 53 | 227 | 275 |
| Galilee Basin | na | Joe Joe Group (all units) | 54 | 5 | 1600 | 25 | 1807 | 420 | 119 | 284 | 786 |
| Galilee subregion geological basement | Basement | Basement | 103 | na | 3732 | na | na | Na | na | na | na |

Basement represents the base of the Galilee subregion, thus statistics on thickness and number of bores that fully intercept a unit cannot be computed.
na = not applicable
Data: Bioregional Assessment Programme (Dataset 8)

### 2.1.2.2.3 Structure

Regional-scale structures identified from historical geological mapping (Table 3), drill data and geophysical surveys are shown in Figure 11. Geological subsurface mapping (Section 2.1.2.2.5; Moya et al., 2015), suggests that disruption and modification of Galilee subregion sequences can occur across some of the large-scale faults and folds. More local-scale faults are apparent on some of the maps presented in Section 2.1.2.2.5.3 (e.g. Figure 22, Figure 27).

Aside from regional structures on published maps, finer-scaled structuring is also evident in the geophysics (Figure 8). Some of these structures are the focus of ongoing research (e.g. the Thomson Orogen and Cork Fault; see Spampinato et al., 2015a, 2015b, 2015c for further detail). A proportion of finer-scale features evident in Figure 8 may only affect geological basement rocks, which underlie Galilee Basin sedimentary rocks. The effect these have on overlying Galilee and Eromanga basins is not always apparent due to the density of drillhole data and the distribution and quality of available seismic line data (Figure 6). However, it is likely that ongoing research will uncover further structures that significantly modify Galilee subregion stratigraphy (e.g. Moya et al., 2015).

Environmental impact statements (EISs) from recent publicly available coal mine development proposals include only limited information on mine-scale geological features such as faults. Some information gleaned from recent reports is as follows:

- Hyde Park: associated with a synclinal fold structure near Galilee Basin margin. Bedding dips 0.5 to 2° west (Saul et al., 2015)
- China Stone: bedding dip varies from north to south ranging from 3 to 6° south-west. A north-north-west trending normal fault, approximately 18 km long with down throws to the east of up to 100 m is present in the northern sections of the mine complex (AGE Consultants Pty Ltd, 2015). This fault offsets the coal seams and has enough displacement to juxtapose Clematis Group sedimentary rocks against Rewan Group sedimentary rocks. The fault runs sub-parallel to nearby regional-scale structures (e.g. Mingobar Monocline) that are situated to the east along the margin of the Galilee subregion (Figure 11)
- Carmichael: four east trending faults with throws in the order of 20 to 40 m were noted in the upper Permian coal measures (GHD, 2013). These faults would have a similar trend to some lineaments present in aeromagnetics data, in the vicinity of the Carmichael development. Bedding dip ranges from 2 to 6° west
- Kevin's Corner and Alpha coal projects: some small-scale faulting was identified in drill core and minor south-west trending faults have been identified outside the mine development area. However, there is little evidence to indicate the presence of larger-scale folds or faults or that the groundwater flow regime was been influenced by more regional-scale structures (URS, 2012a, 2012b). Bedding dips 1 to 2° west.

#### *2.1.2.2.3.1 Regional-scale features in the Galilee subregion*

The Galilee subregion is of the same outline and extent as the geological Galilee basin. The margins of the present-day Galilee Basin are a consequence of erosion and structural control (Figure 11, Figure 29). Isolated erosional remnants that consist of Galilee Basin sedimentary rocks occur to the east of the present-day Galilee Basin boundary. These demonstrate that the basin once had greater extents (Saul et al., 2015).

The main geological features associated with the Galilee Basin are:

**Maneroo Platform**

The western extent of the Galilee subregion and the northern Galilee Basin is partly fault-bounded against the Maneroo Platform (Figure 11). This platform region occurs where overlying Eromanga Basin rests directly on geological basement. The Maneroo Platform was essentially a north–south basement high throughout most deposition of the Galilee Basin, making the basin essentially U-shaped in configuration. Both north-eastern and south-eastern sides of the Maneroo Platform are partly fault bounded. The Hulton-Rand Structure effectively acted as a margin to the basin throughout much of the Permian. The Hulton-Rand and Tara structures were intermittently active through the Mesozoic and Cenozoic (Norvick, 1981). The structural fabric within the platform area is north-trending (Figure 6) north of the Hulton-Rand Structure; the north-eastern margin of the platform comprises a series of north-trending half-grabens where the faults have been reactivated at various times during development of the basin (Figure 11, Figure 32)

**Canaway Ridge**

The Canaway Ridge (Figure 11) is a basement high bounded by the Canaway Fault on its eastern side. It is the boundary between the Cooper and Galilee basins. For a short period during the Late Permian, sedimentation was continuous across this barrier. There was no fault activity during deposition of the Eromanga sequence during the Jurassic to Early Cretaceous, but the ridge was reactivated in the Late Cretaceous to Paleogene with displacement up to 400 m (Ransley et al., 2012).

**Nebine Ridge**

The Nebine Ridge (Figure 11) is a south-south-west plunging basement high extending south from the exposed Anakie Inlier. This ridge is the demarcation between the south-eastern Galilee Basin and the Bowen Basin to the east, as well as the demarcation between the overlying Eromanga Basin and the Surat Basin to the south-east.

**Barcaldine Ridge**

The Barcaldine Ridge forms the boundary between the northern and southern sections of the Galilee Basin. In the Galilee Basin sequence (Figure 32b) this feature is manifested as a drape fold over a basement ridge (Casey, 1970). The ridge extends from the eastern corner of the Maneroo Platform near the town of Barcaldine (in companion product 1.1 for the Galilee subregion (Evans et al., 2014)) and descends eastwards towards the southern limit of the Koburra Trough (Figure 11). The relative influence and prominence of this feature varied considerably during deposition of the Galilee Basin sequences and overlying Eromanga Basin. Spurs off this feature that run into the southern Galilee Basin were uplifted and eroded in the Triassic.

#### *2.1.2.2.3.2 Northern section of the Galilee Basin*

**Koburra Trough**

Also known as the Aberfoyle Syncline, this elongate depocentre (Figure 11) aligns with the eastern margin of the northern Galilee Basin, trending northwards from near the Barcaldine Ridge, then north-north-westwards towards, but short of, Hughenden. The Koburra Trough is 300 km long on its north-west axis and 100 km across (Allen, 1974). The north-eastern margin of the trough is structurally defined as a fold or monocline above eastward-dipping thrust faults (White Mountains Structure, Mingobar Structure).

**North Galilee Rise**

A broad gentle rise in basement extends from the eastern end of the Barcaldine Ridge north-westwards to the Wetherby Terrace and is informally named the 'North Galilee Rise'. This feature creates a subtle divide between the Koburra Trough and the Aramac Depression and other features found along the western margin adjacent to the Maneroo Platform (Figure 8, Figure 11).

**Aramac Depression**

The Aramac Depression is a relatively subdued equant-shaped feature (Figure 11) with a depocentre close to the Hulton-Rand Structure near the margin of the Maneroo Platform. The depression is contained to the north by the Maranthona Monocline, and to the south by the Barcaldine Ridge. Eastwards it shallows slightly onto the North Galilee Rise in basement which then descends as the western flank of the Koburra Trough.

**Lovelle Depression**

Found to the north and west of the Maneroo Platform (Figure 11), this depocentre lies predominantly on the north-western side of a deep narrow basement ridge, the Cork Block-Elderslie Ridge. Towards the south-western extent of the Lovelle Depression, the Galilee sequence descends south-eastwards from this prominent structure. This region remains poorly understood because of an absence of seismic and drillhole data.

**Cork Fault and Holberton Structure**

The Cork Fault and its south-western continuation the Holberton Structure comprise a major tectonic feature within the Australian continent as part of the Tasman Line demarcating the North Australian Craton from the Thomson Orogen. The Cork Fault is part of a pervasive fault complex within the Lovelle Depression, and is the southern-eastern faulted margin of the narrow Cork Block. At its south-western extent in the Lovelle Depression, the Permian sequence over this fault is downthrown to the north-west in the same sense and magnitude as the paralleling Holberton Structure (Harrison and Bauer, 1976). The Cork Fault was active as a strike-slip fault system in the Neoproterozoic, and was repeatedly reactivated in the Paleozoic (Spampinato et al., 2015b). In the early Permian, the fault was active during subsidence in the Lovelle Depression, and experienced reactivation in the Cenozoic with an overall 420 m of displacement (Ransley et al., 2012). This margin of the Galilee Basin is poorly constrained due to insufficient well data and limited seismic control.

**Elderslie Ridge and Cork Block**

The south-west-oriented Cork Block in the Lovelle Depression is a narrow ridge (Figure 11) that has faulted margins defined by the Holberton Structure and the Cork Fault. The ridge is continuous north-eastwards into the Elderslie Ridge where the Wetherby Structure is a north-north-eastward trending bifurcation of the fault on the north-western margin of this ridge. To the south-west, the displacement sense changes on these faults, and the Cork Block transitions to a terrace.

**Wetherby Terrace**

The wedge-shaped Wetherby Terrace lies between the bifurcation of the Wetherby Structure and the Elderslie Ridge and has a gentle plunge to the south (Figure 8, Figure 11).

**Hulton-Rand Structure**

The Hulton-Rand Structure is located along the south-eastern margin of the Maneroo Platform. At depth it is a fault that demarcates part of the western margin of the Galilee Basin. It transitions from a fault at depth to a monoclinal fold structure at surface (Figure 11, Figure 30). This structure acted as a barrier to sedimentation during the late Paleozoic and Mesozoic eras.

**Beryl Ridge, Darriveen Fault and Maranthona Monocline**

Along the north-eastern margin of the Maneroo Platform, north-west of the Aramac Trough, are a series of north-trending half-grabens formed in basement (Figure 11). The Beryl Ridge is a northward-plunging drape fold (Casey, 1970) over a basement ridge that extends northwards off the Maneroo Platform. The Darriveen Fault demarcates the margin of another half-graben. The Maranthona Monocline is another drape fold over a half-graben in basement, and lies between the Darriveen Fault to the north and the Hulton-Rand Structure to the south.

**Mingobar Structure, White Mountains Structure and Belyando Structure**

The White Mountains Structure (Figure 11) is a distinct structural discontinuity on the north-eastern margin of the Galilee Basin and demarcates an abrupt contact of Galilee Basin rocks with underlying basement. The White Mountains Structure, although of different structural expression to the Mingobar Structure, is continuous along strike from where the Mingobar Structure and the Hopkins Thrust appear to converge. The Mingobar Structure is a linear topographic high situated on the margin of the Galilee Basin. It is associated with a west-dipping monoclinal fold and, at depth, thrust faults (Pinchin, 1978). The Belyando Structure was defined as an intense gravity depression on the eastern margin of the Galilee Basin and is co-linear with the Mingobar Structure (Vine, 1965). The more recently defined Belyando Basin (Draper, 2013) occurs in the same area, and there may be some association with the earlier defined Belyando Structure.

**Moocha-Nogoa Structure**

It is possible that a new semi-regional structure, here informally called the Moocha-Nogoa Structure (Figure 12 for location), has been identified as part of the BA for the Galilee subregion. This feature passes through Moocha Creek to the north and the Nogoa Scarplands to the south. Further detail on Nogoa Scarplands can be found in Section 1.1.2.1.1 of companion product 1.1

(Evans et al., 2014)). At surface the Moocha-Nogoa Structure approximates the western margin of a series of ranges that occur where sedimentary rocks of Jurassic age outcrop along the eastern margin of the Eromanga Basin. The structure is expressed at surface as a relict Cenozoic duricrusted surface that bears a gentle westward regional tilt. In its regional arcuate course, the Moocha-Nogoa Structure appears to have similar trends to structures identified along the eastern margin of the Galilee subregion (e.g. Mingobar Structure, White Mountains Structure).

Unsurprisingly, at depth, the Moocha-Nogoa Structure also coincides with the inferred western margins of the underlying Drummond and Belyando basins (Figure 12). The Moocha-Nogoa Structure is interpreted to represent the surface expression of an inferred thrust fault that occurs at depth, and its apparent topographic effect implies reactivation in the Cenozoic with uplift associated with the formation of the Great Dividing Range and erosion of the overlying Eromanga sequence.

#### *2.1.2.2.3.3 Southern section of the Galilee Basin*

The southern Galilee Basin is complicated structurally due to structure inherited from the Adavale Basin, which almost entirely underlies the Powell Depression.

**Powell Depression**

This depression flanks the south-eastern side of the Maneroo Platform, and a thin Galilee sequence deepens south-westwards in a stepped manner from the Barcaldine Ridge, over the Fairlea Anticline/Blackall Ridge and the Grey Range Fault towards the Canaway Ridge (Figure 11). Between the Fairlea Anticline and the Grey Range Fault, the circular Talundilly Structure of some 95 km diameter, contains a brecciated, faulted and disturbed sequence in the Jurassic and Cretaceous sequence of the Eromanga Basin, and presumably in basement rocks. Its origin has been ascribed to a bolide impact at about 125 Ma, during Cadna-owie Formation deposition (Longley, 1989).

**Pleasant Creek Arch**

The Pleasant Creek Arch is a major north-east-trending structure in the underlying Adavale Basin, and flanks the south-eastern side of the Powell Depression (Figure 11). Aligned above the arch is the Warrego Fault. Paralleling these features to the north-west are the Cothalow and Carlow arches. Collectively these arches and the Warrego Fault mark a change south-eastwards in structural style to half-grabens that are aligned north-north-east in the underlying Adavale Basin. In the overlying thin Galilee sequence and thicker Eromanga sequence, this structure has expression as gentle folding in the Noella, Woolga and Biddenham synclines, and Ward River Anticline, which is mapped to the north-east as the Birkhead Anticline.

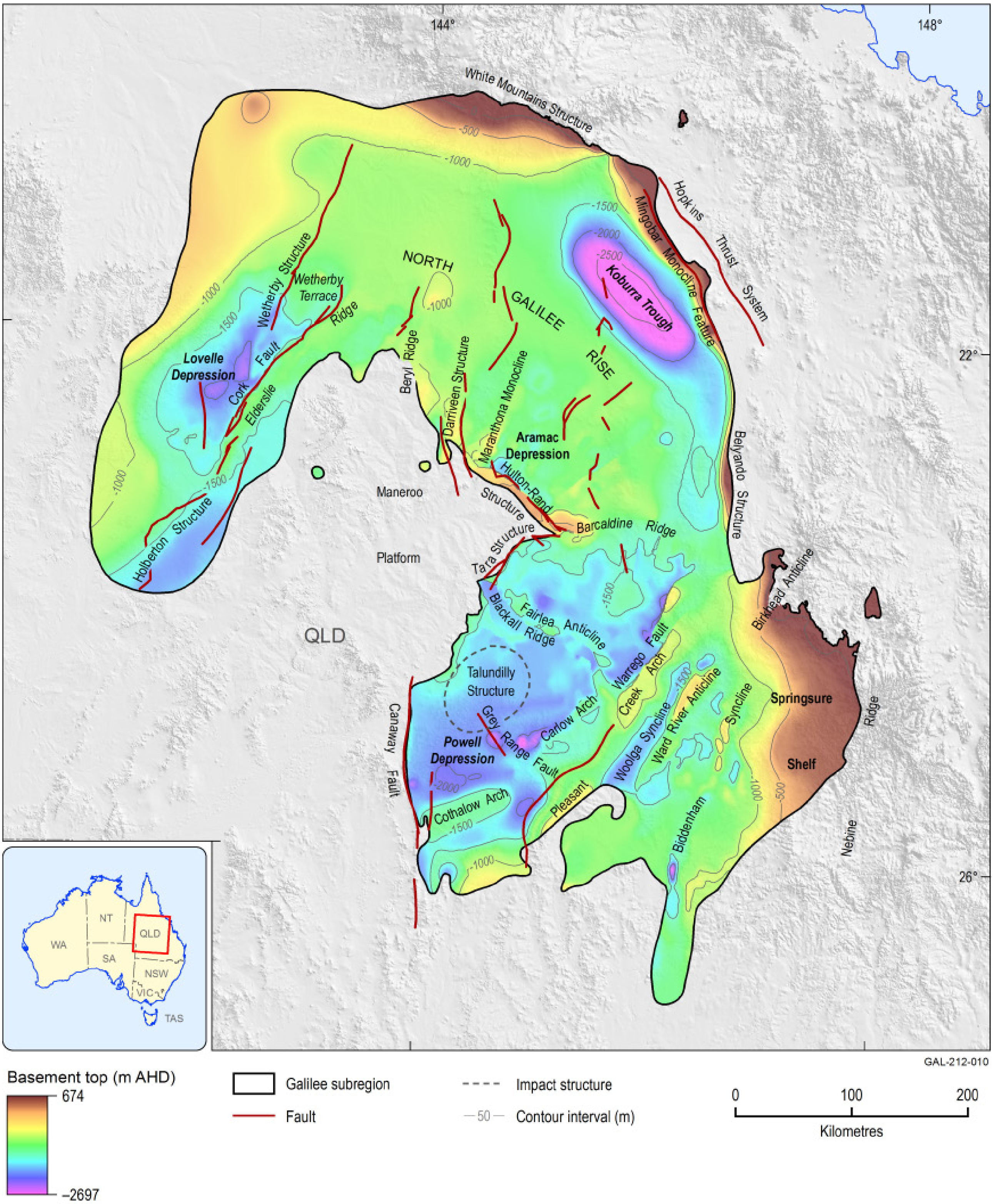


**Figure 11 Significant structures in the Galilee subregion superimposed on basement to the Galilee Basin**

Data: Bioregional Assessment Programme (Dataset 13)

**Tara Structure**

The Tara Structure is located along the south-eastern margin of the Maneroo Platform (Figure 11) that is similar in nature to the Hulton-Rand Structure. At depth it is a fault that grades upward to a monocline at the surface (Casey, 1970). The Tara Structure acted as a barrier to sedimentation during the Late Paleozoic and Triassic eras.

**Springsure Shelf**

The Springsure Shelf is located north-west of the Nebine Ridge and is a transitional zone in the southern Galilee Basin with the Denison Trough of the Bowen Basin to the east.

#### *2.1.2.2.3.4 Geological basement features for the Galilee subregion*

Geological basement includes any rocks that are older than the Late Carboniferous–Middle Triassic Galilee Basin. Geological basement includes any older sedimentary basins, as well rocks assigned to the Thomson Orogen and Mount Isa Inlier. The boundary between Thomson Orogen and Mount Isa Inlier (a part of the North Australia Craton) is demarcated by Cork Fault and Diamantina River Domain (Figure 12).

In the eastern part of the subregion, the Thomson Orogen is partly covered by the Adavale and Belyando basins (Devonian in age) and the Late Devonian–Early Carboniferous Drummond Basin. The age of the Millungera Basin is relatively unknown, but it has to be younger than the North Australia Craton as it overlies it, but older than the Galilee Basin. Collectively, all these geological elements form the geological basement to the Galilee and Eromanga basins. Further information on geological elements that underlie the Galilee Basin is outlined in companion product 1.1 for the Galilee subregion (Evans et al., 2014).

Understanding the potential for hydraulic connectivity between Galilee Basin strata and underlying basement rocks is speculative as the hydrological properties of geological basement are poorly known. However, it is probable that fracture permeability would be the only effective permeability in rocks assigned to the Thomson Orogen, Mount Isa Orogen and the Diamantina River Domain (Figure 12). Fractures are more likely to occur near faults. How permeable a fault or a fracture is at depth is dependent on several factors including: the amount of fault offset, type of fracture infill, and the orientation of a fracture relative to the present-day stress field.

Other potential areas of enhanced structural connectivity may occur where fault bound blocks of basement rocks are fractured, uplifted and juxtaposed against Galilee Basin or Eromanga Basin sedimentary rocks. In the Galilee subregion these areas principally occur along major faults located around the margin of the Maneroo Platform, the Barcaldine Ridge, the Lovelle and Powell depressions and the Warrego Fault.

Another area of potential connectivity between Galilee Basin sediments and underlying basement may be where the Lake Galilee Sandstone overlies older sedimentary basins such as the Drummond Basin. There may also be some structural control on the distribution of Lake Galilee Sandstone as its western margin approximates the edge of the Drummond Basin, the Belyando Basin and the Moocha-Nogoa Structure (Figure 12).

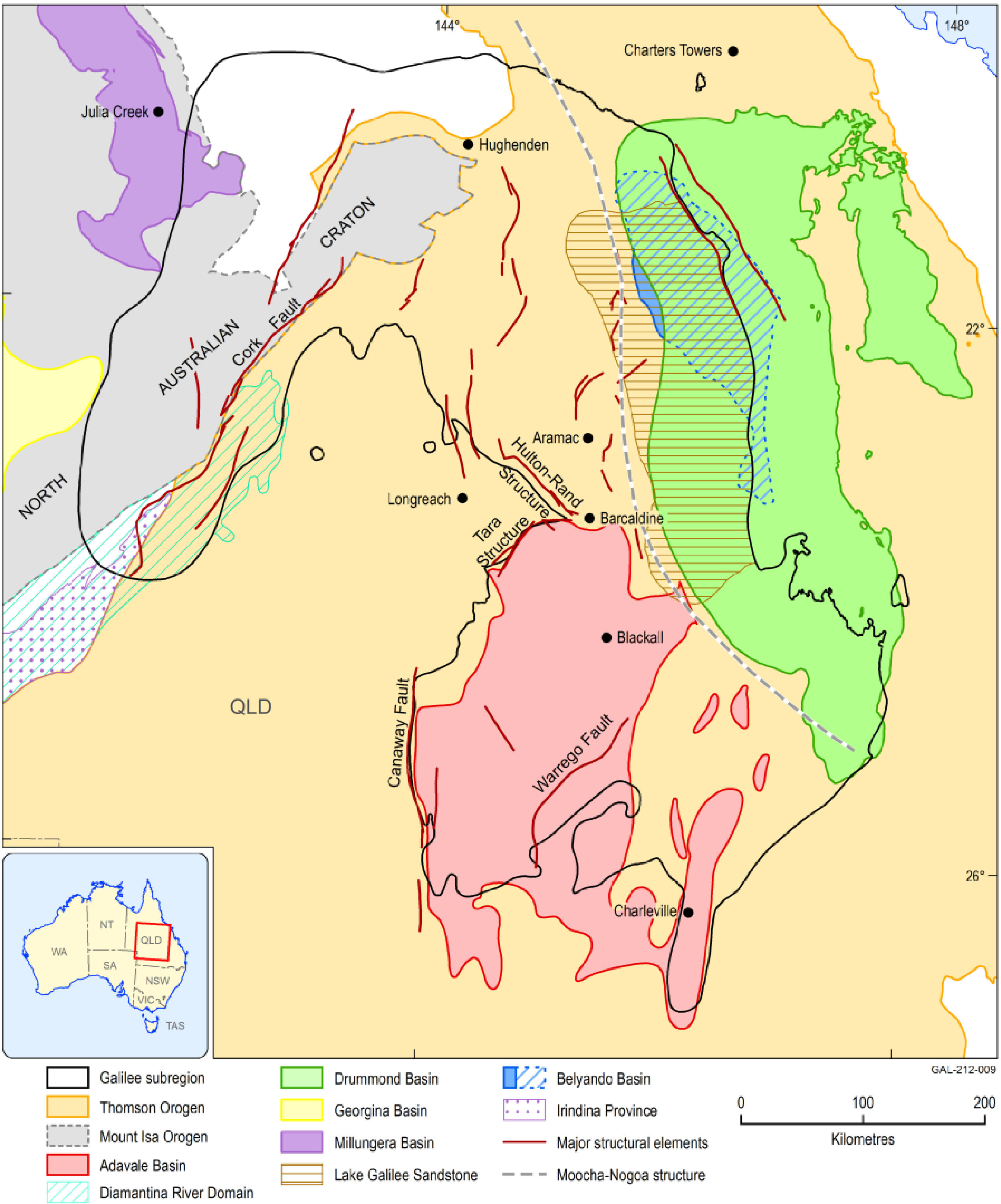


**Figure 12 Underlying geological features that comprise parts of the basement for the Galilee subregion**

Data: Geoscience Australia (Dataset 14), Bioregional Assessment Programme (Dataset 15)

### 2.1.2.2.4 Galilee subregion geological model

This model was developed to be the basis of groundwater modelling and also as a way to present and understand regional geology for the Galilee subregion. The Galilee subregion geological model was developed as a composite of stratigraphic surfaces that were derived from two different approaches. Surfaces for the Galilee Basin sequence were generated in a basement-upwards approach. Surfaces for the overlying Eromanga Basin sequence and uppermost Cenozoic cover were largely adopted from the GAB Atlas (Ransley et al., 2015) and surface elevations were generated from the ground surface downwards.

These contrasting approaches were necessitated by the severely limited borehole data available for the Galilee Basin sequence. To enable extension of this data, existing seismic interpretations were combined with the Phanerozoic basement model OZ SEEBASE (de Vries et al., 2006). This OZ SEEBASE basement surface was itself developed around control offered by very limited borehole data, and extended regionally with the integration of both seismic data available as of 2006, and basement depth estimates modelled from potential field data (gravity and total magnetic intensity).

#### *2.1.2.2.4.1 Galilee Basin geological surfaces*

The Galilee Basin geological surfaces as described in Section 2.1.2.2.5.3 were generated at a semi-regional scale. While the accuracy of each geological surface will vary depending on the density and quality of various datasets, overall the reliable resolution is probably in the order of 1:500,000.

**Datasets**

The Galilee Basin geological model was built entirely from public domain datasets – namely drilling records from petroleum wells and groundwater bores, regional geological mapping, 1-second DEM, regional seismic reflection surveys and OZ SEEBASE.

A brief description of each dataset follows.

- *bores and wells*. (Queensland Department of Natural Resources and Mines, Dataset 16; Geological Survey of Queensland, Dataset 17). All groundwater bores (Queensland Department of Natural Resources and Mines, Dataset 16) and petroleum wells (Geological Survey of Queensland, Dataset 17) within 25 km of the Galilee Basin subregion were included in the project. Well and bore data were used to define the top and bottom of each formation as well as its extent. Stratigraphy was determined from well completion reports (WCR) and drillers' logs. Where naming conflicts existed, a standard nomenclature was developed for the Galilee Basin. Additionally, where generic names were used in the WCR, such as 'undifferentiated Permian', drilling logs and geophysical logs were used to discern the target formations. Depth to formation was converted to metres above the Australian Height Datum (m AHD) by subtracting the height of the drilling rig datum as shown in the well completion report (WCR) by the depth to formation. Where drilling rig datum was not available, height was obtained from the 1-second DEM plus 2 m to represent height of the drilling rig datum. Once a complete dataset of wells and bores was available for each formation, additional quality assurance and quality control was performed on the data to find anomalous wells and bores (i.e. wells and bores with improbable depth to formation). The cause of an anomaly was commonly due to not converting feet to metres or a misidentification of a geologic unit. If the anomaly could not be resolved, then the well or bore was removed from the dataset.

- *published geological maps* (Queensland Department of Natural Resources and Mines, Dataset 18). Outcropping areas of the target formations were chosen from geographical information system (GIS) coverage of Queensland geology and were used to create outcrop maps for each formation. The subsurface well data were used to define the extent of each formation. Subsurface intercepts of the top of each unit were corrected for DEM or kelly bush height to generate the top surface of the formation relative to Australian Height Datum (AHD). The kelly bush is the part of the petroleum drilling rig that connects the drill rods to the rotary table, which in turn rotates the drilling rods during drilling. Drilling depth measurements from petroleum rigs commonly reference the kelly bush rather than ground level.
- *DEM* (Geoscience Australia, Dataset 19). A 1-second DEM was used to determine the ground elevation for wells and bores and also as a proxy for the formation tops where it was outcropping. This dataset offers the highest resolution of topography currently available to cover the entire Galilee subregion.
- *seismic surfaces* (Queensland Department of Natural Resources and Mines, Dataset 20). Two prominent seismic surfaces, bottom of the Galilee Basin and top of the upper Permian coal measures, were chosen from Y80A, W81A, Carmichael, Pendine, T81A, Quilpie, Ward and Powell Creek seismic reflection surveys. Maps from the surveys were georectified and then depth and structures were digitised. The original gridded data for seismic horizon mapping was not available, therefore a velocity model derived from petroleum well check shot surveys could not be built. Depth conversion instead relied on using well and bore depths to convert time contours to depth contours.
- *OZ SEEBASE* (FROGTECH Pty Ltd, Dataset 21). The depth to magnetic basement model, OZ SEEBASE (de Vries et al., 2006), was used as an interpretive template to guide the location and trend of basement structures in areas that were otherwise not covered by available seismic interpretation. However, it must be emphasised that the OZ SEEBASE basement model was limited to pre-2006 data and utilised total magnetic intensity (TMI) data of poorer resolution than available as of 2016. Additionally, this modelled surface represents the magnetic basement. This can be generally assumed to be base Phanerozoic; however, thick Proterozoic basins are known to underlie the north-west of the subregion and magnetic basement would underlie these older basins as well.

##### *2.1.2.2.4.2 Components of the Galilee Basin geological model*

The Galilee geological model was initially developed separately, built from the interpreted basement upwards.

In the Galilee Basin sequence, the top of each stratigraphic unit became the base/container for the overlying unit. Because of the depth of the base of the Galilee Basin (up to 3000 m), a bottom-up approach was initially thought to more accurately portray basement structures and their role in determining depositional centres and groundwater flow direction.

Broadly, there are three components for each stratigraphic unit in the geological model: depth to top/bottom of the unit, stratigraphic unit extent and the influence of faults and basement structure.

**Depth to top/bottom of stratigraphic unit**

While being an essential control, low-density drillhole data are inadequate to represent the spatial complexity of stratigraphic units. In the Galilee Basin geological model, these well intercepts were supplemented by contours derived from interpreted seismic imagery and OZ SEEBASE. The rationale is that the base of the formation (the container) will influence depositional processes and the geometry of the formation above it. Contours from the base of the formation were copied and modified based on well and bore data to represent the top of formation.

Where the component formations of a stratigraphic unit outcropped along the eastern margin of the Galilee Basin, the top of the formation was considered the same as the DEM.

**Stratigraphic unit extent**

The Galilee geological model tried to represent the complexities of the Galilee Basin geology including erosional holes and variable thickness as influenced by deposition, erosion and structure.

On the eastern margin of the Galilee Basin the extent of the stratigraphic units is the same as the outcrop of component formations, as shown in the surface geology. Elsewhere the stratigraphic unit extent and thickness were determined from well and bore data and seismic interpretation. The surface of the unit is guided by the presence of basement structures as evident in seismic imagery and the OZ SEEBASE surface.

**Faults and basement structures**

Faults and basement structures are important parts of the Galilee Basin geological model. They were derived from OZ SEEBASE and seismic surfaces. Underlying structures were extrapolated upwards to overlying units if their influence could be identified in the well and bore data.

**Building the Galilee Basin geological surfaces**

The Galilee Basin geological model was built using the ArcGIS tool 'Topo to Raster', which produced a raster surface of the top of each unit with a cell size of approximately 1 km. The metadata has full details of the inputs for each formation.

Generalised input data were wells, bores, unit specific contours, DEM contours for outcrop and faults (as cliffs). The resulting surface was then clipped by the unit extent to produce a model of the top of unit.

Overlying surfaces were then checked against underlying surfaces and iterative changes to input data were made to ensure that model layers do not interpenetrate.

Each formation in the Galilee Basin geological model has a top, bottom and thickness. The exception is the geological basement model as it represents the base of the whole modelled domain.

#### 2.1.2.2.4.3 Combined Eromanga-Galilee three-dimensional geological model

The three-dimensional geological model for the Galilee subregion is the summed combination of the basal Galilee Basin geological model and a model of surfaces for the Cenozoic cover and Eromanga Basin sequence.

This combined model builds the entire sequence from the ground surface downwards as the ground surface is the most accurately known surface available from the 1-second DEM. This contrasts the bottom-up approach initially used for the geological model of the Galilee Basin sequence.

The top-down approach used thickness maps from the GAB Atlas datasets (Ransley et al., 2015). These thicknesses (isopach maps) were built from lithostratigraphic data from extensive datasets of shallower groundwater bores, and deeper stratigraphic and exploration wells.

The poorest-constrained thickness map in this approach to the upper sequence is that of the Cenozoic. While there is adequate estimation of the Paleogene-Neogene component of Cenozoic cover, estimates of the thickness of the uppermost Quaternary alluvium/colluvium are the least reliable. Although error margins in estimation of this uppermost Cenozoic cover will be in the order of tens of metres, this magnitude is relatively minor – an order of magnitude less compared to the error of estimation of the base Galilee Basin where error margins can be in the order of hundreds of metres where seismic and drillhole data are absent. In data poor areas, error in depths to top of geological features such as formation tops is likely to increase with depth.

The difference between the two models in predicting basement to the Galilee Basin, from between the bottom-up approach (Galilee Basin geological model) and top-down approach (combined Cenozoic-Eromanga-Galilee surfaces), is used as a measure of prediction uncertainty in the overall three-dimensional model for the Galilee subregion (Figure 29). This is discussed below.

The Cenozoic-Eromanga Basin geological model is derived from the GAB Atlas (Ransley et al., 2015; Geoscience Australia, Dataset 22, Dataset 23, Dataset 24, Dataset 25, Dataset 26, Dataset 27, Dataset 28, Dataset 29, Dataset 30, Dataset 31) and consists of isopach data of hydrostratigraphic packages that have been converted to their equivalent grouped lithostratigraphic units: the Paleogene- Neogene Cover, Winton-Mackunda aquifer (Winton and Mackunda formations), Rolling Downs Group aquitard (Wallumbilla Formation, Toolebuc Formation, Allaru Mudstone), Cadna-owie – Hooray aquifer and equivalents (Cadna-owie Formation, Hooray Sandstone, Blantyre Sandstone, and part of the Ronlow beds), the Westbourne aquitard (Westbourne Formation), Adori-Springbok aquifer (Adori Formation), Birkhead-Walloon aquitard (Birkhead Formation), Hutton aquifer (Hutton Sandstone), Evergreen-Poolowanna aquitard (Evergreen Formation) and Precipice Sandstone aquifer (Precipice Sandstone and equivalents). The isopach data were converted to raster surfaces of thickness using ArcGIS and the 'Topo to Raster' tool and then clipped to geological extent. Stratigraphic sequences of the Cenozoic cover and Eromanga Basin were then combined with stratigraphic sequences of the Galilee Basin.

To produce the top and bottom of each formation, the thickness of each layer was subtracted from the bottom of the layers above it, starting with the surface and working downwards.

Once a raster surface (top and bottom) for each formation of the Eromanga-Galilee three dimensional geological model was completed, the rasters were converted into a triangular irregular network model (TIN) by using the 'From Raster' tool in the ArcGIS – 3D Analyst tool set. These were loaded into ArcScene, resulting in the production of Figure 30, Figure 31 and Figure 32.

### 2.1.2.2.5 Structure contours and thickness maps for stratigraphic units

Maps of the tops of formations (structural contours of the upper surface) and isopachs (formation thickness) are key interpretive elements in the framework for geological and hydrogeological models used in the BA for the Galilee subregion. There are three stratigraphic packages: Cenozoic cover, Eromanga Basin and Galilee Basin (Figure 9). Surfaces of formation tops and isopachs map data for the Cenozoic cover and Eromanga Basin are derived from the GAB Atlas isopach maps (Geoscience Australia, Dataset 22, Dataset 23, Dataset 24, Dataset 25, Dataset 26, Dataset 27, Dataset 28, Dataset 29, Dataset 30, Dataset 31, Dataset 32), which are discussed in detail in Ransley et al. (2015). Formation top structure and extent maps and thickness maps for the Galilee Basin sequence were produced as part of the BA. They are covered in detail in Section 2.1.2.2.5.3.

#### *2.1.2.2.5.1 Cenozoic cover*

Cenozoic cover (Figure 13) is predominantly found in the eastern and southern parts of the subregion, as well as following major surface drainage systems. Isopach maps and further detail on the Paleogene-Neogene component of Cenozoic cover can be found in Ransley et al. (2015) and Table 3.

Detailed Cenozoic stratigraphy, as outlined in Figure 9, is commonly not differentiated in drillhole data. As a result for the Galilee BA, it is categorised as either: Quaternary alluvium, Cenozoic sediments or basalt. Table 5 indicates the thickness of alluvium and Cenozoic sediments across the subregion as derived from available drillhole data. These data suggest the Cenozoic cover is thickest in areas such as the Warrego River near Charleville, around Alpha and south-west of Blackall over the Powell Depression.

The most advanced coal mining proposals are located in the headwaters of the Belyando River on the eastern side of the Great Dividing Range. This area is largely blanketed by a cover of Cenozoic sediments. Other than groundwater monitoring bores, most drillhole data for this region are not publicly available. Although most company drillhole data are also currently not available, the following information on Cenozoic sediments was gleaned from publicly available reports:

- *Hyde Park* – upper Permian coal measures are blanketed by Cenozoic sediments (Saul et al., 2015)
- *China Stone* – where Cenozoic cover is present it varies from 10 to 77 m in thickness, but is typically between 30 to 60 m (AGE Consultants Pty Ltd, 2015). There is a regional thickening from west to east
- *Carmichael* – Cenozoic cover is almost ubiquitous across the mine area and generally thickens from west to east. From MSEC (2013) it appears that north of the Carmichael River, Cenozoic cover is generally less than 50 m, whereas south of the river it is typically greater than 50 m and up to 80 m in thickness

- *China First* – Cenozoic sediments almost completely cover the mine area and are generally less than 35 m thick, but can be up to 90 m thick in the eastern region of the mine area (Waratah Coal Pty Ltd, 2013)
- *Kevin's Corner* – the entire mine area has Cenozoic cover with thickness varying from less than 5 m in the west to up to around 60 m eastwards with a mean thickness of 40 m (URS, 2012a)
- *Alpha* – Cenozoic cover has a mean thickness of 40 m, but thins to less than 5 m over topographically high areas found to the west of the mine (URS, 2012b)
- *South Galilee* – the thickness of Cenozoic cover ranges from 3 to 52 m in thickness with a mean thickness of 21 m (Seedsman Geotechnics Pty Ltd, 2012).

This information suggests that Cenozoic sediments in the Belyando River catchment are generally thicker than that indicated from existing drillhole data presented in Table 5.

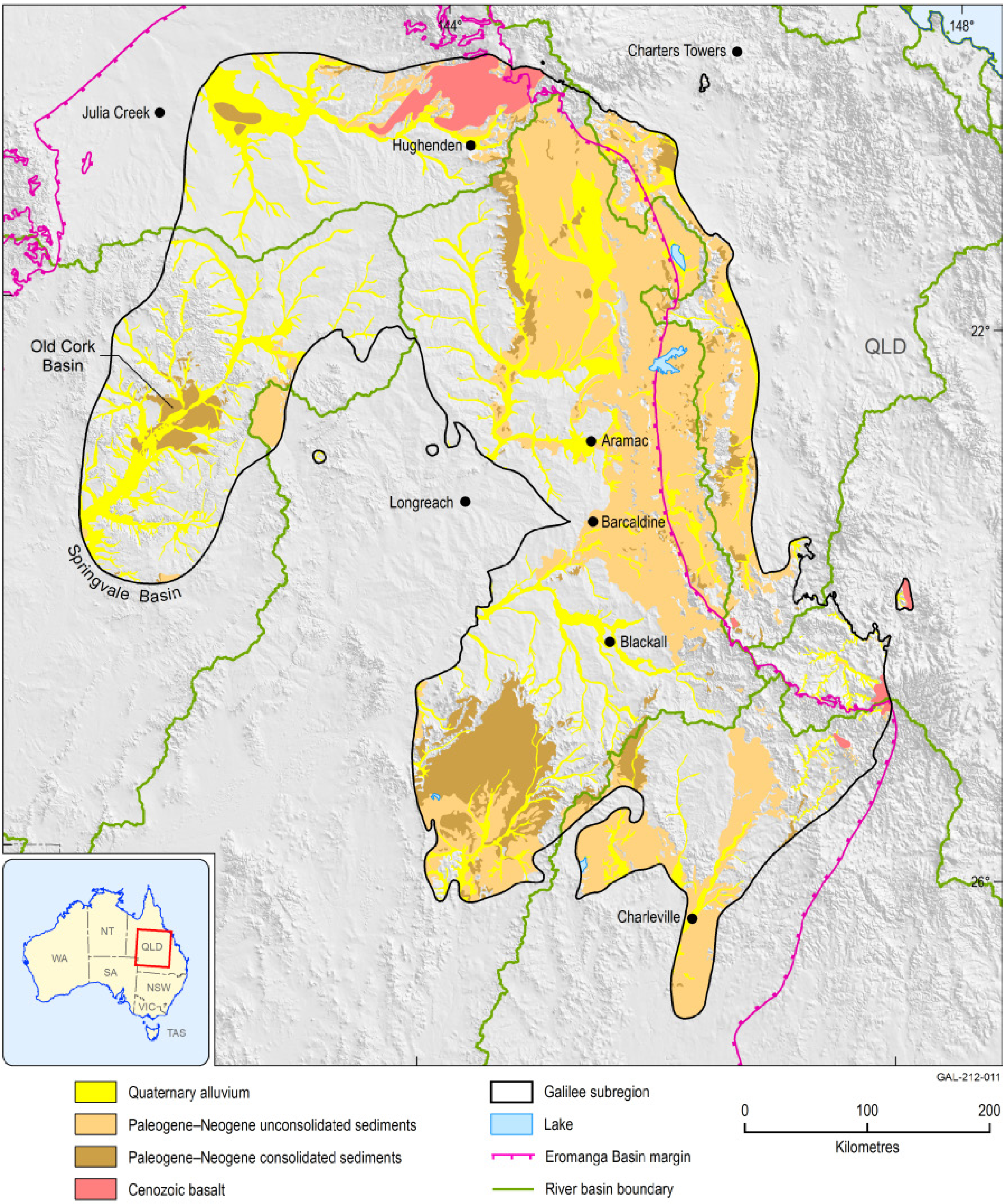


**Figure 13 Extent and differentiation of Cenozoic cover and major geomorphic features in the Galilee subregion**

Data: Geoscience Australia (Dataset 12), Bioregional Assessment Programme (Dataset 33)

### *2.1.2.2.5.2 Eromanga Basin*

For this product, discussion on the Eromanga Basin sequences (Figure 9) will be relatively brief as Eromanga Basin hydrostratigraphic units thickness maps are derived from data presented in detail in Ransley et al. (2015). Further detail on lithology, depositional environments and other aspects of the Eromanga Basin stratigraphic units can be found in Ransley et al. (2015), companion product 1.1 for the Galilee subregion (Evans et al., 2014) and references outlined in Table 3.

**Winton and Mackunda formations**

The Winton and Mackunda formations have been grouped into a thick and widespread regional hydrostratigraphic sequence by Ransley and Smerdon (2012), companion product 1.1 for the Galilee subregion (Evans et al., 2014) and Ransley et al. (2015). The same convention was followed for the numerical and geological models for the Galilee subregion.

The Winton and Mackunda formations cover about half of the subregion and this combined unit thickens to the south-west, attaining over 550 m thickness in the Lovelle Depression (Figure 11), and over 650 m at the south-western limit of the Powell Depression. Along the margin of the Maneroo Platform, this combined sequence thickens northward, from less than 120 m against the Hulton-Rand Structure, to over 250 m at the Elderslie Ridge (Figure 14d). The basal Mackunda Formation is generally consistent in thickness at around 100 m. The Winton Formation constitutes the predominantly thicker and overlying continental part of this combined sequence. The lowermost coal interval within this composite sequence is taken as a convenient demarcation between the Winton Formation and underlying Mackunda Formation. The marginal marine Mackunda Formation has the most persistent lateral permeability of the composite Winton-Mackunda sequence.

Much of the Winton Formation experienced intense periods of weathering during the Cenozoic, as evident in exposed kaolinitised and ferruginised sandstone, mudstone and siltstone. Unweathered outcrop appears restricted to well-cemented, medium-to-coarse-grained sandstone that is commonly nodular.

**Allaru Mudstone, Toolebuc and Wallumbilla formations**

The Allaru Mudstone, Toolebuc Formation and Wallumbilla Formation collectively constitute the Rolling Downs Group aquitard (Figure 14c). These marine units were deposited during a major period of significant sea-level rise and fall in the Cretaceous Eromanga Basin.

The Wallumbilla Formation (Vine et al., 1967) is the most widespread marine unit in the whole of the GAB. Although the Wallumbilla Formation has been subdivided into various members across its extent, they are not readily mappable in the Galilee subregion.

The Wallumbilla Formation was deposited in the Eromanga Basin during a period of rising sea level in the Cretaceous. Its drillhole data (Table 5) indicates it has a mean thickness around 190 m, but can be over 250 m in thickness. The Toolebuc Formation is a distinctive yet thin unit, and is generally less than 30 m in thickness across the subregion. It was deposited at around the time of maximum marine transgression into the Eromanga Basin under anoxic conditions at the seafloor (Ozimic, 1986). The Allaru Mudstone was deposited as the sea receded from the Eromanga Basin. Its drillhole data (Table 5) indicates it has a mean thickness of around 160 m but can be up over 200 m in thickness in places.

These three major units are grouped into a thick and widespread regional sequence known as the ‘Rolling Downs Group Aquitard’ by Ransley and Smerdon (2012), companion product 1.1 for the

Galilee subregion (Evans et al., 2014) and Ransley et al. (2015). Across the Galilee subregion, this sequence thickens from its outcrop to locally reaching over 500 m over parts of the Lovelle Depression in the north of the subregion and the Powell Depression in the south (Figure 14). For the Rolling Downs Group aquitard, 90% of intercepts were greater than 77 m in thickness and the overall mean thickness is 292 m (Table 5).

**Wyandra Sandstone Member, Cadna-owie Formation and Hooray Sandstone**

The Wyandra Sandstone Member, Cadna-owie Formation, Hooray Sandstone, and equivalents have been grouped into a thick and widespread regional hydrostratigraphic sequence (Figure 14b) by Ransley and Smerdon (2012), companion product 1.1 for the Galilee subregion (Evans et al., 2014) and Ransley et al. (2015). In the Galilee subregion portion of the Eromanga Basin, several marginal sandstone facies are differentiated as equivalents and include the Longsight and Blantyre sandstones and part of the section of the Ronlow beds.

According to its drillhole data (Table 5), the Hooray Sandstone averages 60 to 70 m in thickness, the Cadna-owie Formation is around 50 m in thickness, and the Wyandra Sandstone Member is around 18 m in thickness.

The Cadna-owie – Hooray sequence is widespread and its drillhole data (Table 5) indicates it has a mean thickness of 116 m. It extends westwards and northwards from its outcrop areas across the Galilee subregion. Outcrop forms quite a prominent ridge that for the most part is separate from the Great Dividing Range (Figure 13). It is quite thin where it subcrops along the northern margin of Galilee subregion – variably less than 20 m thick. However, it progressively thickens southwards along its outcropping margin to 120 m in thickness at the Nebine Ridge, at the south-eastern limit of the Galilee subregion.

Away from outcrop areas the Cadna-owie – Hooray sequence progressively thickens, reaching up to 260 m in parts of the south-western Lovelle Depression, about 90 m along the north-eastern margin of the Maneroo Platform, and approaching or exceeding 200 m in thickness in the southern Galilee Basin against the Canaway and Nebine ridges (Figure 14b).

The Cadna-owie Formation (Wopfner et al., 1970) is transitional with the underlying Hooray Sandstone. Although relatively thin over the Lovelle Depression and eastern Galilee Basin, this subsurface unit thickens to the south and south-west in the Powell Depression. Some unusual features that formed around the time of the deposition of the Cadna-owie Formation are the Talundilly and Tookoonooka structures. For example, the Tallundilly Structure is some 95 km in diameter, contains impermeable chaotically disturbed strata down sequence from this unit and has been ascribed to a bolide impact (Longley, 1989).

Deposition of the Cadna-owie Formation was in coastal to shallow marine environments and represented the first major marine transgression into the Eromanga Basin sequence, with the Wyandra Sandstone Member possibly being indicative of beach facies (Senior et al., 1975) or a reworked sand sheet from around the upraised Talundilly and Tookoonooka impact features (Gorter et al., 1989).

**Injune Creek Group**

In the Galilee subregion, the Injune Creek Group comprises the Westbourne Formation, Adori Sandstone, and Birkhead Formation. Drillhole data for the subregion (Table 5) indicates the mean thickness for the Injune Creek Group is 163 m with 90% of intercepts less than 283 m. The uppermost Westbourne Formation, although widespread across the subregion, is thin in subsurface across the northern Galilee Basin where it is less than 30 m in thickness (Figure 14a). Southwards, around the Barcaldine Ridge and into the southern Galilee Basin, the formation thickens regionally to above 80 m and continues to thicken southwards to greater than 120 m around the south-eastern Galilee subregion boundary, the Nebine Ridge (Figure 11).

Underlying the Westbourne Formation is the Adori Sandstone. It unconformably overlies the Birkhead Formation, however, it is conformable with the Westbourne Formation. The Adori Sandstone, although widespread, generally (Figure 15e) only has a mean thickness of 31 m (Table 5). The Adori Sandstone has lateral equivalence to the Springbok Sandstone in the Surat Basin.

The Birkhead Formation has a comparable extent across the subregion as the Hutton Sandstone but is generally not as thick as the Hutton Sandstone (Figure 15d). In the northern Galilee Basin, it is generally less than 50 m thick except for localised increases to 85 m in thickness. In contrast, the formation thickens into the southern Galilee Basin where it is generally greater than 100 m in thickness and thickest south-east of the Warrego Fault (see Figure 11 for location). The Birkhead Formation is laterally continuous eastwards across the Nebine Ridge with the Walloon Coal Measures in the Surat Basin. While the Walloon Coal Measures is the focus of CSG production in the Surat Basin, there is little coal present in the Birkhead Formation in the Galilee subregion.

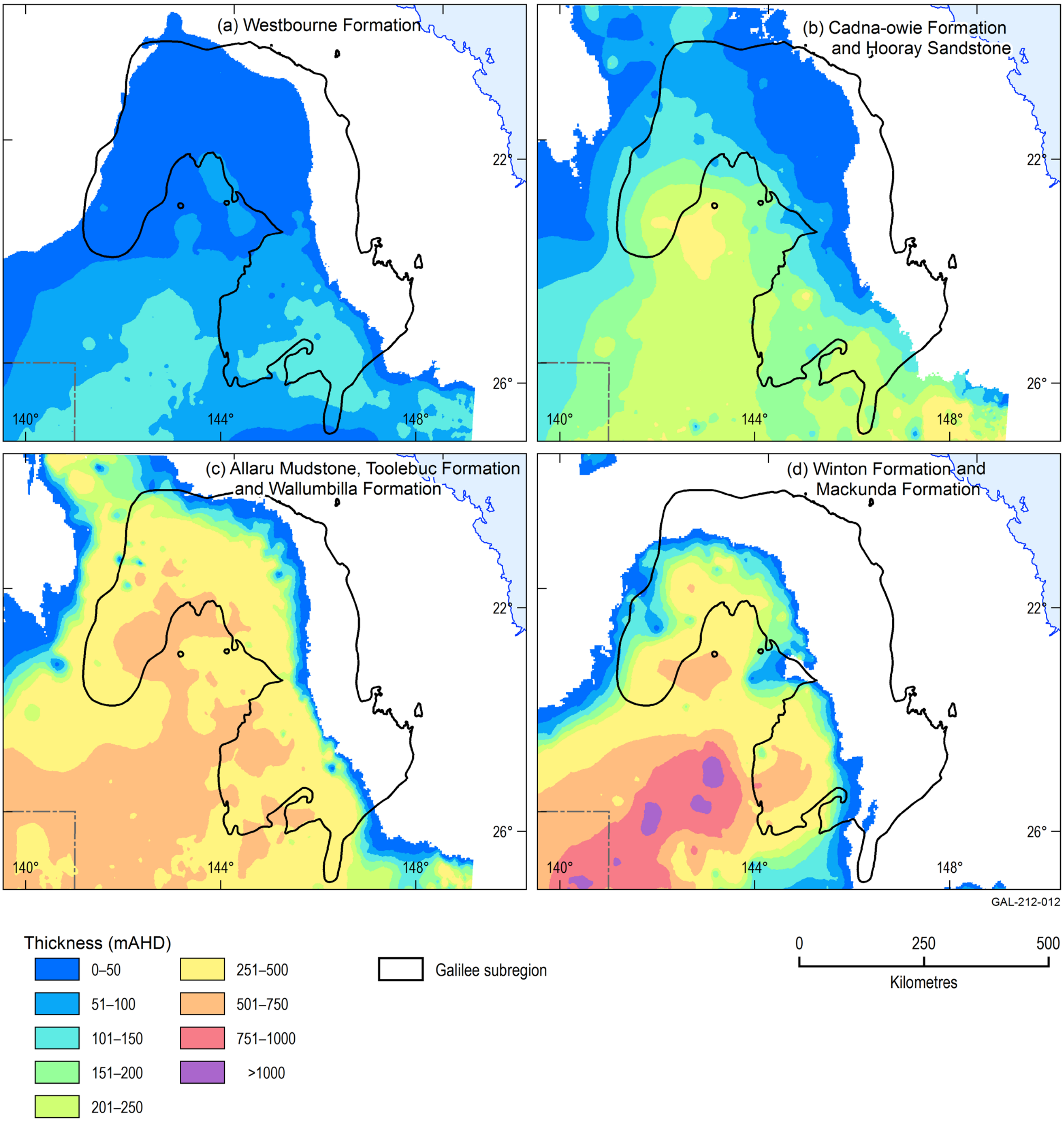


**Figure 14 Extent and thickness variations of the Jurassic-Cretaceous sequence of the Eromanga Basin**

(a) Westbourne Formation, (b) Cadna-owie Formation and Hooray Sandstone, (c) Allaru Mudstone, Toolebuc Formation and Wallumbilla Formation (Rolling Downs Group aquitard), (d) Winton Formation and Mackunda Formation
Data: Bioregional Assessment Programme (Dataset 13)

### Hutton Sandstone and Ronlow beds

The Hutton Sandstone extends in the subsurface over the entire subregion west of its outcrop. North of Jericho, its lateral equivalent in outcrop is the Ronlow beds.

The Ronlow beds is a mapped unit of discontinuous outcrop (Vine et al., 1965) of 30 to 150 m in thickness. It is thought to be a basin margin equivalent of the sequence from Hutton Sandstone up to the Cadna-owie Formation. The incomplete nature of the sequence in the Ronlow beds is probably due to thinning and a depositional hiatus (Cook et al., 2013).

The Hutton Sandstone is widespread in the subregion and although it has an overall mean thickness of around 135 m, it can thicken to over 200 m in the southern Galilee Basin. In the northern Galilee Basin, from the northern flank of the Barcaldine Ridge, the Hutton Sandstone thins both north-westwards and towards and across the Maneroo Platform. There are some locally thick areas up to 150 m on the north-western side of the Koburra Trough (in the areas of the North Galilee Rise) and in the depocentre of the Lovelle Depression (Figure 15c). This suggests that there was some active subsidence at the time of deposition in these areas in the north Galilee Basin.

**Evergreen Formation**

The Early Jurassic Evergreen Formation has a continuous extent in the southern Galilee Basin where it is variably 30 to 40 m in thickness but has some thicker subsurface pockets south-west of its outcrop (Figure 15b). Along the Springsure Shelf in the southern Galilee Basin, the Boxvale Sandstone Member of this formation is predominant (Exon, 1970) and assumes aquifer characteristics. The Evergreen Formation has a generally comparable extent to the underlying Precipice Sandstone except that it is contiguous with the Poolowanna Formation to the south-west over the Canaway Ridge, outside of the Galilee subregion.

The isolated areas of known basal Jurassic (Precipice) and Evergreen equivalents across the northern Galilee Basin suggest that there was an erosional event in this region and that the Evergreen Formation is disconformably overlain by the Hutton Sandstone (Figure 9). This is consistent with what has been outlined for other parts of the Eromanga Basin (e.g. Ransley et al., 2015). The drillhole data (Table 5) indicate the mean thickness for both units is 77 m.

**Precipice Sandstone**

The Early Jurassic Precipice Sandstone extent is limited to the southern Galilee Basin where it thickens eastwards in outcrop and subsurface to about 81 m, near the Birkhead Anticline, and maintains that thickness towards the Nebine Ridge. The unit thins south-westwards and wedges out within the subregion in the vicinity of the Canaway Fault (Figure 15a).

Scattered linear occurrences of a basal Jurassic sandstone exist in the northern Galilee Basin (Ransley et al., 2015). Early exploration drilling ascribed these intersections of about 28 to 74 m in thickness to either basal Jurassic Sandstone or basal Jurassic where an upper facies of Evergreen Formation equivalent was sometimes present (Archer and Armstrong, 1986; Bell, 1985). This Precipice Sandstone equivalent occurs as isolated narrow linear belts up to 80 m in thickness against some of the more significant structures such as the Cork Fault and Beryl Ridge.

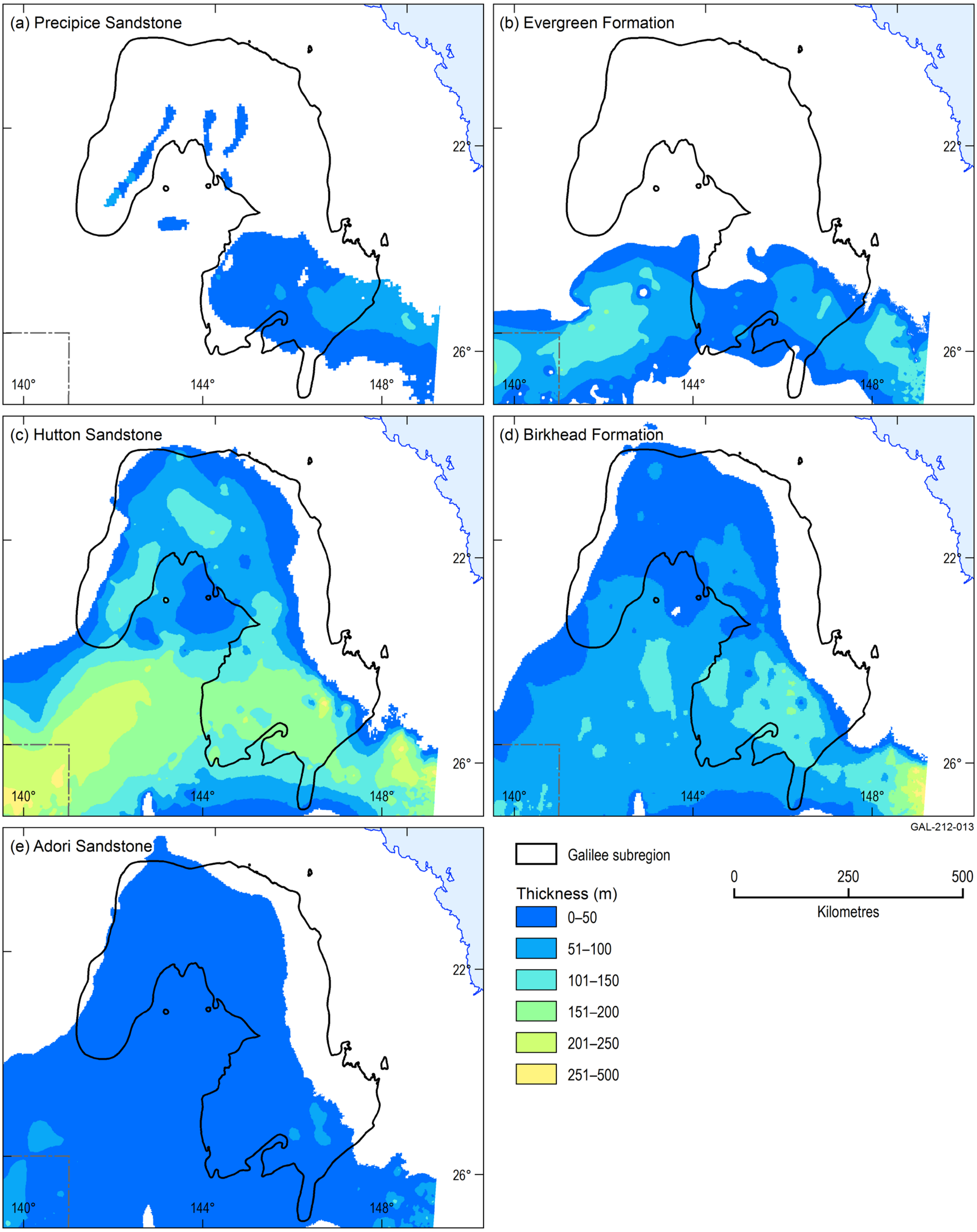


**Figure 15 Extent and thickness of the lower stratigraphic sequence of the Eromanga Basin**

(a) Precipice Sandstone, (b) Evergreen Formation, (c) Hutton Sandstone, (d) Birkhead Formation, (e) Adori Sandstone
Data: Bioregional Assessment Programme (Dataset 13)

#### *2.1.2.2.5.3 Galilee Basin*

Structure contour maps for the upper surface of major stratigraphic units as well as thickness (isopach) maps have been generated for the Galilee Basin as part of the BA for the Galilee subregion. These stratigraphic packages include: Moolayember Formation, Clematis Group, Rewan Group, upper Permian coal measures and Joe Joe Group. A surface of structural contours has also been generated for the top of basement to the Galilee Basin (Figure 11).

Table 6 presents some basic statistics on formation thickness for the modelled layers in the Galilee Basin. Some differences are evident in figures presented for each formation in Table 5 and Table 6. A major reason why that is the case is that data presented in Table 6 are derived from grids interpolated from a number of sources (including geological mapping derived from seismic reflection surveys) as well as some of the drillhole data presented in Table 5.

**Table 6 Statistics on thickness of stratigraphic units in the Galilee Basin as calculated from the modelled layers**

| Stratigraphic unit | Maximum (m) | Mean (m) | Median (m) | 10th percentile (m) | 90th percentile (m) |
|---|---|---|---|---|---|
| Moolayember Formation | 706 | 182 | 156 | 48 | 364 |
| Clematis Group | 401 | 117 | 100 | 57 | 213 |
| Rewan Group | 474 | 148 | 128 | 27 | 297 |
| Upper Permian coal measures | 219 | 93 | 87 | 37 | 162 |
| Joe Joe Group | 1920 | 466 | 340 | 102 | 1079 |

Data: Bioregional Assessment Programme (Dataset 13)

Further details on methods used to produce the models are outlined in Section 2.1.2.2.4. Only stratigraphic intercepts considered fit for purpose, and consistent with other data, are used to model a particular surface. This is due to the potential issues associated with using archival data as outlined in Section 2.1.2.1.5.1.

**Moolayember Formation**

The Moolayember Formation has a broad extent across the Galilee Basin (Figure 16, Figure 17). It comprises predominantly mudstone and siltstone, with minor medium- to coarse-grained pebbly lithic sandstone. Outcrop is only found along the eastern margin of the Galilee Basin, particularly along the crest, and just west of the Great Dividing Range.

The Moolayember Formation conformably overlies the Clematis Group and other underlying units such as the Warang Sandstone. The top of the Moolayember Formation is eroded to varying degrees; this erosional surface (unconformity) forms much of the contact with the overlying Eromanga Basin in the Galilee subregion.

Figure 16 demonstrates that the Moolayember Formation has a regional westerly to south-westerly dip, reaching its greatest depth at 1214 m below sea level (BSL) in the Lovelle Trough. It is absent from the Powell Depression, much of Balcaldine Ridge and the western margin of the Galilee Basin.

Overall the Moolayember Formation has a mean thickness of 182 m with 90% of it being less than 364 m (Table 6). The Moolayember Formation is thickest (Figure 17) in the northern Galilee Basin in the Koburra Trough (upwards of 600 m). It also locally thickens up to 405 m adjacent to the Cork Fault in the Lovelle Depression. It thins to the south of the Barcaldine Ridge, along the Springsure Shelf and along its western margin.

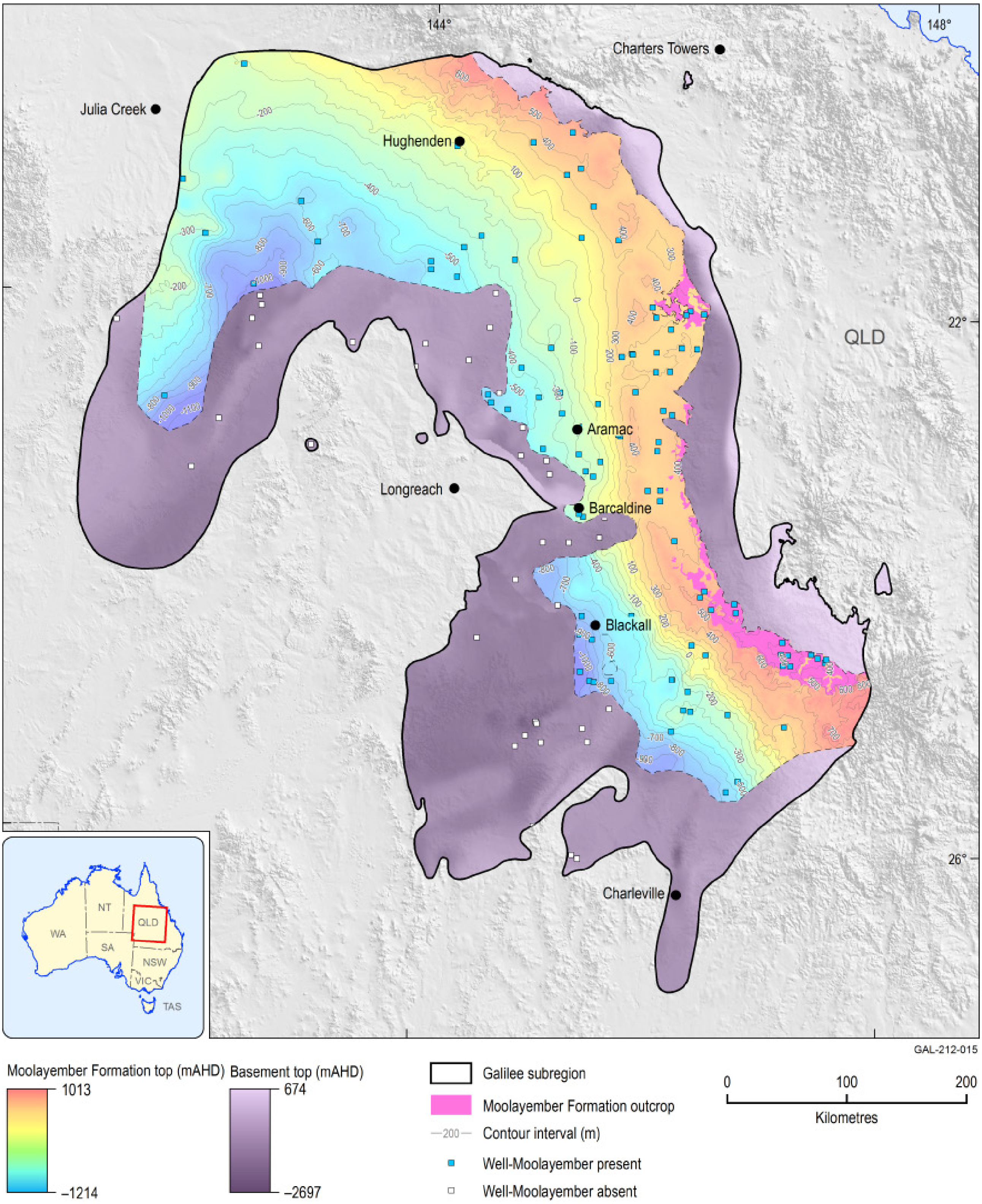


**Figure 16 Elevation of the top of the Moolayember Formation in the Galilee Basin**

Data: Bioregional Assessment Programme (Dataset 13)

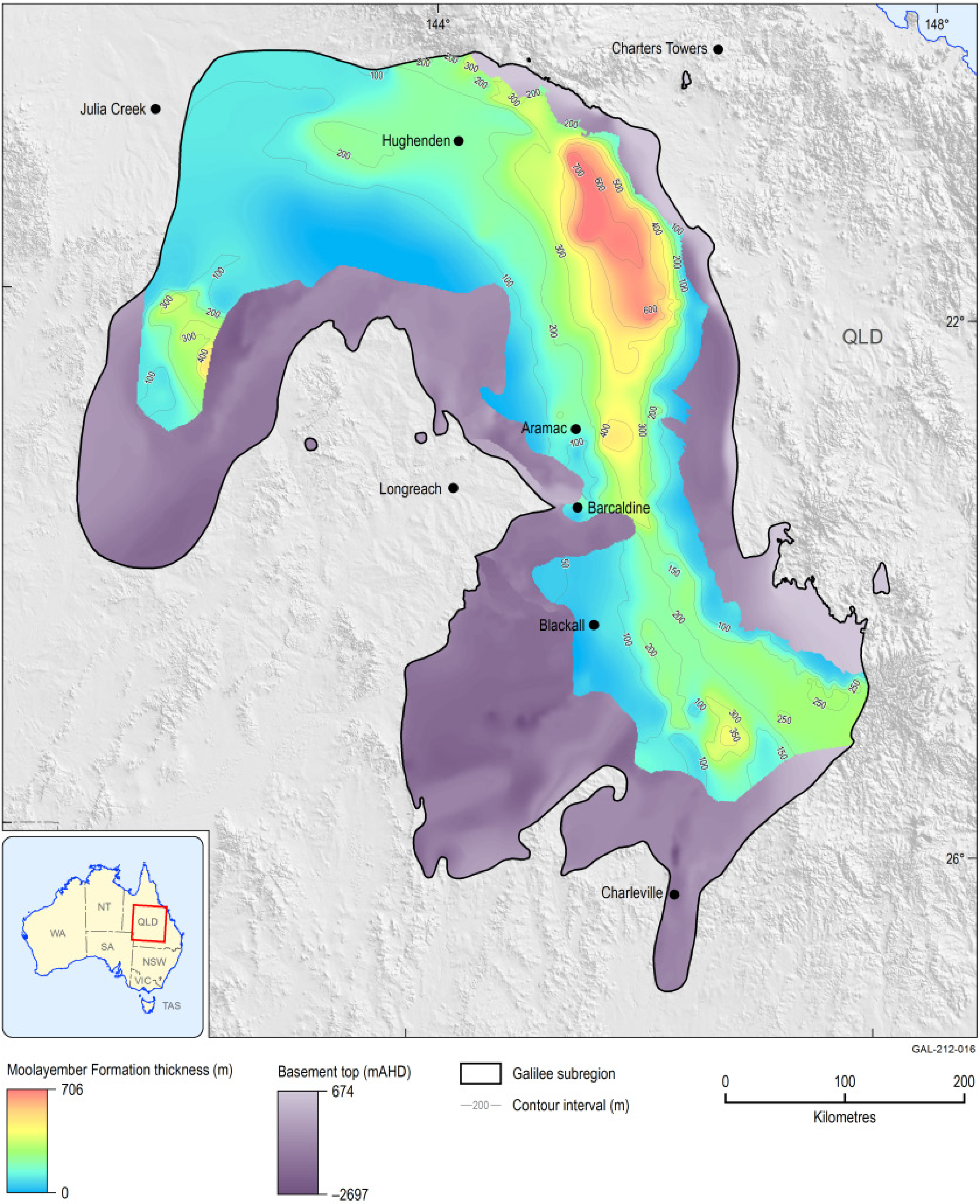


**Figure 17 Extent and thickness of the Moolayember Formation in the Galilee Basin**

Data: Bioregional Assessment Programme (Dataset 13)

### Clematis Group and Warang Sandstone

Due to a relative lack of data, the Warang Sandstone is included as part of the Clematis Group. The Warang Sandstone outcrops along the north-eastern margin of the Galilee Basin and has limited extent south-westwards into the Lovelle Depression.

The Warang Sandstone is in part a lateral equivalent of the Clematis Group (Figure 9). The Clematis Group unconformably overlies the Rewan Group but is conformably overlain by the Moolayember Formation.

The Clematis Sandstone comprises fine- to very coarse-grained quartzose sandstone that are friable and porous with lesser siltstone and mudstone. The Warang Sandstone consists predominantly of poorly sorted kaolinitic sandstone with interbedded siltstone, mudstone and conglomerate (Gray, 1977). Sandstones are medium- to very coarse-grained, generally poorly sorted with calcitic cements. The apparent differences in sedimentology and provenance are likely to cause differences in the hydraulic properties of the Warang Sandstone and Clematis Group. Sandstones of the Clematis Group accumulated under braided fluvial conditions.

Clematis Group and Warang Sandstone outcrop occur along the eastern margins of the Galilee Basin (Figure 18), near the crest of the Great Dividing Range. The contour spacing (Figure 18) suggests there can be relatively considerable variation in the degree of dip. In general these formations dip west to south-west. Unlike what occurs in the overlying Moolayember Formation, the top of the Clematis Group appears to have quite variable dip in the vicinity of the Koburra Trough. The reason for the difference is that the morphology of the top of Moolayember Formation (Figure 16) is largely a result of the significant erosion that occurred after deposition of sediments ceased in the Galilee Basin. Erosion of the Clematis Group (Figure 18) appears to have been more confined to around the margins and thus there is a greater likelihood of preserving features active around the time of deposition.

The Clematis Group has been intercepted down to about 1214 m BSL (Figure 18) in the southern Galilee Basin. It is largely absent from the Lovelle and Powell depressions and along much of the south-western margins of the Galilee Basin. A significant erosional hole is centred along the Barcaldine Ridge.

The Clematis Group has a mean thickness of 117 m with 90% of it being less than 213 m thick (Table 6). It is thick in the Koburra Trough (Figure 19) but is thickest near the northern margin of the Galilee subregion (up to 390 m) near Warang Sandstone outcrop. The Clematis Group generally thins westwards and southwards to less than 100 m. In the southern Galilee Basin, along and south-east of the Pleasant Creek Arch, there is a regional thickening of the unit up to 270 m. Thicker sections (greater than 250 m) align with the trends of regional folds and structure in the area.

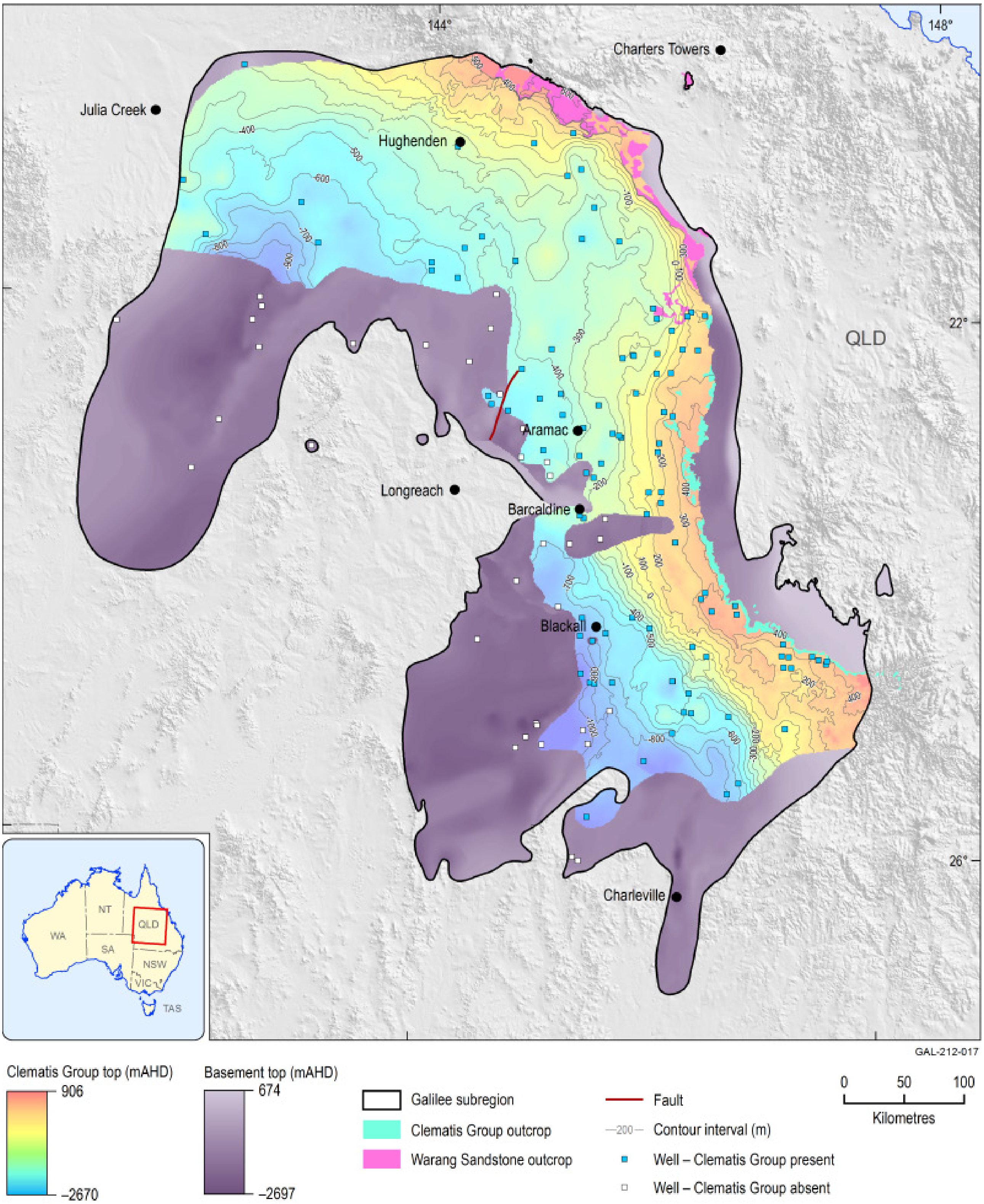


**Figure 18 Elevation of the top of the Clematis Group in the Galilee Basin**

Top of formation mapping incorporates both top of Warang Sandstone and top of Clematis Group.
Data: Bioregional Assessment Programme (Dataset 13)

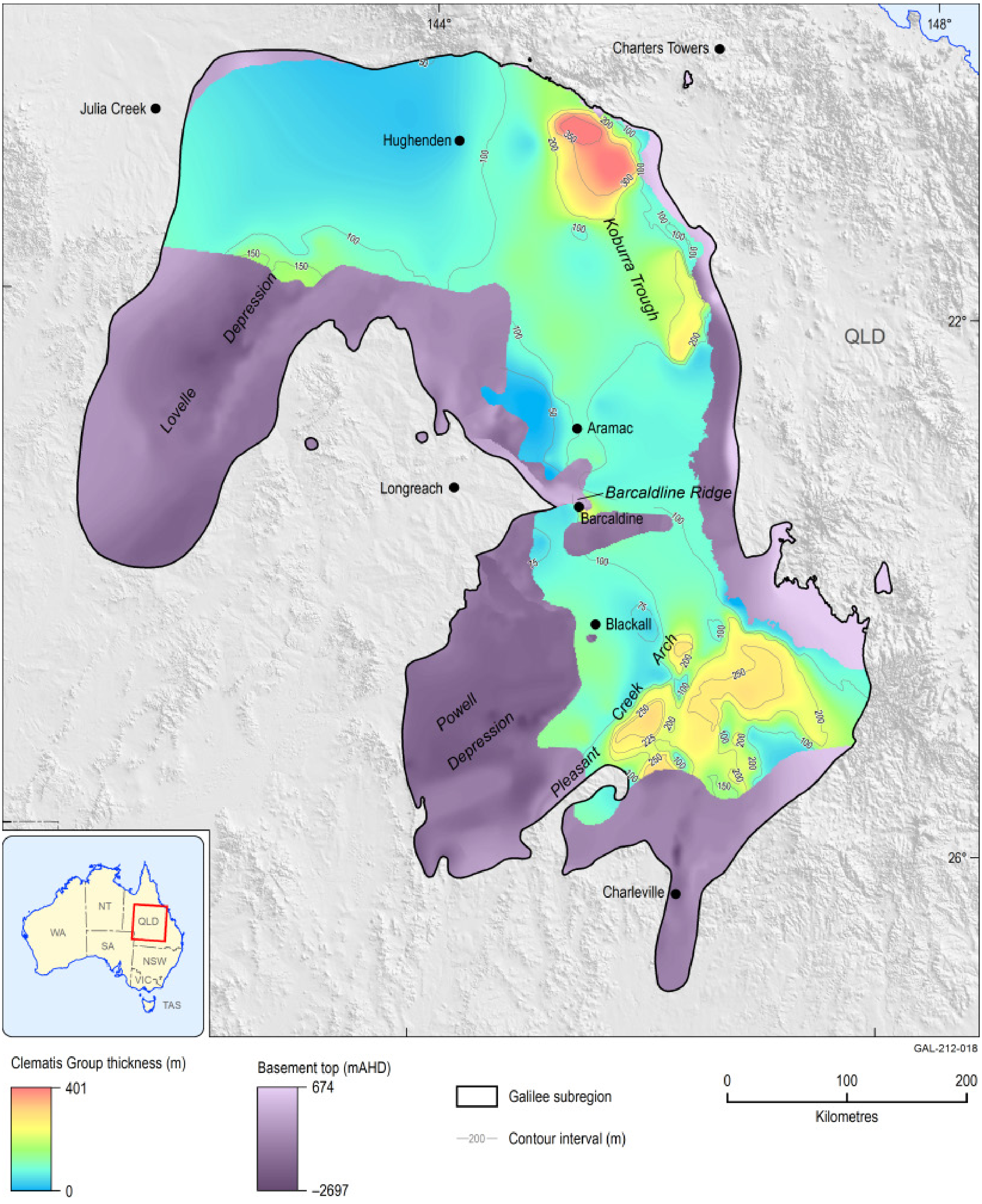


**Figure 19 Extent and thickness of the Clematis Group in the Galilee Basin**

Thickness map is inclusive of the Warang Sandstone and Clematis Group

Data: Bioregional Assessment Programme (Dataset 13)

### Rewan Group

In the Galilee Basin, the Rewan Group includes both the Rewan Formation and the Dunda beds (Figure 9). Although use of the term 'Rewan Group' has previously been generally unique to the Bowen Basin, it is used here for the Galilee Basin sequence to be inclusive of the Rewan Formation and Dunda beds as per McKellar and Henderson (2013). The Dunda beds only occur along the eastern margin of the northern Galilee Basin. The Rewan Group unconformably overlies the upper Permian coal measures, and is in turn disconformably to unconformably overlain by the Clematis Group.

The Rewan Formation consists of interbedded sandstone, distinctive grey to green siltstone and mudstone. Fine to coarse-grained sandstones are frequently occluded with calcitic cement. These sedimentary rocks were deposited as continental fluvial red beds with a significant input of volcanolithic sediment under hot climatic conditions. This formation is an excellent aquitard across much of its extent.

The Dunda beds (Vine et al., 1965) extend across the eastern Koburra Trough but are limited southwards. This unit is a sandier facies that is superimposed over and interdigitates with the Rewan Formation. The Dunda beds predominantly consist of sandstone in the lower half, but with a transition to mudstone and siltstone in the upper sequence.

The Rewan Group (Figure 20) outcrops along the eastern margin of Galilee Basin, just east of the crest of the Great Dividing Range and reaches its deepest point at around 1200 m BSL into the Lovelle Depression. It has similar regional dips to those of the overlying Clematis Group. The Rewan Group, is largely absent from the Lovelle Depression and across much of the south-western part of the southern Galilee Basin; however, it does extend along the Springsure Shelf to the Nebine Ridge. Of significance is the erosional absence of this aquitard at the western end, and it is very thin across the eastern end of the Barcaldine Ridge (Figure 19, Figure 20), which enables upper Permian coal measures to be in direct contact with the overlying Eromanga Basin sequence and specifically the Hutton Sandstone. The Rewan Group is also missing along the north-north-eastern margin of the Galilee Basin which would allow the Warang Sandstone to be in direct contact with the upper Permian coal measures. This may have implications for connectivity between the two units in these areas.

The Rewan Group has an overall mean thickness of around 148 m with 90% of it being less than 297 m in thickness (Table 6). The Rewan Group extends across the entire Koburra Trough where it reaches a maximum thickness of over 400 m centrally, but thins and wedges out westwards towards the Maneroo Platform (Figure 21). The Rewan Group thins south-eastwards across the north-eastern part of the Springsure Shelf, and is absent south-westwards beyond the Fairlea Anticline in the Powell Depression.

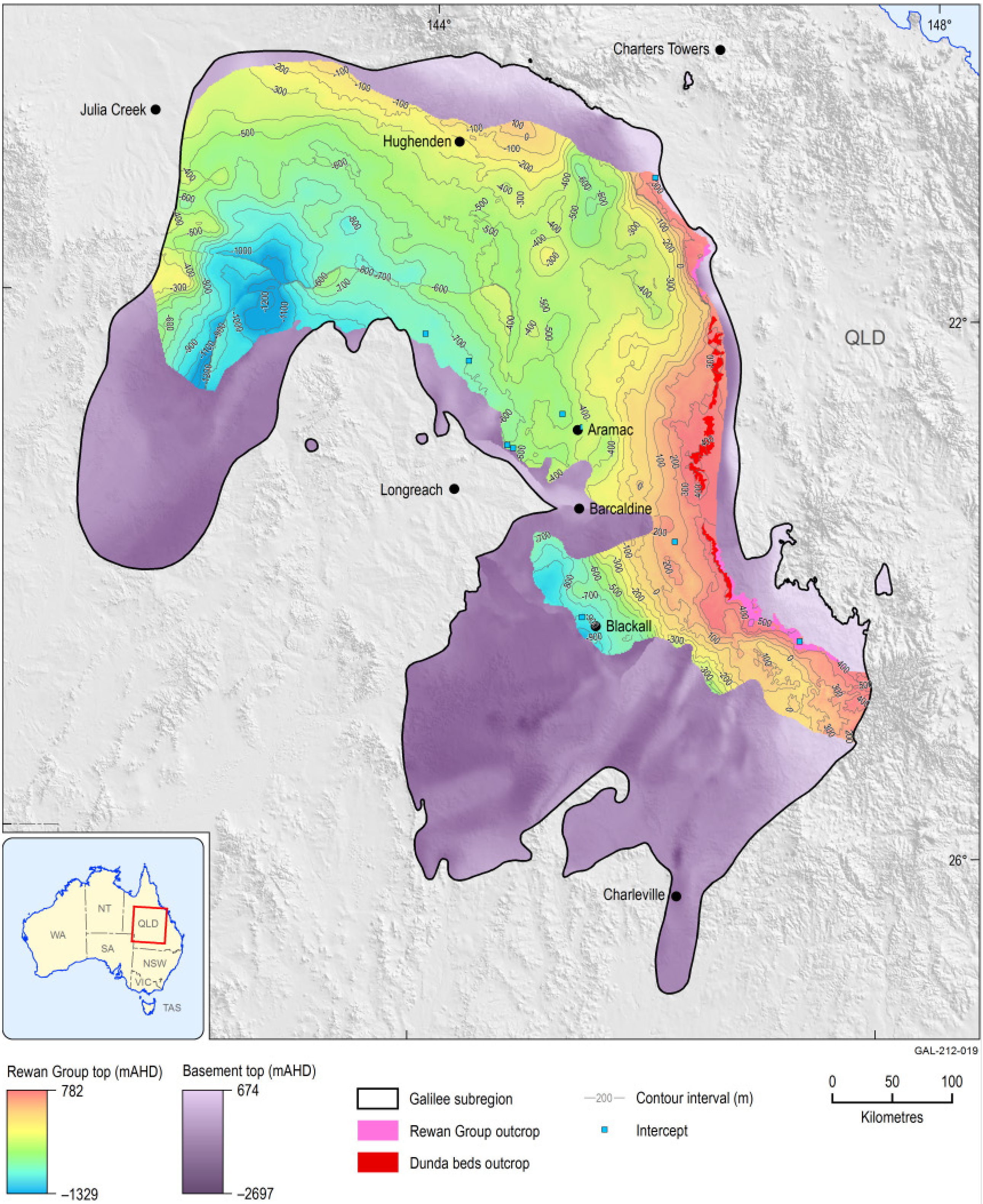


**Figure 20 Elevation of the top of the Rewan Group in the Galilee Basin**

Data: Bioregional Assessment Programme (Dataset 13)

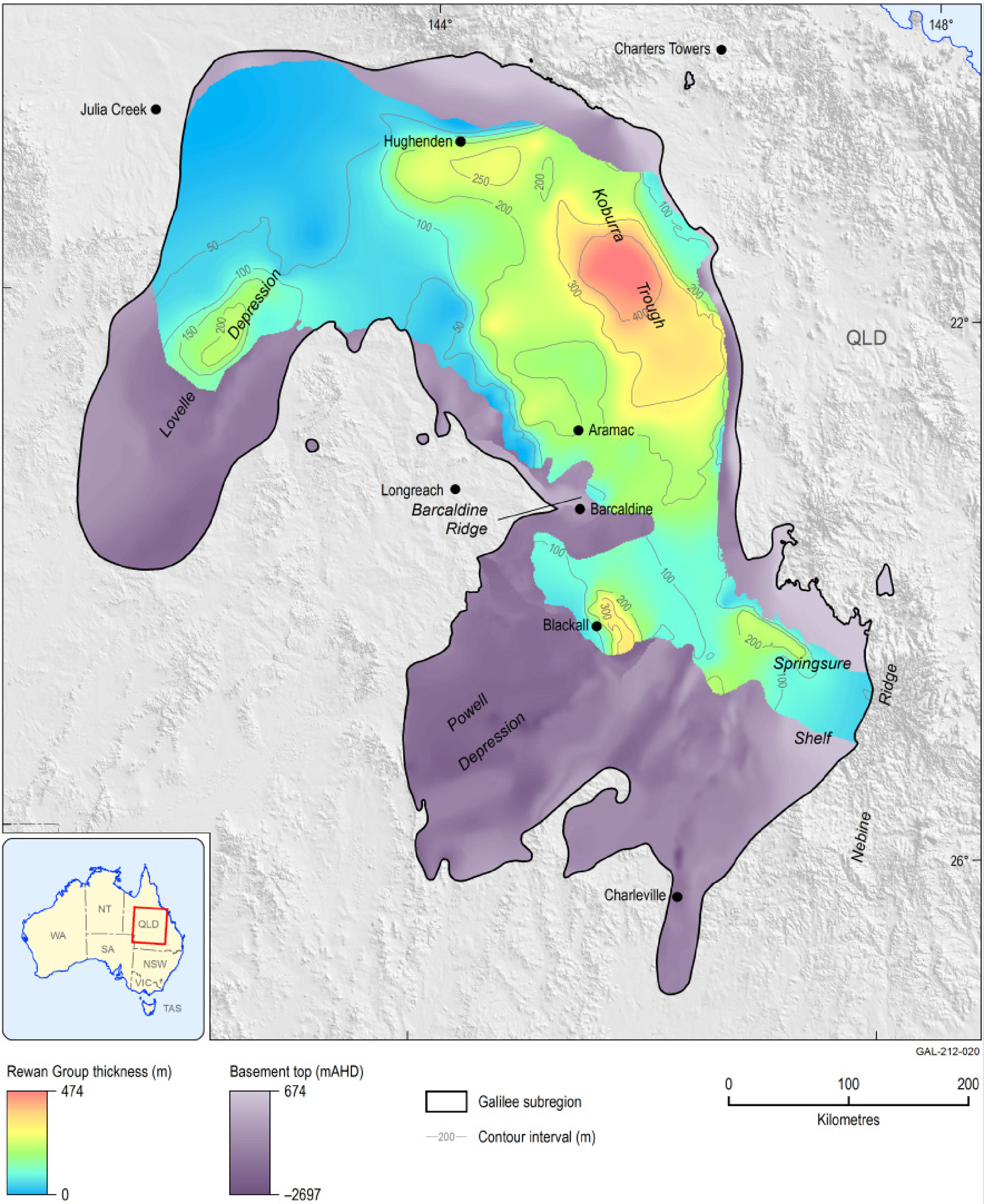


**Figure 21 Extent and thickness of the Rewan Group in the Galilee Basin**

Data: Bioregional Assessment Programme (Dataset 13)

### Upper Permian coal measures

For the Galilee subregion, the name 'upper Permian coal measures' refers to the Betts Creek beds, Bandanna Formation, Black Alley Shale, Peawaddy Formation and Colinlea Sandstone. Figure 9 and Phillips et al. (2015) show that the Betts Creek beds are the lateral equivalent of the Bandanna

Formation, Black Alley Shale, Peawaddy Formation and Colinlea Sandstone. Further detail on upper Permian stratigraphic units can be found in Phillips et al. (2015, 2016), Nicoll et al. (2015), companion product 1.1 for the Galilee subregion (Evans et al., 2014), McKellar and Henderson (2013), Blanco (2010), Allen and Fielding (2007), Scott et al. (1995), Scott and Hawkins (1992), Wells (1989) and references listed in Table 3.

Within the upper Permian coal measures, individual coal seams will merge and split depending on local geological factors such as subsidence rates, compaction and sediment influx at the time of coal deposition. Up to seven major coal seams designated A to G, have been delineated in the upper Permian coal measures (Scott and Hawkins, 1992). Coal seams A and B were included in the Bandanna Formation. Recent work by Phillips et al. (2015, 2016) has identified further coal seam groups.

The coal seam nomenclature in Scott and Hawkins (1992) has been adopted by most coal companies operating in the Galilee Basin. However, whether a particular seam is included stratigraphically in the Betts Creek beds, the Bandanna Formation or Colinlea Sandstone varies between the different coal mine developments. For instance, at Hyde Park, seams A through to D2 are included in the Betts Creek beds, with seams D1 to G incorporated into the Colinlea Sandstone (Saul et al., 2015). At Carmichael Coal Project, seams A to C are included in the Bandanna Formation with seams D to F included in the Colinlea Sandstone (GHD, 2013). At Alpha, seams A and B are included in the Bandanna Formation with seams C to F included in the Colinlea Sandstone (Hancock Prospecting Pty Ltd, 2011). In South Galilee, however, seam D is included in the Bandanna Formation (SGCP, 2012). Other conventions of coal seam nomenclature based on CSG wells are adopted for some of the deeper parts of the Galilee Basin (Phillips et al., 2015). The variety of coal seam nomenclature can cause issues for correlation, which in turn influences the degree of detail and certainty that geology can be modelled on a semi-regional basis.

Phillips et al. (2015, 2016) suggest that at a semi-regional scale, there are issues that need to be addressed with correlations between the different stratigraphic units that comprise the upper Permian coal measures sequence.

Phillips et al. (2015, 2016) present a stratigraphic framework for correlation of coal seams across the entire Galilee Basin. Primarily using geophysical well logs and other drillhole data, Phillips et al. (2015) designated 11 major coal seams, A through K, with seams A and B in the Bandanna Formation and seams C to I in the Colinlea Sandstone. Seams J to K are newly recognised lithological subdivisions in the coal measures and are yet to be assigned to a stratigraphic unit. The Betts Creek beds included all seam packages. Phillips et al. (2015) then correlated the coal seams across the Galilee Basin using seam C as a distinctive marker horizon. Seams B to G, were found to occur across the Galilee Basin while Seam A was only found to occur around the eastern margin and central parts of the Koburra Trough. Seams H and I are localised to deep parts of the Koburra Trough. Seams J and K occurred along the western margin of the northern Galilee Basin, in particular in the Aramac Trough. According to Phillips et al. (2015), the variation in seams suggests there is compartmentalisation in the Galilee Basin possibly due to variations in tectonics, subsidence and differential compaction. Phillips et al. (2015) suggested that correlations presented in their study should be further tested using biostratigraphy and geochronology.

Nicoll et al. (2015) reported on some preliminary age dating results that are part of these ongoing studies.

Due to limited available data for the individual stratigraphic units that comprise upper Permian coal measures and discrepancies between drillhole stratigraphic picks, only the top and base were modelled for the Galilee subregion geological model.

The upper Permian coal measures are unconformably overlain by the Rewan Group across much of the subregion (Figure 9). Around the north-eastern margin of the subregion the upper Permian coal measures are unconformably overlain by Warang Sandstone. Most of the Barcaldine High and the upper Permian coal measures, in parts of the southern Galilee Basin and along parts of the western margin of Galilee Basin respectively, are in direct contact with the overlying Eromanga Basin (specifically the Hutton Sandstone or Precipice Sandstone).

The upper Permian coal measures outcrop just east of the Great Dividing Range in the upper reaches of the Belyando river basin. However, most of the outcrop is obscured by a cover of Cenozoic sediment (see Section 2.1.2.2.5.1). Although the upper Permian coal measures occur throughout much of the Galilee Basin (Figure 22), drillhole data suggest they are missing along the western margin of the Galilee Basin and from much of the Lovelle Depression. The deepest intervals occur at a depth around 1800 m BSL in the Powell Depression. Further information on the distribution of individual stratigraphic units that comprise the upper Permian coal measures can be found in companion product 1.1 for the Galilee subregion (Evans et al., 2014) and Wells (1989). Figure 20 in Evans et al. (2014) outlines the general distribution of Betts Creek beds, Bandanna Formation and Colinlea Sandstone in the upper Permian coal measures. Wells (1989) outlined the distribution of all coal-bearing formations in the Galilee Basin as well as the Peawaddy Formation and Black Alley Shale. It is likely that these maps will be able to be refined in the future by referring to the work of Phillips et al. (2015, 2016) and by utilising recent company CSG and coal drilling data.

Overall, Figure 22 demonstrates that the top of the upper Permian coal measures have westerly and southerly dip direction patterns, which is similar to what occurs in the overlying Rewan and Clematis groups (Figure 18, Figure 20). However, in the structure contours it is evident that there is more complexity (Figure 22). Part of the reason why there is more complexity could be because existing seismic mapping was incorporated into the development of Figure 23 (Section 2.1.2.2.4). The presence of significant thicknesses of coal makes the top of the upper Permian coal measures a relatively easy horizon to pick from seismic techniques (Marsh et al., 2008). Some of the complexity in Figure 23 involves a series of north-easterly trending troughs and highs (e.g. the Aramac Trough) near the western margin of the northern Galilee Basin. These troughs and highs are separated from the Koburra Trough by the North Galilee Rise (Section 2.1.2.2.3). In the southern Galilee Basin, the south-west trending Pleasant Creek Arch and Warrego Fault are prominent and segregate the Powell Trough from Springsure Shelf. Also evident are some of the south-west trending fold closures on the Springsure Shelf and the complicated nature of the Barcaldine Ridge (see also Section 2.3.2 of companion product 2.3 for the Galilee subregion (Evans et al., 2018)).

The upper Permian coal measures are much thinner south of the Barcaldine Ridge compared to north of it (Figure 23). Overall the upper Permian coal measures have a mean thickness of around

93 m with 90% of it being less than 162 m in thickness (Table 6). It reaches a maximum of around 210 m in thickness in southern sections of Koburra Trough and in the Aramac Depression. In the central Lovelle Depression, the upper Permian coal measures steadily thicken to a maximum of 125 m. In other areas, the upper Permian coal measures thin considerably, to generally less than 50 m.

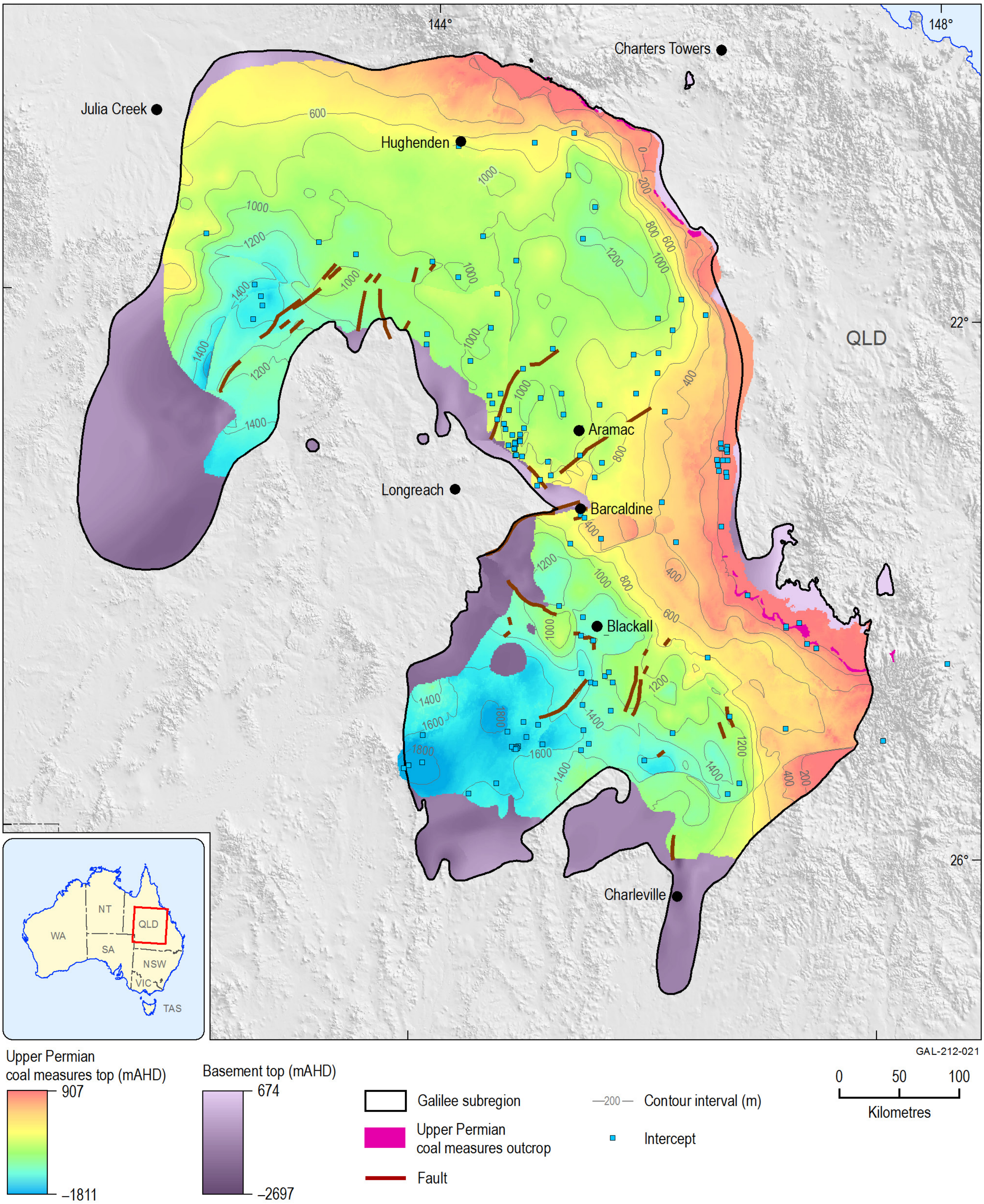


**Figure 22 Elevation of the top of the upper Permian coal measures in the Galilee Basin**

Data: Bioregional Assessment Programme (Dataset 34)

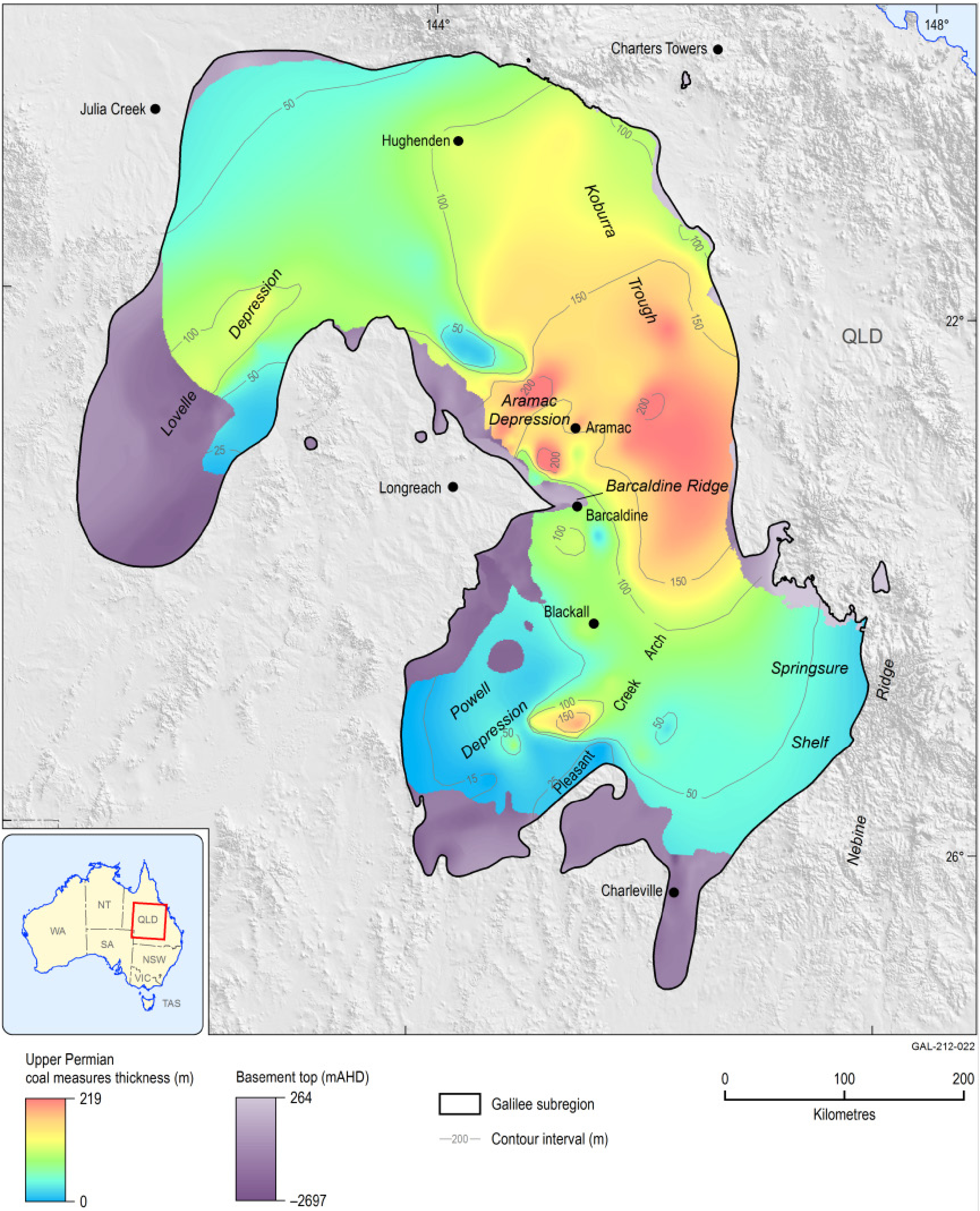


**Figure 23 Extent and thickness (m) of the upper Permian coal measures**

Data: Bioregional Assessment Programme (Dataset 13)

### *2.1.2.2.5.4 Distribution of coal seam gas in the upper Permian coal measures*

While many aspects of CSG studies are beyond the scope of the BA, some information is pertinent as it has a bearing on the formation and distribution of gas in Galilee subregion. This in turn may provide additional information on the hydrodynamics of the Galilee Basin groundwater systems and for the qualitative risk and impact analysis that will be reported in companion products 3 and 4 of the BA for the Galilee subregion. Further discussion on CSG and its possible relationship with groundwater systems in the Galilee Basin is provided in Section 2.3.2.2.2 of companion product 2.3 for the Galilee subregion (Evans et al., 2018).

I'Anson (2013) investigated various aspects of coal and CSG from the upper Permian and Aramac coal measures in the Galilee Basin. More data have become available since the publication of I'Anson (2013). Relevant aspects of some CSG data that were collated for the BA for the Galilee subregion are outlined below.

The CSG content from a drill core sample is typically reported as raw gas content. If additional information such as the moisture content and inert mineral content (ash) of the coal from which the gas has been extracted is available, then the raw gas content value can be standardised to a dry ash free (DAF) gas content. Standardisation allows for a more direct comparison of gas content data from different seams and regions. For the BA for the Galilee subregion, DAF gas contents are used for comparison, as samples from different seams but within the same coal-bearing sequence are being clumped into two broad groups. The two broad groups are the upper Permian coal measures and Aramac coal measures.

I'Anson (2013) showed that vitrinite reflectance for upper Permian coal measures ranges from around 0.4 to 0.8 %Ro, while for the more deeply buried Aramac Coal Measures the vitrinite reflectance range from 0.5 to 0.9 %Ro. In the upper Permian and Aramac coal measures the highest DAF gas content from drill core samples occur between 900 and 1200 m (Figure 24). Gas content decreases significantly below 1300 m. The apparent increase in gas content below 1600 m (Figure 24) may relate more to the coal samples having a tendency towards higher ash contents, rather than the raw gas content actually beginning to increase again with depth. A discrete peak in gas content is one line of evidence that is suggestive that the gas was largely derived through a biogenic pathway. Such a distribution has been observed in other coal-bearing basins, for example Sydney Basin (Burra et al., 2014) and Surat Basin (Hamilton et al., 2015). However, unlike in the previous examples, there do not appear to be an obvious conceptual flow pathways that could connect groundwater recharge to areas in the Galilee Basin where higher CSG contents are present in the upper Permian coal measures (see also Section 2.3.2.2.2 of companion product 2.3 for the Galilee subregion (Evans et al., 2018)).

CSG is produced primarily via two major processes: biogenic (microbial) or thermogenic (geological) pathways. Hamilton et al. (2012) and Golding et al. (2014) detailed a number of discriminating factors that can be used to determine the origins of CSG. These include gas composition, thermal maturity of the coal and the isotopic composition of carbon and hydrogen in methane and other gases that make up the CSG. Detailed analysis of all these aspects was not required for the BA. The only discriminant considered here is the carbon isotopic composition of methane. According to Golding et al. (2014), a $\delta^{13}C$ value of –50 approximates the boundary between biogenic and thermogenic gas. CSG can be described as having a biogenic, mixed or thermogenic origin.

As shown in Figure 25, carbon isotope data for the methane component of CSG from the Galilee subregion is sparse. Available data suggests that CSG from upper Permian and Aramac coal measures is primarily biogenic to mixed-biogenic origin above 1400 m. Limited sampling from below 1600 m suggests that, at deeper levels, CSG has more of a thermogenic origin. In general, gases of biogenic origin are thought to be associated with topographic-driven groundwater systems (Burra et al., 2014; Hamilton et al., 2015) rather than groundwater systems driven by other geological pressure regimes (e.g. over-pressurisation due to gas at depth). The lower CSG contents found between 1300 to 1600 m also support the interpretation that CSG is biogenic rather than thermogenic and that the system has not been pressured by gas sources from deeper levels in the coal seams.

Figure 26 shows the variation in the distribution of the average CSG gas content for upper Permian coal measures. Higher average gas contents tend to be clustered in the vicinity of CSG project areas (Figure 26) in central parts of the northern Galilee Basin. Overall, however, a zone of higher gas content forms a north-east trending fairway. I'Anson (2013) also noted a similar gas content trend in the upper Permian coal measures. The zone of higher gas contents appears to butt up against the Maneroo Platform, along the western margin of Galilee Basin. Faults that are known to occur have also been overlain on Figure 26. Many of these faults have a near-parallel trend to CSG fairway, which suggests some structural control is influencing the distribution of the gas. In Figure 26, the north-east trending fault along the southern margin of the gas fairway appears to form a boundary between high and low gas contents, which suggests that there is some compartmentalisation in the coal measures. This may also have some bearing on potential for groundwater flow. As shown in Section 2.3.2.2.2 of companion product 2.3 for the Galilee subregion (Evans et al., 2018), the potential groundwater flow direction is parallel to some faults as well as the trend in higher gas contents (the gas fairway) in the upper Permian coal measures. Evans et al. (2016) postulated that structures and hydrodynamics may be influencing the distribution of CSG. In turn, the CSG distribution suggests that some compartmentalisation of the reservoir is apparent in the upper Permian coal measures, which may locally influence the hydrodynamics of this unit.

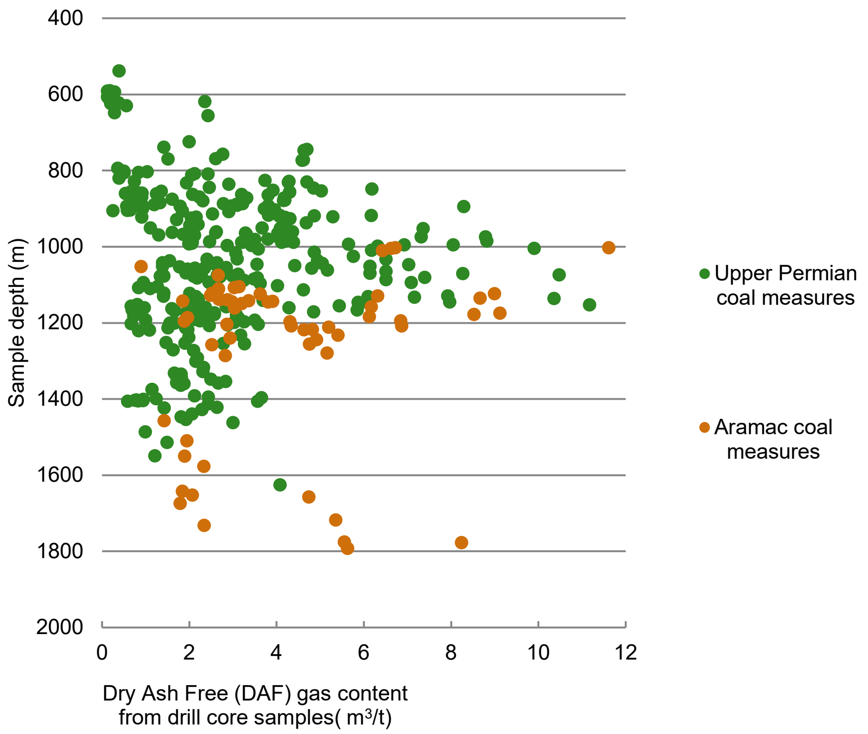


**Figure 24 Dry Ash Free gas contents for upper Permian and Aramac coal measures relative to depth**

Data: Bioregional Assessment Programme (Dataset 35)

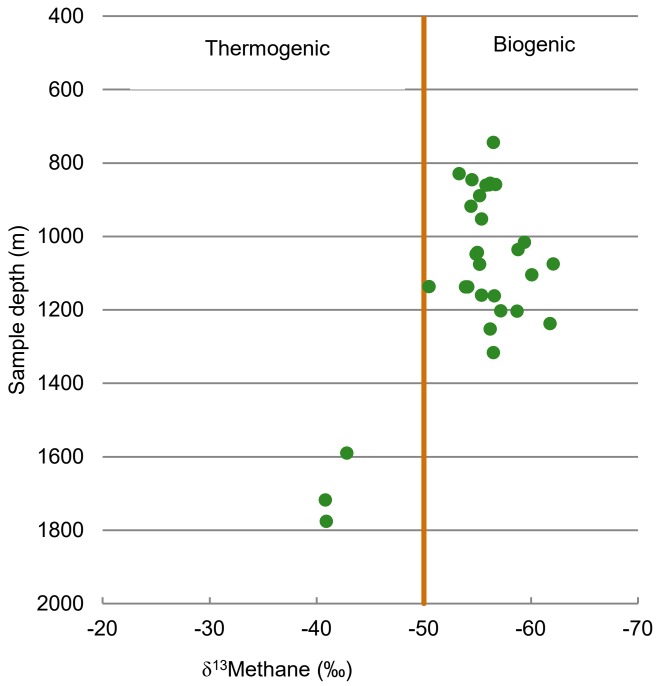


**Figure 25 Methane carbon isotope values relative to depth and interpretation of the origin of coal seam gas**

$\delta^{13}$Methane is a measure of the isotopic composition of the Carbon (C) atom in the methane molecule. $\delta^{13}$C is the ratio of $^{13}$C to $^{12}$C isotopes of the carbon in the methane gas, relative to the isotopic ratio of $^{13}$C to $^{12}$C in a standard reference material. As described in the text, a $\delta^{13}$C value less than –50 indicates a biogenic origin for the methane.

Data: Bioregional Assessment Programme (Dataset 35)

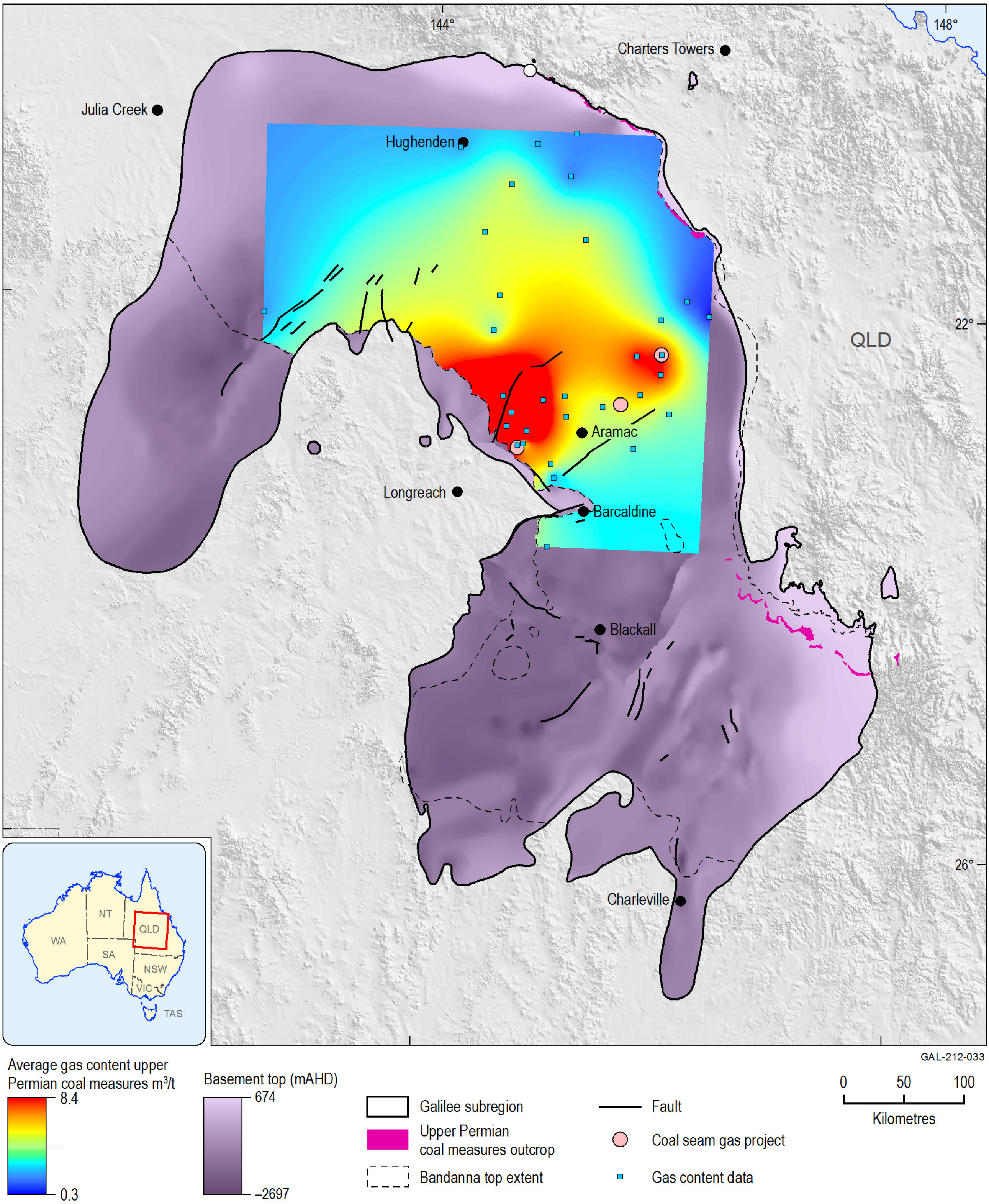


**Figure 26 Distribution of average gas contents for the upper Permian coal measures**

Data: Bioregional Assessment Programme (Dataset 36)

### Joe Joe Group

The Late Carboniferous to early Permian Joe Joe Group represents the lowermost stratigraphic sequence in the Galilee Basin. It was in part deposited in glacial, fluvial glacial and lacustrine environments. Figure 9 outlines the stratigraphy for the Joe Joe Group, which is comprised of four main stratigraphic units. These are the: Lake Galilee Sandstone, Jericho Formation, Jochmus Formation and the Aramac Coal Measures. The Edie Tuff Member occurs in the upper part of the Jochmus Formation while the Oakleigh Siltstone Member is a part of the Jericho Formation. The Boonderoo beds are a basin margin facies restricted to the north-eastern margin of the Galilee Basin.

For the purposes of the BA for the Galilee subregion, the Joe Joe Group was modelled as one unit as most coal mine projects (the exception being coal mine projects in the Winton Formation) are situated stratigraphically above the Joe Joe Group, in units that comprise the upper Permian coal measures (see companion product 1.2 for the Galilee subregion (Lewis et al., 2014)). The Aramac Coal Measures, while an exploration target for CSG, are yet to be included in a declared CSG gas resource. Further detail on the Joe Joe Group is available from Phillips et al. (2015), Nicoll et al. (2015), companion product 1.1 for the Galilee subregion (Evans et al., 2014), McKellar and Henderson (2013), Jones and Fielding (2008), Scott et al. (1995) and references listed in Table 3.

The Joe Joe Group has the broadest extent across the Galilee Basin. It outcrops along the eastern margin of the Galilee subregion, east of the Great Dividing Range in the Burdekin river basin. The top of the Joe Joe Group (Figure 28) is at its deepest in the main depocentres – the Koburra Trough, the Lovelle Depression and the Powell Depression at respectively around 1200 m, 1700 m and 1800 m BSL. The Aramac Trough is another prominent depression situated near the western margin of the northern Galilee Basin. Overall, it has a westerly to southerly dip from its eastern and northern margins into the Galilee Basin.

The Joe Joe Group has a highly variable thickness, which locally reflects its infill of irregular terrain and the influence of basin-forming tectonic events in the early Permian. Erosion and uplift that occurred during the Permian but post deposition have also modified the distribution and thickness of the Joe Joe Group. There is more structural complexity in the top of Joe Joe Group (Figure 27), when compared with others (e.g. Figure 18, Figure 20, Figure 22) as the various depo-centres within the Galilee Basin were at their most active during deposition of the Joe Joe Group. The Joe Joe Group is thickest in the Koburra Trough (over 1600 m thick). It also exceeds 1000 m thickness over parts of the Barcaldine Ridge, northern parts of the Springsure Shelf and bits of the Aramac Trough.

However, the Joe Joe Group is generally less than average thickness in the Powell and Lovelle depressions. Overall, the Joe Joe Group has a modelled mean thickness of 466 m and 90% of it is less than 1079 m thick (Table 6).

Table 5 outlines statistics based on drillhole data for the various stratigraphic units that comprise the Joe Joe Group. The various stratigraphic units that comprise the Joe Joe Group are not distributed evenly across the basin (Scott et al., 1995). The Lake Galilee Sandstone is restricted to eastern and central parts of the Koburra Trough. The Jericho and Jochmus formations are more widespread; the Jochmus Formation is commonly the basal sequence across much of the Galilee Basin.

The Aramac Coal Measures has limited extent in the northern Galilee Basin, from the mid-region of the Lovelle Depression, around the Maneroo Platform into the Aramac Depression, and eastwards into the western margin of the Koburra Trough. There are varying views that the distribution of the Aramac Coal Measures has been either the uppermost eroded remnant of the Joe Joe Group, or that it is largely controlled by syndepositional structural movements, with the thickest coal seams accumulated in fault-controlled grabens and half-grabens (Scott and Hawkins, 1992; Scott et al, 1995). The drillhole data (Table 5) indicate that although it can be up to 272 m in thickness in the Lovelle Depression, it has a mean thickness of 106 m with 90% of drillhole intercepts being less than 194 m in thickness.

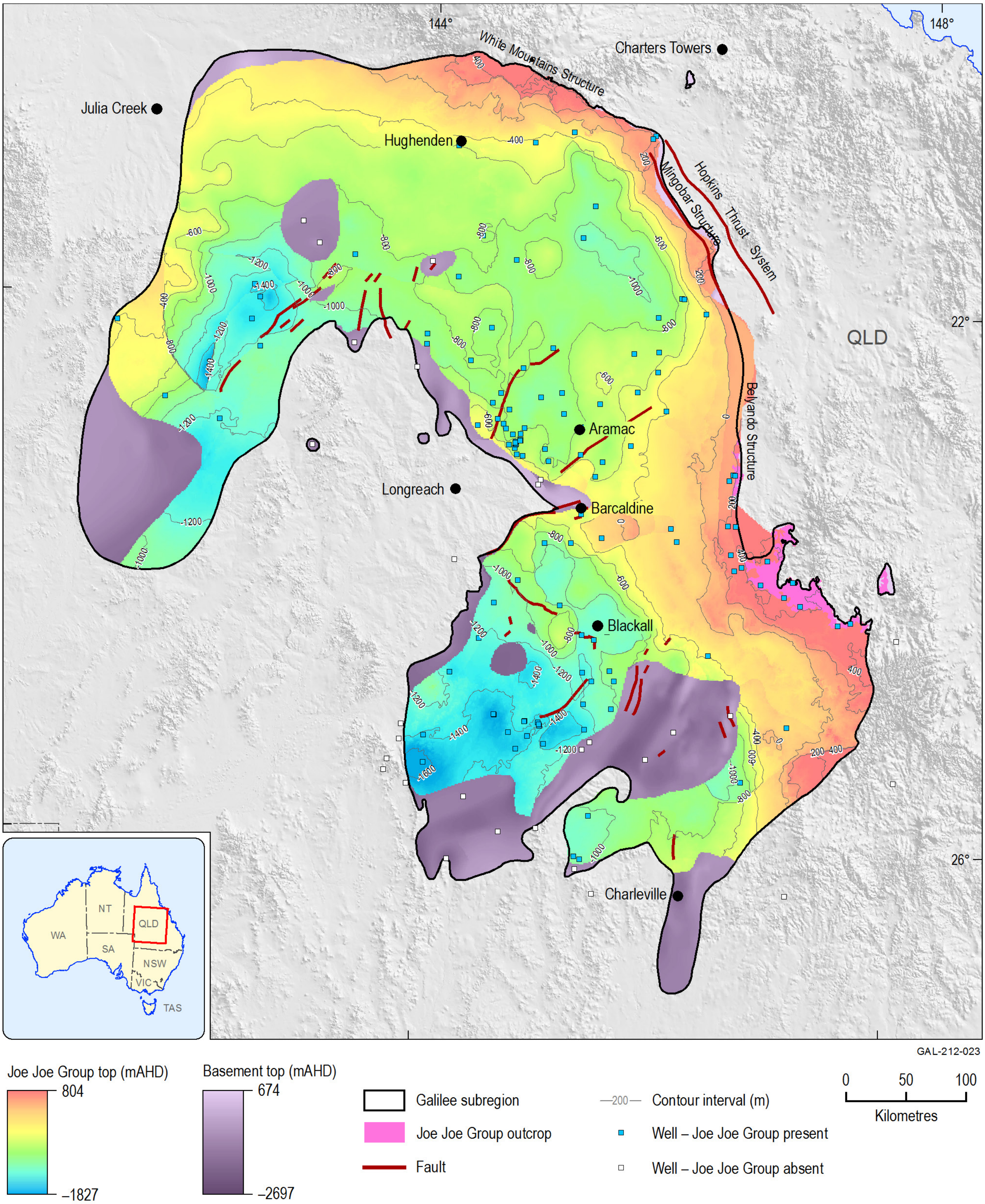


**Figure 27 Depth to top of the Joe Joe Group in the Galilee Basin**

Data: Bioregional Assessment Programme (Dataset 13)

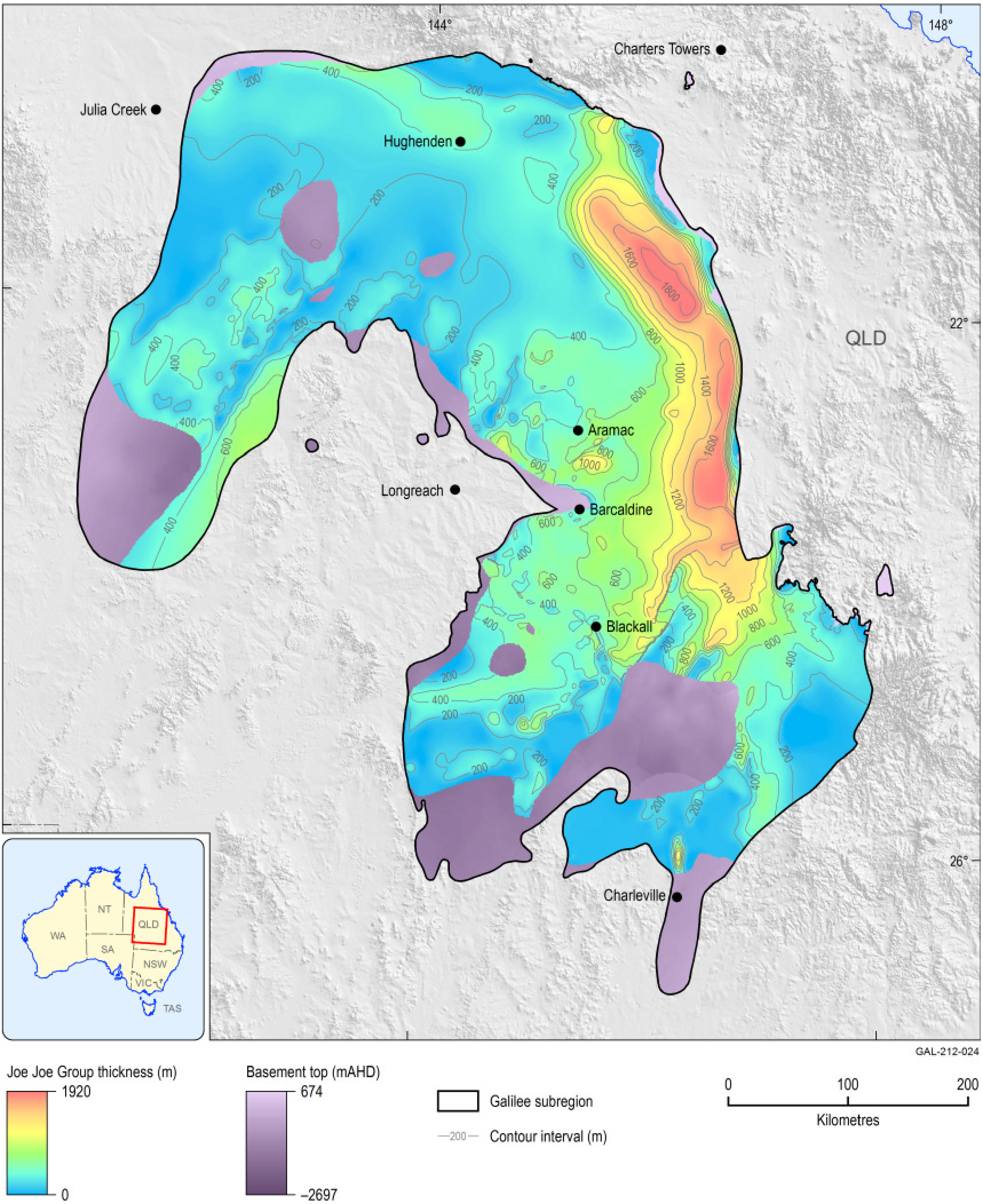


Figure 28 Extent and thickness of the Joe Joe Group in the Galilee Basin

Data: Bioregional Assessment Programme (Dataset 13)

### Top of basement

The top of basement surface is represented by structural contours of the base of the Galilee Basin (Figure 29). Basement rocks outcrop to the east of the Galilee subregion. Many of the faults that are evident in basement do not necessarily have surface expression. However, many faults have repeatedly influenced deposition and erosion through their reactivation at various stages during the history of basin development in the Galilee subregion (companion product 1.1 (Evans et al., 2014)).

The three main depocentres for the Galilee Basin form prominent depressions in the top of basement. Along parts of the eastern margin of the Galilee Basin, depth to basement drops significantly into the Koburra Trough with the deepest areas being in the order of 2600 m BSL. The southern margin of the Koburra Trough may terminate against the Warrego Fault and Pleasant Creek Arch.

In the northern Galilee Basin, the Aramac Trough and Barcaldine Ridge are also prominent, as are the complex series of basement highs associated with the north-eastern margin of the Maneroo Platform. In the southern Galilee Basin, a series of faults bound the north-eastern margin of the Powell Depression, whereas the Warrego Fault and Pleasant Creek Arch cross-cut the basin just to the south-east of Blackall.

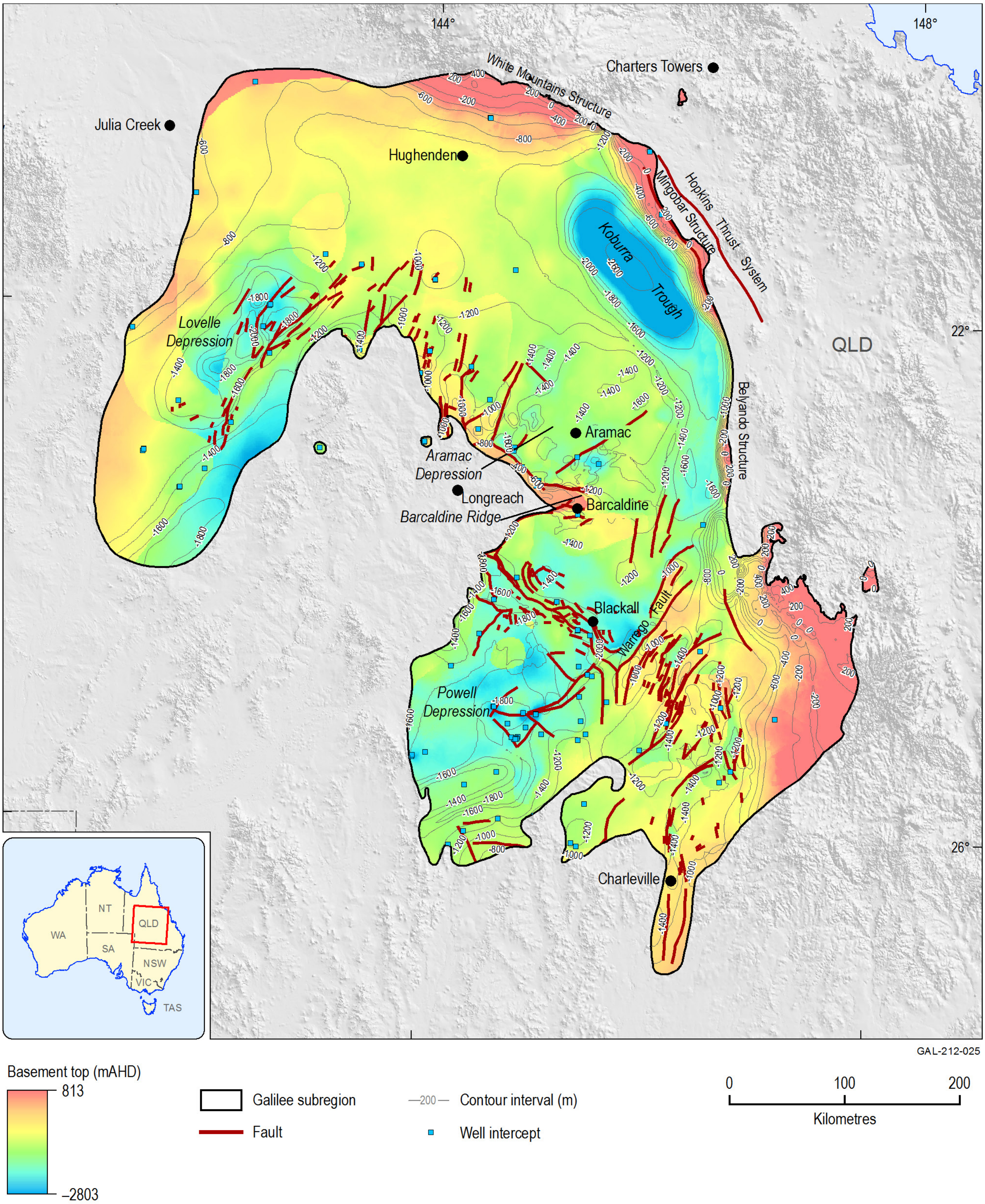


**Figure 29 Depth to basement of the Galilee Basin**

Data: Bioregional Assessment Programme (Dataset 13)

### *2.1.2.2.5.5 Combined geological model sections and uncertainty*

In Figure 30a, the Galilee Basin sequence is overlain by rocks of the Eromanga Basin and superficial Cenozoic sediments. The Eromanga Basin sequence can be up to 1 km thick with the recharge beds for the Eromanga Basin aquifers outcropping at the north end of section (Figure 30).

Additionally, the Rewan Group is missing and upper Permian Coal measures are directly overlain by Clematis Group and the Moolayember Formation. Heading south into the Galilee Basin, the Rewan Group occurs but the Moolayember Formation thins out. In the far south the edge of the Galilee Basin is faulted out against the Maneroo Platform and thus Eromanga Basin sequences are resting on basement rocks (Maneroo Platform).

Figure 30b and Figure 30c are cross-sections from the western Galilee Basin margin across the Koburra and Aramac troughs, to the eastern margin of the Galilee subregion. The Koburra and Aramac troughs are separated by the North Galilee Rise (Section 2.1.2.2.3). Near the eastern edge of Figure 30b, the upper Permian coal measures, Rewan Formation and Clematis Group outcrop to the east or near the crest of the Great Dividing Range. West of the Great Dividing Range the outcrop is dominated by Moolayember Formation until the edge of the Eromanga Basin is reached around the centre of the section. Here, the recharge beds for the GAB outcrop. Recharge bed outcrop (Figure 30b) consists predominantly of Hutton Sandstone and Cadna-owie – Hooray Sandstone. Further west the recharge beds are buried by the Wallumbilla Formation and the Winton-Mackunda formations. In the far south-west the Galilee Basin margin is faulted against the Maneroo Platform by the Hulton–Rand Structure (Section 2.1.2.2.3).

Figure 31 includes two cross-sections located in the southern Galilee Basin. Figure 31a runs from the eastern margin of the Galilee Basin through the Powell Depression to terminate near the Canaway Fault. Outcrop of Galilee Basin sedimentary rocks occurs east of the Great Dividing Range on the Springsure Shelf (Section 2.1.2.2.3). At depth most of the Galilee Basin sedimentary fill consists of Joe Joe Group. Once off the Springsure Shelf the Rewan Group is largely missing and the upper Permian coal measures pinch out as they go into the Powell Depression. Most of the sedimentary fill in the Powell Depression consists of Eromanga Basin strata, in particular the Winton-Mackunda and Wallumbilla formations.

Figure 31b runs from north-west to south-east across the Powell Depression. The Galilee Basin sequence is relatively thin and partially preserved in fault-bounded blocks beneath a thick sequence of Eromanga Basin sedimentary rocks. Faults in this section appear to not have been active after the deposition of Galilee Basin sedimentary rocks. There are areas where upper Permian coal measures and Clematis Group are in direct contact with base of the Eromanga sequence. The whole Galilee subregion sedimentary sequence has been deformed into a series of open folds east of the Pleasant Creek Arch.

Figure 32a presents a regional section along the Koburra Trough and the eastern margin of the Galilee subregion. The main feature is the Koburra Trough with late Permian sedimentary packages dipping into it from the north and the south. On the northern flank of the Koburra Trough, the Rewan Group pinches out allowing the Clematis Group (probably Warang Sandstone) to be in direct contact with upper Permian coal measures.

Figure 32b is a regional section, running along the western margin of the Galilee subregion, then once south of the Barcaldine Ridge, it cuts across the trends of major structures in the southern Galilee Basin. The Barcaldine Ridge (Figure 23b) forms the boundary between northern and southern Galilee Basin. On the Barcaldine Ridge itself, much of the Galilee Basin sequence is missing, allowing upper Permian coal measures to be in direct contact with the Hutton Sandstone. On either side of the ridge the full Galilee Basin sequence is present. However, it is significantly thicker north of the Barcaldine Ridge than it is to the south. This suggests that the Barcaldine Ridge structures were active during deposition of the upper Permian and Triassic Galilee Basin sequences. Another feature of interest is the three jagged ‘peaks’ in the basement, north of the Aramac Depression. These ‘peaks’ are the fault-bound ridges that run northwards off the Maneroo Platform (Marathona Monocline, Darriveen Structure and Beryl Ridge). The upfaulted block in the far northern part of the section is associated with the Cork Fault and the Wetherby Terrace.

Figure 32c is a long-section down the Lovelle Depression. Here the Galilee Basin sequence is relatively thin when compared to other parts of the Galilee Basin. The upper Permian coal measures do not occur in much of the Lovelle Depression. Much of the sedimentary fill in the Lovelle Depression is assigned to the Eromanga Basin, in particular the Wallumbilla Formation and Winton-Mackunda formations.

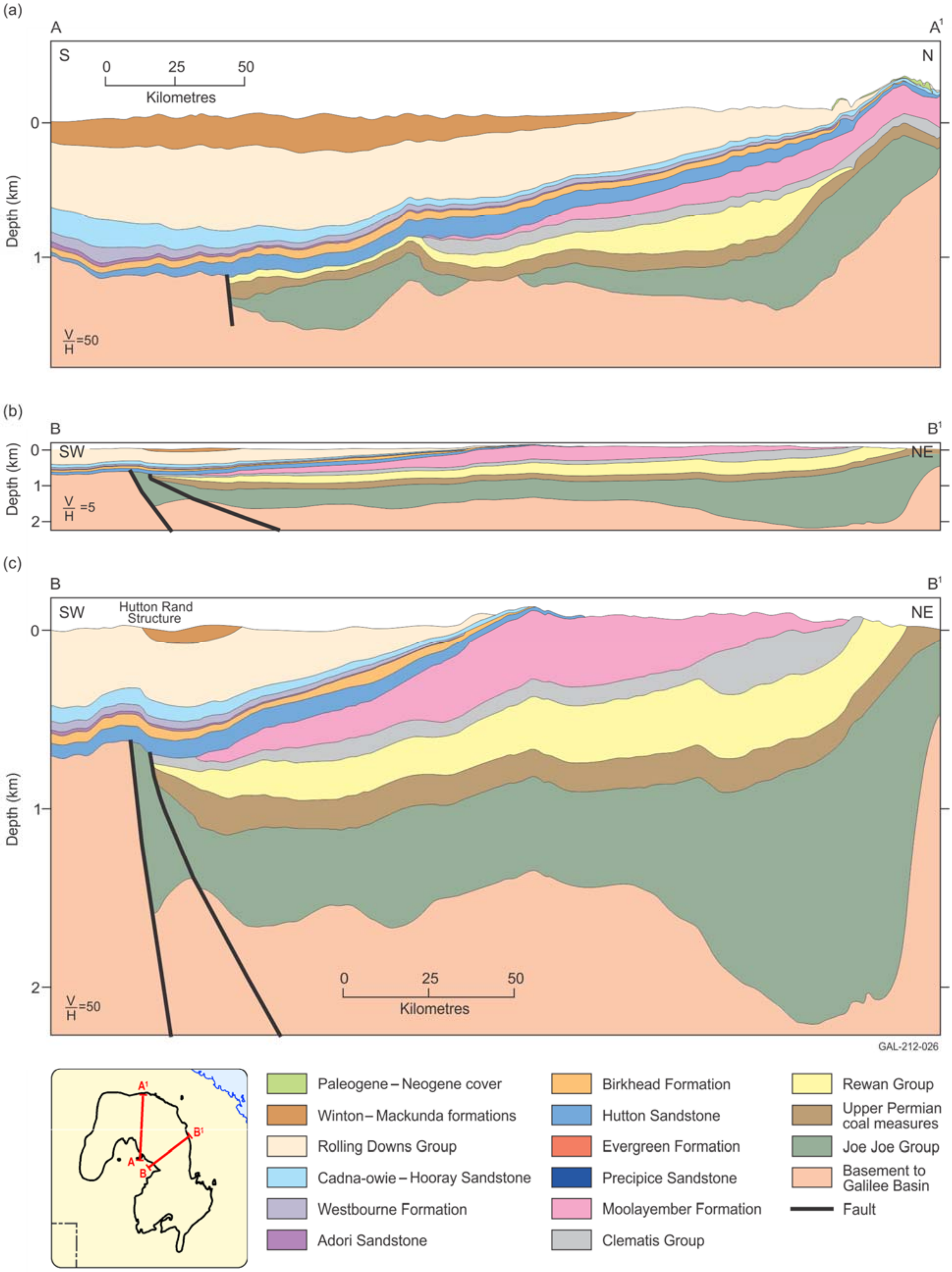


**Figure 30 Regional cross-sections for the northern parts of the Galilee subregion**

Data: Bioregional Assessment Programme (Dataset 13)

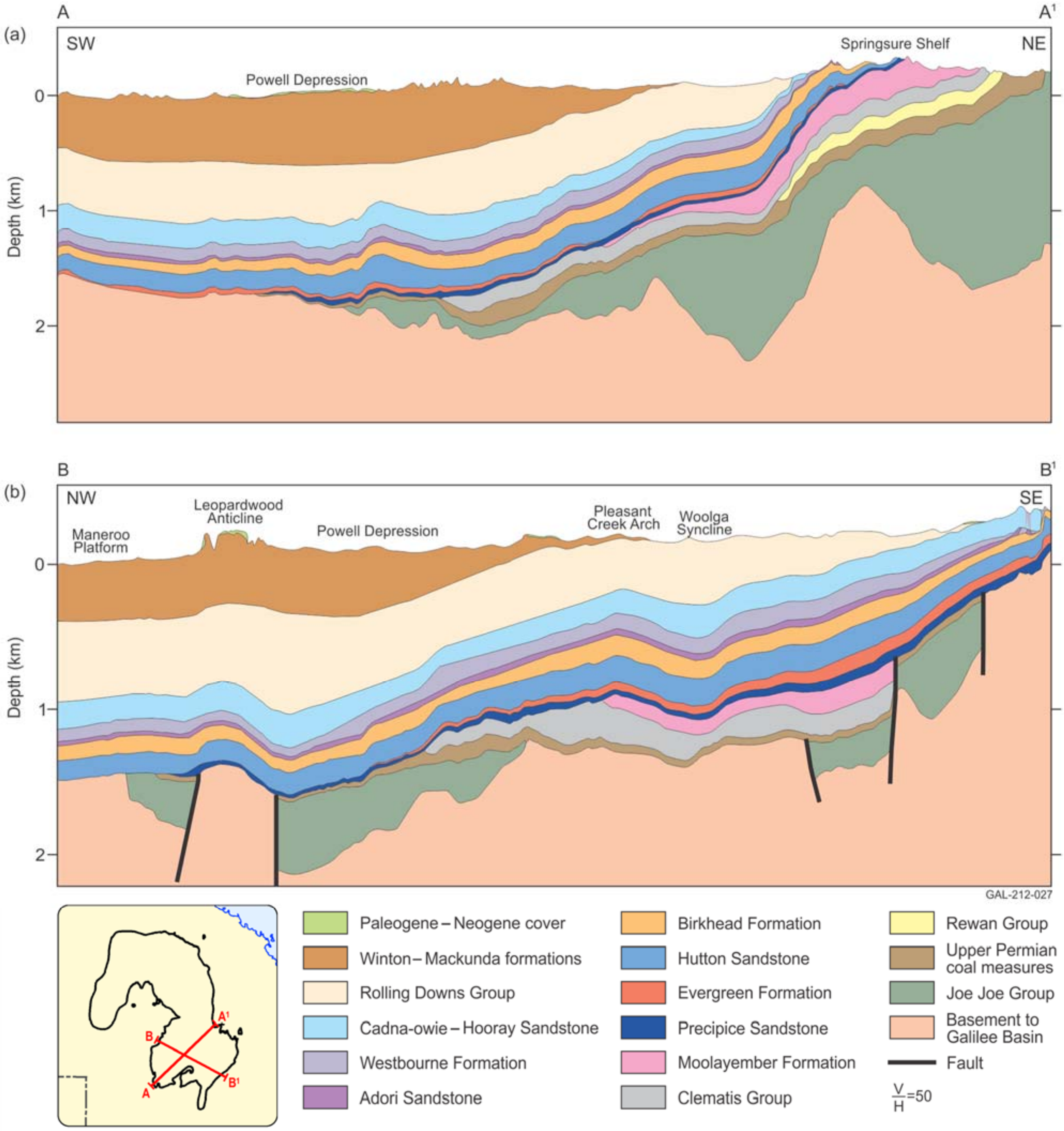


**Figure 31 Regional cross-sections for the southern portions of the Galilee subregion**

H = horizontal, V = vertical
Data: Bioregional Assessment Programme (Dataset 13)

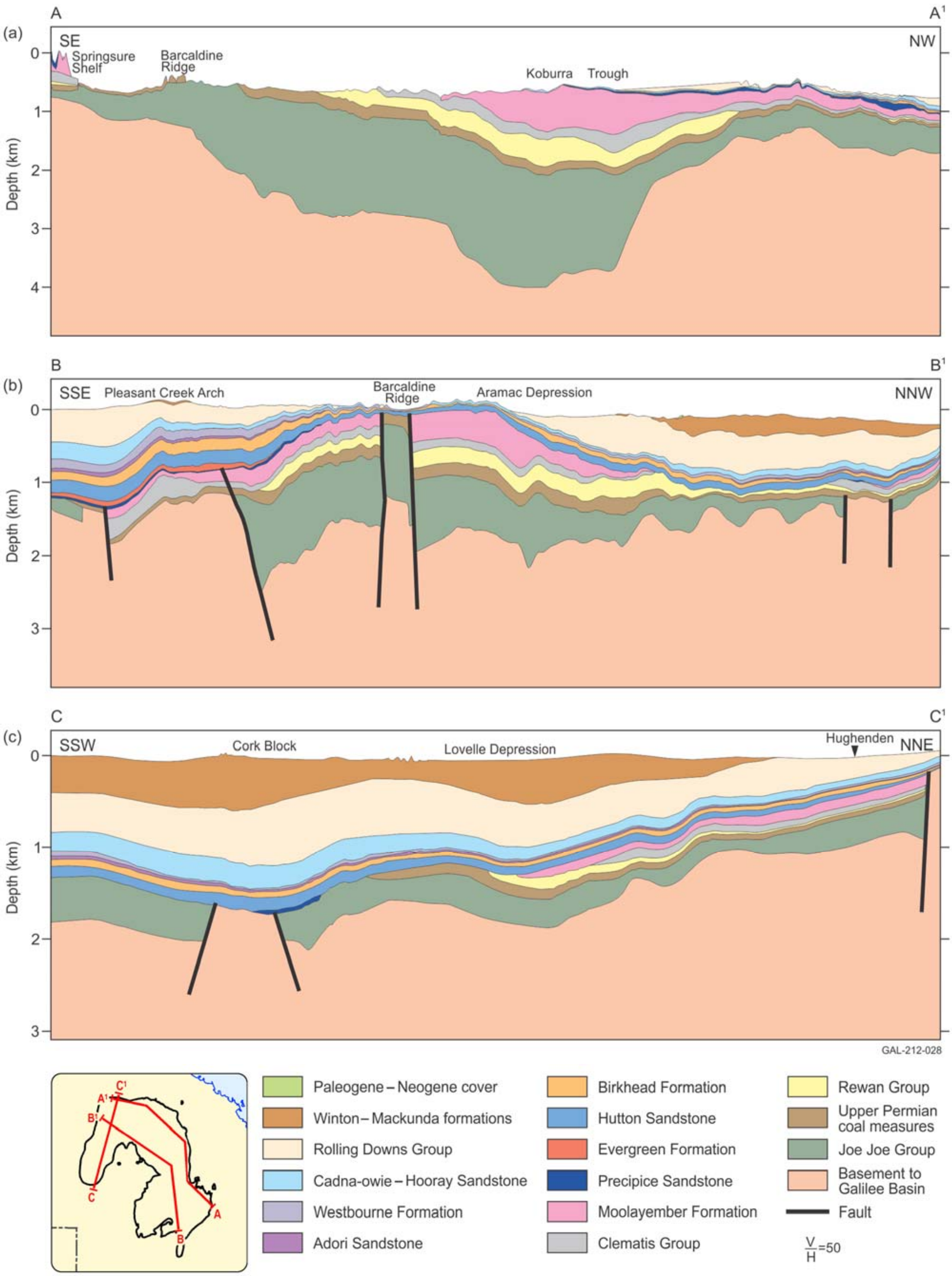


**Figure 32 Regional long sections for the Galilee subregion**

(a) cross-section A to A1. Eastern margin of the Galilee subregion (section looking to the south-west)
(b) cross-section B to B1. Centre of the Galilee subregion (section looking to the south-west)
(c) cross-section C to C1. Lovelle Depression (section looking to the north-west)
Data: Bioregional Assessment Programme (Dataset 13)

#### *2.1.2.2.5.6 Eromanga–Galilee three-dimensional geological model: limitations and uncertainty*

A stratigraphic model was originally constructed for the Galilee Basin from basement upwards because the templates of basement faults and an interpreted magnetic basement surface (OZ SEEBASE) were already available. The OZ SEEBASE surface is an interpretation of depth to magnetic basement which, apart from intrusions, may occur at various stratigraphic levels within the geological basement itself. The implication is that in the absence of other data, such as seismic interpretation or drillhole intercepts, the OZ SEEBASE basement surface won't always coincide with the actual interface between overlying sedimentary basins and geological basement. A basement surface for the Galilee Basin was developed from the OZ SEEBASE basement surface through depth correction from drill data and/or available seismic interpretation.

When the isopach data for the Eromanga Basin sequence was later added and compiled from ground surface downwards to the first iteration of the modelled Galilee stratigraphic layers, it became apparent that there were disparities in the order of hundreds of metres, between the top of Galilee and base of Eromanga basins. As a result, it was decided to compile all layers of Eromanga and Galilee basins from the ground surface down to the top of geological basement (bottom of the Galilee Basin). This resulted in a second iteration of all Galilee stratigraphic layers as well as geological basement.

It was found that utilising the top down approach minimises the introduction of errors from the OZ SEEBASE dataset. Also, uncertainty would increase with depth in part due to a decrease in drillhole data reaching a maximum value at the base of the model (top of basement). Confidence in geological modelling would be lowest at depth in areas where there is little drillhole data or seismic mapping. Confidence would be higher at shallower levels, in areas with higher density of drillhole data and seismic coverage.

As an example of an estimate of uncertainty, the two top of basement surfaces for the Galilee Basin – one generated from the basement up and the other from the ground surface down approach – were compared to generate a percentage of uncertainty. Accordingly, this level of uncertainty is a 'worst case scenario situation' as geological basement is the deepest layer.

One uncertainty that remains in the top-down approach to modelling was the estimation of thickness of Cenozoic (Quaternary) sediments. These data are not available from the GAB Atlas (Ransley et al., 2015). However, anticipated error in estimation of the Quaternary thickness is an order of magnitude lower than prediction error at the basement to the Galilee Basin.

The level of confidence of the subsurface extent of the Galilee Basin and individual units within the sequence is variable to low in the south-east and north-west (Figure 33). Seismic reflection survey lines are mainly clustered in the Powell Depression, the margin of the Maneroo Platform and around to the central region of the Lovelle Depression. Only a few seismic reflection survey lines traverse the Koburra Trough (Figure 33). Along the margins of the Galilee Basin the category of higher relative uncertainty is mostly the result of little or no publicly available data, as well as increased relative error at shallow depth.

Predictably for areas with sufficient data, the disparity between the two approaches is minimal, although significant disparities exist in data-poor areas. If required, stratigraphic data gaps in data poor areas could be decreased through the drilling of stratigraphic wells or undertaking geophysical surveys such as seismic reflection surveys.

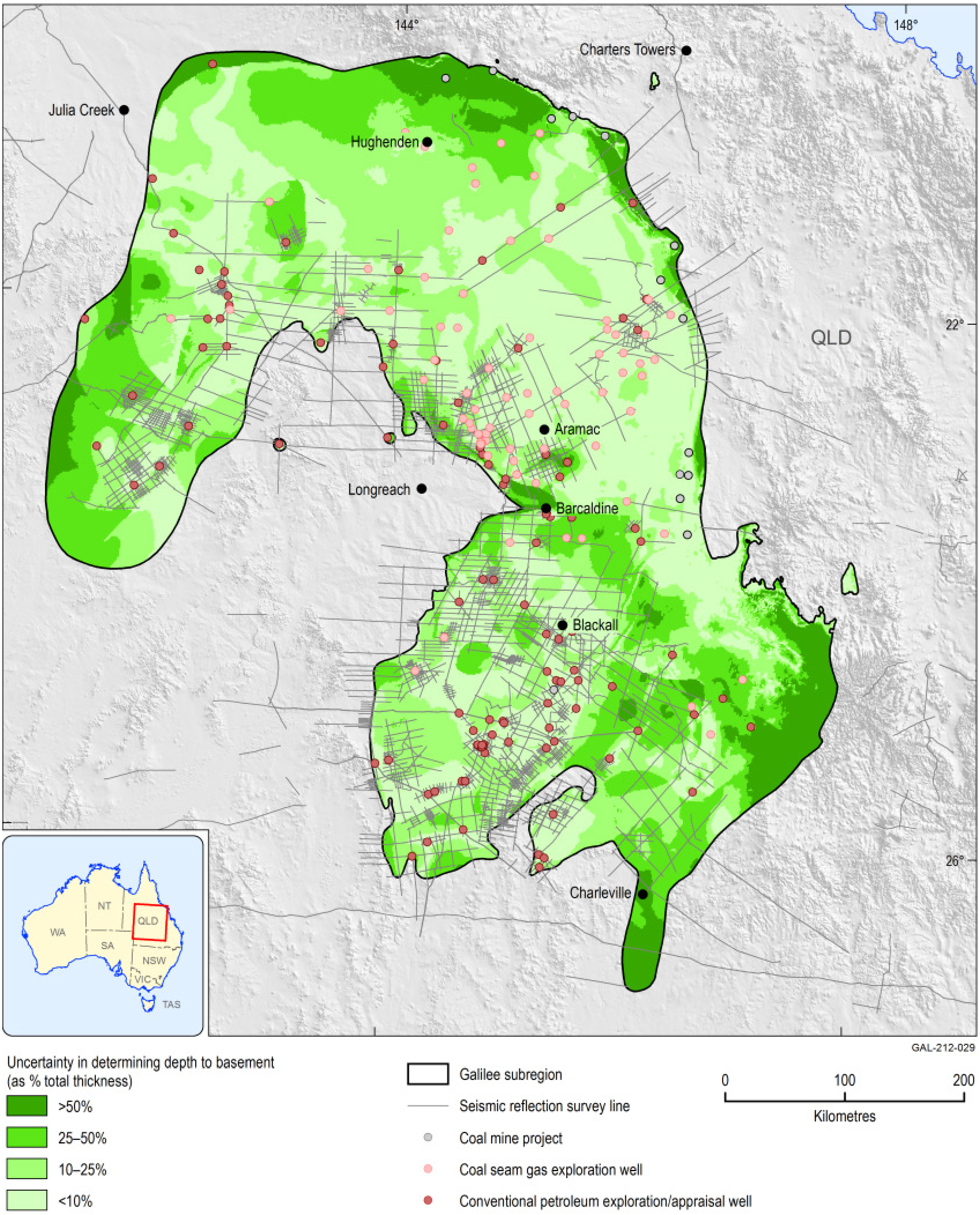


**Figure 33 An estimate of modelling uncertainty for top of Galilee basement**

Uncertainty in the estimate of depth to basement is presented as a percentage difference in depth estimates between modelling geological layers by the basement-up and from the top-down approach. Where reliable data sources, such as deep drillholes or seismic reflection surveys are present, the results of the two approaches are very similar.
Data: Bureau of Meteorology (Dataset 1), Bioregional Assessment Programme (Dataset 13)

### 2.1.2.3 Gaps

There are several geological data gaps for the Galilee subregion:

- Approximately 8% of all groundwater bores are missing drillhole depth measurements.
- Currently, approximately 70% of groundwater bores in the Galilee subregion either have no stratigraphic data, or do not have usable data for geological modelling. Also, data analysis workflows would be streamlined if existing stratigraphic data records could be standardised; for example, removing spelling errors or variations in spelling, errant characters and include (if available) top and bottom information for each stratigraphic entry. Most groundwater bores are missing ground elevation measurements. Additionally, some existing elevation data in Queensland Department of Natural Resources and Mines (Dataset 16) were recorded relative to a state elevation datum rather than the national elevation datum. It may be useful to convert existing elevation data as required so that they reference the national elevation datum.
- No reference elevation data are included in Queensland Department of Natural Resources and Mines (Dataset 16) for petroleum and CSG wells. While elevation data can be sourced from relevant well completion reports, workflows would be streamlined if these data could be included in the digital databases.
- Access to at least some company coal drilling data would greatly improve the accuracy of geological models in the vicinity of coal mine project areas along the eastern margin of the Galilee subregion. Not all of that drilling data would be required, but ideally bore location data, stratigraphic picks and, if possible, some geophysical well logs.
- Some bores drilled for stratigraphic investigations in the 1960s to 1970s appear to be missing stratigraphic data records. It would be useful to access and incorporate these missing data into the databases.
- The geological Galilee Basin boundary, in particular areas along its eastern margin, need to be updated in light of the geological modelling presented here. Any update should consider utilising regional geophysical datasets to refine the boundary and, if available, recent company coal and CSG drillhole data and more detailed surface mapping. Access to more detailed company geological mapping (including structural mapping) would also improve the Galilee geological models, particularly along the Galilee subregion’s eastern boundary. These data would assist in resolving the discrepancies that exist in available geological surface mapping.
- Some stratigraphic correlations, particularly in the upper Permian and Triassic sequences of the Galilee Basin, could be refined by more age dating and biostratigraphy. This would lessen uncertainty in regional correlation and thus geological modelling. Some of this work is already underway (e.g. Nicoll et al., 2015; Phillips et al., 2015, 2016). Future refinements of the Galilee subregion geological model should consider incorporating upper Permian stratigraphy outlined in Phillips et al. (2015, 2016) if data are available.
- Further detailed interpretation of existing two-dimensional seismic and geophysical well logs and incorporation of updated interpretations would improve geological models. If available seismic and well log information is considered fit for purpose, they could be used for other

purposes such as distribution and variation in lithology, porosity and more detailed structural analysis.

- Although there is a general understanding of regional structure, there seems to be little available information on local structures that may exist in the Galilee subregion. More localised structures do exist and have been documented from recent reporting (Section 2.1.2.2.3). Use of regional geophysical datasets, and available seismic, well logs and coal company data are likely to provide further understanding on more local-scale structures. A more detailed understanding of structures would improve geological and hydrogeological modelling.
- Figure 33 shows the worst case scenario of uncertainty of Galilee basement position across the Galilee subregion. This is especially the case near basin margins and highlights the paucity of available stratigraphic control and the need for regional seismic transects to extend control across the entire subregion. Some of this uncertainty could potentially be alleviated by the incorporation of company drillhole data into the geological models.
- Present understanding of regional structure has evolved from regional mapping, seismic reflection surveys and exploration drilling. These investigations could be used to improve the interpretation of structural elements that are graphically indicated in potential field imagery, that of gravity and magnetics (Figure 8). Lower resolution datasets had been the basis of the OZ SEEBASE model of magnetic basement (de Vries et al., 2006), but with recent upgrading of dataset resolution, there is a need for a new iteration of interpretive modelling of magnetic basement. However, even with improvement in a modelled magnetic basement, the uncertainties of thickness of underlying sedimentary sequences in the Adavale, Drummond and Belyando basins remain dependent on additional seismic data, given the very limited number of drillholes in these areas.
- Knowledge of the thickness, structure and lithological variations within Cenozoic sequences is very limited across the Galilee subregion. One option that would improve understanding of the Cenozoic sediments would be acquisition of airborne electromagnetic (AEM) data in the subregion. If required, the AEM survey could be complemented by a shallow drilling program or use of existing company-supplied drilling data (if applicable), to provide stratigraphic control for modelling the thickness and characteristics of the near-surface cover. The AEM data would also provide information on shallow groundwater systems, and potentially identify areas of connectivity between Cenozoic cover and underlying regional GAB aquifers.

## *References*

AGE Consultants Pty Ltd (2015) Project China Stone groundwater report: Project China Stone Draft EIS Appendix I groundwater report dated 25 July 2015. Viewed 6 November 2015, http://www.hansenbailey.com.au/documents/stone/Project_China_Stone_EIS_I_Groundwater.pdf.

Allen RJ (1974) Hydrocarbon significance of Upper Palaeozoic sediments associated with the Koburra trough, Galilee Basin. Journal of the Australian Petroleum Exploration Association 14, 59–65.

Allen JP and Fielding CR (2007) Sequence architecture within a low accommodation setting: an example from the Permian of Galilee and Bowen basins, Queensland, Australia. AAPG Bulletin 91(11), 1503–1539.

Archer DW and Armstrong KD (1986) Holberton No.1 well completion report Eromanga Hydrocarbons N.L., Company Report 15985, QDEX Queensland Department of Mines.

Bell RM (1985) Jillaroo No.1 well completion report, Authority to Prospect 279P, Volume 1. Company report 14205 (A) QDEX Queensland Department of Mines.

Blanco E (2010) Coal lithotype response to changing depositional sequences in the Betts Creek beds, Galilee Basin. Unpublished honours thesis, School of Earth Sciences, University of Queensland, Brisbane.

Burra A, Esterle JS and Golding SD (2014) Coal seam gas distribution and hydrodynamics of the Sydney Basin, NSW, Australia. Australian Journal of Earth Sciences 61, 427–451.

Casey DJ (1965a) Explanatory notes on the Manuka geological sheet. Bureau of Mineral Resources, Geology and Geophysics, Canberra.

Casey DJ (1965b) Explanatory notes on the Winton geological sheet. Bureau of Mineral Resources, Geology and Geophysics, Canberra.

Casey DJ (1969) Tangorin, Queensland: Sheet SE/52-9 international index. Bureau of Mineral Resources, Geology and Geophysics, Canberra.

Casey DJ (1970) Northern Eromanga Basin. Report 41. Geological Survey of Queensland, Brisbane.

Casey DJ (1971) Blackall, Qld: Sheet SG/55-1 international index. Bureau of Mineral Resources, Geology and Geophysics, Canberra.

Clarke DE (1970) Charters Towers, Qld. Sheet SF/55-2 international index. Bureau of Mineral Resources, Geology and Geophysics, Canberra.

Cook AG, McKellar JL and Draper JJ (2013) Eromanga Basin. In: Jell PA (ed) Geology of Queensland. Geological Survey of Queensland, 523–533, Brisbane.

de Vries S, Fry N and Pryer L (2006) OZ SEEBASE Proterozoic basins July 2006. FrOG Tech PR107.

DME (2008) Mount Tutah 1:100,000 mapsheet. Queensland Department of Mines and Energy. Published by Geological Survey of Queensland.

Draper JJ (2013) Belyando Basin. In: Jell PA (ed) Geology of Queensland. Geological Survey of Queensland, 174–175, Brisbane.

Evans T, Pavey C, Cassel R, Ransley T, Sparrow A, Kellett J, Lewis S, Galinec V, Dehelean A, Caruana L and Kilgour P (2018) Conceptual modelling for the Galilee subregion. Product 2.3 for the Galilee subregion from the Lake Eyre Basin Bioregional Assessment. Department of the Environment and Energy, Bureau of Meteorology, CSIRO and Geoscience Australia, Australia. http://data.bioregionalassessments.gov.au/product/LEB/GAL/2.3.

Evans T, Karim F, Cassel R, and Harris-Pascal C (2015) Current water accounts and water quality for the Galilee subregion. Product 1.5 for the Galilee subregion from the Lake Eyre Basin Bioregional Assessment. Department of the Environment, Bureau of Meteorology, CSIRO and Geoscience Australia, Australia. Viewed 18 November 2015, http://data.bioregionalassessments.gov.au/product/LEB/GAL/1.5.

Evans T, Tan KP, Magee J, Karim F, Sparrow A, Lewis S, Marshall S, Kellett J and Galinec V (2014) Context statement for the Galilee subregion. Product 1.1 from the Lake Eyre Basin Bioregional Assessment. Department of the Environment, Bureau of Meteorology, CSIRO and Geoscience Australia, Australia. Viewed 2 April 2016, http://data.bioregionalassessments.gov.au/product/LEB/GAL/1.1.

Exon NF (1968) Eddystone, Queensland: Sheet SG/55-7 international index. Bureau of Mineral Resources, Geology and Geophysics, Canberra.

Exon NF (1970) Tambo, Queensland: Sheet SG/55-2 international index. Bureau of Mineral Resources, Geology and Geophysics, Canberra.

Galloway MC (1970a) Adavale, Qld: Sheet SG/55-5 international index. Bureau of Mineral Resources, Geology and Geophysics, Canberra.

Galloway MC (1970b) Augathella, Qld: Sheet SG/55-6 international index. Bureau of Mineral Resources, Geology and Geophysics, Canberra.

Geoscience Australia (2015) GADDS-Geophysical Archive Data Delivery System. Viewed 19 November 2015, http://www.geoscience.gov.au/cgi-bin/mapserv?map=/nas/web/ops/prod/apps/mapserver/gadds/wms_map/gadds.map&mode=browse.

GHD (2013) Report for updated mine project description. Carmichael coal mine and rail project SEIS. Appendix B – updated mine project description of the Carmichael supplementary environmental Impact statement, dated 18 October 2013. Viewed 15 October 2015, http://eisdocs.dsdip.qld.gov.au/Carmichael%20Coal%20Mine%20and%20Rail/SEIS/Appendices/Appendix-B-Updated-Mine-Project-Description.pdf.

Golding SD, Boreham CJ and Esterle JS (2013) Stable isotope geochemistry of coal bed and shale gas and related production waters: a review. International Journal of Coal Geology 120, 24–40.

Gorter JD, Gostin VA and Plummer P (1989) The Tookoonooka Structure: An enigmatic subsurface feature in the Eromanga Basin, its impact origin and implications for petroleum exploration. In: O’Neil BJ (ed) The Cooper and Eromanga Basins Australia. Proceedings of Petroleum Exploration Society of Australia, Society of Petroleum Engineers, Australian Society of Exploration Geophysicists (SA Branches), 441–456.

Gray ARG (1977) Stratigraphic drilling in the Hughenden 1:250,000 Sheet Area, 1974-75. Queensland Government Mining Journal 78, 382–392.

Gregory CM (1969) Windorah, Qld: Sheet SG/54-8 international index. Bureau of Mineral Resources, Geology and Geophysics, Canberra.

Hamilton SK, Esterle JS and Golding SD (2012) Geological interpretation of gas content trends, Walloon Subgroup, eastern Surat Basin, Queensland, Australia. International Journal of Coal Geology 101, 21–35.

Hamilton SK, Golding SD, Baublys KA and Esterle JS (2015) Conceptual exploration targeting for microbially enhanced coal bed methane (MECoM) in the Walloon Subgroup, eastern Surat Basin, Queensland, Australia. International Journal of Coal Geology 138, 68–82.

Hancock Prospecting Pty Ltd (2011) Coal mine - groundwater and final void report. Appendix N – Alpha Coal project supplementary environmental Impact statement Issue 4A, dated August 2011. Viewed 15 October 2015, http://gvkhancockcoal.com/documents/Publications/EIS/ACPSEIS2011/Volume2/Volume%202%20Appendix%20%20N%20Groundwater%20and%20Final%20Void%20Report%20Issue%203%20Final.pdf.

Harrison PL and Bauer JA (1976) Galilee Basin seismic survey, Queensland. Operational report. Bureau of Mineral Resources Record 27.

I'Anson A (2013) Coal seam gas in the Galilee Basin, Queensland. Unpublished honours thesis. University of Sydney.

Jauncey W (1962) Explanatory notes, Brighton Downs Sheet, Queensland (BMR Explanatory Notes and Map). Bureau of Mineral Resources, Geology and Geophysics, Canberra.

Jauncey W (1965) Explanatory notes on the Maneroo geological sheet. Bureau of Mineral Resources, Geology and Geophysics, Canberra.

Jones AT and Fielding CR (2008) Sedimentary facies of a glacially influenced continental succession in the Pennsylvanian Jericho Formation, Galilee Basin, Australia. Sedimentology 55, 531–556.

Lewis S, Cassel R and Galinec V (2014) Coal and coal seam gas resource assessment for the Galilee subregion. Product 1.2 for the Galilee subregion from the Lake Eyre Basin Bioregional Assessment. Department of the Environment, Bureau of Meteorology, CSIRO and Geoscience Australia, Australia. Viewed 18 November 2015, http://data.bioregionalassessments.gov.au/product/LEB/GAL/1.2.

Lewis S, Evans T, Pavey C, Holland KL, Henderson BL, Kilgour P, Dehelean A, Karim F, Viney NR, Post DA, Schmidt RK, Sudholz C, Brandon C, Zhang YQ, Lymburner L, Dunn B, Mount R, Gonzales D, Peeters LJM, O' Grady A, Dunne R, Ickowicz A, Hosack G, Hayes KR, Dambacher J, Barry S (2018) Impact and risk analysis for the Galilee subregion. Product 3-4 for the Galilee subregion from the Lake Eyre Basin Bioregional Assessment. Department of the Environment and Energy, Bureau of Meteorology, CSIRO and Geoscience Australia, Australia. http://data.bioregionalassessments.gov.au/product/LEB/GAL/3-4.

Longley IM (1989) The Talundilly anomaly and its implications for hydrocarbon exploration of Eromanga astroblemes. In: O'Neil BJ (ed.) Proceedings of Petroleum Exploration Society of Australia, Society of Petroleum Engineers, Australian Society of Exploration Geophysicists (SA Branches), 473–490.

Marsh C, Rawsthorn K, Causebrook R, Kalinowski A, and Newlands I (2008) A geological review of the Galilee Basin, Queensland for possible storage of carbon dioxide. Cooperative Research Centre for Greenhouse Gas Technologies, Canberra, Australia. CO2CRC Report No. RPT08-0983.

McKellar JL and Henderson RA (2013) Galilee Basin. In: Jell PA (ed) Geology of Queensland. Geological Survey of Queensland, 196–202, Brisbane.

Mollan RG (1967) Springsure, Qld: Sheet SG/55-3 international index. Bureau of Mineral Resources, Geology and Geophysics, Canberra.

Moya CE, Raiber M, and Cox ME (2014) Three dimensional geological modelling of the Galilee and central Eromanga basins, Australia: New insights into aquifer/aquitard geometry and potential influence of faults on inter-connectivity. Journal of Hydrology: Regional Studies 2, 119–139.

MSEC (2013) Carmichael Project – revised subsidence assessment: In support of the Environmental Impact Assessment: Carmichael Coal and Rail Project SEIS Appendix I1, 25 November 2013. Viewed 2 November 2015, http://www.adanimining.com/Common/Uploads/SEISDocuments/101_SEISDoc_Appendix%20I1%20-%20Revised%20Subsidence%20Assessment%20Report.pdf.

Nakamura A and Milligan PR (2015) Total magnetic intensity (TMI) image of Australia with variable reduction to pole (VRTP) greyscale. Geoscience Australia, Canberra.

Nicoll R, McKellar J, Areeba A, Laurie J, Esterle J, Crowley J, Wood G and Bodorkos S (2015) CA-IDTIMS dating of tuffs, calibration of palynostratigraphy and stratigraphy of the Bowen and Galilee basins. In: Beeston, J.W. (Ed.) Bowen Basin Symposium 2015—Bowen Basin and Beyond. Geological Society of Australia Inc. Coal Geology Group and the Bowen Basin Geologists Group, Brisbane, October, 2015, 211–218.

Norvick M (1981) Permian and Late Carboniferous palynostratigraphy of the Galilee Basin, Queensland. Report 219, Bureau of Mineral Resources, Geology and Geophysics, 219.

Olgers F (1969) Emerald, Queensland: Sheet SF/55-15 international index. Bureau of Mineral Resources, Geology and Geophysics, Canberra.

Olgers F (1970) Buchanan, Queensland: Sheet SF/55-6 international index. Bureau of Mineral Resources, Geology and Geophysics, Canberra.

Ozimic S (1986) The geology and petrophysics of the Toolebuc Formation and its time equivalents, Eromanga and Carpentaria Basins. In: Gravestock DI, Moore PS and Pitt GM (eds) Contributions to the geology and hydrocarbon potential of the Eromanga Basin. Geological Society of Australia, Special Publication 12, 119–137.

Pinchin J (1978) A seismic investigation of the eastern margin of the Galilee Basin, Queensland. BMR Journal of Australian Geology and Geophysics 3, 1978, 193–202.

Phillips LJ, Esterle JS and Silwa R (2015) Rationalising the Late Permian coal seam stratigraphy of the Koburra Trough, Galilee Basin. In: Beeston, J.W. (Ed.) Bowen Basin Symposium 2015—Bowen Basin and Beyond. Geological Society of Australia Inc. Coal Geology Group and the Bowen Basin Geologists Group, Brisbane, October, 2015, 219–226.

Phillips L; Bianchi V and Esterle J (2016) Sedimentary trends in Late Permian coal measures of the Galilee Basin. Poster presented at Australian Earth Sciences Convention, Adelaide, June, 2016.

Ransley TR, Radke BM, Feitz AJ, Kellett JR, Owens R, Bell J, Stewart G and Carey H (2015) Hydrogeological Atlas of the Great Artesian Basin. Geoscience Australia, Canberra. Viewed 18 November 2015, http://dx.doi.org/10.11636/9781925124668.

Ransley TR and Smerdon BD (2012) Hydrostratigraphy, hydrogeology and system conceptualisation of the Great Artesian Basin. A technical report to the Australian Government from the CSIRO Great Artesian Basin Water Resource Assessment. Viewed 15 October 2015, https://publications.csiro.au/rpr/download?pid=csiro:EP132693&dsid=DS5.

Saul G, Spargo S, Skinner M, Biggs N, Hansen A, and Coulls R (2015) The geology of the Hyde Park coal project. In: Beeston JW (ed) Bowen Basin Symposium 2015—Bowen Basin and Beyond. Geological Society of Australia Inc. Coal Geology Group and the Bowen Basin Geologists Group, Brisbane, October, 2015, 235–246.

Scott SG, Beeston JW and Carr AF (1995) Galilee Basin. In: Ward CR, Harrington HJ, Mallett CW and Beeston JW (eds) Geology of Australian Coal Basins. Geological Society of Australia – Coal Geology Group 1, 341–353.

Scott SG and Hawkins PJ (1992) Coal geology of the northern Galilee Basin and its implications for coalbed methane investigations. Symposium on coalbed methane research and development in Australia, Townsville November 1992, James Cook University of North Queensland.

Seedsman Geotechnics Pty Ltd (2012) South Galilee Coal Project life of mine subsidence deformations: South Galilee Coal Project EIS Appendix H – subsidence technical report. Viewed 6 November 2015, http://www.southgalilee.com.au/files/EIS/SGCP_EIS_Appendix_H_Subsidence_Technical_Report.pdf.

Senior BR (1969a) Connemara, Queensland: Sheet SG/54-3 international index. Bureau of Mineral Resources, Geology and Geophysics, Canberra.

Senior BR (1969b) Jundah, Queensland: Sheet SG/54-4 international index. Bureau of Mineral Resources, Geology and Geophysics, Canberra.

Senior BR (1971a) Quilpie, Queensland: Sheet SG/55-9 international index. Bureau of Mineral Resources, Geology and Geophysics, Canberra.

Senior BR, Exon NF and Burger D (1975) The Cadna-owie and Toolebuc Formations in the Eromanga Basin, Queensland. Queensland Government Mining Journal 76, 445–455.

Senior D (1971b) Charleville, Queensland: Sheet SG/55-10 international index. Bureau of Mineral Resources, Geology and Geophysics, Canberra.

Senior D (1973) Jericho, Queensland: Sheet SF/55-14 international index. Australian Government Publishing Service, Canberra.

SGCP (2012) Chapter 4 - project description. South Galilee coal project environmental impact statement dated 20 October 2012. Viewed 15 October 2015, http://www.southgalilee.com.au/files/EIS/SGCP_EIS_04_Project_Description.pdf.

Spampinato GPT, Ailleres L, Betts PG and Armit RJ (2015a) Imaging the basement architecture across the Cork Fault in Queensland using magnetic and gravity data. Precambrian Research 264, 63–81.

Spampinato GPT, Betts PG, Ailleres L and Armit RJ (2015b) Early tectonic evolution of the Thomson Orogen in Queensland inferred from constrained magnetic and gravity data. Tectonophysics 651-652, 99–120.

Spampinato GPT, Betts PG and Armit RJ (2015c) Crustal architecture of the Thomson Orogen in Queensland inferred from potential field forward modelling, Australian Journal of Earth Sciences 62(5), 581–603.

URS (2012a) Kevin's Corner SEIS groundwater report: SEIS Volume 2 Appendix L groundwater report dated 18 May 2012. Viewed 6 November 2015, http://gvkhancockcoal.com/documents/Publications/EIS/KevinsCornerSEIS2012/Volume2/Volume%202%20-%20App%20L%20Groundwater%20Report.pdf.

URS (2012b) Groundwater modelling report – Alpha Coal Project: supplementary environmental reports dated 28 March 2012. Viewed 2 November 2015, http://gvkhancockcoal.com/documents/Publications/EIS/ACPSup2012/Alpha%20Coal%20Project%20Groundwater%20Report%20March%202012.pdf.

Vine RR (1962a) Explanatory notes, Julia Creek Sheet, Queensland. (BMR Explan. Notes and Map). Bureau of Mineral Resources, Geology and Geophysics, Canberra.

Vine RR (1962b) Explanatory notes, Mackunda Sheet, Queensland. (BMR Explan. Notes and Map.). Bureau of Mineral Resources, Geology and Geophysics, Canberra.

Vine RR (1962c) Explanatory notes, McKinlay Sheet, Queensland. (BMR Explan. Notes and Map). Bureau of Mineral Resources, Geology and Geophysics, Canberra.

Vine RR, Jauncey W, Casey DJ and Galloway MC (1965) The geology of the Longreach-Jericho-Lake Buchanan area, Queensland. Bureau of Mineral Resources, Australia, Record 1965/245.

Vine RR (1970a) Longreach, Queensland: Sheet SF/53-13 international index. Bureau of Mineral Resources, Geology and Geophysics, Canberra.

Vine RR (1970b) Muttaburra, Queensland: Sheet SF/55-9 international index. Bureau of Mineral Resources, Geology and Geophysics, Canberra.

Vine RR (1970c) Richmond, Queensland: Sheet SF/54-4 international index. Bureau of Mineral Resources, Geology and Geophysics, Canberra.

Vine RR (1972) Galilee, Queensland: Sheet SF/55-10 international index. Australian Government Publishing Service, Canberra.

Vine RR (1974) Hughenden, Queensland: Sheet SF/55-1 international index. Australian Government Publishing Service, Canberra.

Waratah Coal Pty Ltd (2013) Longwall mining subsidence report China First coal project – Galilee Basin. Appendix 41 supplementary EIS dated March 2013. Viewed 15 October 2015, http://waratahcoal.com/publications/.

Wells AT (1989) Chapter 10 - Stratigraphy and Permian Coal Measures of the Galilee Basin, Queensland. In: Harrington HJ (ed) Permian coals of Eastern Australia. Bureau of Mineral Resources Bulletin 231. Australian Government Publishing Service, Canberra. Viewed 15 October 2015, http://www.ga.gov.au/metadata-gateway/metadata/record/gcat_a05f7892-9cf7-7506-e044-00144fdd4fa6/Permian+coals+of+Eastern+Australia.

Wopfner H, Freytag IB and Heath GR (1970) Basal Jurassic-Cretaceous rocks of the western Great Artesian Basin, South Australia: Stratigraphy and environment. AAPG Bulletin 54(3), 381–416.

### *Datasets*

Dataset 1 Bureau of Meteorology (2013) National Groundwater Information System - Geological Survey of QLD and Queensland Petroleum Exploration Data. Bioregional Assessment Source Dataset. Viewed 11 April 2016, http://data.bioregionalassessments.gov.au/dataset/2d8225dd-d0c2-4f7d-aaaa-c2b387ab3df6.

Dataset 2 Geological Survey of Queensland (2011) Queensland Petroleum Exploration Data QPED Wells - July 2011. Bioregional Assessment Source Dataset. Viewed 09 September 2016, http://data.bioregionalassessments.gov.au/dataset/55a2192c-13a8-43d8-918d-72027f666f49.

Dataset 3 Bioregional Assessment Programme (2015) Galilee subregion coal seam gas well locations. Bioregional Assessment Derived Dataset. Viewed 11 April 2016, http://data.bioregionalassessments.gov.au/dataset/362fc1a5-3c8e-45f5-9b6c-806342de164e.

Dataset 4 Bioregional Assessment Programme (2014) Coal deposits and projects in the Galilee Basin. Bioregional Assessment Derived Dataset. Viewed 11 April 2016, http://data.bioregionalassessments.gov.au/dataset/784b7534-f2ae-426b-a60c-345d5dd08332.

Dataset 5 Queensland Department of Natural Resources and Mines (2015) Petroleum survey licences - Queensland. Bioregional Assessment Source Dataset. Viewed 11 April 2016, http://data.bioregionalassessments.gov.au/dataset/64841d4c-6458-4250-84f1-a4a0934f0f23.

Dataset 6 Queensland Department of Natural Resources and Mines (2015) QLD DNRM Seismic survey deep - Queensland. Bioregional Assessment Source Dataset. Viewed 11 April 2016, http://data.bioregionalassessments.gov.au/dataset/00656ea3-336d-4fa5-9070-3aa8d6fc522e.

Dataset 7 Bioregional Assessment Programme (2015) QLD DNRM Seismic survey 2D - Galilee subregion. Bioregional Assessment Derived Dataset. Viewed 11 April 2016, http://data.bioregionalassessments.gov.au/dataset/3718c61f-d5d4-4a99-96e9-029d7bb4f5ae.

Dataset 8 Bioregional Assessment Programme (2016) Stratigraphy and statistics for the Galilee subregion. Bioregional Assessment Derived Dataset. Viewed 11 April 2016, http://data.bioregionalassessments.gov.au/dataset/0e611b46-def6-42ee-a518-4c2fd2d07fce.

Dataset 9 Geoscience Australia (2009) Onshore geodetic Spherical Cap Bouguer gravity anomalies. Bioregional Assessment Source Dataset. Viewed 11 April 2016, http://data.bioregionalassessments.gov.au/dataset/90c0e7ac-587b-45d7-adfd-931e53ba5ead.

Dataset 10 Bioregional Assessment Programme (2015) Galilee clip of GA magmap v6 2014 VRTP 1VD. Bioregional Assessment Derived Dataset. Viewed 11 April 2016, http://data.bioregionalassessments.gov.au/dataset/4dff0093-da1a-4d16-93de-789d9ae01cf6.

Dataset 11 Geoscience Australia (2006) GEODATA TOPO 250K Series 3. Bioregional Assessment Source Dataset. Viewed 09 September 2016, http://data.bioregionalassessments.gov.au/dataset/a0650f18-518a-4b99-a553-44f82f28bb5f.

Dataset 12 Geoscience Australia (2012) Surface Geology of Australia, 1:2 500 000 scale, 2012 edition. Bioregional Assessment Source Dataset. Viewed 11 April 2016, http://data.bioregionalassessments.gov.au/dataset/4a91fff8-ed51-4994-b358-066497e25c8c.

Dataset 13 Bioregional Assessment Programme (2015) Galilee geological model 25-05-15. Bioregional Assessment Derived Dataset. Viewed 11 April 2016, http://data.bioregionalassessments.gov.au/dataset/bd1c35a0-52c4-421b-ac7d-651556670eb9.

Dataset 14 Geoscience Australia (2013) Australian Geological Provinces, v02. Bioregional Assessment Source Dataset. Viewed 01 July 2016, http://data.bioregionalassessments.gov.au/dataset/13ad6933-ee80-4c51-a97b-bac1e8bef16d.

Dataset 15 Bioregional Assessment Programme (2014) Diamantina river domain. Bioregional Assessment Derived Dataset. Viewed 16 November 2016, http://data.bioregionalassessments.gov.au/dataset/d5710fad-6bf1-4eb0-8f70-efd00596a51b.

Dataset 16 Queensland Department of Natural Resources and Mines (2014) QLD Department of Natural Resources and Mines Groundwater Database Extract 20142808. Bioregional Assessment Source Dataset. Viewed 16 November 2016, http://data.bioregionalassessments.gov.au/dataset/a5c5cbdb-1152-43f7-9533-a123027b7ce1.

Dataset 17 Geological Survey of Queensland (2014) Queensland petroleum exploration data - QPED. Bioregional Assessment Source Dataset. Viewed 09 September 2016, http://data.bioregionalassessments.gov.au/dataset/cb357721-bf22-45c9-a82e-828807912dd4.

Dataset 18 Queensland Department of Natural Resources and Mines (2012) Queensland Geological Digital Data - Detailed state extent, regional. November 2012. Bioregional Assessment Source Dataset. Viewed 11 April 2016, http://data.bioregionalassessments.gov.au/dataset/03ea9d87-55f1-400e-86c0-b8f7492984c4.

Dataset 19 Geoscience Australia (2011) Geoscience Australia, 1 second SRTM Digital Elevation Model (DEM). Bioregional Assessment Source Dataset. Viewed 11 April 2016, http://data.bioregionalassessments.gov.au/dataset/9a9284b6-eb45-4a13-97d0-91bf25f1187b.

Dataset 20 Queensland Department of Natural Resources and Mines (2015) QLD DNRM Seismic survey 2D - Queensland. Bioregional Assessment Source Dataset. Viewed 11 April 2016, http://data.bioregionalassessments.gov.au/dataset/fc3ecd06-6725-498a-98b4-8f46dc05274a.

Dataset 21 FROGTECH (2014) Phanerozoic OZ SEEBASE v2 GIS. Bioregional Assessment Source Dataset. Viewed 16 November 2016, http://data.bioregionalassessments.gov.au/dataset/26e0fbd9-d8d0-4212-be52-ca317e27b3bd.

Dataset 22 Geoscience Australia (2015) Great Artesian Basin - Paleogene-Neogene Cover - Thickness and Extent. Bioregional Assessment Source Dataset. Viewed 11 April 2016, http://data.bioregionalassessments.gov.au/dataset/26335d25-e904-462b-b075-50cfe5dc9b31.

Dataset 23 Geoscience Australia (2014) GABATLAS 15 Winton Mackunda aquifer and equivalents. Bioregional Assessment Source Dataset. Viewed 16 November 2016, http://data.bioregionalassessments.gov.au/dataset/2e1e0572-a43c-448e-be15-18abf848ab5c.

Dataset 24 Geoscience Australia (2015) GABATLAS - Rolling Downs Aquitard - Thickness and Extent. Bioregional Assessment Source Dataset. Viewed 11 April 2016, http://data.bioregionalassessments.gov.au/dataset/0c4f0e0e-2d1d-4dee-9a57-36ecdd1d9a1f.

Dataset 25 Geoscience Australia (2015) GABATLAS - Cadna-owie-Hooray Aquifer and Equivalents - Thickness and Extent. Bioregional Assessment Source Dataset. Viewed 11 April 2016, http://data.bioregionalassessments.gov.au/dataset/bc55589c-1c6f-47ba-a1ac-f81b0151c630.

Dataset 26 Geoscience Australia (2015) Great Artesian Basin, Westbourne Aquitard - thickness and extent. Bioregional Assessment Source Dataset. Viewed 16 November 2016, http://data.bioregionalassessments.gov.au/dataset/cba1a795-5502-44f4-80e8-d03bd4f5ae5a.

Dataset 27 Geoscience Australia (2015) GABATLAS - Adori-Springbok Aquifer - Thickness and Extent. Bioregional Assessment Source Dataset. Viewed 11 April 2016, http://data.bioregionalassessments.gov.au/dataset/6df0da09-5e9f-4656-b2f8-b87e5dbfde92.

Dataset 28 Geoscience Australia (2015) GABATLAS - Birkhead-Walloon Aquitard - Thickness and Extent. Bioregional Assessment Source Dataset. Viewed 11 April 2016, http://data.bioregionalassessments.gov.au/dataset/a5912292-10cd-42e2-aefe-49aae2eead4b.

Dataset 29 Geoscience Australia (2015) GABATLAS - Hutton Aquifer and Equivalents - Thickness and Extent. Bioregional Assessment Source Dataset. Viewed 11 April 2016, http://data.bioregionalassessments.gov.au/dataset/97def8b6-2c88-41cf-b77a-3433dfdc4470.

Dataset 30 Geoscience Australia (2015) GABATLAS - Evergreen-Poolowanna Aquitard and Equivalents - Thickness and Extent. Bioregional Assessment Source Dataset. Viewed 11 April 2016, http://data.bioregionalassessments.gov.au/dataset/b9c0d451-e7f0-4810-95eb-51fa6d9f552b.

Dataset 31 Geoscience Australia (2015) GABATLAS - Precipice Aquifer & Equivalents - Thickness and Extent. Bioregional Assessment Source Dataset. Viewed 11 April 2016, http://data.bioregionalassessments.gov.au/dataset/aeeead0e-9637-4f6f-b870-df4bc66dc81c.

Dataset 32 Geoscience Australia (2013) Thickness of Cenozoic weathering in the Great Artesian Basin. Bioregional Assessment Source Dataset. Viewed 11 April 2016, http://data.bioregionalassessments.gov.au/dataset/788a990e-77d5-4341-954d-aae72fc3d8b6.

Dataset 33 Bioregional Assessment Programme (2014) Galilee - Alluvium and Cenozoic 1M surface Geology. Bioregional Assessment Derived Dataset. Viewed 11 April 2016, http://data.bioregionalassessments.gov.au/dataset/552d5323-bb28-43e9-b137-8dd2d81f7d3c.

Dataset 34 Bioregional Assessment Programme (2014) Galilee top of formation elevations v03. Bioregional Assessment Derived Dataset. Viewed 16 November 2016, http://data.bioregionalassessments.gov.au/dataset/8911f763-a618-452f-829b-58497369f8e8.

Dataset 35 Bioregional Assessment Programme (2016) Galilee Upper Permian coal measures gas contents from WCR. Bioregional Assessment Derived Dataset. Viewed 13 September 2016, http://data.bioregionalassessments.gov.au/dataset/81130c47-15e0-4e0d-873c-9e008a874819.

Dataset 36 Bioregional Assessment Programme (2016) GAL212 Average gas content upper Permian coal measures. Bioregional Assessment Derived Dataset. Viewed 12 September 2016, http://data.bioregionalassessments.gov.au/dataset/d6c77474-1c2f-4db4-bf23-ff9e84158fdc.

## 2.1.3 Hydrogeology and groundwater quality


### *Summary*

**Hydrochemistry**

Hydrochemistry data were available for three regional aquifers (Cadna-owie – Hooray Sandstone, Hutton Sandstone and Clematis Sandstone), three regional partial aquifers (Winton-Mackunda formations, upper Permian coal measures and Joe Joe Group) and three regional aquitards (Rolling Downs Group, Injune Creek Group and Moolayember Formation). All of the hydrogeologic units in the Galilee subregion show high variability in solute concentrations, ion:chloride (Cl) ratios, and sample depth. Based on major ion chemistry, hydrogeologic units in the subregion can be grouped into three hydrochemical systems: two in the Eromanga Basin and one in the Galilee Basin. In stratigraphic order these are: a strongly Na-Cl dominated system with minor $SO_4$, consisting of the Winton-Mackunda formations partial aquifer and the Rolling Downs Group aquitard; a Na-$HCO_3$-Cl dominated system, consisting of the Cadna-owie – Hooray Sandstone aquifer, the Injune Creek Group aquitard and the Hutton Sandstone aquifer; and a Na-Cl system with minor to significant $HCO_3$, consisting of the Clematis Group aquifer, the upper Permian coal measures and the Joe Joe Group.

The distinctive hydrochemical signature, evident within each hydrogeologic unit, suggests that each is hydraulically separated at a regional scale by aquitards. However, at a local scale there may be some mixing of waters between aquifers. For instance, available data suggests mixing of groundwater may be occurring where the Hutton Sandstone aquifer is in contact with Galilee Basin aquifers in areas adjacent to the Maneroo Platform.

Salinity values are highest in Eromanga Basin units on the Maneroo Platform, coinciding with where the Moolayember Formation and Clematis Group pinch out.

**Water levels**

Potentiometric surfaces developed from water level observations in the Cenozoic aquifers (Quaternary alluvium and Cenozoic sediments) indicate that these units comprise local flow systems which are highly influenced by topography. The curvature of potentials around certain streams indicate that Jordan Creek, the Alice River and the Belyando River are potentially gaining streams and Dunda Creek, Tallarenha Creek and Lagoon Creek are potentially losing streams.

In the Eromanga Basin, the potentiometric surface of the Winton-Mackunda formations indicates a potential for regional flow from east to west, with some local groundwater mounding in areas of higher topography indicating a local component to flow. The underlying confined aquifers (Hooray Sandstone and correlatives, and Hutton Sandstone and correlatives) show a much smoother regional flow pattern from the intake beds in the east towards the west. Hydraulic gradients are much higher in these units in the area of the intake beds than further west, and this is believed to be due to reduced permeability in the outcrop areas due to weathering.

The potentiometric surfaces of the Galilee Basin units (Clematis Group, upper Permian coal measures, and Joe Joe Group) all show a basin centred groundwater divide in the vicinity of the Galilee and Jericho 1:250,000 scale geological map sheets, with potential for groundwater flow on one side going east toward the Belyando river basin and outcrop areas, and on the other side flowing to the west. Also, significant variability in vertical hydraulic gradients in the upper Permian coal measures partial aquifer was found. To further understand the complexity, water level data were further split between three hydrogeological sub-units, which from top to bottom are informally designated BC1, BC2 and BC3. The partitioning was done on the basis of approximately similar groundwater pressures existing in each sub-unit.

**Water level trends**

Time series groundwater level data for a number of observation wells were collected from the Queensland groundwater database.

The distribution of observation wells is weighted slightly to the east of the subregion, with a number of clusters of bores located around proposed areas of coal resource development.

The majority of bores in the observation dataset are non-artesian but a number of artesian bores were located in the Jurassic and Cretaceous units in the western part of the subregion.

Time series data from all bores in the dataset were analysed by the Theil-Sen regression method to identify whether there were statistically significant trends in the time series of the observation bores.

Filtering of the dataset was required to ensure that interpretations were made on reliable information. Many bores had time series of less than two years and were analysed separately from bores with longer records.

The majority of non-artesian bores with a statistically significant trend and records longer than two years showed a decreasing trend in water levels over the recording period.

The majority of artesian bores did not show any statistically significant trend in the data. For some bores this is likely due to the small number of observations available for statistical analysis (only three or four points for some bores), but for many bores a change in the hydrological regime caused by the Great Artesian Basin Sustainability Initiative (GABSI) program may be the reason. The hydrographs of several bores in which a statistically significant trend could not be identified show stable water levels, or a decline in water levels, until sometime in the 1990s, after which water levels begin to rise.

Both increasing and decreasing trends in water level were seen in most hydrostratigraphic units.

**Head differences**

When head differences between adjacent aquifers are in the range –10 m to +10 m, this is considered to be a necessary but not sufficient condition for the aquitard to be leaky and for inter-aquifer leakage to be occurring. Conversely, where the head difference is less than –10 m or greater than +10 m, such areas may be interpreted as indicating where the aquitard forms a tight seal and that negligible inter-aquifer leakage occurs.

Regions where the head in the Hutton Sandstone is higher than the head in the Hooray Sandstone occur near the intake beds in the eastern zone (where the outcrop of Hutton Sandstone is topographically higher than the Hooray Sandstone) and in the western artesian areas on the Winton and Mackunda 1:250,000 sheets. These are areas where it appears that the intervening aquitard, the Injune Creek Group, forms a tight seal. Elsewhere, in the central eastern, and in parts of the central western and western zones, the Injune Creek Group aquitard appears to be leaky.

About 40% of the Injune Creek Group aquitard forms a tight seal and the remaining 60% is leaky. The notion of a significant component of the Injune Creek Group being leaky is supported by the hydrochemistry data. The dominant vertical flow direction through the leaky aquitard would be upwards from the Hutton Sandstone because chemically the Injune Creek Group is closer to the Hutton Sandstone than the Hooray Sandstone.

Analysis of the head difference between the Hutton Sandstone and Clematis Group indicates that the Moolayember Formation forms a tight seal near the intake beds of the Hutton Sandstone in the eastern zone and parts of the central eastern zone, and is leaky over the majority of the central eastern zone and for all of the Manuka 1:250,000 sheet in the central western zone.

Examination of head difference between the Clematis Group aquifer and the BC1 partial aquifer (of the upper Permian coal measures) indicates that in most places the intervening aquitard, the Dunda beds and Rewan Formation, forms a tight seal.

Analysis of the head differences between the BC1 and BC2 partial aquifers indicates that on the Muttaburra and Jericho 1:250,000 sheets the aquitard at the top of BC2 (the BC interburden sandstone) forms a tight seal to exclude vertical hydraulic connection between BC1 and BC2 and is approximately collinear with the groundwater divide. The tight aquitard occurs across about 40% of the mapped area but is leaky elsewhere.

Examination of the head difference between the BC2 and BC3 partial aquifers indicates that the intervening aquitard (DE interburden sandstone) forms a tight seal on the Tangorin, Muttaburra, Galilee, Jericho and Springsure 1:250,000 sheets. Elsewhere, on the eastern and western margins the DE interburden sandstone aquitard appears to be leaky.

Investigation of the head difference between the BC3 partial aquifer of the upper Permian coal measures and the Joe Joe Group aquitard reveals the head in the Joe Joe Group is higher than the head in BC3 over about 75% of the mapped area. While there is a potential for vertical upwards flow, leakage is excluded by the tight seal afforded by the Joe Joe Group aquitard (Jochmus Formation). The head difference map shows an area on the western margin, and a smaller one on the eastern margin, where the Joe Joe Group aquitard appears to be leaky.

**Recharge**

In the bioregional assessment (BA) programme only the rock outcrop areas of the aquifers have been used to estimate groundwater recharge rates using the chloride mass balance method. The sub-crop areas are assumed to be blanketed by dense, plastic Cenozoic clay which greatly impedes recharge. Consequently, an assumed recharge rate of 0.2 mm/year has been applied to such areas, irrespective of the substrate.

The estimated recharge flux for the Hutton Sandstone and Hooray Sandstone are 18,672 ML/year and 12,252 ML/year. This contrasts with previous estimates by Kellett et al. (2003) of 25,710 ML/year and 21,360 ML/year. The significant decreases in these revised recharge estimates are due to only mapped areas of outcrop being considered as applicable for receiving direct recharge from rainfall due to the potential for Cenozoic cover to impede recharge. Whereas, these effects of Cenozoic cover on recharge were not taken into account in the original estimates by Kellet et al. (2003).

A total recharge flux of approximately 101,000 ML/year was estimated across the subregion. Recharge to the Winton-Mackunda formations occurs over the entire area of occurrence, but the recharge rate is not uniform. In many places, the Winton-Mackunda formations are blanketed by a thick layer of saprolite and the lower horizon of the weathered profile greatly impedes downward infiltration of the wetting front and therefore also recharge. Groundwater (recharge) mounds occur in those places where the saprolite has been eroded exposing relatively unaltered rock. Recharge rates in such areas are about 1 mm/year, but in places where the saprolite cover has been preserved, recharge rates are of the order of 0.1 mm/year.

The recharge fluxes for the Rewan Group, upper Permian coal measures and the Joe Joe Group are particularly low (<700 ML/year).

**Discharge**

Artificial discharge of groundwater by pumping from bores, or discharge from free-flowing artesian wells, is a component of groundwater discharge for every formation in the Galilee subregion. For the Hooray and Hutton sandstones, flow from controlled or uncontrolled artesian water wells is by far the largest proportion of discharge from these aquifers. The remainder of the groundwater flux in these two aquifers, except for a minor component of flow to rejected recharge springs in the Barcaldine Springs complex, is ultimately naturally discharged in springs, salt lakes or vertical leakage in the south-west Eromanga Basin.

Natural groundwater discharge occurs from several groups of springs in the Galilee subregion. The source aquifer for the Barcaldine Springs complex is the Ronlow beds (mainly Hooray Sandstone equivalent). The source aquifer for the Doongmabulla Springs complex (about 10 km west of the proposed Carmichael Coal Mine) is primarily the Clematis Group aquifer. The Colinlea Sandstone is the source aquifer of the Mellaluka Springs complex and Albro

Springs in the east of the subregion. The Dunda beds are source aquifer for some small springs including Hector Springs.

With the notable exception of the Clematis Group aquifer, artificial groundwater discharge by pumping from wells is negligible for the Galilee Basin formations. However this is set to change dramatically when dewatering of the upper Permian coal measures begins in 2018. Initially it is proposed to pump 6,000 ML/year from the upper Permian coal measures, ramping up to 11,350 ML/year over 30 years.

A component of flow in the upper Permian coal measures partial aquifer and the Joe Joe Group aquitard discharges eastwards towards the Belyando River valley, but the majority of the groundwater flux in these formations is towards the west. It appears that the groundwater discharge from these formations is dominantly vertical upwards leakage into the overlying formations at the western margins of the Galilee Basin where the strata pinch out. This also appears to be the case for the Triassic units of the Galilee Basin sequence, with the exception of the Clematis Group.

**Gaps**

A significant amount of data could not be used due to insufficient information being available to adequately determine which geological unit the data were obtained from. Additional hydrochemical data collection and analysis (e.g. cluster analysis and isotopic data) would help in identifying inter-aquifer mixing and regions where different chemical processes are dominant.

Water level and water level monitoring data are sparse and unevenly distributed in the subregion. Few nested piezometers exist to enable direct comparison between aquifers at a single location.

### *2.1.3.1 Observed data*

Nine existing datasets with useful hydrogeological information were analysed for the bioregional assessment of the Galilee subregion. Table 7 lists the datasets and identifies the information that was analysed.

**Table 7 Data used for hydrogeological analysis of the Galilee subregion**

| Dataset title | Source | Information analysed |
| --- | --- | --- |
| Hydrochemistry analysis of the Galilee subregion | Bioregional Assessment Programme (Dataset 1) | Major ions, alkalinity, total dissolved solids (TDS), trace elements, sodium absorption ratio (SAR) |
| QLD Department of Natural Resources and Mining Groundwater Database Extract 20142808 | Queensland Department of Natural Resources and Mines (Dataset 2) | Location, water level, standing water level, bore construction, hydrostratigraphy, water chemistry |
| Queensland petroleum exploration data - QPED | Geological Survey of Queensland, Department of Natural Resources and Mines (Dataset 3) | Locations, stratigraphy, drill stem formation tests (DST) e.g. temperature, salinity |
| QDEX Well Completion Reports (WCR) - Galilee v01 | Queensland Department of Employment, Economic Development and Innovation (Dataset 4) | Stratigraphy, drill stem formation tests (DST) e.g. pressure, temperature, salinity data, not included in QPED, from open file well completion reports |
| Carmichael Coal Mine and Rail Project Environmental Impact Statement | Queensland Government Department of State Development, Infrastructure and Planning (Dataset 5) | Bore location, stratigraphy, water levels, hydraulic head (mAHD), well screen intervals, temperature and water chemistry |
| China First Galilee Coal Project Environmental Impact Assessment | Waratah Coal Pty Ltd (Dataset 6) | Bore location, stratigraphy, water levels, hydraulic head (mAHD), well screen intervals, temperature and water chemistry |
| Kevin's Corner Project Environmental Impact Statement | Hancock Galilee Pty Ltd (Dataset 7) | Bore location, stratigraphy, water levels, hydraulic head (mAHD), well screen intervals, temperature and water chemistry |
| South Galilee Coal Project Environmental Impact Statement | AMCI (Alpha) Pty Ltd (Dataset 8) | Bore location, stratigraphy, water levels, hydraulic head (mAHD), well screen intervals, temperature and water chemistry |
| QLD Dept. of Natural Resources and Mines, Groundwater Entitlements linked to bores and NGIS v4 28072014 | Bioregional Assessment Programme (Dataset 9) | Borehole stratigraphy |

The primary source for groundwater data is the Queensland Department of Natural Resources and Mines Groundwater Database (Dataset 2). It contains information on registered groundwater bores in the state of Queensland. The bore database has a number of tables which include data on: bore registration (location information), bore construction; stratigraphy, lithology, water levels, aquifer test data, water quality data, as well as other bore related information. Department of Natural Resources and Mines (DNRM, 2013) provides detail on groundwater database structure and content.

Other significant sources of groundwater data were environmental impact statements (EISs) (Dataset 5 to Dataset 8) for proposed coal resource developments in the Galilee subregion and formation tests undertaken in wells drilled for coal seam gas (CSG) and petroleum exploration

(Dataset 3 and Dataset 4). EISs are a key source of information as they contain recent data pertaining to groundwater systems in and near proposed development areas. Formation tests are one of the few sources of information on pressures in the deeper groundwater flow systems.

### 2.1.3.1.1 Hydrostratigraphy

The Galilee subregion BA is focused on two stacked geological basins – the Eromanga Basin and the Galilee Basin – that in some places are overlain by Cenozoic sediments. While parts of the Drummond, Adavale and Belyando basins are in contact with the base of the Galilee Basin, these basins are isolated from the areas of coal resource development and are not considered further.

The Galilee subregion includes the following geological environments which generally represent individual (or in some cases connected) groundwater systems:

- Cenozoic aquifers
- Early Jurassic to Early Cretaceous layered aquifers and aquitards of the Eromanga Basin (Great Artesian Basin (GAB))
- Late Carboniferous, Permian to Late Triassic layered aquifers and aquitards of the Galilee Basin. The upper Permian coal measures and correlatives host the coal seams that are targeted for mining.

Previous hydrogeological investigations within the Galilee subregion have been mainly restricted to local scale investigations focused in and around areas of potential coal mining developments. As such, prior to this BA, the understanding of the regional hydrogeology of the Galilee Basin was limited.

For the purposes of this bioregional assessment, a number of analyses have been undertaken to better understand the current hydrogeological characteristics of the region, which, in turn, allows an enhanced conceptual understanding of the effects of potential coal mining developments modelled in BA companion products 2.6.1 (Karim et al., 2018b) and 2.6.2 (Peeters et al., 2018) for the Galilee subregion.

The analyses include the following:

- statistical analysis of hydrochemistry data
- water level mapping for all of the main aquifers and the upper Permian coal measures
- monitoring bore water level trend analysis
- aquifer pressure comparison – for analysis of seal characteristics
- recharge and discharge analysis.

The above analyses are aimed specifically at improving our understanding of: the hydrodynamics of the system – groundwater flow, chemical evolution, areas of possible inter-aquifer leakage and recharge and discharge processes; and the current water level trends prior to coal resource development.

The hydrostratigraphy of the Galilee subregion is summarised in Figure 34.

The hydrostratigraphic units to which samples were assigned are outlined in companion product 1.5 for the Galilee subregion (Evans et al., 2014), with the following amendments:

- The Wyandra-Hooray grouping is hereafter referred to as the Cadna-owie – Hooray aquifer because the majority of samples available are sourced from the Cadna-owie Formation or Hooray Sandstone.
- The Injune Creek Group includes the Westbourne Formation, Adori Sandstone and Birkhead Formation.
- The Clematis-Warang Sandstone is now referred to as the Clematis Group aquifer as outlined in Section 2.1.2 of this product.
- The Betts Creek beds are now referred to as the upper Permian coal measures.

These changes in title have not changed the hydrostratigraphic units that any samples were assigned to.

There is some variation between the geological units used for each type of analyses undertaken in the following sections. This is due to variability in the amount and spatial distribution of the available data for each individual geological unit. Hydrochemistry, water level mapping and aquifer pressure comparison analyses use hydrostratigraphic groupings for some units with similar hydrogeological characteristics. Whereas, the water level trend and recharge analyses are reported based on individual stratigraphic units. Descriptions of the units and groupings used are provided at the beginning of each respective section.

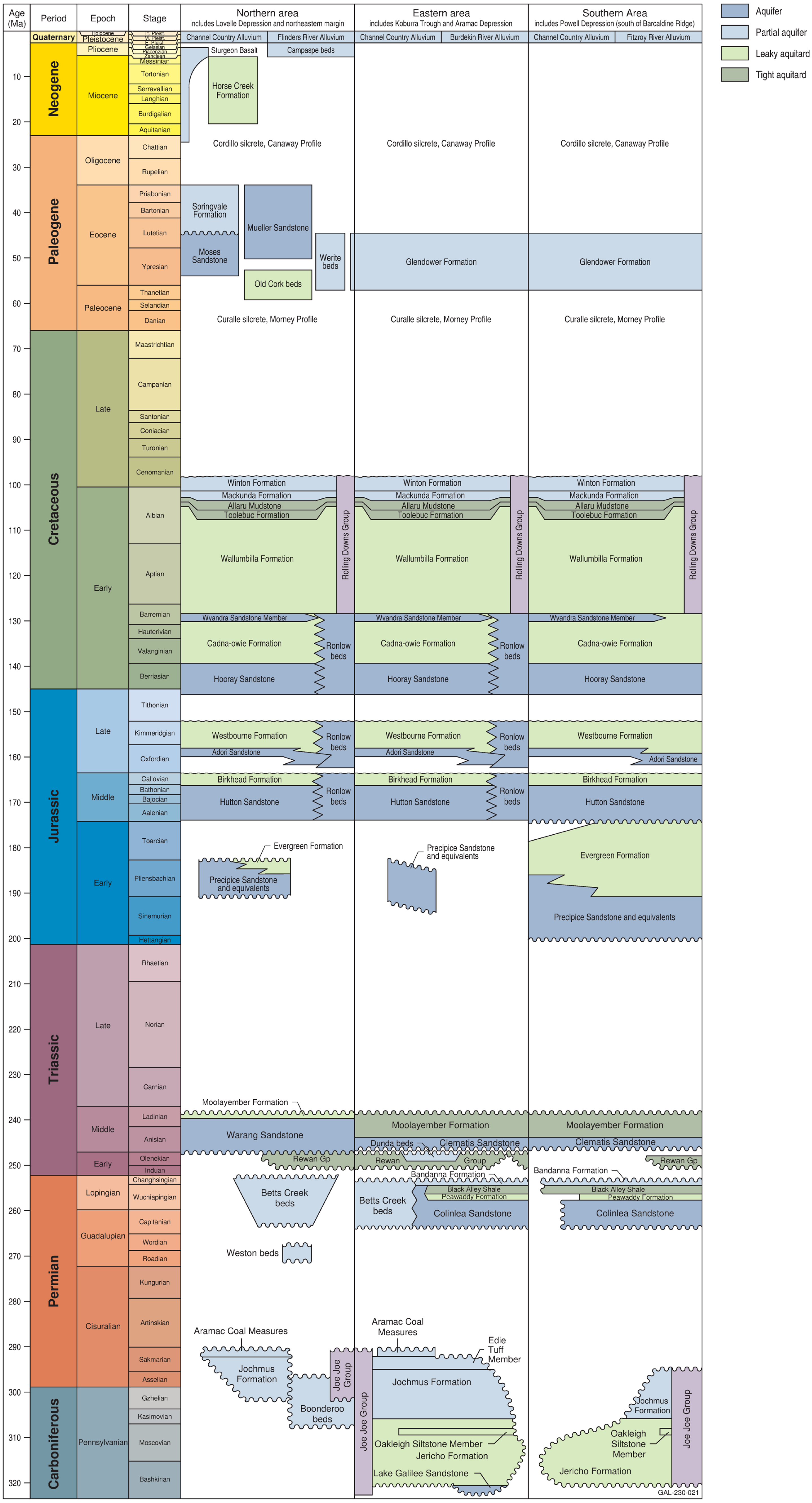


**Figure 34 Hydrostratigraphic sequence of the Cenozoic cover, Eromanga Basin and Galilee Basin**

This figure has been optimised for printing on A3 paper (297 mm x 420 mm).

## 2.1.3.1.2 Hydrochemistry data and processing

Hydrochemistry data were obtained from the Queensland DNRM groundwater bore database. A subset of this dataset was extracted for the Galilee subregion. Few bores had a complete suite of analyses for hydrochemistry, and data quality was highly variable. In some instances insufficient information (e.g. a description of the aquifer tapped and/or casing and depth information) was available to confidently determine the source aquifer for particular analyses. In such cases these analyses were discarded and not used for the subsequent interpretation. The initial hydrochemical dataset comprised 5680 samples with information for:

- bore identification (RN) and location
- data source
- aquifer information for some bores, including formations intercepted by monitoring wells and screened intervals
- sample information (e.g. date sampled)
- field parameters (pH, electrical conductivity, temperature, dissolved oxygen, redox)
- total dissolved solids (TDS)
- alkalinity
- major ions
- selected trace elements.

### *2.1.3.1.2.1 Quality assurance / quality control analysis of data*

Prior to analysis all hydrochemistry data were assessed for reliability by quality assurance/quality control (QA/QC) procedures. A data audit and verification were performed using various quality checking procedures including identification and verification of outliers.

The charge balance of major ions in each sample was used to assess the reliability of the data. In some cases, alkalinity was expressed as calcium carbonate which required conversion to alkalinity as bicarbonate to achieve ionic charge balance.

The charge balance of each sample was determined using the following equation:

$$Charge\ balance = 100 * \frac{\sum Cat - \sum An}{\sum \mathrm{Cat} + \sum An} \qquad (1)$$

where *Cat* = the concentration of all cations in solution in milliequivalents per litre (meq/L), and *An* = the concentration of all anions in meq/L. Using milliequivalents accounts for the charge and molecular weight of each ion.

Theoretically the meq/L of anions in solution should be equal to the meq/L of cations, since natural solutions are electrically neutral. This means the deviation from zero in the charge balance calculation gives an indication of the potential error associated with the sample data. Given the age range and geographical extent of the groundwater data analysed by the BA programme, an ionic charge balance of 10% was deemed acceptable. Samples which exceeded this error threshold were discarded.

Measurements of field electrical conductivity (EC) data were limited, with many zero or missing values present. An initial investigation of the EC-TDS ratio of each sample within a particular hydrogeologic unit revealed a range of ratios from 0.2 to 12. To avoid the influence of outliers and obvious EC measurement errors, interpolation of TDS from the EC-TDS regression was only applied to the EC range between 0.50 and 0.90.

Further filtering of the data was required for some of the hydrochemical methods employed. This will be discussed in Section 2.1.3.2.1.

To interpret the hydrochemistry data it was necessary to assign each sample to a hydrogeologic unit. Data that passed the initial QA/QC procedures were checked against borehole construction and stratigraphic records to determine aquifer intercepts. Data were discarded in cases where there was no recorded screen interval or depth information that could be cross referenced with borehole stratigraphy, or where bores were screened in multiple aquifers. A total of 4624 samples which passed the initial QA/QC process had sufficient stratigraphic data to be assigned to a hydrogeologic unit.

#### 2.1.3.1.3 Standing water level and hydraulic head

Standing water level (SWL) is a measurement of the depth below a reference point to the water level in a bore. SWL data were converted to hydraulic head (groundwater level above a reference point, usually the Australian Height Datum). Certain types of hydrogeological analyses require SWL to be compared between water bores. In such cases, hydraulic head is corrected to an equivalent fresh water hydraulic head. The correction requires the measurement reference point elevation to convert SWL to uncorrected hydraulic head. In turn, water salinity and temperature data are required to calculate equivalent fresh water hydraulic head.

Regional plots of water level depth are used to infer hydraulic processes such as potential groundwater flow direction and recharge processes.

To interpret SWL data, the hydrostratigraphic unit(s) in which the bore is screened must be determined. In some cases a bore may be drawing water from more than one hydrostratigraphic unit. Section 2.1.3.1.1 and Evans et al. (2014) details the stratigraphy and hydrostratigraphy for the Galilee subregion.

#### *2.1.3.1.3.1 Datasets and processing*

**QLD Department of Natural Resources and Mining Groundwater Database (Dataset 2)**

SWL data for groundwater bores are primarily stored in the 'water levels' table in Dataset 2. Some SWL data, mainly for artesian bores, are also available from the 'pumping test and design' table of Dataset 2. Many of these measurements are also duplicated in the water levels table. SWL and other relevant data for hydrogeological analysis were extracted from Dataset 2 and incorporated with data from other sources using the following steps:

1. Using a GIS package, select bores located within the Galilee preliminary assessment extent (PAE) area. Based on the Registered Number (RN) from the filtered GIS dataset, extract and join data from the following tables contained in Dataset 2: registrations, aquifers, stratigraphy, construction, lithology, water analysis, field water quality and elevation.
2. Check and assign elevation data that referenced the Australian Height Datum (AHD) and were derived from a survey or GPS elevation measurement. Where no elevation data were available in Dataset 2 (mostly private bores), the elevation was derived from the 1-second digital elevation model (DEM) (Geoscience Australia, Dataset 10).
3. Determine screened intervals using the construction table in Dataset 2. In the construction table these intervals are designated in the material description column as either: open, perforated, screened or VWPZ (vibrating wire piezometer). Sometimes bores can have multiple ingress points for groundwater. In the BA dataset, the screen 'From' measurement represents uppermost interval and screen 'To' represents the base of the interval at which groundwater can enter a bore.
4. Determine hydrostratigraphic unit sample intercept by cross checking screened interval with hydrostratigraphic interval interpretation. In Dataset 2, stratigraphic information is sourced from the aquifer and stratigraphy tables. Stratigraphic data from these sources can be missing, incomplete, or the stratigraphic interpretation may have changed since data were originally input. To infill data gaps, extra stratigraphic data were incorporated from a number of additional datasets including groundwater bore entitlements and licences (Bioregional Assessment Programme, Dataset 9) and Queensland Petroleum Exploration Data (Department of Employment, Economic Development and Innovation, Dataset 4). Stratigraphic data were queried for each bore and compared for consistency and completeness. A number of bores draw groundwater from multiple aquifers.

For bores with missing or incomplete screen interval data, the maximum recorded drilling depth was used as a proxy for the base of screened interval. However, it should be noted that in some cases using total depth as a proxy for base of screens may not be representative of the screened interval. For example in some cases a bore may be uncased below a certain depth and the open interval in the bore could be large and intersect multiple aquifers.

**Queensland petroleum exploration data - QPED (Dataset 3) and QDEX Well Completion Reports (WCR) (Dataset 4)**

Basic data from petroleum and CSG wells are archived in the Department of Employment, Economic Development and Innovation (Dataset 4).Open file well completion reports (WCR) can be downloaded as required from the Department of Employment, Economic Development and Innovation (Dataset 4), which is the Queensland Digital Exploration Reports system. Detailed results such as pressures, recorded by formation tests were obtained from the WCR and associated datasets.

Various types of formation testing are commonly undertaken in petroleum and CSG wells as part of petroleum resource assessments. Over discrete intervals these tests can be used to assess: the presence of hydrocarbons, determine reservoir properties (pressures, temperatures, flow rates), well performance, and obtain samples of reservoir fluids.

Formation test and other data, for use in bioregional assessments, were data-mined using the following steps:

1. Identify which bores are located within the Galilee PAE area, using a GIS package.
2. Record drilling datum and ground levels in mAHD.
3. Where available, record detailed stratigraphy in the coal-bearing sequences, not already in the Queensland Petroleum Exploration Database (QPED) database.
4. Formation test data: record test type, depth; formation tested; salinity (if available); pressure measurement units; inside and outside gauge pressures; gauge temperature, interpreted test results (if available) and any comments on test performance.
5. Record water analysis data not already in QPED database.

**Datasets 5 to 8 – environmental impact statements**

Groundwater bore data were obtained from available company EISs and tabulated in spreadsheets. Data included bore location, stratigraphy, water levels, hydraulic head (mAHD), well screen intervals, temperature and chemistry. Stratigraphic data in most of the EIS are more detailed (mine scale stratigraphy) than those available in Queensland Department of Natural Resources and Mines (Dataset 2). This level of detail was required for the BA groundwater model (in companion product 2.6.2 for the Galilee subregion (Peeters et al., 2018)).

### 2.1.3.1.4 Corrected hydraulic head calculation

#### *2.1.3.1.4.1 Corrected hydraulic head from Dataset 2 and Dataset 5 to Dataset 8*

Where possible, hydraulic head was corrected to a fresh water equivalent hydraulic head. Water salinity and temperature data are required to calculate equivalent fresh water hydraulic head using the process described in Post et al. (2007). Many water level measurements could not be corrected due to an absence of corresponding temperature or salinity measurements.

To correct hydraulic head to an equivalent freshwater hydraulic head the following steps were undertaken:

1. Data from Dataset 2, and Dataset 5 to Dataset 8 were combined.
2. Water level records missing temperature readings: to fill in gaps, temperature data from non-flowing groundwater bores and all formation tests were plotted on a temperature versus depth plot. A linear regression line based on the data provided the formula to which an approximate temperature for a given depth could be calculated.

3. Water level records missing salinity readings: to fill data gaps, from the compiled data, the mean EC for a given formation was used as a proxy for salinity.
4. Salinity: EC measurements (including calculated EC) were converted to TDS in mg/L in order to calculate corrected hydraulic head. Further discussion on the factors used for conversion from EC to TDS can be found in Section 2.1.3.2.
5. Equivalent freshwater hydraulic head was calculated using methods outlined in Post et al. (2007).

##### *2.1.3.1.4.2 Corrected hydraulic head from formation pressure test data*

Additional steps are required to obtain a freshwater equivalent hydraulic head from formation test pressure measurements. Firstly, quality assurance protocols were applied to the available data, before pressure measurements were converted to freshwater equivalent hydraulic head.

The QA process and corrected head calculation involved:

1. quality assurance checks such as: Was the formation test classed as successful by the operator and all test gauges operational? Were all data present? Was final shut-in pressure less than final hydrostatic pressure? Did the pressure build-up phase of the test stabilise around a final value? Further detail on formation test quality control can be found in Hortle et al. (2013)
2. for successful tests, ensuring that final shut-in pressures reference pounds per square inch gauge (PSIG) and not pounds per square inch absolute (PSIA). PSIG was chosen as the reference because there is no information on whether SWL readings were corrected for atmospheric pressure changes at the time the SWL measurement was made
3. converting final shut-in pressure (PSIG) to fresh water equivalent hydraulic head as per steps 4 and 5 in the previous section.

Most formation tests had temperature data, although they lacked salinity data. Where no salinity data were available, water salinity was assumed to be the mean aquifer salinity.

Water level maps of hydraulic head are presented in Section 2.1.3.2.2. In areas where groundwater level data were unavailable, formation test data obtained from Dataset 3 and Dataset 4 were used to aid interpretation.

With the exception of Cenozoic aquifer water levels maps, all potentiometric surfaces are corrected to a common datum of 25 ˚C and equivalent fresh water head.

### *2.1.3.2 Statistical analysis and interpolation*

#### 2.1.3.2.1 Hydrochemistry

In descending stratigraphic order the hydrostratigraphic units used in this section are:

- Winton-Mackunda partial aquifer
- Rolling Downs Group aquitard (includes Allaru Mudstone, Toolebuc Formation, Wallumbilla Formation)
- Cadna-owie – Hooray Sandstone aquifer

- Injune Creek Group aquitard (includes Westbourne Formation, Adori Sandstone, Birkhead Formation)
- Hutton Sandstone aquifer
- Moolayember Formation aquitard
- Clematis Group aquifer (includes Warang Sandstone)
- upper Permian coal measures partial aquifer
- Joe Joe Group partial aquifer.

As expected the majority of samples are from major regional aquifers, with some samples from local aquifers situated within regional aquitards (i.e. the Injune Creek Group aquitard and the Moolayember Formation aquitard).

Hydrochemical trends in the hydrogeologic units were investigated using a variety of techniques discussed below.

#### *2.1.3.2.1.1 Ion:chloride ratios*

Chloride (Cl) is often assumed to be a conservative ion in solution. Once it is introduced into a groundwater system it remains dissolved because there is no water–rock interaction that can remove chloride from groundwater (Appelo and Postma, 2006), although halite dissolution processes may increase its concentration. In contrast, the other major ions can enter or leave a groundwater system through adsorption and desorption, or precipitation and dissolution.

The chemical processes which are not related to surface processes such as evapotranspiration can be identified by the changes in ion:Cl ratios in groundwater. The $HCO_3$:Cl, (Na+K):Cl and (Ca+Mg):Cl ratios can be used to compare concentrations of ions (units meq/L) in excess of their respective recharge ratios. The concentrations are a measure of the input of ions to groundwater from water–rock interactions or mixing of different water bodies, relative to the concentration of ocean-derived salts in rainfall. Ion:Cl ratios were used to examine the sources of major ions in solution for the different hydrogeologic units.

#### *2.1.3.2.1.2 Sodium Absorption Ratio*

Sodium, magnesium and calcium are the dominant cations in natural waters. The sodium absorption ratio (SAR) is the fraction of exchangeable sodium over the square root of half of the sum of the calcium and magnesium concentrations (Fetter, 2001). High sodic groundwater, when used in surface environments (e.g. irrigation cropping), can affect soil quality and result in soil dispersibility. Calcium and magnesium ions are preferentially held over sodium ions in cation exchange sites in clays. Where sodium concentrations are high relative to calcium and magnesium, sodium may displace them from the cation exchange sites. Sodium has a large hydrated ionic radius and it tends to push the layered lattices of clay minerals apart, ultimately causing disaggregation and loss of soil structure.

SAR is expressed as:

$$SAR = \frac{Na^{+}}{0.5 * (Ca^{2+} + Mg^{2+})^{0.5}} \tag{2}$$

where $Na^{+}$, $Ca^{2+}$ and $Mg^{2+}$ are expressed as milliequivalents per litre (meq/L) (Appelo and Postma, 2006). SAR was used in conjunction with ion:Cl ratios to examine which aquifer properties may be responsible for changes in groundwater chemistry.

#### *2.1.3.2.1.3 Hydrochemical characterisation*

In this section hydrogeologic units are assigned to hydrochemical systems based on major ion abundances. Hydrochemical trends in each hydrogeologic unit are identified using ion-TDS and ion-chloride relationships which are summarised in Table 8. It should be noted that the hydrogeological units used conform to the hydrostratigraphic units used for the Galilee groundwater model (see companion product 2.6.2 for the Galilee subregion (Peeters et al., 2018)).

The data used in this study are composited from analyses accumulated over a long timescale, from 1938 to 2013. Approximately 70% of samples were collected between 1970 and 2013. It is assumed that given the long residence time of water in the GAB there would be little short-term variation in the data, and, given the absence of significant resource development in the region, only minor changes in the water chemistry over the time period are represented by the samples. This view is supported by Moya et al. (2015) who performed hierarchical cluster analysis on samples from the Galilee subregion and observed that samples collected from the same bore at different times were consistently assigned to the same hierarchical cluster group. The data discussed below therefore represent a generalised picture of the hydrochemistry of the subregion over several decades. Such data should be appropriate for investigating regional trends and processes operating over a large part of the basin, but may not necessarily be suited to a detailed study of localised processes.

**Major ions**

Major ion abundances were used to classify the hydrogeologic units into hydrochemical systems. Figure 35 shows the abundances of major ions relative to TDS for the different hydrogeologic units in the subregion. Table 8 shows $R^2$ values for regressions undertaken on major ion relationships to TDS. On the basis of the relative abundances of major ions, three distinct groundwater types can be differentiated:

- Na-Cl dominated groundwater type with minor $SO_4$ (Winton-Mackunda partial aquifer and Rolling Downs Group aquitard)
- pH dependent, Na-$HCO_3$-Cl groundwater type (the Cadna-owie – Hooray Sandstone aquifer, Injune Creek Group aquitard, and Hutton Sandstone aquifer)
- Na-Cl type with minor $HCO_3$ (the Clematis Group aquifer, upper Permian coal measures partial aquifer, and Joe Joe Group partial aquifer).

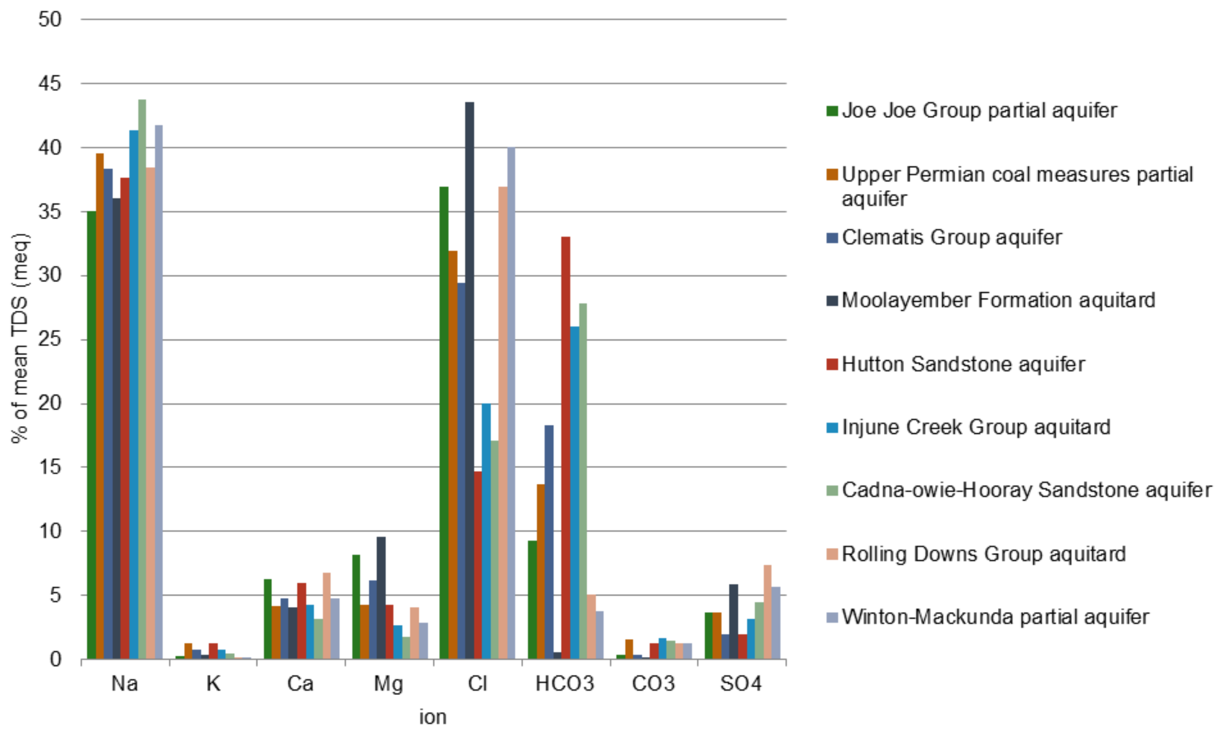


**Figure 35 Relative average abundances of elements in hydrogeologic units for the Galilee subregion**

TDS = total dissolved solids
Data: Bioregional Assessment Programme (Dataset 1)

**Table 8 Ion-TDS $R^2$ values for hydrogeologic units in the Galilee subregion**

| Hydrogeologic unit or group | EC[a] TDS relationship | Cl TDS relationship | Na TDS relationship | $HCO_3$ TDS relationship | Hydrochemistry system |
|---|---|---|---|---|---|
| Winton-Mackunda partial aquifer | 0.97 | 0.95[b] | 0.97 | 0.01 | Na-Cl |
| Rolling Downs Group aquitard | 0.98 | 0.92 | 0.94 | 0.04[c] | Na-Cl |
| Wyandra-Cadna-owie – Hooray Sandstone aquifer | 0.99 | 0.49 | 0.95 | 0.54[c] | Na-$HCO_3$-Cl |
| Injune Creek Group aquitard | 0.99 | 0.32 | 0.94 | 0.65 | Na-$HCO_3$-Cl |
| Hutton Sandstone aquifer | 0.96 | 0.60 | 0.89 | 0.72[c] | Na-$HCO_3$-Cl |
| Clematis Group aquifer | 0.99 | 0.93 | 0.98 | 0.02 | Na-Cl with minor $HCO_3$ |
| Upper Permian coal measures | 0.99 | 0.74 | 0.90 | 0.15 | Na-Cl with minor $HCO_3$ |
| Joe Joe Group | 0.99 | 0.96 | 0.97 | 0.02 | Na-Cl with minor $HCO_3$ |

[a]regression fitted to samples with TDS-EC relationships between 0.50 and 0.90, after eliminating EC data points with zero values and obvious errors
[b]Moolayember Formation data has virtually same Cl-TDS slope
[c]regression limited to groundwater samples with pH
TDS = total dissolved solids, EC = electrical conductivity
Data: Bioregional Assessment Programme (Dataset 1)

The reason for these different water types is likely due to a combination of mineralogical and depositional characteristics of the host material of the aquifers, and differences in hydrochemical evolution along flow paths. The hydrochemical evolution may be largely an indication of the age of the groundwater. The clustering of groundwater types closely mirrors the stratigraphy of the hydrogeologic units; each hydrochemical system in the subregion consists of a number of hydrogeologic units that overlie one another.

This suggests that there is limited flow across the regional aquitards identified in the subregion. These are the Rolling Downs Group aquitard, which separates the Winton-Mackunda partial aquifer from the Cadna-owie – Hooray Sandstone aquifer, and the Moolayember Formation, which separates the Hutton Sandstone aquifer from the Clematis Group aquifer. Between these regional aquitards there may be hydraulic continuity between overlying hydrogeologic units, causing similarities in groundwater chemistry.

It is worth noting that despite the relatively high average abundance of $HCO_3$ in the Clematis Group aquifer, upper Permian coal measures and Joe Joe Group partial aquifers, the $R^2$ values for $HCO_3$ and TDS in these units are 0.02, 0.15 and 0.02 respectively. This suggests that $HCO_3$ reaches high concentrations locally, but may not be a significant component of TDS through the full extent of these hydrogeologic units.

These hydrochemical groupings are slightly different from a revised hydrochemical stratigraphy proposed by Moya et al. (2015). Using a combination of hierarchical clustering, principal component analysis (PCA) and factor analysis, they identified three hydrochemical groups:

- a Na-Cl dominated group containing brackish waters, seen in the Winton-Mackunda formations, Allaru Mudstone and Toolebuc Formation. Similar to the Na-Cl dominated group identified with the exception that they exclude the Wallumbilla Formation based on a lower mean TDS
- a Na-$HCO_3$-Cl group containing slightly brackish waters, seen in the Wallumbilla Formation, Cadna-owie Formation, Hooray Sandstone and Westbourne Formation. These aquifers are recognised as containing dissolved gas which is believed to be primarily $CO_2$. This again is similar to the Na-$HCO_3$-Cl group identified by the BA programme, though Moya et al. (2015) exclude the Hutton Sandstone from this group and include the Wallumbilla Formation
- a Na-$HCO_3$ dominated group containing largely fresh waters and more dissolved gas than overlying units, occurring within the Adori Sandstone, Birkhead Formation, Hutton Sandstone and Clematis Sandstone.

The Na-$HCO_3$ group differs significantly from the hydrochemical system for the Galilee Basin units identified by the BA programme, which is a Na-Cl dominated system seen in the Clematis Group, upper Permian coal measures and Joe Joe Group.

Key differences between the hydrochemical classification of Moya et al. (2015) and this work are the inclusion by Moya et al. (2015) of the Wallumbilla Formation (Rolling Downs Group aquitard) in the Na-$HCO_3$-Cl system, and the grouping of the Hutton Sandstone with the Clematis Group in a Na-$HCO_3$ type system. No hierarchical clustering was undertaken in the Galilee subregion BA, and hydrochemical systems were defined on the basis of average ionic abundance as a fraction of TDS, and the ions with which TDS was highly correlated. Significant data were included in the Galilee subregion BA for the upper Permian coal measures and Joe Joe Group, which were not analysed by Moya et al. (2015). The data indicates to these authors that the units underlying the Moolayember Formation comprise a generally more brackish hydrochemical system than the units overlying the Moolayember Formation, with a predominance of Na and Cl and a weaker relationship to $HCO_3$ than in the Eromanga Basin aquifers. The possibility of a hydrological disconnect between the Hutton Sandstone and Clematis Group aquifers is discussed by Moya et al. (2015) who conclude that it seems probable that the Moolayember Formation forms a tight aquitard between these units, but there are insufficient data to discount the possibility of water being exchanged between these units. In this product the possibility of leakage across the Moolayember Formation is explored through a number of different methods.

Detailed hydrochemistry of each hydrogeologic unit is summarised below. These data have been treated as a regionally representative dataset to examine the processes controlling water quality in each hydrogeologic unit at a regional scale. However, differences in hydrochemical processes present at smaller scales have not been examined for each hydrogeologic unit. The complexity of the data suggests that there may be different processes acting along different flow paths for each hydrogeologic unit, rather than groundwater evolving over a single chemical pathway in the subregion.

### Winton-Mackunda partial aquifer

The Winton-Mackunda partial aquifer overlies the Rolling Downs Group aquitard. A total of 611 samples passed the QC process. Of these, 440 had pH data available for the multivariate analysis. Salinity has a very broad range, with TDS from 79 to 20,400 mg/L. The principal ions are Na and Cl, with minor $SO_4$. Their relative abundances are 32%, 47% and 9% respectively (Table 9, Figure 36).

**Table 9 Hydrochemistry of the Winton-Mackunda partial aquifer**

| | pH | Na (mg/L) | K (mg/L) | Ca (mg/L) | Mg (mg/L) | Cl (mg/L) | Alk (mg/L) | $CO_3$ (mg/L) | $SO_4$ (mg/L) | SAR | TDS (mg/L) |
|---|---|---|---|---|---|---|---|---|---|---|---|
| **Mean** | 7.66 | 1133 | 1.8 | 111.7 | 40.5 | 1676 | 270.2 | 44.4 | 318.1 | 31.1 | 3541 |
| **Mean/TDS** | NA | 32% | 0% | 3% | 1% | 47% | 8% | 1% | 9% | NA | NA |
| **Std dev** | 0.70 | 908 | 6 | 182 | 64 | 1647 | 287 | 70 | 403 | 19 | 2881 |
| **10th percentile** | 6.90 | 287 | 0 | 6 | 1 | 259 | 70 | 0 | 0 | 10 | 1029 |
| **Median** | 7.70 | 990 | 0 | 56 | 19 | 1319 | 201 | 4 | 150 | 30 | 3028 |
| **90th percentile** | 8.30 | 2334 | 708 | 283 | 105 | 3880 | 540 | 150 | 877 | 55 | 7398 |

NA = data not available, SAR = sodium absorption ratio, TDS = total dissolved solids, std dev = standard deviation
Data: Bioregional Assessment Programme (Dataset 1)

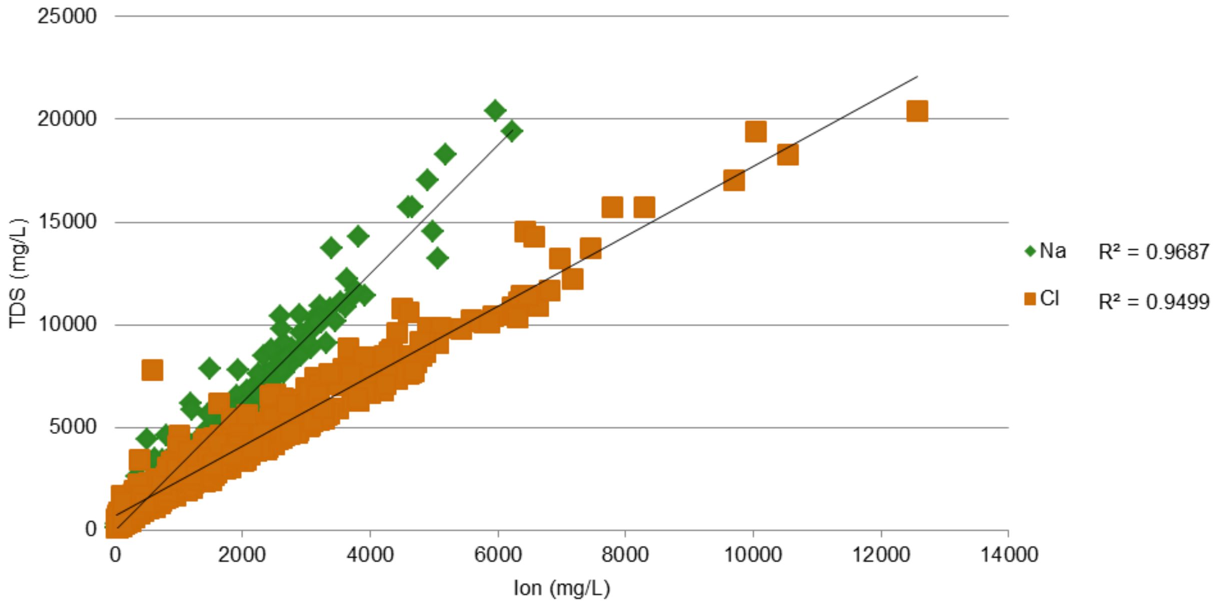


**Figure 36 Chloride (Cl) and sodium (Na) relationships to total dissolved solids (TDS) in the Winton-Mackunda partial aquifer**

Data: Bioregional Assessment Programme (Dataset 1)

Distribution of TDS is variable in the Winton-Mackunda partial aquifer, with a number of areas of higher salinity occurring through the subregion. The Winton-Mackunda partial aquifer shows little change in ion:Cl ratios with TDS (Figure 37).

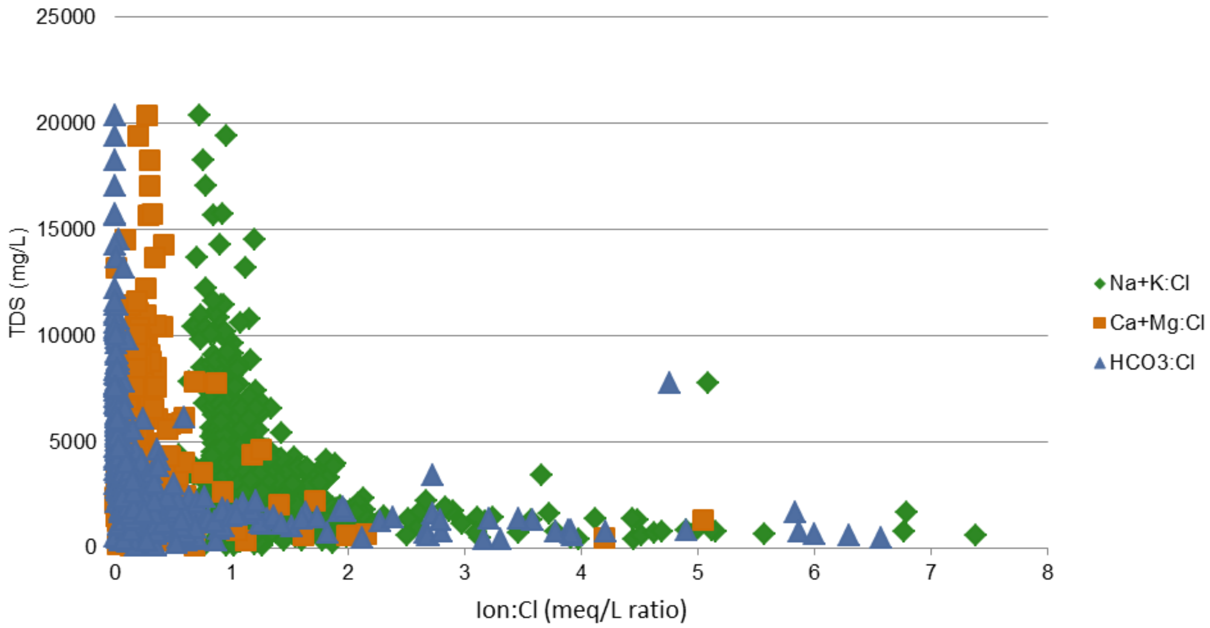


**Figure 37 Ion:chloride (Cl) ratios versus total dissolved solids (TDS) in the Winton-Mackunda partial aquifer**

TDS = total dissolved solids

Data: Bioregional Assessment Programme (Dataset 1)

### Rolling Downs Group aquitard

The Rolling Downs Group aquitard overlies the Cadna-owie – Hooray Sandstone aquifer. A total of 159 samples passed the QC process. Of these, 127 had pH values available for the multivariate analysis. Salinity shows a broad range, with TDS from 170 to 12,735 mg/L. The principal ions are Na and Cl, with minor $SO_4$. Their respective abundances are 29%, 43% and 12% (Table 10, Figure 38). It is apparent that some samples on Figure 38 have anomalous ionic concentrations, for example low Cl or $HCO_3$ relative to TDS. Further investigation may be warranted to determine whether the anomalies are due to hydrogeological processes or is a sample artefact.

**Table 10 Hydrochemistry of the Rolling Downs Group aquitard**

| | pH | Na (mg/L) | K (mg/L) | Ca (mg/L) | Mg (mg/L) | Cl (mg/L) | Alk (mg/L) | $CO_3$ (mg/L) | $SO_4$ (mg/L) | SAR | TDS (mg/L) |
|---|---|---|---|---|---|---|---|---|---|---|---|
| **Mean** | 7.82 | 688 | 3 | 104.8 | 38.1 | 1019.3 | 238.4 | 30.6 | 276.2 | 20.58 | 2377 |
| **Mean/TDS** | NA | 29% | 0.001% | 4% | 2% | 43% | 10% | 1% | 12% | NA | NA |
| **Std dev** | 0.61 | 733 | 6 | 187 | 68 | 1336 | 158 | 55 | 508 | 16 | 2507 |
| **10th percentile** | 7.20 | 96 | 0 | 2 | 0 | 51 | 87 | 0 | 0 | 5 | 360 |
| **Median** | 7.90 | 333 | 0 | 20 | 8 | 265 | 212 | 2 | 75 | 17 | 1155 |
| **90th percentile** | 8.50 | 1773 | 8 | 268 | 99 | 2712 | 518 | 108 | 750 | 38 | 5811 |

NA = data not available, SAR = sodium absorption ratio, TDS = total dissolved solids, std dev = standard deviation
Data: Bioregional Assessment Programme (Dataset 1)

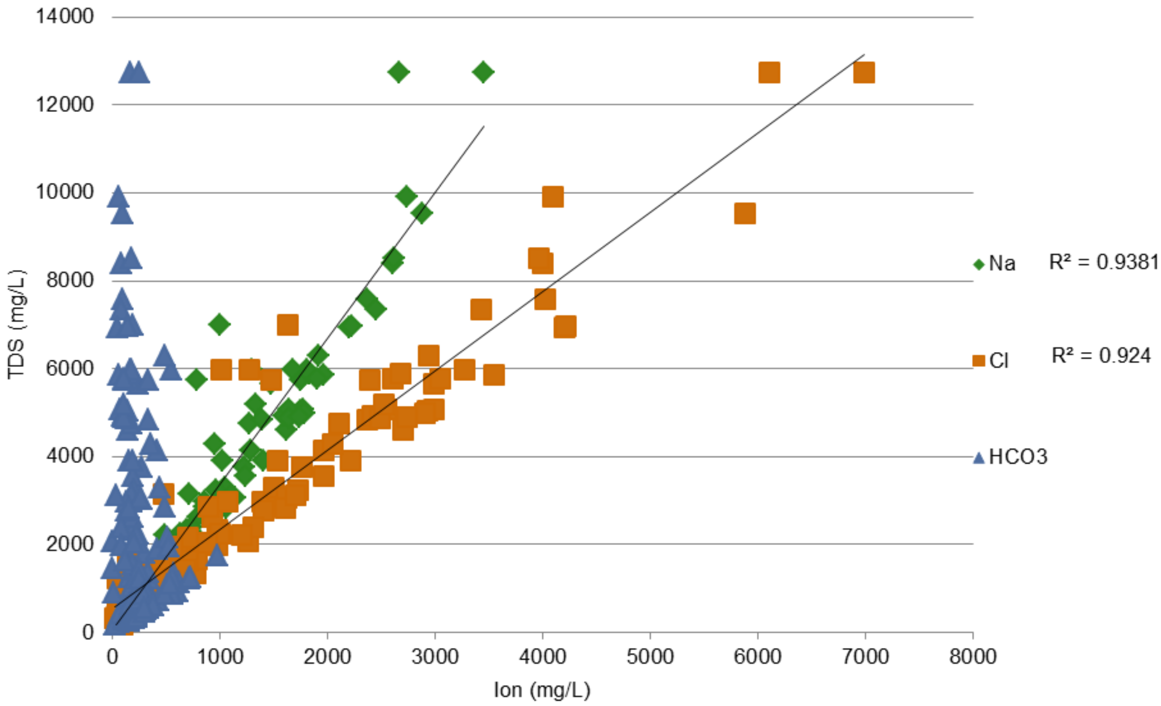


**Figure 38 Chloride (Cl) and sodium (Na) relationship to total dissolved solids (TDS) in the Rolling Downs Group aquitard**

Data: Bioregional Assessment Programme (Dataset 1)

Water in the Rolling Downs Group aquitard is generally fresh with an area of higher salinity in the south of the subregion. Ion:Cl ratios show little variability with TDS (Figure 39). Other than some high Na+K:Cl and $HCO_3$:Cl ratios in the fresher samples, ion:Cl ratios occupy a very narrow band.

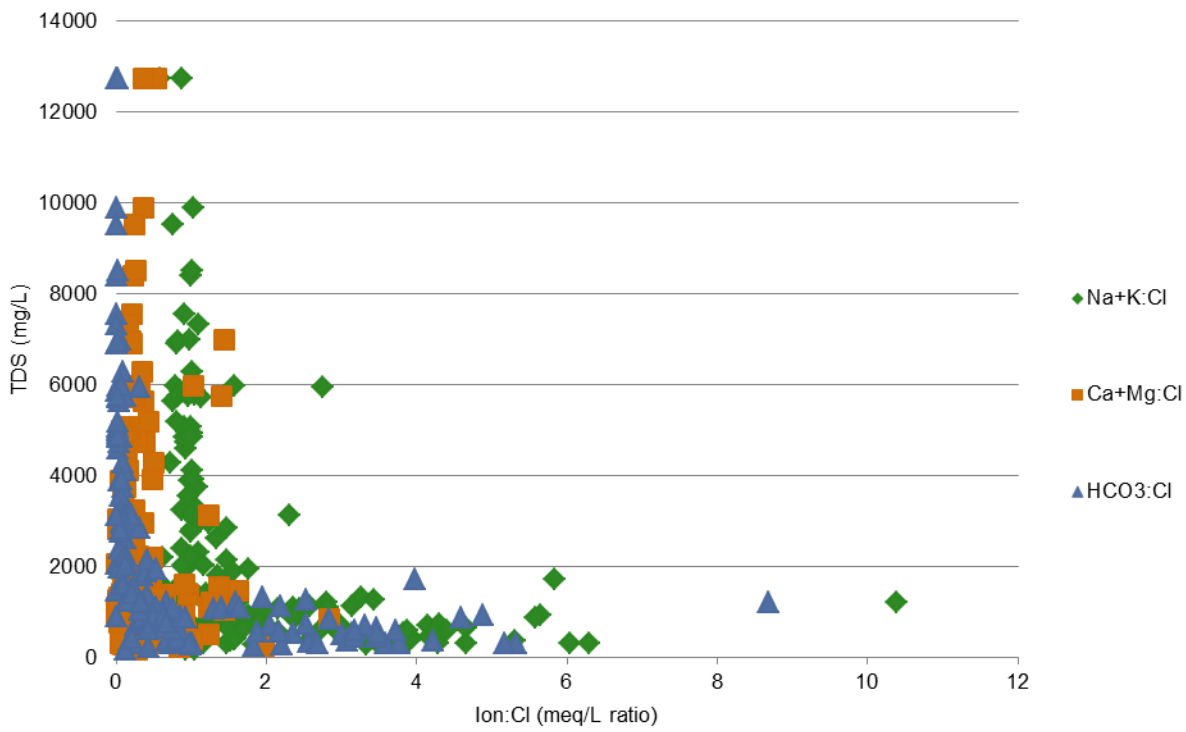


**Figure 39 Ion:chloride (Cl) ratios versus total dissolved solids (TDS) in the Rolling Downs Group aquitard**

TDS = total dissolved solids
Data: Bioregional Assessment Programme (Dataset 1)

### Cadna-owie – Hooray Sandstone aquifer

There were 1302 samples for the Cadna-owie – Hooray sandstone aquifer after QA/QC filtering, of which 1269 samples had pH values. Samples were collected in the formation at a depth of up to 2920 m. The Cadna-owie – Hooray Sandstone aquifer shows a broad range in salinity as measured by TDS (180–7136 mg/L). The major ions are Cl, Na and $HCO_3$. The mean concentrations of these ions as a percentage of TDS are 17%, 28% and 47% respectively (Table 11, Figure 40). It is apparent that some samples shown on Figure 40 have anomalous ionic concentrations, for example low Cl or $HCO_3$ relative to TDS. Further investigation in the future may determine whether the anomalies are due to a hydrogeological process or are an artefact of the sample.

**Table 11 Hydrochemistry of the Cadna-owie – Hooray Sandstone aquifer**

| | pH | Na (mg/L) | K (mg/L) | Ca (mg/L) | Mg (mg/L) | Cl (mg/L) | Alk (mg/L) | $CO_3$ (mg/L) | $SO_4$ (mg/L) | SAR | TDS (mg/L) |
|---|---|---|---|---|---|---|---|---|---|---|---|
| **Mean** | 8.16 | 231.8 | 4.1 | 14.4 | 5 | 139.9 | 390.6 | 10.2 | 49.6 | 27.7 | 834 |
| **Mean/TDS** | NA | 28% | 0.005% | 2% | 1% | 17% | 47% | 1% | 6% | NA | NA |
| **Std dev** | 0.45 | 192 | 5 | 33 | 13 | 200 | 322 | 24 | 134 | 25 | 643 |
| **10th percentile** | 7.60 | 64 | 0 | 2 | 0 | 36 | 171 | 0 | 0 | 3 | 335 |
| **Median** | 8.20 | 197 | 2 | 4 | 1 | 88 | 322 | 3 | 11 | 27 | 619 |
| **90th percentile** | 8.60 | 480 | 11 | 22 | 11 | 250 | 900 | 28 | 87 | 65 | 1603 |

NA = data not available, SAR = sodium absorption ratio, TDS = total dissolved solids, std dev = standard deviation
Data: Bioregional Assessment Programme (Dataset 1)

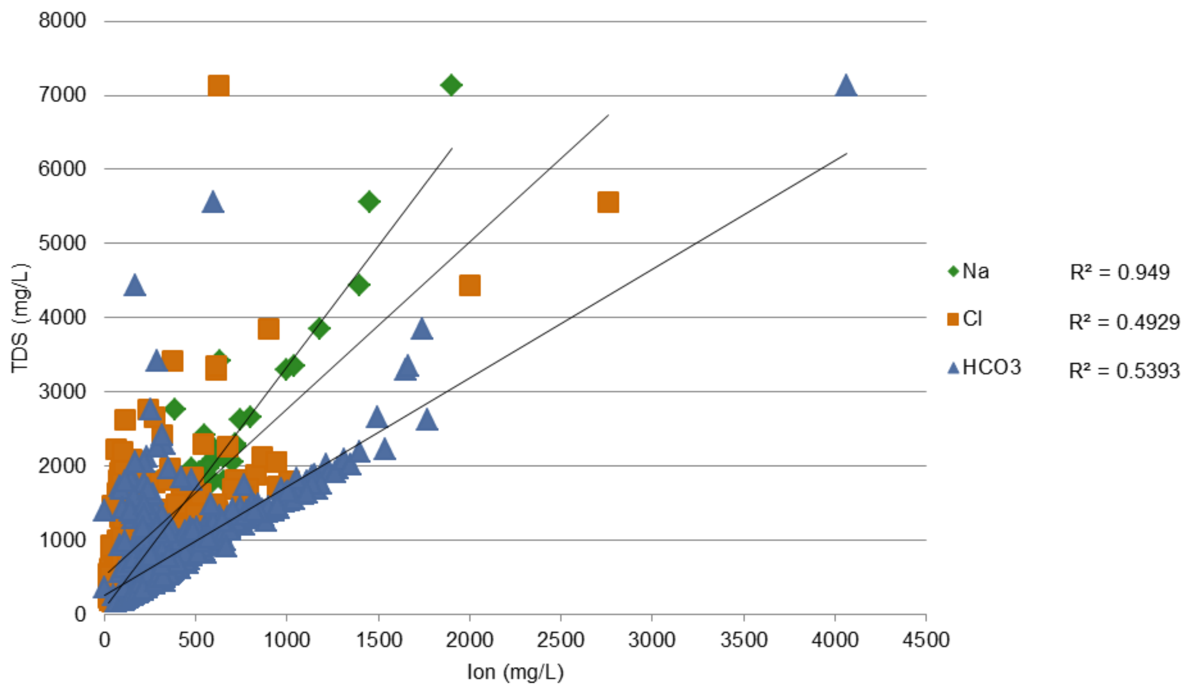


**Figure 40 Chloride (Cl), sodium (Na) and bicarbonate ($HCO_3$) relationships to total dissolved solids (TDS) in the Cadna-owie – Hooray Sandstone aquifer**

Data: Bioregional Assessment Programme (Dataset 1)

Like the Injune Creek Group and Hutton Sandstone aquifer, the Cadna-owie – Hooray Sandstone aquifer is generally fresh (TDS < 1000 mg/L) with higher salinities occurring on the Maneroo Platform. Ion:Cl ratios are variable where TDS is below about 2000 mg/L, but has a lower variance where TDS is greater than 2000 mg/L (Figure 41).

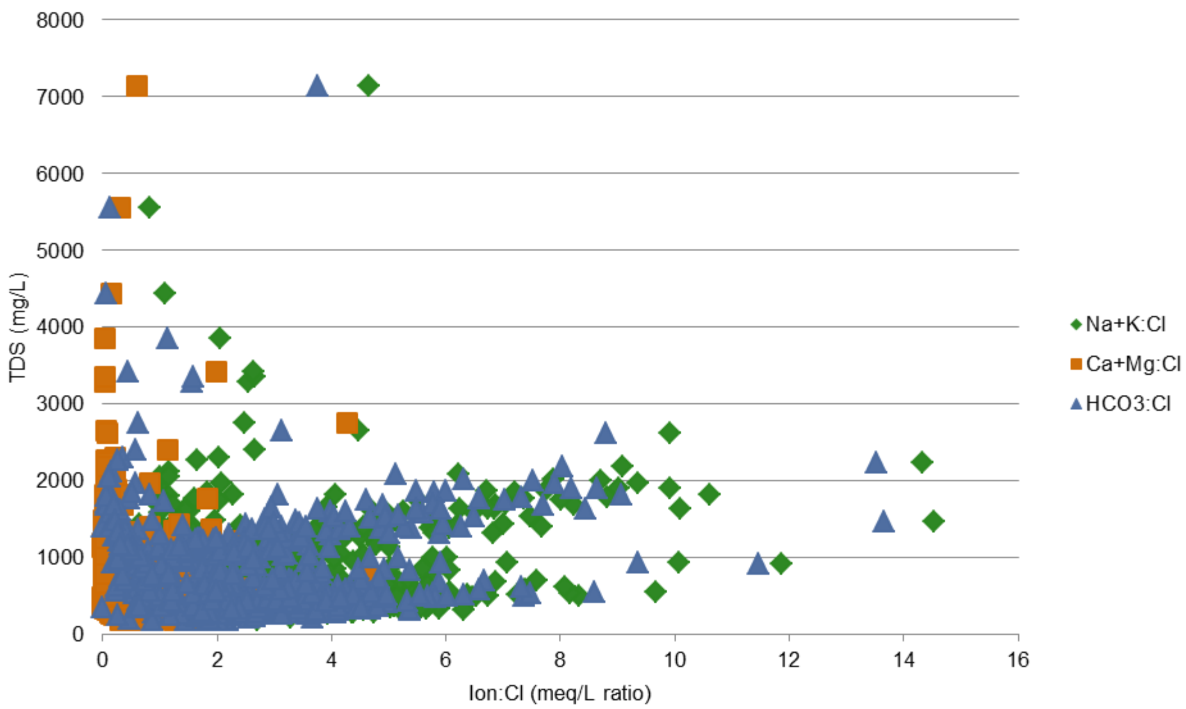


**Figure 41 Ion:chloride (Cl) ratios versus total dissolved solids (TDS) in the Cadna-owie – Hooray Sandstone aquifer**

TDS = total dissolved solids
Data: Bioregional Assessment Programme (Dataset 1)

### Injune Creek Group aquitard

The Injune Creek Group aquitard overlies the Hutton Sandstone aquifer. A summary of the hydrochemical data for the Injune Creek Group aquitard is presented in Table 12. There were 146 samples available for analysis after QA/QC filtering, of which 134 samples had pH values.

**Table 12 Hydrochemistry of the Injune Creek Group aquitard**

| | pH | Na (mg/L) | K (mg/L) | Ca (mg/L) | Mg (mg/L) | Cl (mg/L) | Alk (mg/L) | $CO_3$ (mg/L) | $SO_4$ (mg/L) | SAR | TDS (mg/L) |
|---|---|---|---|---|---|---|---|---|---|---|---|
| **Mean** | 8.07 | 159.9 | 5 | 14.2 | 5.44 | 119.26 | 267.15 | 8.68 | 25.8 | 16.6 | 597 |
| **Mean/TDS** | NA | 27% | 1% | 2% | 1% | 20% | 45% | 1% | 4% | NA | NA |
| **Std dev** | 0.53 | 127 | 6 | 15 | 11 | 122 | 242 | 24 | 38 | 19 | 396 |
| **10th percentile** | 7.4 | 45 | 0 | 2 | 0 | 36 | 113 | 0 | 1 | 3 | 283 |
| **Median** | 8.2 | 131 | 1 | 8 | 2 | 75 | 239 | 1 | 12 | 11 | 493 |
| **90th percentile** | 8.6 | 381 | 13 | 32 | 14 | 197 | 678 | 19 | 54 | 45 | 1322 |

NA = data not available, SAR = sodium absorption ratio, TDS = total dissolved solids, std dev = standard deviation
Data: Bioregional Assessment Programme (Dataset 1)

Injune Creek Group aquitard shows a broad range in salinity (286–9541 mg/L TDS). The major ions are Cl, Na and $HCO_3$. The mean concentrations of these ions as a percentage of TDS are 20%, 27% and 45% respectively (Figure 42).

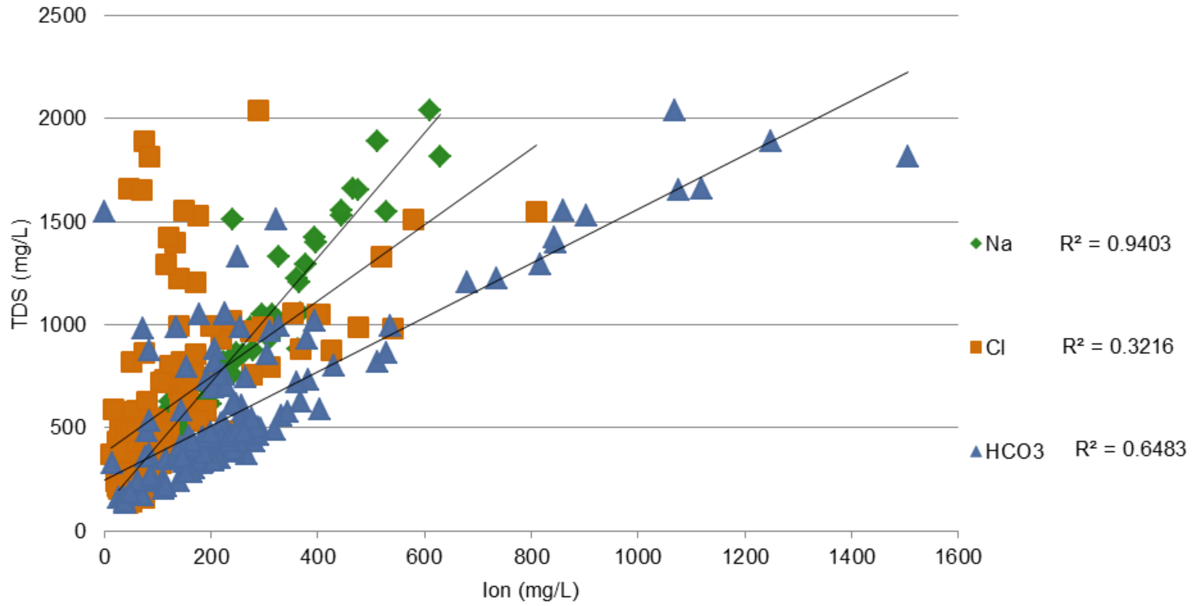


**Figure 42 Chloride (Cl), sodium (Na), and bicarbonate ($HCO_3$) relationship to total dissolved solids (TDS) in the Injune Creek Group aquitard**

Data: Bioregional Assessment Programme (Dataset 1)

Like the Hutton Sandstone aquifer, the Injune Creek Group aquitard is fresh in much of the subregion, with higher salinities occurring on the Maneroo Platform. This may be an indication of hydraulic connection between these two hydrogeologic units, or may reflect similarities in the composition of aquifer material. Ion:Cl ratios are variable in the Injune Creek Group aquitard, indicating a variety of processes acting on solute concentrations (Figure 43). There is a tendency for low Ca+Mg:Cl ratios where TDS is high.

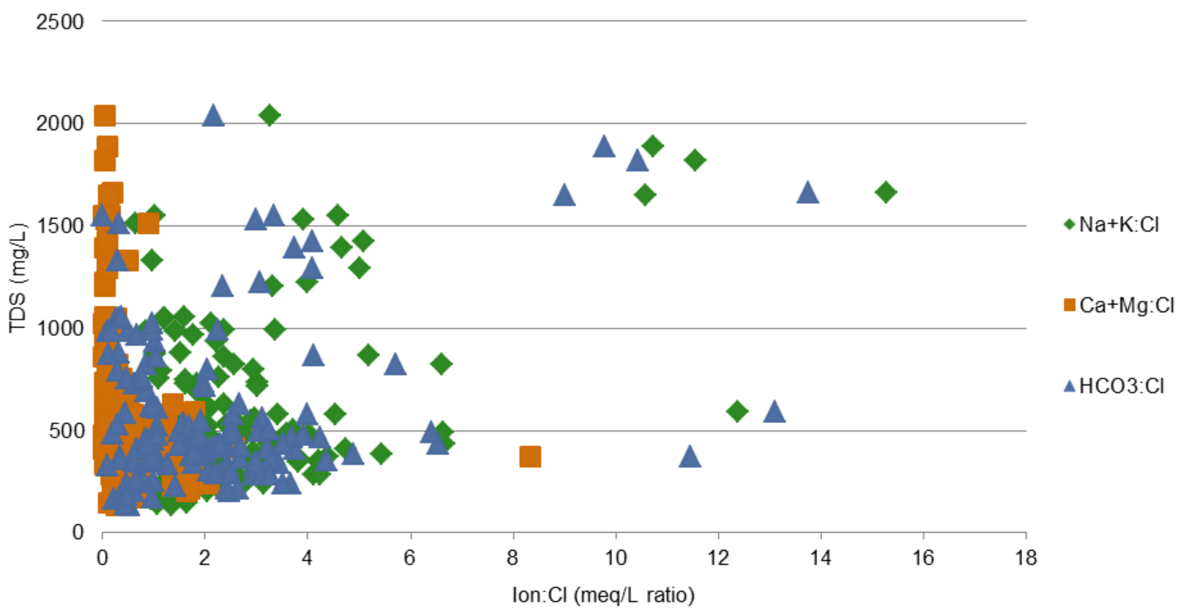


**Figure 43 Ion:chloride (Cl) ratios versus total dissolved solids (TDS) in the Injune Creek Group aquitard**

TDS = total dissolved solids

Data: Bioregional Assessment Programme (Dataset 1)

### Hutton Sandstone aquifer

The Hutton Sandstone aquifer overlies the Clematis Group aquifer, separated by the Moolayember Formation which acts as a regional aquitard (see companion product 1.1 for the Galilee subregion (Evans et al., 2014)). There were 1302 samples for the Hutton Sandstone after QA/QC filtering, of which 1269 samples had pH values. The Hutton Sandstone shows a significant range in salinity (55–3579 mg/L TDS). The major ions are Cl, Na and $HCO_3$. The mean concentrations of these ions as a percentage of TDS are 14%, 23% and 54% respectively (Table 13, Figure 44). It is apparent that some samples shown on Figure 44 have anomalous ionic concentrations, for example low or high $HCO_3$ relative to TDS. Further investigation may be warranted in the future to determine whether the anomalies are due to a hydrogeological process or is an artefact of the sample.

**Table 13 Hydrochemistry of the Hutton Sandstone aquifer**

| | pH | Na (mg/L) | K (mg/L) | Ca (mg/L) | Mg (mg/L) | Cl (mg/L) | Alk (mg/L) | $CO_3$ (mg/L) | $SO_4$ (mg/L) | SAR | TDS (mg/L) |
|---|---|---|---|---|---|---|---|---|---|---|---|
| Mean | 8.03 | 112.4 | 6.5 | 15.5 | 6.7 | 67.4 | 261.6 | 5 | 12.2 | 11.8 | 482 |
| Mean/TDS | NA | 23% | 1% | 3% | 1% | 14% | 54% | 1% | 3% | NA | NA |
| Std dev | 0.47 | 108 | 6 | 21 | 9 | 99 | 165 | 19 | 27 | 14 | 335 |
| 10th percentile | 7.4 | 42 | 0 | 2 | 0 | 27 | 128 | 0 | 0 | 2 | 261 |
| Median | 8.1 | 89 | 4 | 8 | 2 | 45 | 231 | 1 | 7 | 8 | 406 |
| 90th percentile | 8.5 | 270 | 15 | 30 | 16 | 130 | 534 | 12 | 22 | 35 | 959 |

NA = data not available, SAR = sodium absorption ratio, TDS = total dissolved solids, std dev = standard deviation
Data: Bioregional Assessment Programme (Dataset 1)

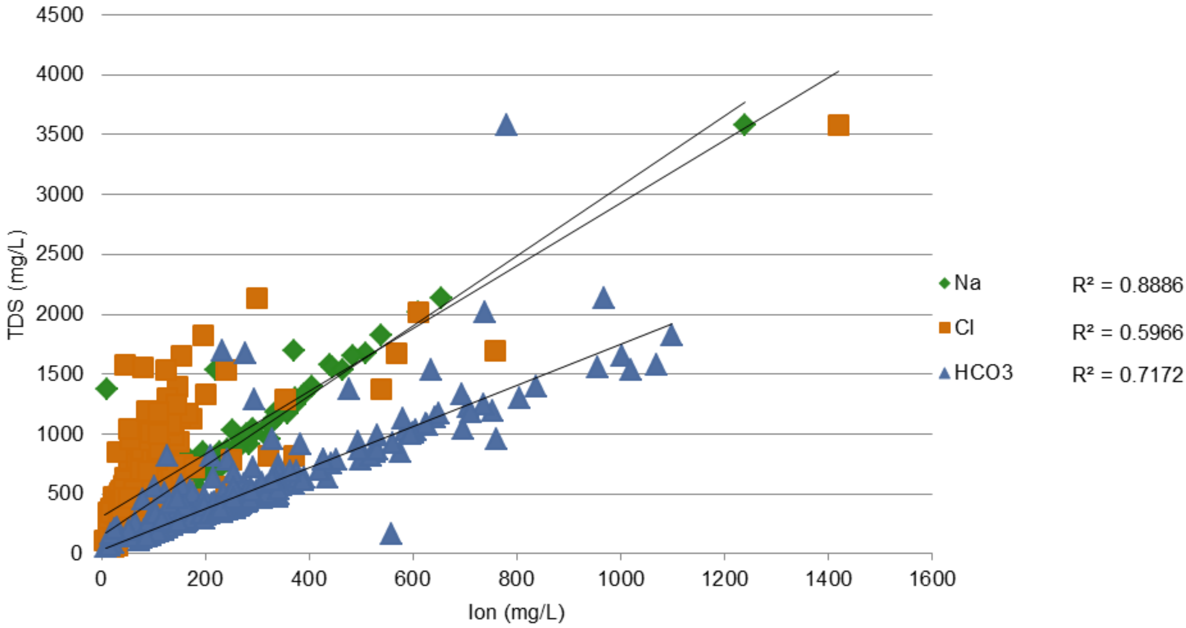


**Figure 44 Chloride (Cl), sodium (Na) and bicarbonate ($HCO_3$) relationship to total dissolved solids (TDS) in the Hutton Sandstone aquifer**

Data: Bioregional Assessment Programme (Dataset 1)

Hutton Sandstone aquifer is predominantly fresh (TDS < 1000 mg/L), with higher salinities on the Maneroo Platform. Ion:Cl ratios are highly variable in the Hutton Sandstone aquifer, indicating a variety of processes affecting solute loads (Figure 45). These may include evapotranspiration, mixing of waters from different hydrogeologic units, and water–rock interactions.

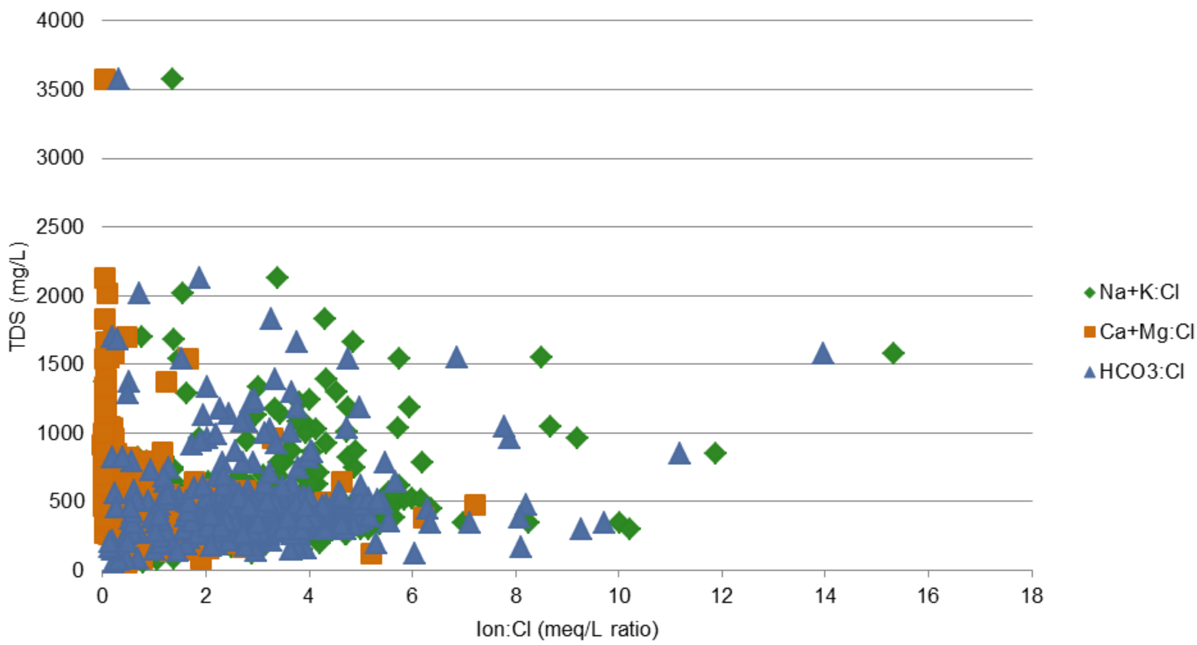


**Figure 45 Ion:chloride (Cl) ratios versus total dissolved solids (TDS) for the Hutton Sandstone aquifer**

Data: Bioregional Assessment Programme (Dataset 1)

### Clematis Group aquifer

The Clematis Group aquifer overlies the upper Permian coal measures and underlies the Moolayember Formation, which is thought to keep it hydraulically separate from the overlying Hutton Sandstone aquifer (see companion product 1.1 for the Galilee subregion (Evans et al., 2014)). A summary of the hydrochemical data is presented in Table 14. There were 98 samples available for analysis after QA/QC filtering, of which 88 samples had pH values for multivariate analysis.

**Table 14 Hydrochemistry of the Clematis Group aquifer**

| | pH | Na (mg/L) | K (mg/L) | Ca (mg/L) | Mg (mg/L) | Cl (mg/L) | Alk (mg/L) | $CO_3$ (mg/L) | $SO_4$ (mg/L) | SAR | TDS (mg/L) |
|---|---|---|---|---|---|---|---|---|---|---|---|
| **Mean** | 7.73 | 151.2 | 16.2 | 16.4 | 12.8 | 179.2 | 191.2 | 1.8 | 16 | 10.7 | 574 |
| **Mean/TDS** | NA | 26% | 1% | 3% | 2% | 31% | 33% | 0.003% | 3% | NA | NA |
| **Std dev** | 0.60 | 149 | 5 | 28 | 33 | 321 | 114 | 6 | 38 | 7 | 549 |
| **10th percentile** | 7.2 | 51 | 0 | 2 | 0 | 33 | 31 | 0 | 0 | 4 | 202 |
| **Median** | 7.8 | 125 | 4 | 6 | 3 | 70 | 205 | 0 | 5 | 9 | 468 |
| **90th percentile** | 8.2 | 264 | 17 | 48 | 29 | 365 | 305 | 2 | 44 | 22 | 919 |

NA = data not available, SAR = sodium absorption ratio, TDS = total dissolved solids, std dev = standard deviation
Data: Bioregional Assessment Programme (Dataset 1)

Salinity in the Clematis Group aquifer shows a broad range (103–3290 mg/L TDS). The major ions are Cl, Na and $HCO_3$. The mean concentrations of these ions as a percentage of TDS are 31%, 26% and 33% respectively, with minor Ca (3%) and sulfate (3%) (Figure 46). The groundwater in the Clematis Group aquifer can be generally described as Na-Cl-$HCO_3$.

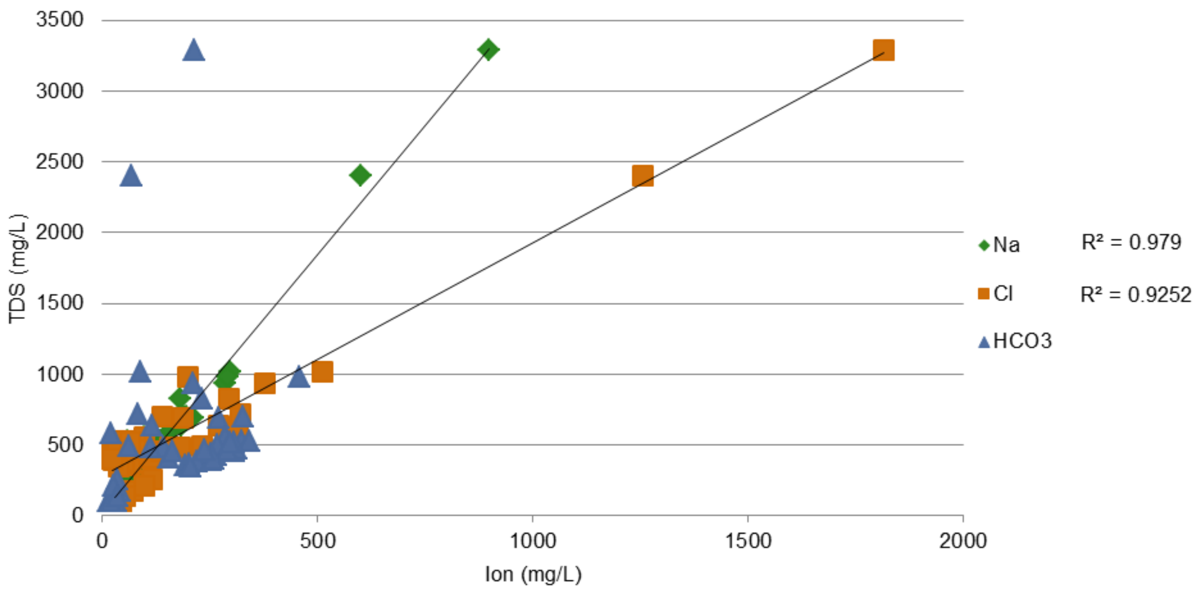


**Figure 46 Chloride (Cl) and sodium (Na) and bicarbonate ($HCO_3$) relationship to total dissolved solids (TDS) in the Clematis Group aquifer**

Data: Bioregional Assessment Programme (Dataset 1)

It is apparent that some samples shown on Figure 46 have anomalous ionic concentrations, for example low $HCO_3$ relative to TDS. Further investigation in the future may determine whether these anomalies are due to hydrogeological processes or are an artefact of the sample.

Groundwaters in the Clematis Group aquifer are fresh (TDS 100–200 mg/L) close to the Clematis Group outcrop in the east of the subregion. Further west salinities are higher (up to 3000 mg/L TDS). Close to the western extent of the Clematis Group aquifer, in the central part of the Galilee subregion between the Maneroo Platform and Aramac, groundwater in the Clematis Group has lower salinity (300–500 mg/L TDS).

Ion:Cl ratios in the Clematis Group aquifer (Figure 47) show little variation with TDS, much like the upper Permian coal measures (Figure 49) and Joe Joe Group, except for a region of elevated Na+K:Cl ratios and $HCO_3$:Cl ratios at relatively low TDS.

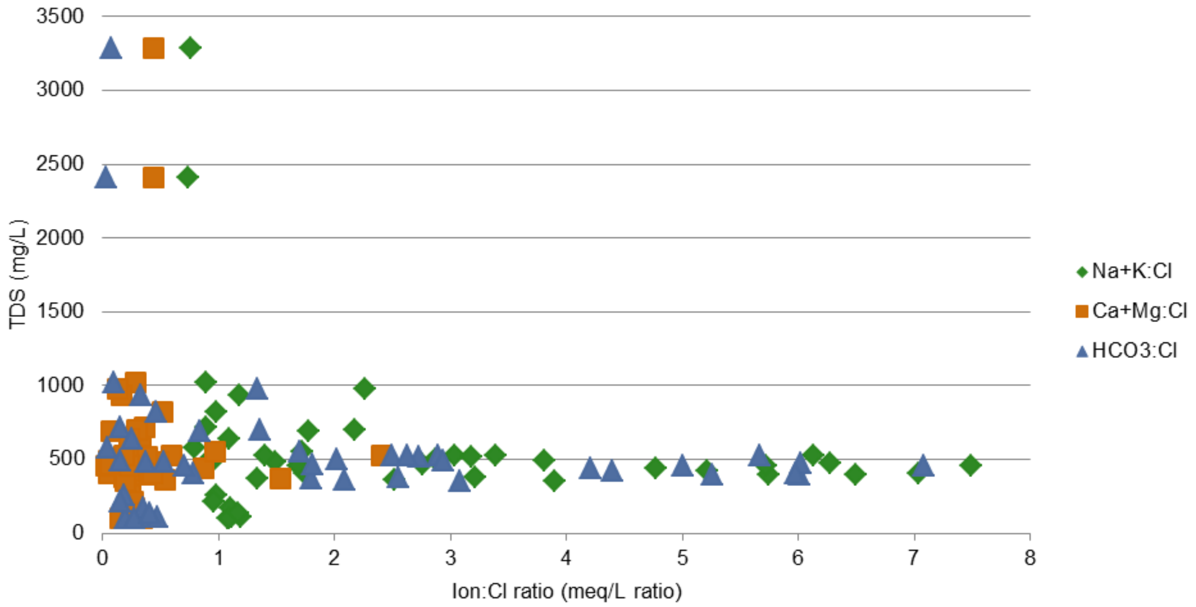


**Figure 47 Ion:chloride (Cl) ratios versus total dissolved solids (TDS) in the Clematis Group**

TDS = total dissolved solids
Data: Bioregional Assessment Programme (Dataset 1)

### Upper Permian coal measures partial aquifer

The upper Permian coal measures overlies the Joe Joe Group and underlies the Clematis Group. A summary of the hydrochemical data for the upper Permian coal measures is presented in Table 15. There were 132 samples available for analysis after QA/QC filtering, of which 46 samples had pH values for the multivariate analysis.

Salinity in the upper Permian coal measures shows a broad range. The major ions are Cl, Na and $HCO_3$. The mean concentrations of these ions as a percentage of TDS are 34%, 28% and 26% respectively, with minor Ca (3%) and Mg (2%) and $SO_4$ (5%) (Figure 48). The groundwater can be generally described as Na-Cl-$HCO_3$ with possible calcium-magnesium carbonate species. The possibility of secondary gypsum or dolomite forming in the aquifer material should be investigated further.

**Table 15 Hydrochemistry of the upper Permian coal measures partial aquifer**

| | pH | Na (mg/L) | K (mg/L) | Ca (mg/L) | Mg (mg/L) | Cl (mg/L) | Alk (mg/L) | $CO_3$ (mg/L) | $SO_4$ (mg/L) | SAR | TDS (mg/L) |
|---|---|---|---|---|---|---|---|---|---|---|---|
| **Mean** | 7.24 | 298.6 | 16.2 | 27.2 | 16.9 | 371.4 | 275 | 15.6 | 57.6 | 14.8 | 1078 |
| **Mean/TDS** | NA | 28% | 2% | 3% | 2% | 34% | 26% | 1% | 5% | NA | NA |
| **Std dev** | 1.41 | 173 | 25 | 23 | 20 | 264 | 194 | 64 | 93 | 12 | 516 |
| **10th percentile** | 5.78 | 134 | 3 | 6 | 2 | 88 | 104 | 0 | 1 | 7 | 570 |
| **Median** | 7.70 | 242 | 8 | 18 | 6 | 232 | 218 | 5 | 24 | 14 | 858 |
| **90th percentile** | 8.28 | 450 | 22 | 45 | 39 | 634 | 556 | 16 | 134 | 22 | 1581 |

NA = data not available, SAR = sodium absorption ratio, TDS = total dissolved solids, std dev = standard deviation
Data: Bioregional Assessment Programme (Dataset 1)

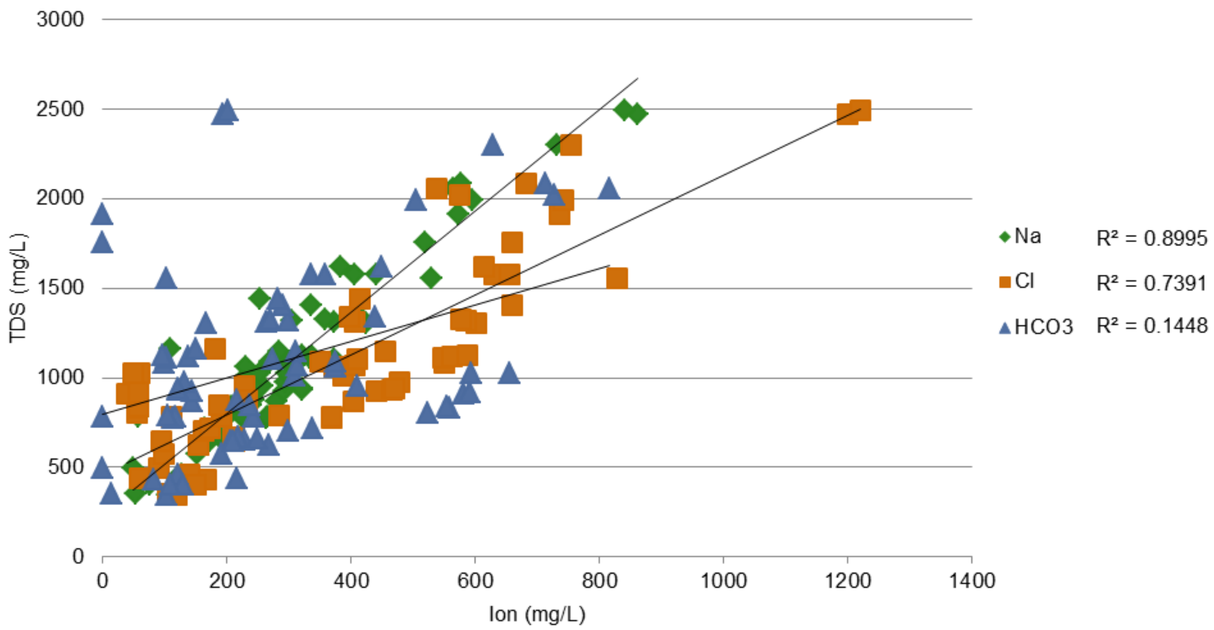


**Figure 48 Plot of chloride (Cl), sodium (Na), and bicarbonate ($HCO_3$) relationship with total dissolved solids (TDS) in the upper Permian coal measures partial aquifer**

Data: Bioregional Assessment Programme (Dataset 1)

Bores screened in the upper Permian coal measures partial aquifer have a limited distribution. The freshest water is located around areas of outcrop where recharge occurs (see companion product 1.5 for the Galilee subregion (Evans et al., 2015)). Ion:Cl ratios in the upper Permian coal measures partial aquifer show little variation with TDS (Figure 49). It is apparent that some samples shown on Figure 48 have anomalous ionic concentrations, for example low $HCO_3$ relative to TDS. Further investigation may be warranted to determine whether these anomalies are due to hydrogeological processes or are a sample artefact.

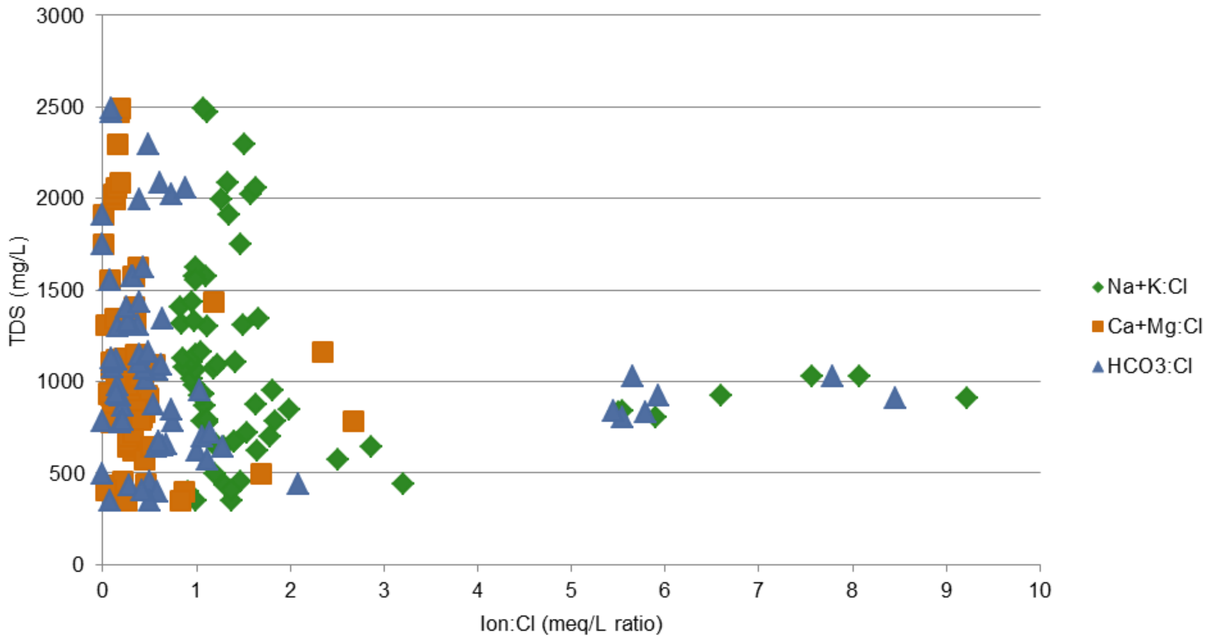


**Figure 49 Ion:chloride (Cl) ratios versus total dissolved solids (TDS) in the upper Permian coal measures**

TDS = total dissolved solids
Data: Bioregional Assessment Programme (Dataset 1)

### Joe Joe Group partial aquifer

The Joe Joe Group partial aquifer is the lowermost hydrogeologic unit in the Galilee Basin sequence. A summary of the hydrochemical data are presented in Table 16. There were 106 samples available for analysis after QA/QC filtering, of which 99 samples had pH values for the multivariate analysis.

Salinity in the Joe Joe Group aquifer shows a broad range (175–11,060 mg/L TDS). The major ions are Cl, Na and $HCO_3$. The mean concentrations of these ions as a percentage of TDS are 36%, 23% and 24% respectively with minor Ca (4%) and $SO_4$ (6%). The groundwater can be generally described as Na-Cl with minor bicarbonate.

**Table 16 Hydrochemistry of the Joe Joe Group partial aquifer**

| | pH | Na (mg/L) | K (mg/L) | Ca (mg/L) | Mg (mg/L) | Cl (mg/L) | Alk (mg/L) | $CO_3$ (mg/L) | $SO_4$ (mg/L) | SAR | TDS (mg/L) |
|---|---|---|---|---|---|---|---|---|---|---|---|
| **Mean** | 7.5 | 372 | 8 | 81 | 58 | 572 | 393 | 11 | 132 | 7 | 1607 |
| **Mean/TDS** | NA | 23% | 0.005% | 5% | 4% | 36% | 24% | 1% | 8% | NA | NA |
| **Std dev** | 0.99 | 600 | 10 | 112 | 50 | 1082 | 295 | 31 | 210 | 8 | 1967 |
| **10th percentile** | 6.52 | 30 | 0 | 19 | 9 | 38 | 49 | 0 | 0 | 1 | 313 |
| **Median** | 8 | 140 | 3 | 48 | 45 | 120 | 400 | 1 | 55 | 4 | 928 |
| **90th percentile** | 8.2 | 1024 | 24 | 180 | 136 | 1978 | 714 | 24 | 262 | 18 | 4155 |

NA = data not available, SAR = sodium absorption ratio, TDS = total dissolved solids, std dev = standard deviation
Data: Bioregional Assessment Programme (Dataset 1)

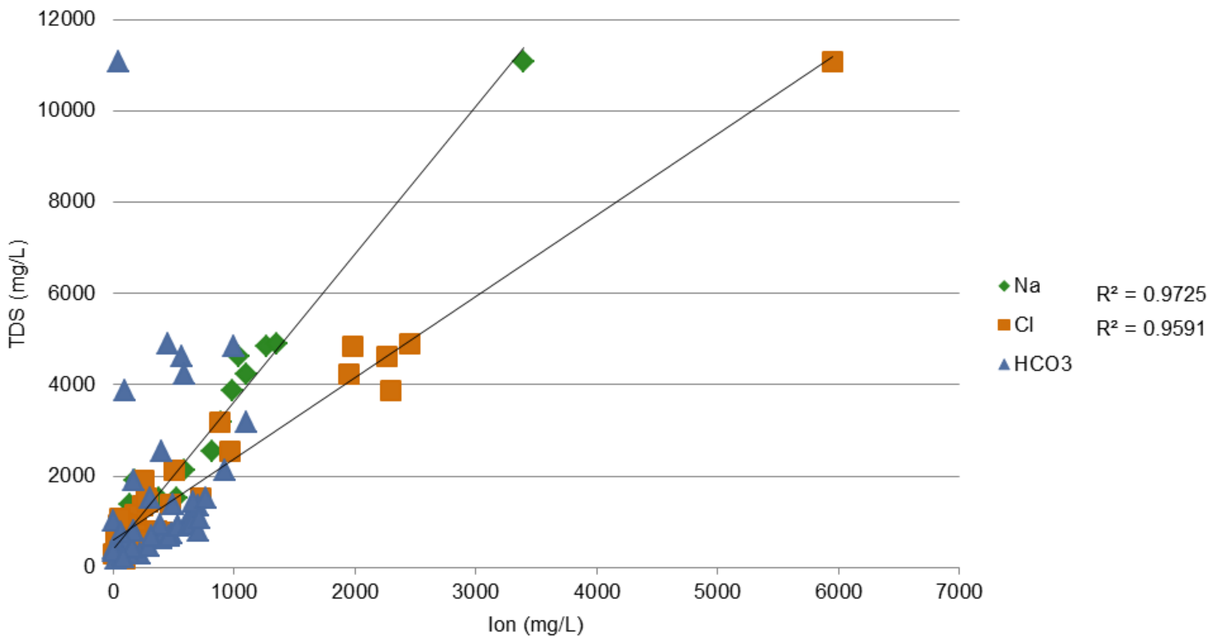


**Figure 50 Sodium (Na), chloride (Cl) and bicarbonate ($HCO_3$) relationship to total dissolved solids (TDS) in the Joe Joe Group partial aquifer**

Data: Bioregional Assessment Programme (Dataset 1)

The strong correlation between TDS and sodium and chloride (Figure 50) indicates that these two elements account for the majority of salinity changes in the Joe Joe Group. In the south of the Galilee subregion a small area of high bicarbonate concentration is at odds with this trend. Anomalously, TDS for the Joe Joe Group is highest in the north-east of the Galilee subregion, close to where the Permian and Carboniferous rocks outcrop. This may be an indication that recharge does not occur in this region, or that potential for flow is from the deep central parts of the basin to the margins. Ion:Cl ratios in the Joe Joe Group show very little variation with TDS (Figure 51).

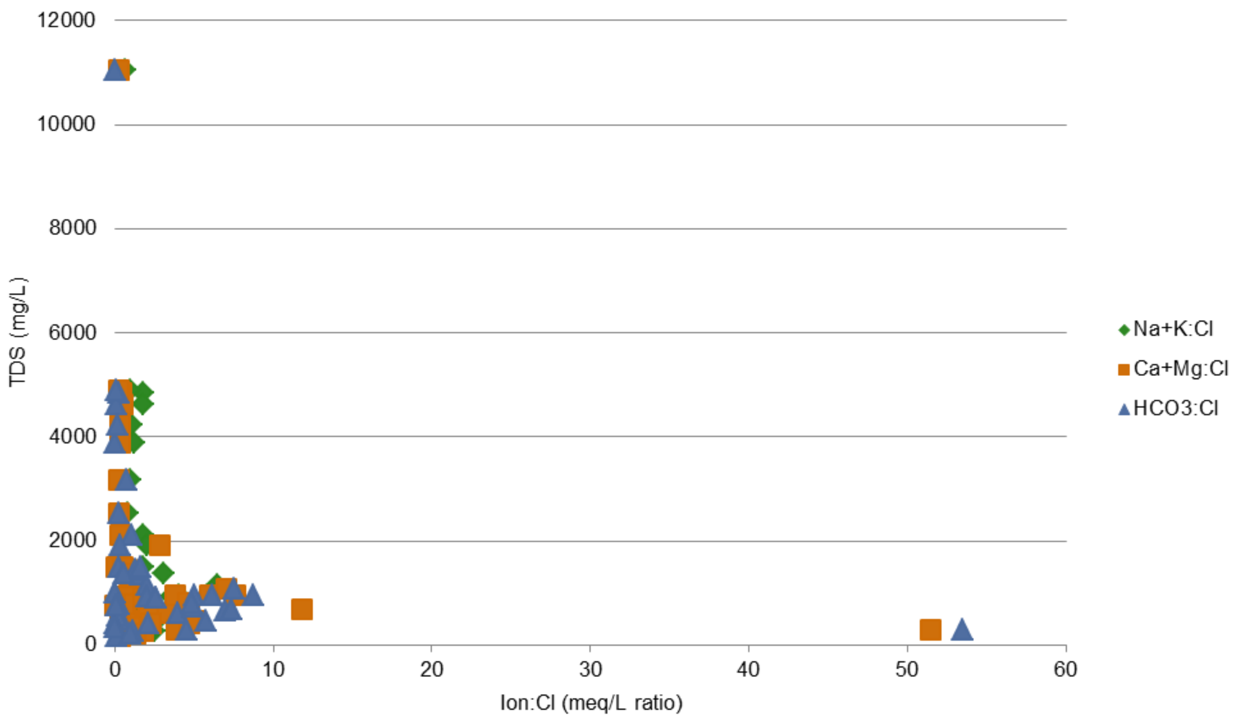


**Figure 51 Ion:chloride (Cl) ratios versus total dissolved solids (TDS) in the Joe Joe Group partial aquifer**

TDS = total dissolved solids
Data: Bioregional Assessment Programme (Dataset 1)

#### *2.1.3.2.1.4 Discussion*

**Solute sources**

Defining the sources of solutes to groundwater is important for understanding how groundwater will evolve along a flow path, and to understand the potential for connectivity between different hydrogeologic units. Moya et al. (2015) concluded that in the recharge area in the east of the basin, evaporative concentration of cyclic salts is an important process and leads to a dominance of Na and Cl ions. This is a trend which is common to many of the hydrogeologic units studied here, with the exception of samples collected from the central and western parts of the Galilee subregion. As stated above, the complexity of the dataset indicates that more than one process operates in each hydrogeologic unit in different parts of the subregion. The following discussion attempts to define the major processes operating in each hydrogeologic unit but may not identify local processes operating only in a small area of the subregion.

**Na-Cl system (Winton-Mackunda partial aquifer, Rolling Downs Group aquitard)**

Both the Winton-Mackunda partial aquifer and the Rolling Downs Group aquitard show very high TDS values in some samples (> 10,000 mg/L). Both these units show ion:Cl ratios to be unaffected by increases in TDS at higher salinities; beyond 5,000 mg/L in the Winton-Mackunda partial aquifer, and beyond 2,000 mg/L in the Rolling Downs Group aquitard. This may be indicative of evaporative concentration, which increases TDS without altering the ion:Cl ratio. Radke et al. (2000) suggested that diffusion of original marine salts contained within the marine units of the Rolling Downs Group aquitard and the Mackunda Formation were a controlling factor on high solute loads.

It seems likely that marine salts are the dominant control on very high TDS values. The greater variance in ion:Cl ratios where TDS values are low may represent variable ion:Cl ratios in recharge water, or a mixing signal between marine salts and the cyclic salts contained in recharge water, which becomes overprinted by the marine salt signal as water flows through the system.

**Na-$HCO_3$-Cl system (Cadna-owie – Hooray Sandstone aquifer, Injune Creek Group aquitard, Hutton Sandstone aquifer)**

All three units in this hydrochemical system show greater variability in ion:Cl ratios than the Na-Cl system, and do not show the same restriction of ion:Cl ratios where TDS is high. The variability in ion:Cl ratios may reflect an increased importance of water–rock interaction, such as carbonate dissolution, in this system.

The bicarbonate concentrations of the Hutton Sandstone aquifer and Injune Creek Group aquitard are up to twice that observed in the Joe Joe Group and upper Permian coal measures partial aquifers, or Clematis Group aquifer. This is consistent with observations of carbonate cements in the Jurassic and Cretaceous sequence of the Eromanga Basin (Draper, 2002).

All three units in this hydrochemical system display a wide range of Na+K:Cl, Ca+Mg:Cl, and $HCO_3$:Cl ratios where TDS is low (below 1000–2000 mg/L). Where TDS values are higher, Na+K and $HCO_3$:Cl values may also be high, but Ca+Mg:Cl ratios are consistently low. High Na+K:Cl ratios where TDS is high coupled with low Ca+Mg:Cl ratios may be an indication of cation exchange processes in the aquifer. Herczeg et al. (1991) observed a similar trend and suggested that a combination of carbonate dissolution and cation exchange was the dominant influence on solute concentrations in the Hutton Sandstone aquifer. Based on similarities in the hydrochemistry, this process may also be operating in the Cadna-owie – Hooray Sandstone aquifer and Injune Creek Group aquitard. This process is further explored using the sodium absorption ratio (SAR).

SAR is a measure of the ratio of sodium to calcium and magnesium in solution. In the Galilee subregion, SAR shows a positive correlation with TDS in most units. This is most pronounced in the Hutton Sandstone aquifer, Injune Creek Group aquitard, and Cadna-owie – Hooray Sandstone aquifer. Carbonate dissolution would create high $HCO_3$:Cl ratios, but would be expected to be accompanied by a rise in Ca+Mg:Cl ratios (or reduction in SAR) as well. Instead, elevated SAR levels occur where $HCO_3$:Cl ratios are high. Herczeg et al. (1991) observed a similar trend in samples from the western region of the Eromanga Basin, and suggested that carbonate dissolution may be followed by cation exchange processes, in which Na in clay minerals is exchanged for Ca and Mg in solution, reducing the ratio of Ca+Mg:Cl and allowing SAR to increase where $HCO_3$ concentrations are high.

Another process which could lead to high $HCO_3$:Cl and Na:Cl ratios with low Ca:Cl ratios is albite dissolution, which contributes sodium, bicarbonate and dissolved silica to solution. However, Si:Cl ratios are lowest where SAR is high (Figure 52), which is inconsistent with silicate mineral dissolution contributing solutes to groundwater. The process of carbonate dissolution followed by cation exchange, outlined by Herczeg et al. (1991), adequately explains the trends seen in the data and is assumed to be the dominant control on solute loads in the Na-$HCO_3$-Cl hydrochemical system.

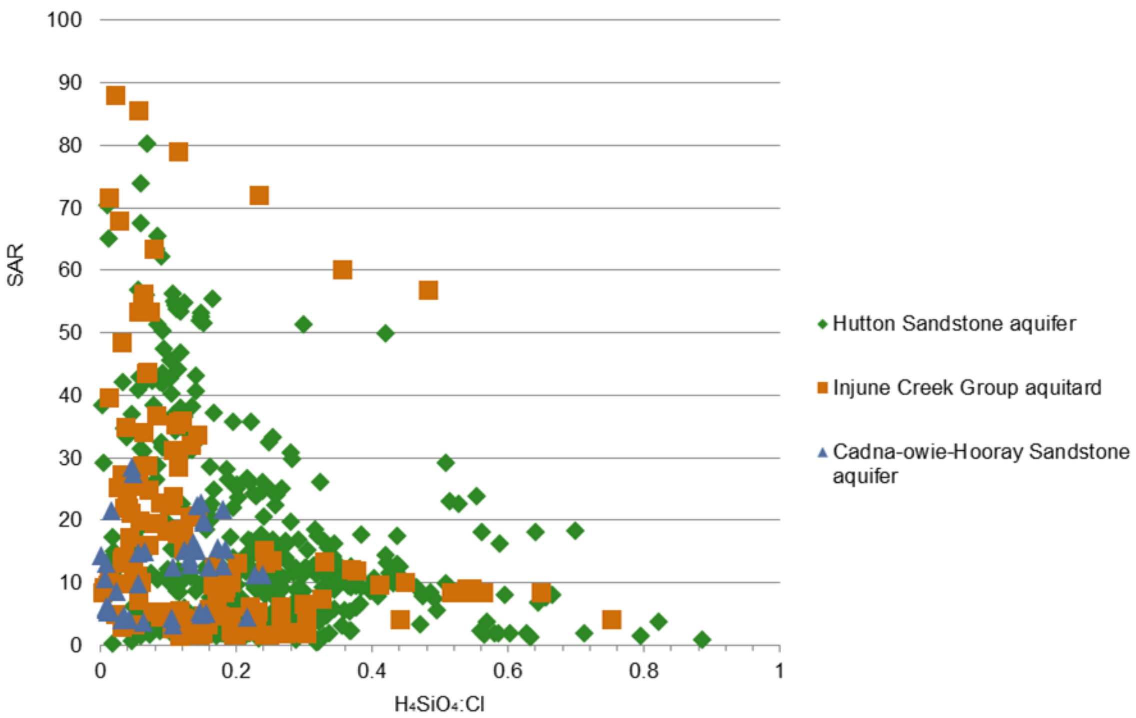


**Figure 52 Sodium absorption ratio (SAR) over dissolved silica ($H_4SiO_4$):chloride ratio in the Na-$HCO_3$-Cl hydrochemical system**

Data: Bioregional Assessment Programme (Dataset 1)

Carbonate dissolution is also considered to be a dominant process in controlling groundwater chemistry by Moya et al. (2015), who observed degassing of groundwater samples, probably associated with dissolved $CO_2$, from the Jurassic, Triassic and Cretaceous units when pumped to the surface.

### Na-Cl system with minor $HCO_3$ (Clematis Group, upper Permian coal measures, Joe Joe Group)

This hydrochemical group shows greater variability in the relative average abundance of ions than the Na-Cl or Na-$HCO_3$-Cl systems, however, they are grouped as a single hydrochemical system based on the similarity in ion-TDS relationships; all three units show high $R^2$ values for Cl and Na with respect to TDS. While $HCO_3$ is high in some Clematis Group aquifer, and upper Permian coal measures partial aquifer samples, there is poor correlation between $HCO_3$ and TDS in these units ($R^2 < 0.2$), indicating that high $HCO_3$ values are a local phenomenon rather than a regional trend.

The distribution of solutes in the Clematis Group aquifer is difficult to explain given that low salinity (TDS < 500 mg/L) groundwater is found to the west of much higher salinity (TDS up to 3000 mg/L TDS) groundwater, at depths of 600 m where no recent recharge is expected. These low salinity groundwaters, in the area between the Maneroo Platform and Aramac, also tend to have higher $HCO_3$:Cl ratios than samples further east. A possible explanation for low salinity and elevated $HCO_3$ concentrations in the Clematis Group is the interactions with fresher, $HCO_3$-rich water from the Hutton Sandstone aquifer. This hypothesis is discussed further in the 'Inter-aquifer mixing' section.

Another possible reason for elevated $HCO_3$ concentrations in the Clematis Group aquifer is upward migration of $CO_2$ from the underlying upper Permian coal measures, though this would not account for the low salinity of these samples when groundwater in the Clematis Group is of higher salinity further east. Potentiometric head difference maps in Section 2.1.3.2.4 show the upper Permian coal measures, which are known to have potentially economic gas contents, has a higher potentiometric surface than the Clematis Group aquifer between the Maneroo Platform and Aramac, meaning upward migration of gas containing $CO_2$ is possible given the hydrologic pressure regime in this area.

Finally, it should be noted that there is a groundwater divide in the Clematis Group aquifer in the central part of the subregion, which may separate the high TDS groundwater in the east, and low TDS groundwater in the west (Section 2.1.3.2.2). The implication here is that low salinity samples close to the Maneroo Platform may not be connected to possible recharge areas of the Clematis Group aquifer, that are thought to occur in areas of outcrop along the eastern margin. This compartmentalisation of the Clematis Group aquifer makes it a complex and unusual hydrogeologic system, and further work is needed to fully understand its hydrogeologic processes.

The region of high TDS in the Clematis Group aquifer, with low hydraulic gradients and high hydraulic heads, may represent an area of stagnant groundwater where solute concentrations are high due to long residence times allowing for high levels of water–rock interaction.

In the Joe Joe Group the independence of ion:Cl ratios with respect to TDS suggests that evaporative concentration dominates the solute budget. Higher Ca+Mg:Cl and $HCO_3$:Cl ratios in some fresh samples may indicate carbonate dissolution.

**Inter-aquifer mixing**

A primary objective of this hydrochemical analysis is to help confirm whether inter-aquifer mixing may be occurring between the Galilee Basin hydrogeologic units and the main basal hydrogeologic unit of the Eromanga Basin, the Hutton Sandstone aquifer. The Hutton Sandstone is generally separated from the Clematis Group by the Moolayember Formation. However, there are areas adjacent to the Maneroo Platform margin where the Moolayember Formation is absent, allowing the Hutton Sandstone to be in direct contact with Clematis Sandstone and other Galilee Basin stratigraphic units (Figure 55). Leakage of this sort would require either flow through the

Moolayember Formation aquitard, or flow in areas where the Moolayember Formation pinches out.

The distribution of TDS and $HCO_3$ concentrations in the Clematis Group aquifer are consistent with possible interactions occurring between the Hutton Sandstone aquifer and the Clematis Group aquifer. High $HCO_3$:Cl ratios only occur in the Clematis Group in comparatively low TDS range samples. This is consistent with mixing with water from the Hutton Sandstone aquifer, as increasing the bicarbonate concentration of the Clematis Group enough to raise the $HCO_3$:Cl ratio would require the addition of significant amounts of fresher water from the Hutton Sandstone aquifer.

As stated above, the high $HCO_3$:Cl and Na+K:Cl ratios in the Clematis Group are consistent with carbonate dissolution followed by cation exchange. Primary carbonates or carbonate cements are not commonly reported in the upper Permian coal measures and Clematis Group, meaning this process seems unlikely in these hydrogeologic units. Biological activity, such as acetate fermentation may account for the high $HCO_3$ concentrations in some samples (Herczeg et al., 1991; Burra et al., 2014), but cannot explain the high Na+K:Cl and low Ca+Mg:Cl ratios observed. Figure 53 and Figure 54 show the chemistry of Clematis Group and Hutton Sandstone aquifer groundwater samples in a Piper diagram. Two distinct paths of groundwater evolution can be seen in the Clematis Group aquifer: an increasingly Na-Cl dominated groundwater type with minor $SO_4$, which mirrors the groundwaters of the upper Permian coal measures, and a groundwater type with significant bicarbonate, which seems to follow the trend of increasing bicarbonate dominance seen in the Hutton Sandstone aquifer. Hydraulic head differences presented in Section 2.1.3.2.4 show the Hutton Sandstone aquifer to have generally higher hydraulic head than the Clematis Group aquifer, indicating that the proposed direction of mixing is possible based on relative pressure in the aquifers.

Moya et al. (2015) noted that for Hutton Sandstone aquifer that the majority of hydrochemistry samples clustered into one hierarchical cluster group, however, there was also some clustering of samples in other hierarchical groups. This indicates that some groundwater exchange may be occurring with other aquifers. In the Moya et al. (2015) study area this was attributed to connectivity created by the Hulton-Rand structure (the location of the structure is outlined in Figure 55).

In addition to the possibility of water in the Hutton Sandstone aquifer mixing with waters of the Clematis Group aquifer, it is possible that near the margin of the Maneroo Platform the Hutton Sandstone aquifer receives water from deeper units such as the upper Permian coal measures and Joe Joe Group. In the western parts of the subregion the Moolayember Formation is absent, and the Hutton Sandstone aquifer directly overlies the upper Permian coal measures, Clematis Group, or Joe Joe Group. With only a few exceptions, bores with TDS above the 90th percentile of samples in the Hutton Sandstone aquifer are located in areas where the Moolayember Formation is absent (Figure 55). Figure 54 shows the chemistry of samples from the Hutton Sandstone aquifer with anomalously high TDS, as well as groundwaters in the upper Permian coal measures and Clematis Group, on a Piper diagram. The samples from the Hutton Sandstone aquifer with anomalous TDS values are consistent with hydrochemical trends for groundwater from aquifers in the Galilee Basin.

Samples from the Hutton Sandstone with anomalous TDS also show a marked difference in some major ion $R^2$ values with respect to TDS. Samples with TDS below the 90th percentile (underlain by the Moolayember Formation) have $R^2$ values for Cl and alkalinity with respect to TDS of 0.60 and 0.72. In samples with TDS above the 90th percentile (mostly not underlain by the Moolayember Formation), the $R^2$ value for Cl rises to 0.83, and the value for alkalinity is reduced to 0.37. In the Joe Joe group, $R^2$ values for Cl and alkalinity with respect to TDS are 0.96 and 0.02 respectively. This is a strong indication that the high TDS values in the Hutton Sandstone aquifer to the west of the subregion are the result of mixing with Na-Cl dominated water from underlying aquifers in the Galilee Basin.

Overall there is potential for some leakage to occur between aquifers in the Galilee Basin and the Hutton Sandstone aquifer in areas where the Moolayember Formation is either absent, thin (acts as a leaky aquitard) or in areas where faulting has significantly offset the aquifers.

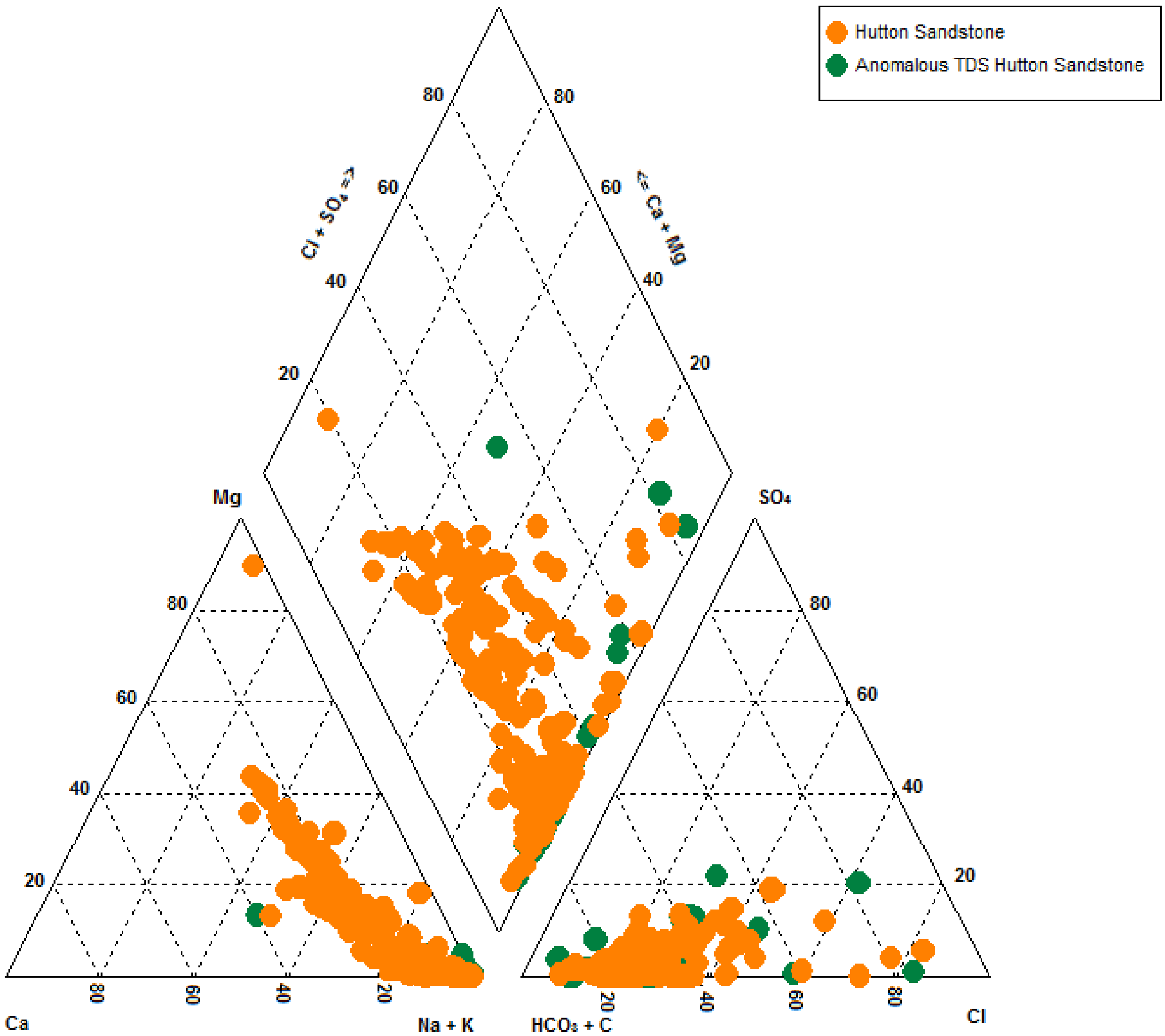


**Figure 53 Piper diagram showing groundwater chemistry of samples from the Hutton Sandstone aquifer, split into anomalous (greater than 90th percentile) TDS and low (lower than 90th percentile) TDS values**

Due to the large number of samples available, this plot is limited to samples collected after 1990.
Data: Bioregional Assessment Programme (Dataset 11)

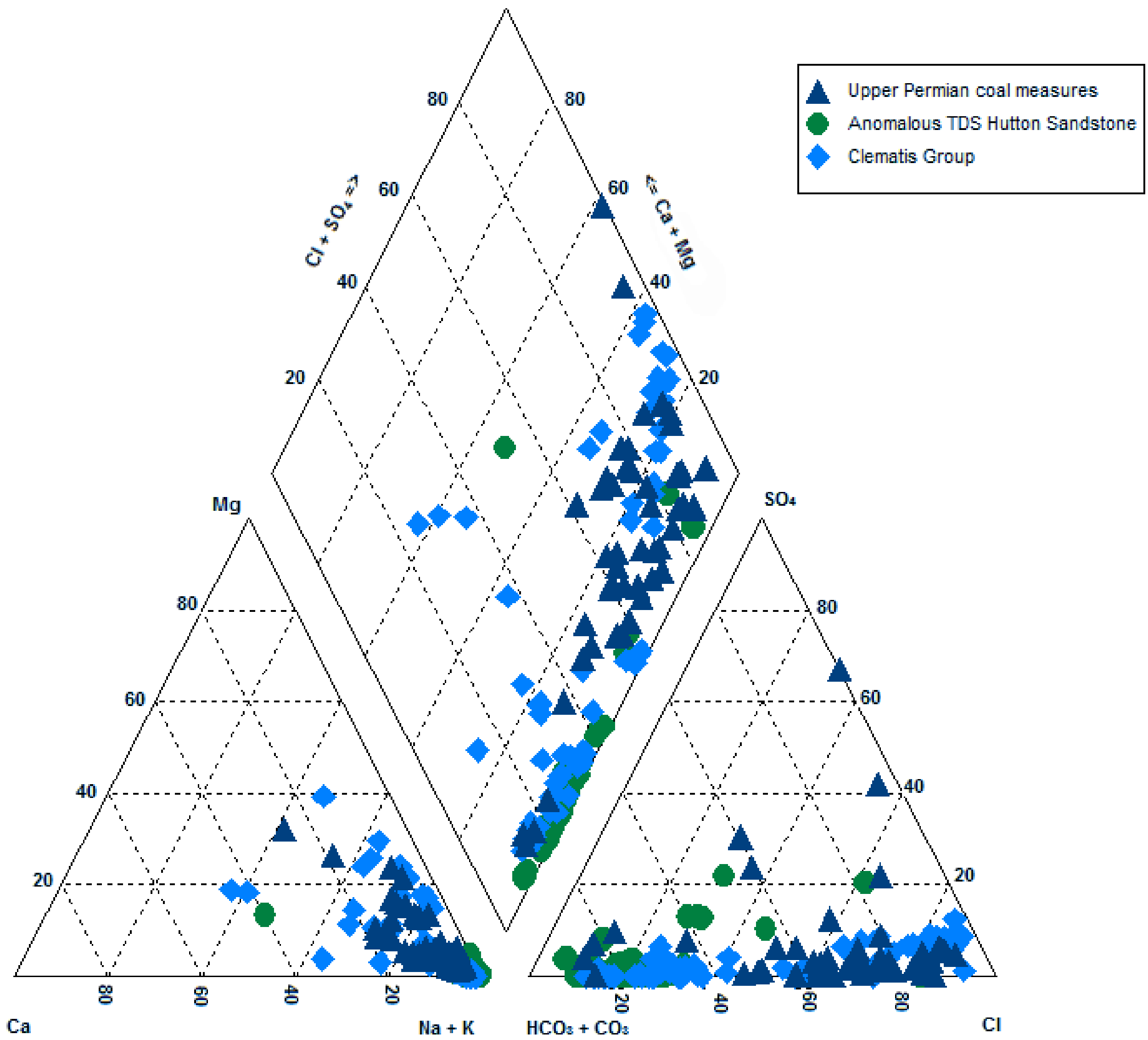


**Figure 54 Piper diagram showing groundwater chemistry of samples from the Clematis Group aquifer, upper Permian coal measures partial aquifer, and anomalous total dissolved solids (TDS) samples from the Hutton Sandstone aquifer**

Data: Bioregional Assessment Programme (Dataset 11)

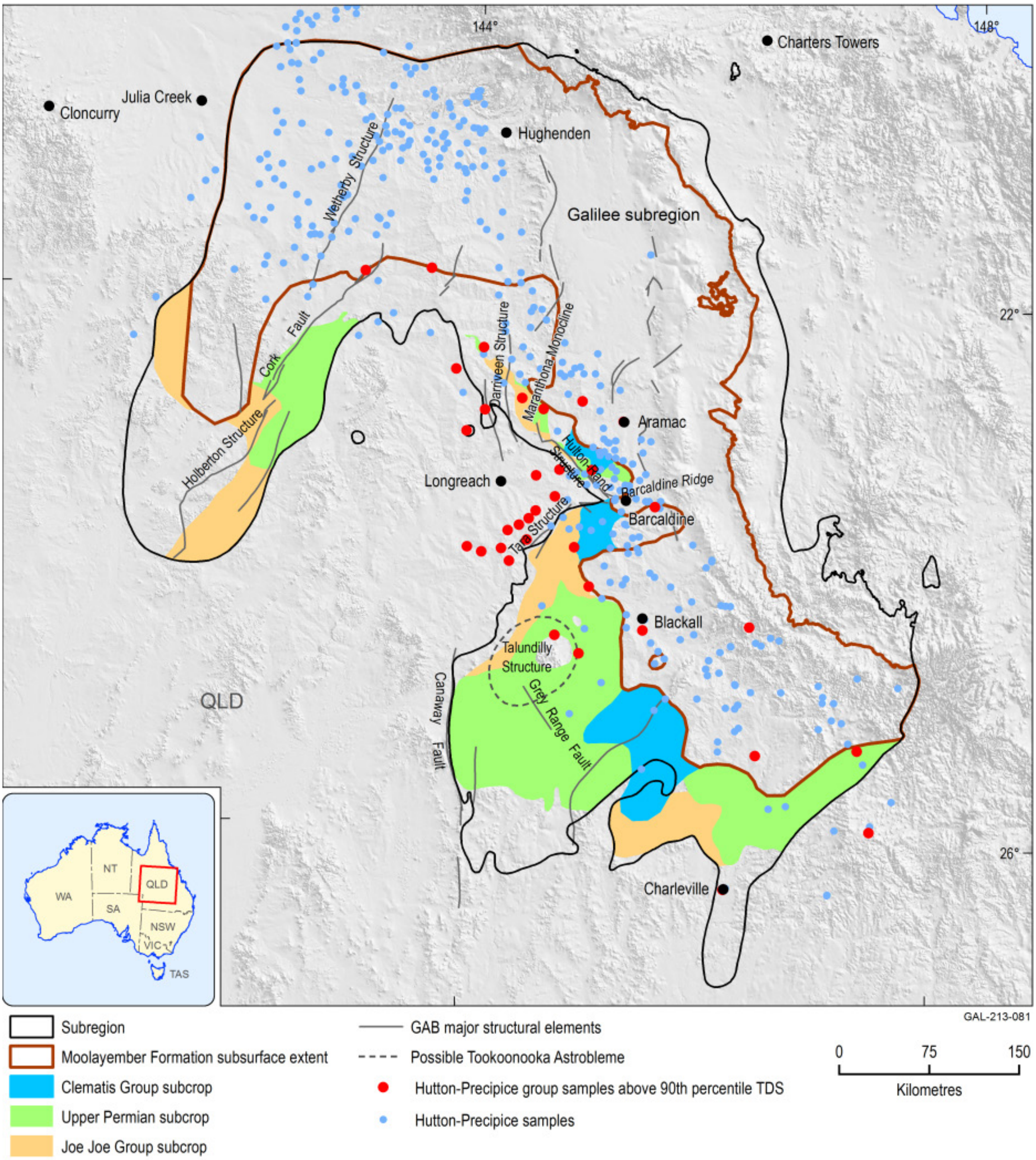


**Figure 55 Location of Hutton Sandstone aquifer groundwater samples with total dissolved solids (TDS) greater than 90th percentile of all samples and their relationship to Galilee Basin subcrop, major structures, and the edge of the Moolayember Formation**

High TDS samples in the Hutton Sandstone aquifer tend to occur where the Moolayember Formation is thin (less than 100 m thick) or absent. High TDS samples can occur in areas where aquifers in the Galilee Basin are in direct contact with the Hutton Sandstone aquifer.

Data: Bioregional Assessment Programme (Dataset 12, Dataset 13), Geoscience Australia (Dataset 14)

#### *2.1.3.2.1.5 Summary*

Groundwaters of all the hydrogeologic units in the subregion show high variability in solute concentrations, ion:Cl ratios, and sample depth. Based on major ion chemistry, hydrogeologic units in the subregion can be grouped into three hydrochemical systems: two are recognised in the Eromanga Basin and one in the Galilee Basin. In descending hydrostratigraphic order these are: a strongly Na-Cl dominated system with minor $SO_4$, recognised in the Winton-Mackunda partial aquifer and the Rolling Downs Group aquitard; a Na-$HCO_3$-Cl dominated system, evident in the Cadna-owie – Hooray Sandstone aquifer, the Injune Creek Group aquitard, and the Hutton Sandstone aquifer; and a Na-Cl system with minor to significant $HCO_3$, within the Clematis Group aquifer, the upper Permian coal measures partial aquifer and the Joe Joe Group partial aquifer.

These hydrochemical systems appear to be hydraulically separated at a regional scale by aquitards: siltstones and mudstones in the Rolling Downs Group aquitard separating the Winton-Mackunda partial aquifer from the Cadna-owie – Hooray Sandstone aquifer, and the Moolayember Formation separating the Hutton Sandstone aquifer from the Clematis Group aquifer.

Very high salinities are observed in the Na-Cl hydrochemical system in the upper Eromanga sequence. These are attributed to a combination of evaporative concentration of cyclic salts and diffusion of connate marine salts held in the Mackunda Formation and Rolling Downs Group aquitard.

Bicarbonate concentrations in the Na-$HCO_3$-Cl hydrochemical system of the Jurassic and Lower Cretaceous Eromanga Basin are up to twice those in the Na-Cl and minor $HCO_3$ hydrochemical system in the Galilee Basin. The high $HCO_3$ concentrations may be the result of dissolution of secondary carbonate cement, however Ca+Mg:Cl ratios do not tend to increase where $HCO_3$:Cl ratios do, as would be expected during carbonate dissolution. Herczeg et al. (1991) observed a similar pattern in groundwater from the GAB, and suggested that Ca and Mg:Cl values were reduced through cation exchange for Na. This process accounts for the high Na:Cl values also observed in samples with high $HCO_3$:Cl.

Two possible pathways for vertical flow between the Hutton Sandstone aquifer and a number of units in the Galilee Basin sequence are outlined:

1. At a local scale there may be the potential for some downward vertical flow from the Hutton Sandstone aquifer into the Clematis Group aquifer, resulting in locally high $HCO_3$:Cl ratios and low TDS in the Clematis Group aquifer. This process may occur in a small area east of the Maneroo Platform and west of Aramac. Vertical flow from the Hutton Sandstone into the Clematis Group would require the Moolayember Formation to act as a leaky aquitard, which may be caused by small-scale faults, erosional holes, or areas where the Moolayember Formation is anomalously thin. Investigations of inter-aquifer mixing would benefit from study at a finer scale than the regional work reported here.
2. In the west of the subregion, particularly around and on the Maneroo Platform, there is potential for upward vertical flow to occur from the upper Permian coal measures and Joe Joe Group partial aquifers into the Hutton Sandstone aquifer where the Moolayember Formation is absent, and where these units directly underlie the Hutton Sandstone aquifer. Salinity values are highest in the Hutton Sandstone aquifer where the Moolayember Formation and Clematis Group pinch out, and TDS in the samples from the Hutton Sandstone aquifer in this area show an anomalously high correlation with Cl, similar to that

seen in the upper Permian coal measures and Joe Joe Group partial aquifers. It seems likely that the higher salinities on the Maneroo Platform are caused by more saline water from units in the Galilee Basin sequence entering the Hutton Sandstone aquifer where they pinch out.

### 2.1.3.2.2 Water levels

In descending stratigraphic order the hydrostratigraphic units used in this section are:

- Cenozoic aquifers
- Wallumbilla and Winton-Mackunda partial aquifer
- Cadna-owie – Hooray Sandstone aquifer
- Hutton Sandstone aquifer
- Moolayember Formation aquitard
- Clematis Group aquifer (includes Warang Sandstone)
- upper Permian coal measures partial aquifer split into BC1, BC2 and BC3 units
- Joe Joe Group partial aquifer.

#### ***2.1.3.2.2.1 Cenozoic groundwater system***

**Cenozoic aquifers**

Figure 56 shows the potentiometric surface of the Cenozoic unconsolidated sediments in the eastern zone of the Galilee subregion. The pressure surface was constructed from recent water levels in bores screened in both the Quaternary and Cenozoic aquifers and assumes the two are hydraulically connected. Figure 56 can be considered to be a plot of the watertable in the eastern zone. The Cenozoic aquifers obviously comprise a local flow system having a strong relationship with the surface drainage system. Figure 56 indicates from the curvature of potentials around certain streams (Jordan Creek, the Alice River and the Belyando River) that these are potentially gaining streams. Conversely, Dunda Creek, Tallarenha Creek and Lagoon Creek are potentially losing streams. This aspect will be further explored in Section 2.1.5 on surface water – groundwater interaction.

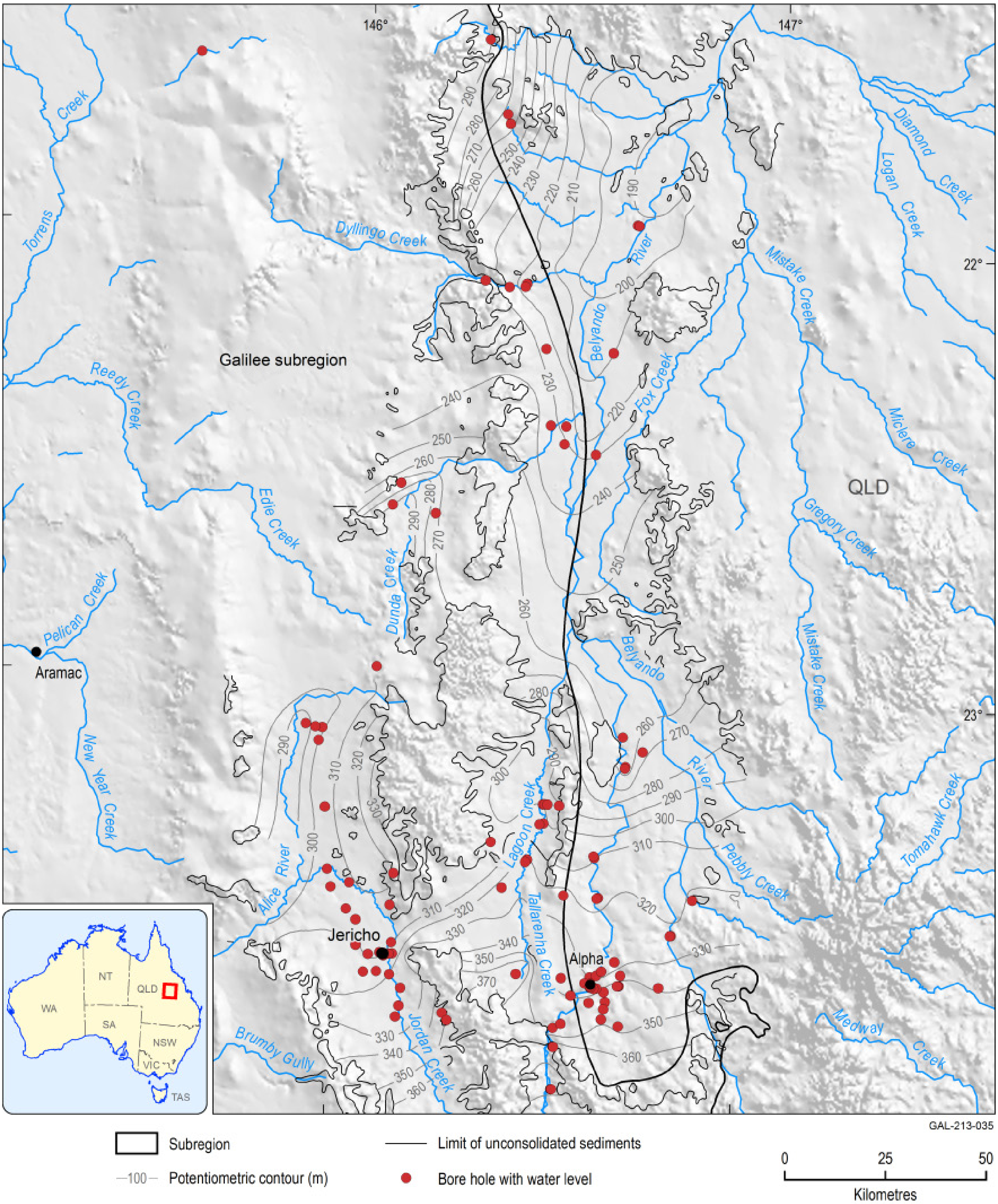


## Figure 56 Watertable in the eastern zone of the Galilee subregion

Contours are constructed from recent water levels in bores screened in both the Quaternary and Cenozoic aquifers and assume vertical hydraulic connectivity between the two systems.
Data: Bioregional Assessment Programme (Dataset 15, Dataset 16)

##### *2.1.3.2.2.2 Eromanga Basin (GAB) groundwater system*

**Wallumbilla Formation and Winton-Mackunda formations partial aquifer**

Many location descriptions referenced in this section refer to 1:250,000 map sheets that cover the Galilee subregion. Refer to Figure 69 and Table 3 in Section 2.1.2 for further information on these maps sheet locations. The Winton Formation includes some brown coal resource developments (for further detail see Section 2.3.4 in companion product 2.3 for the Galilee subregion (Evans et al., 2018)).

Figure 57 and Figure 58 show the potentiometric surface in the Wallumbilla Formation and Winton-Mackunda formations in the central eastern, central western and western zones of the Galilee subregion. These pressure surfaces are considered to represent the Eromanga Basin regional watertable, as the groundwater head in these units equilibrates with the first water cut. The contours are well constrained by water levels from over a thousand bores. In most places, the watertable appears to transition smoothly from the Wallumbilla Formation to the Mackunda Formation except on the Muttaburra and Tangorin 1:250,000 geological map sheets. In the case of the latter, the watertable in the Wallumbilla Formation appears to be higher than that in the Mackunda Formation, but the reverse is true in the former sheet. Although normally regarded as an aquitard, the Wallumbilla Formation supplies over 200 water bores in the eastern zone, some with remarkably fresh water. The majority of these bores are located in the south on the Augathella sheet (n = 82), Charleville sheet (n = 61) and Mitchell sheet (n = 30). Most of the bores that take from the Wallumbilla Formation are screened in sand beds near the base of the Doncaster Member – the basal member of the Wallumbilla Formation.

Figure 57 and Figure 58 indicate that the groundwater flow directions in the Winton-Mackunda formations approximately follow the regional dip and topography to the west and south-west. Although the flow system is a regional one, it nevertheless displays some groundwater mounding in topographically higher areas more typical of a local groundwater flow system. Such areas include the Forsythe Range on the southern Winton 1:250,000 sheet (Figure 57), Yellow Mountain and Opal Hill on the south-eastern Jundah 1:250,000 sheet (Figure 58) and the Grey and Gowan Ranges on the southern Blackall and northern Adavale 1:250,000 sheets.

The Winton-Mackunda formations are classified as a partial aquifer because it is by no means certain that it will supply sufficient quantities of good quality groundwater to a waterbore. There have been a significant number of dry wells drilled in this formation and there have been others where the supply was described as ‘insufficient’ (<0.1 L/sec). There have also been reports of equipped bores in the Winton-Mackunda formations which have been abandoned because the groundwater became saline with continued pumping. Most of the acceptable supplies, in terms of both well yield and salinity, have been obtained from sand beds in the lower part of the Winton Formation or in the underlying Mackunda Formation. It is generally true that all groundwater intersections throughout the Winton-Mackunda formations rise to equilibrate with the level of the first water cut, indicating good vertical hydraulic connection.

Water bores in the Winton-Mackunda formations are all sub-artesian. The watertable in the Winton-Mackunda formations generally lies about 50 to 60 m below ground surface in the eastern and central eastern zones, however, the depth to water can extend to 80 to 100 m in some topographically higher areas (e.g. the aforementioned Grey and Gowan Ranges). The watertable dips more shallowly than the regional topographic slope and depth to water in the central western and western zones is between 20 and 40 m below ground surface. In the north-west, the watertable in the Winton-Mackunda formations lies 10 m or less below ground surface over most of the Julia Creek and Richmond sheets (see Figure 10 in Section 2.1.2).

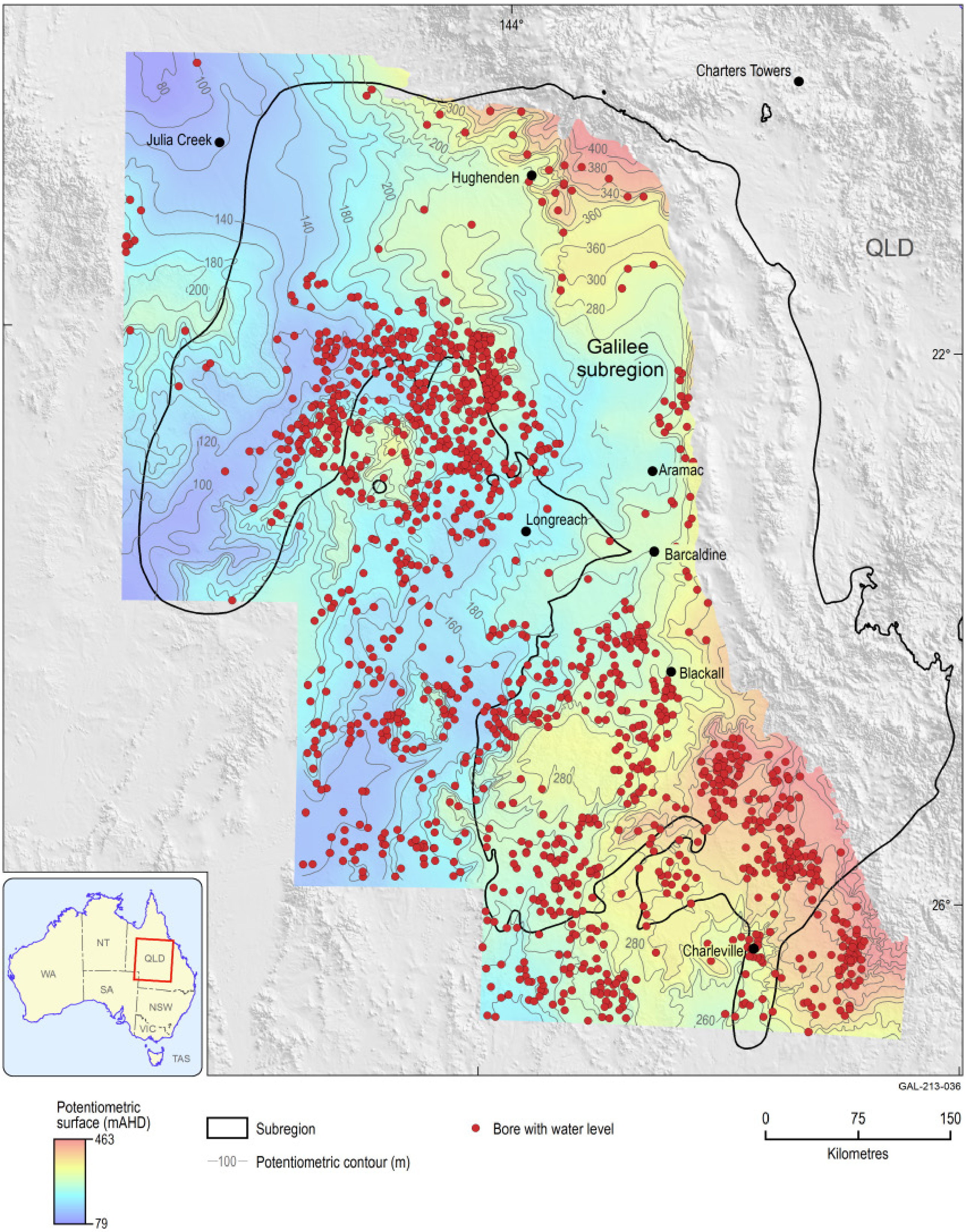


**Figure 57 Regional watertable in the Wallumbilla Formation and Winton-Mackunda formations in the Galilee subregion**

Data: Bioregional Assessment Programme (Dataset 16, Dataset 17)

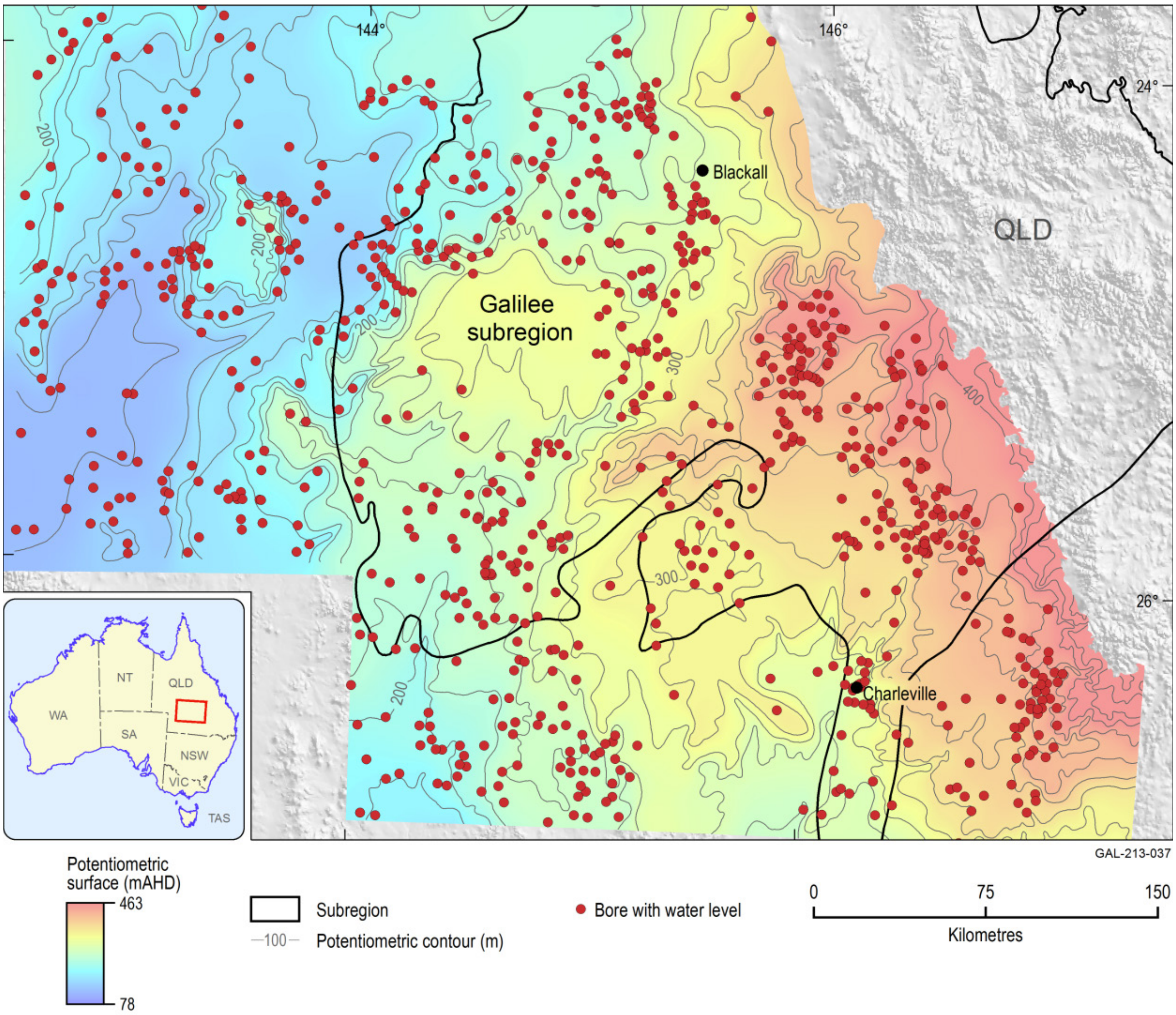


**Figure 58 Regional watertable in the Wallumbilla Formation and Winton-Mackunda formations in the Galilee subregion (south)**

Data: Bioregional Assessment Programme (Dataset 15, Dataset 16, Dataset 17)

### Cadna-owie – Hooray Sandstone aquifer

Figure 59 and Figure 60 show the potentiometric surface for the Cadna-owie – Hooray Sandstone aquifer. The potentiometric contours are generally smoother and spaced further apart than those in the overlying Winton-Mackunda partial aquifer and do not show any relationship with the topography except where the aquifer is unconfined near the intake beds in the eastern zone. The steep hydraulic gradients near the intake beds are probably due to weathering of the rock outcrop which has produced a lower hydraulic conductivity in the rock outcrop. The groundwater flow potential is to the west and south-west, except around the Thomson River channel on the Muttaburra and Longreach 1:250,000 sheets. Here the configuration of the potentials suggests upward leakage from the aquifer into the bed of the Thomson River.

The Hooray Sandstone aquifer is a GAB icon with extensive areas of flowing artesian bores in the central eastern, central western and western zones of the Galilee subregion. Before development in the late nineteenth century, the extent of artesian conditions was even larger than it is today. The water yielded by the Hooray Sandstone is fresh (mean TDS 834 mg/L) but the salinity range is high (180–7136 mg/L, n = 1302). Most of the fresh waters are produced either from the highly permeable and high yielding Wyandra Sandstone at the top of the sequence, or from coarse-grained sand beds near the base of the Hooray Sandstone. Groundwater salinity increases to the west of the Galilee subregion, where the aquifer overlies the Maneroo Platform (see companion product 1.5 for the Galilee subregion (Evans et al., 2015)). Here, most of the bores are drawing groundwater from the Cadna-owie Formation, which immediately underlies the Wyandra Sandstone member. In marked contrast to the overlying Allaru Mudstone / Wallumbilla Formation, and Winton-Mackunda formations waters, the hydrochemical water type of Hooray Sandstone groundwater is Na-HCO3-Cl dominant.

In compiling the potentiometric surface of the Hooray Sandstone in the eastern zone it was necessary to partition the Ronlow beds into the three Jurassic members – Hooray Sandstone, Injune Creek Group and Hutton Sandstone. The Ronlow beds are mapped on three geological sheets – Buchanan, Galilee and Jericho (Figure 59). Vine and Doutch (1972) describe the Ronlow beds as a marginal sandstone facies of the complete Early Jurassic to Early Cretaceous terrestrial sequence from the Hutton to the Hooray Sandstone. These authors were of the opinion that most of the eastern Ronlow beds in the south were equivalent to the Hutton Sandstone but that the sequence younged northward. With these criteria in mind, the Ronlow beds were partitioned into the three Jurassic members shown in Figure 61.

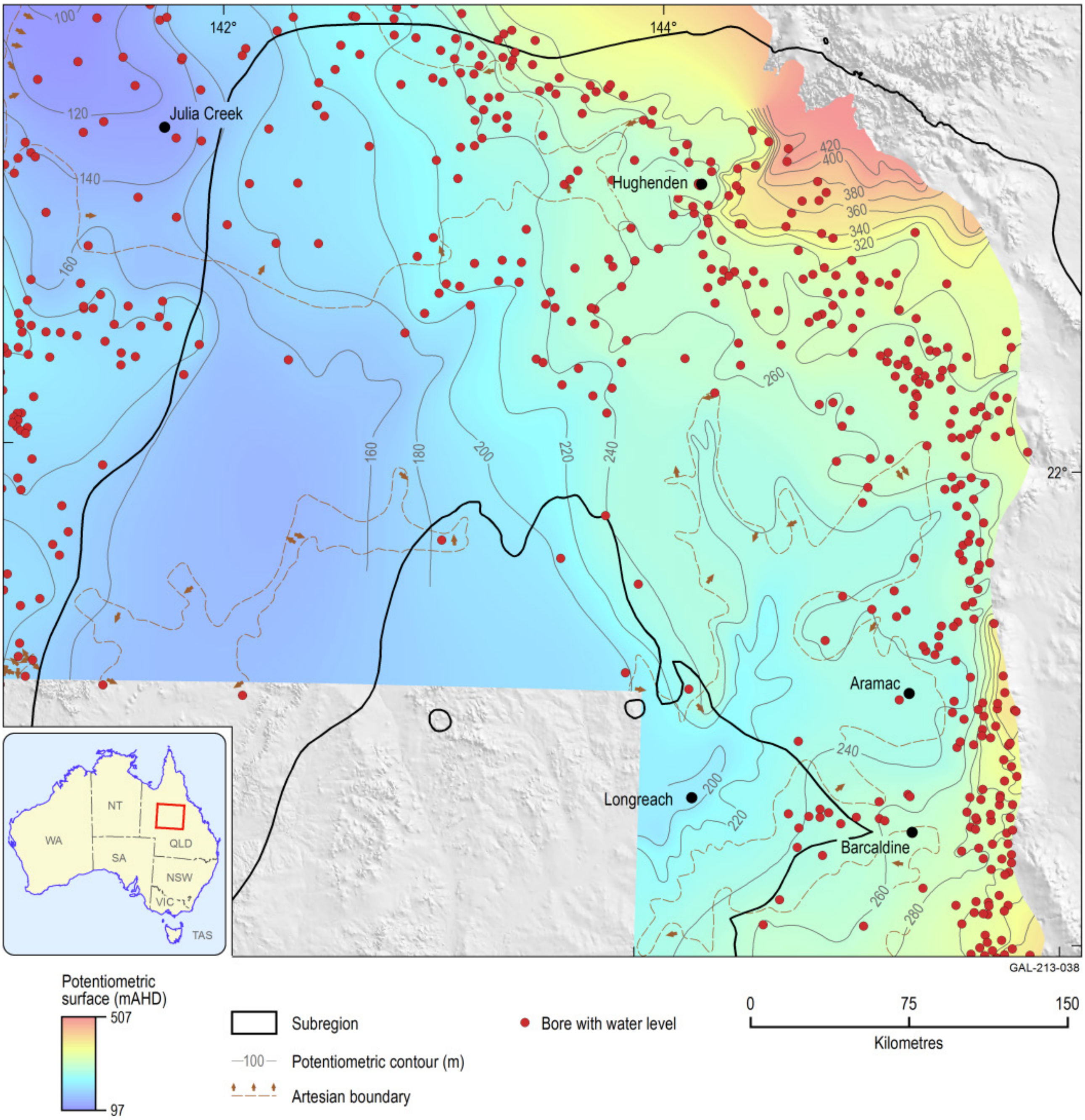


**Figure 59 Potentiometric surface of the Cadna-owie – Hooray Sandstone aquifer, Galilee subregion (north)**

Data points are adjusted to a datum of 25 ˚C and equivalent fresh water head

Data: Bioregional Assessment Programme (Dataset 15, Dataset 16, Dataset 17)

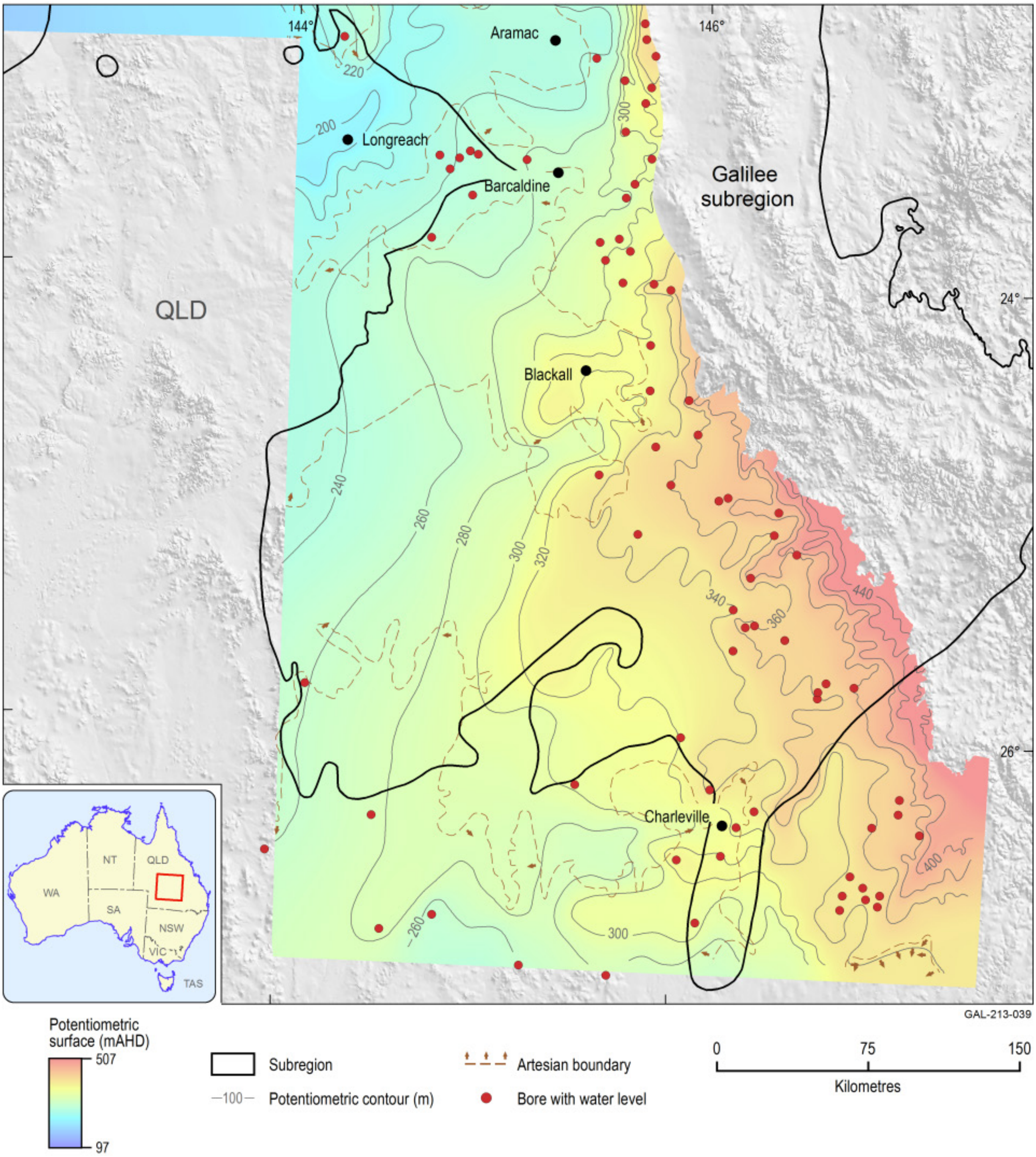


**Figure 60 Potentiometric surface of the Cadna-owie – Hooray Sandstone aquifer, Galilee subregion (south)**

Data points are adjusted to a datum of 25 ˚C and equivalent fresh water head

Data: Bioregional Assessment Programme (Dataset 15, Dataset 16, Dataset 17)

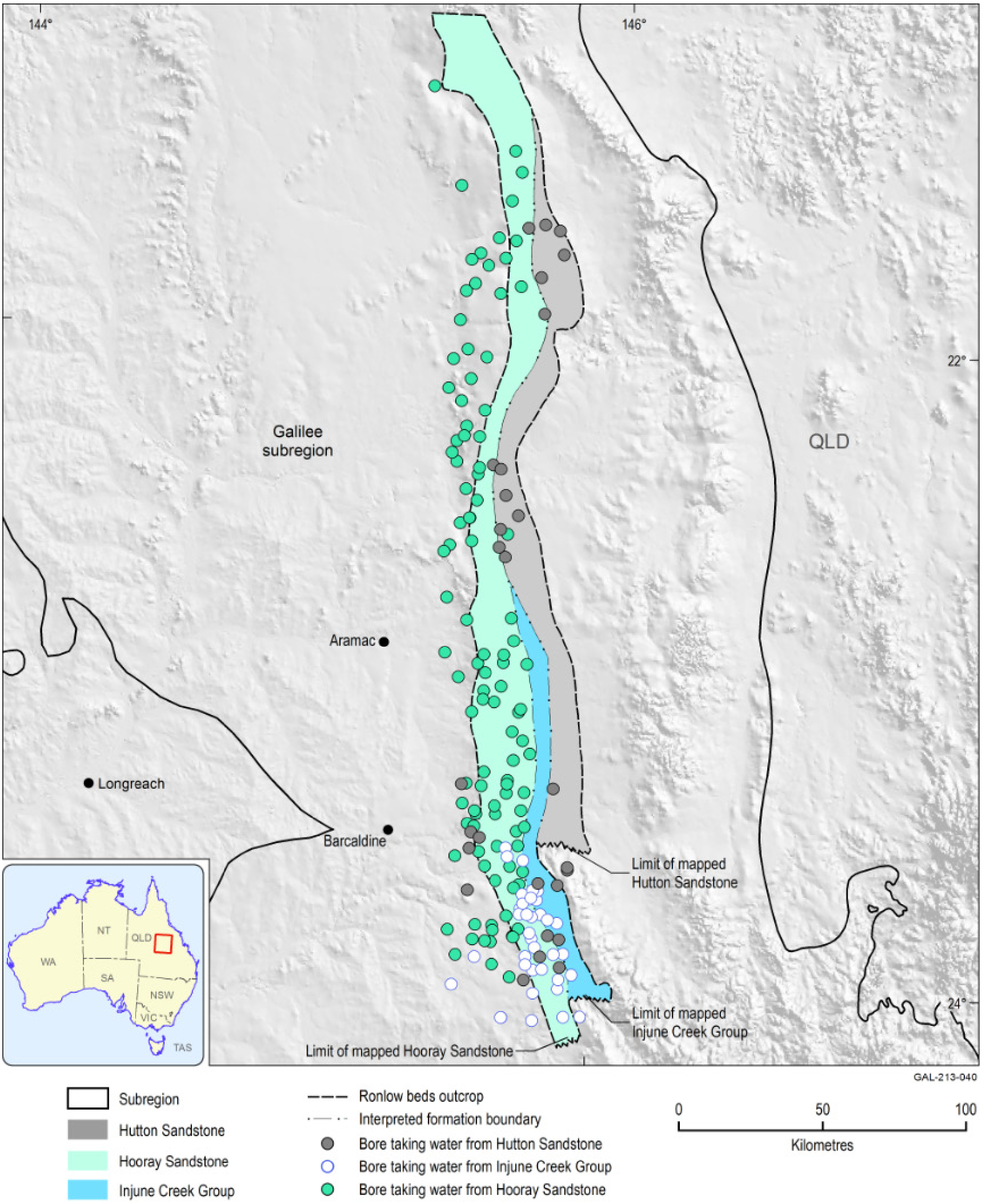


**Figure 61 Partitioning of Ronlow beds into three Jurassic members – Hooray Sandstone, Injune Creek Group and Hutton Sandstone**

Data: Bioregional Assessment Programme (Dataset 12, Dataset 18, Dataset 19)

**Hutton Sandstone aquifer**

Figure 62 shows the potentiometric surface (corrected for temperature and salinity) of the Hutton Sandstone. This pressure surface looks very much like that of the Hooray Sandstone and the same patterns are common to both. Groundwater flow is to the west or south-west, except on the Julia Creek sheet which indicates an additional minor northerly component of flow across the Euroka Arch into the Carpentaria Basin. Like the Hooray Sandstone, hydraulic gradients are steepest in the area of the intake beds of the Hutton Sandstone, and the same causal factor of rock weathering is advanced here.

The area of flowing artesian bores in the Hutton Sandstone is slightly larger than that of the Hooray Sandstone and throughout most of the central eastern zone, and over much of the central western and western zones, heads in the Hutton Sandstone are higher than heads in the Hooray Sandstone. In some places this head difference is up to 50 m. The Hutton Sandstone aquifer yields the best quality groundwater of any of the Galilee subregion aquifers.

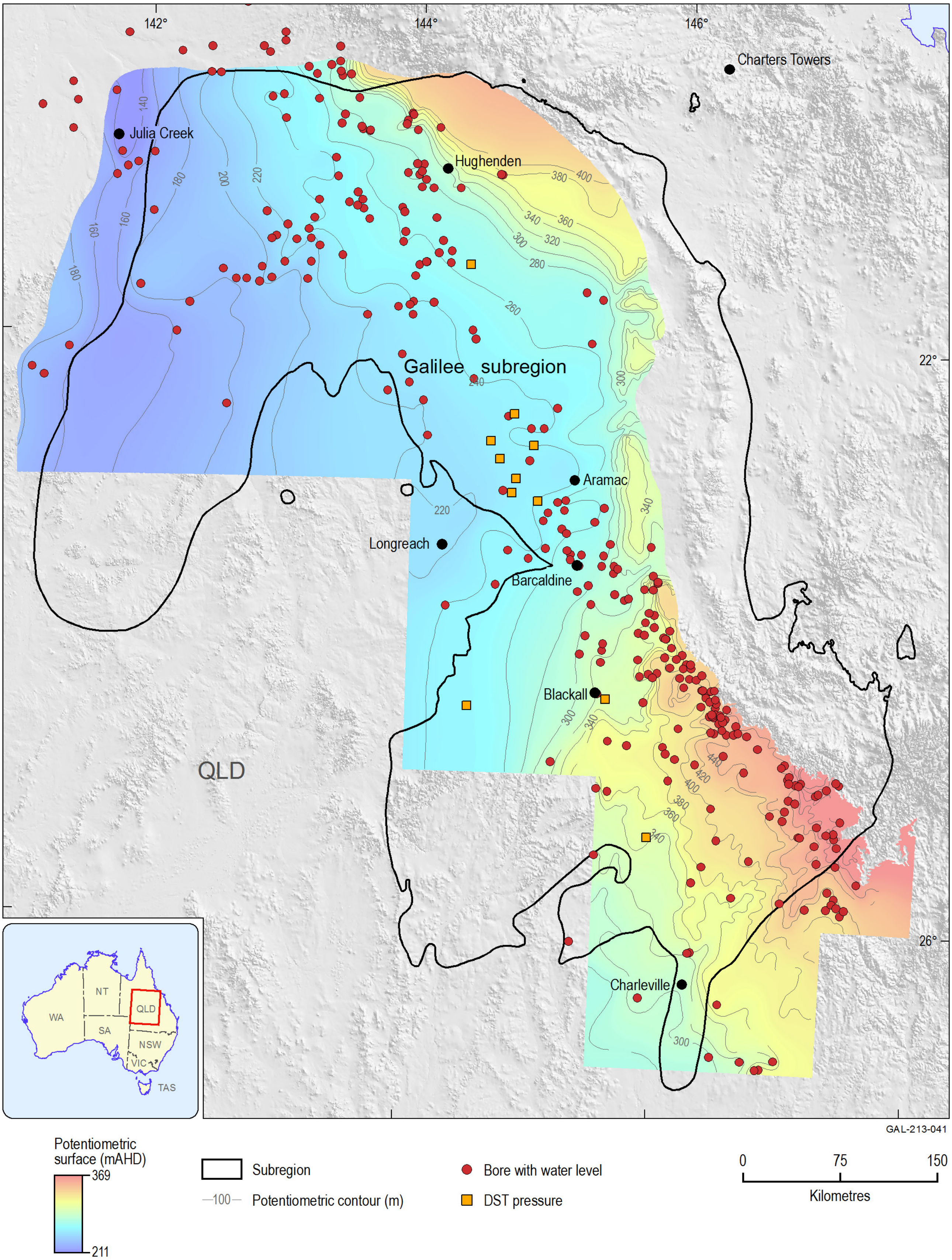


**Figure 62 Potentiometric surface of the Hutton Sandstone, Galilee subregion**

Data points are adjusted to a datum of 25 ˚C and equivalent fresh water head

DST = drill stem tests

Data: Bioregional Assessment Programme (Dataset 15, Dataset 16, Dataset 17, Dataset 19)

#### *2.1.3.2.2.3 Galilee Basin groundwater system*

**Clematis Group aquifer**

Figure 63 shows the potentiometric surface of the Clematis Group aquifer (corrected for temperature and salinity). Groundwater flow directions are slightly different to those of the overlying Eromanga Basin aquifers. For the Clematis Group in the south, the potential groundwater flow direction is to the north-west; in the central area the potential groundwater flow direction is westward, and in the north the groundwater flow direction in the Warang Sandstone is to the south-west. A minor but significant exception to this general pattern occurs in the Carmichael area. Here, a component of potential groundwater flow is to the east, and focuses towards the Carmichael River and the Doongmabulla Springs complex. This means that there must be a groundwater divide separating the easterly and westerly flow regimes. Its inferred location is shown in Figure 63. The groundwater divide occurs to the west of the Carmichael river basin and approximates a topographically elevated area found between the Great Dividing Range and prominent ridges along the margin of the Eromanga Basin.

The Clematis Group aquifer subcrops near surface in the vicinity of the Doongmabulla Springs complex, in the headwaters of the Carmichael river basin. The focusing of potential groundwater flow in the Clematis Group aquifer eastwards towards these areas suggests there is potential for discharge from the Clematis Group aquifer to provide baseflow to the Carmichael River and to be a source aquifer for the Doongmabulla Springs complex. Further discussion on the origin of the groundwater divide and the source aquifer for Doongmabulla Springs complex is provided in Section 2.3.2 of companion product 2.3 (Evans et al., 2018) as well as Section 3.4 and Section 3.5 of companion product 3-4 (Lewis et al., 2018).

Most bores in the Clematis Group are sub-artesian but there are some minor artesian areas near the limits of the formation in the west. Bore yields are generally significantly lower than those of the overlying Hutton Sandstone. Nevertheless this aquifer produces good quality water.

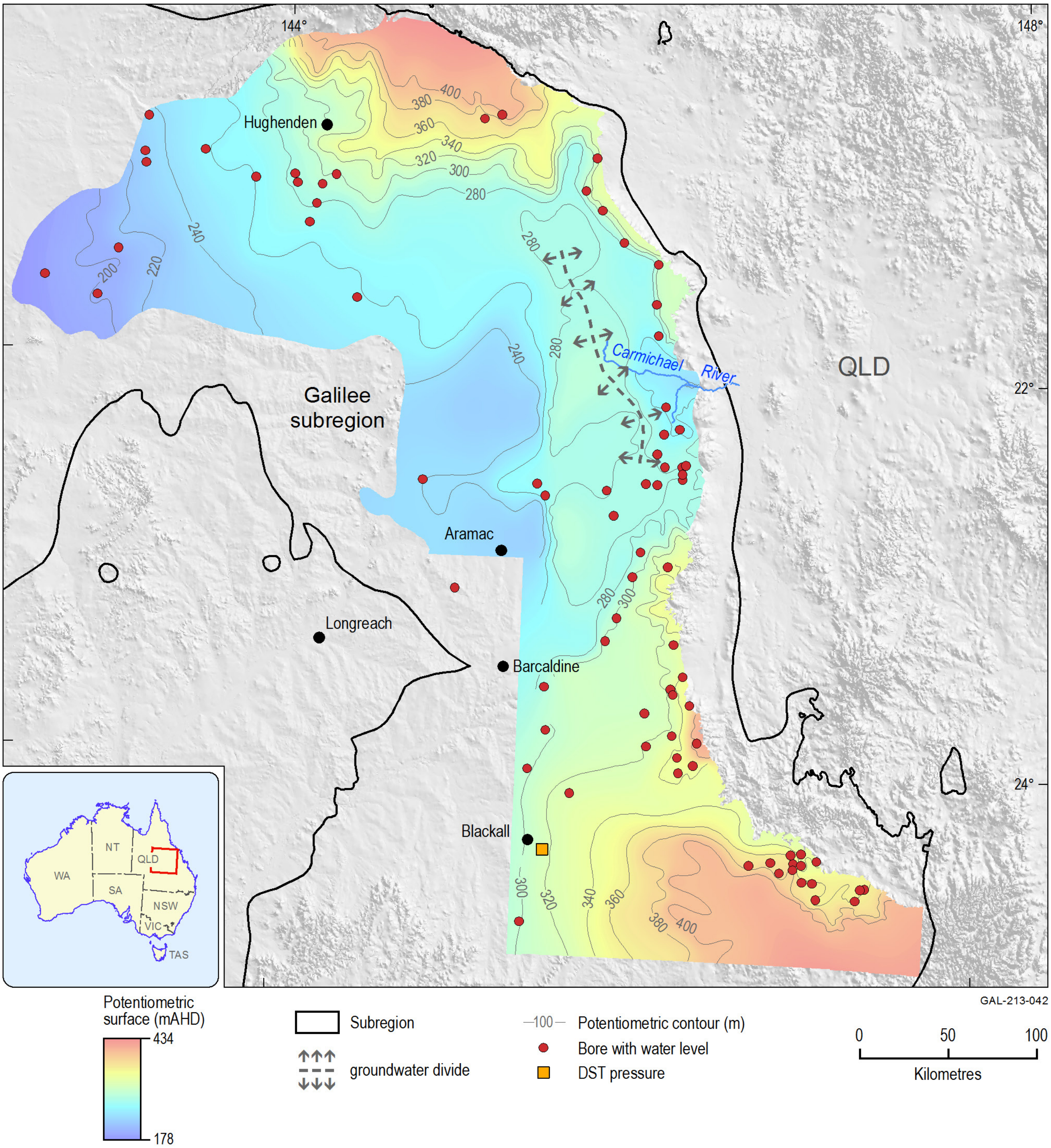


**Figure 63 Potentiometric surface of the Clematis Group aquifer, Galilee subregion**

Data points are adjusted to a datum of 25 ˚C and equivalent fresh water head
DST = drill stem tests
Data: Bioregional Assessment Programme (Dataset 15, Dataset 16, Dataset 17, Dataset 19)

### Upper Permian coal measures partial aquifer

Coal seams in the upper Permian coal measures are the primary target for CSG exploration in the Galilee subregion as well as coal mining proposals located along the eastern margin of the Galilee subregion (for further detail see Section 2.3.4 in companion product 2.3 for the Galilee subregion (Evans et al., 2018)). The formal stratigraphic units included in the upper Permian coal measures are outlined in Section 2.1.2. In general, six major seams separated by interburden sandstones, ranging from the A seam in the Bandanna Formation at the top of the upper Permian coal measures, to the F seam in the upper Permian coal measures at the base, with the upper split in the D seam referred to as DU or D1, and the lower split called DL or D2. The coal seams are highly variable in thickness, ranging from 0.1 m for the E seam at Kevin's Corner to 18 m for the A seam at Carmichael (data from Bleakley et al., 2014). The mean thickness of the coal seams is about 3 m. The thickest total accumulation of coal occurs at Carmichael with a total thickness of 39 m; the thinnest accumulation is at South Galilee where the total coal thickness is considerably less – 14.5 m. The interburden sandstones are thicker than the coal seams, with the thickest being the BC interburden. This unit ranges in thickness from 60 m at Carmichael to 90 m at Kevin's Corner, Galilee and South Galilee (Bleakley et al., 2014).

The mining proponents have established extensive bore monitoring networks, measuring water levels in all coal seams and interburden sandstones. The company water level data show significant vertical hydraulic gradients exist through the upper Permian coal measures. For this reason, and to more adequately model the complexity of the upper Permian coal measures, the upper Permian coal measures have been split into three hydrogeological sub-units. From top to bottom these sub-units are informally designated BC1, BC2 and BC3. The partitioning was done on the basis of approximately similar groundwater pressures existing in each sub-unit (Table 17).

**Table 17 Subdivision of the upper Permian coal measures**

| Sub-unit | Formation | Marker bed |
|---|---|---|
| BC1 | Bandanna Formation / Blackwater Group | Top Bandanna Formation to base B seam |
| BC2 | Peawaddy Formation / Black Alley Shale / Colinlea Sandstone | Base B seam to base E seam |
| BC3 | Colinlea Sandstone (lower) | Top E seam to base Colinlea Sandstone |

The upper Permian coal measures are designated as a partial aquifer because of their low hydraulic conductivity (*Kh* < 0.2 m/day). Figure 64 shows the *Kh* profiles at China First, Kevin's Corner and Carmichael coal projects. The data points are from Bleakley et al. (2014). A few aspects of these plots are notable:

- The plots show a trend (albeit with only three sites) of *Kh* being highest in the south at China First (Galilee) and decreasing northwards to a minimum at Carmichael. The implication is that there are broad trends in hydraulic conductivity, with it decreasing (getting tighter) to the north. Detailed numerical modelling may need to take these trends into consideration.
- There is no consistent trend of *Kh* with depth. One interpretation is that a trend of *Kh* increasing with depth in BC2 at Kevin's Corner and China First (Galilee) down to the C seam with *Kh* then decreasing in the DU and DL seams near the base of BC2, but the reverse trend is displayed at Carmichael. Here *Kh* is maximised in the DU and DL seams, and in the interburden sandstone.
- In coal basins like the Bowen Basin there is anecdotal evidence to support the theory of preferential flow of groundwater through cleats in the coal and minimal groundwater flow through the interburden layers. This appears not to be so in the Galilee Basin. The *Kh* plots in Figure 64 show that, in general, the hydraulic conductivity in the interburden sandstones is higher than in the coal seams.

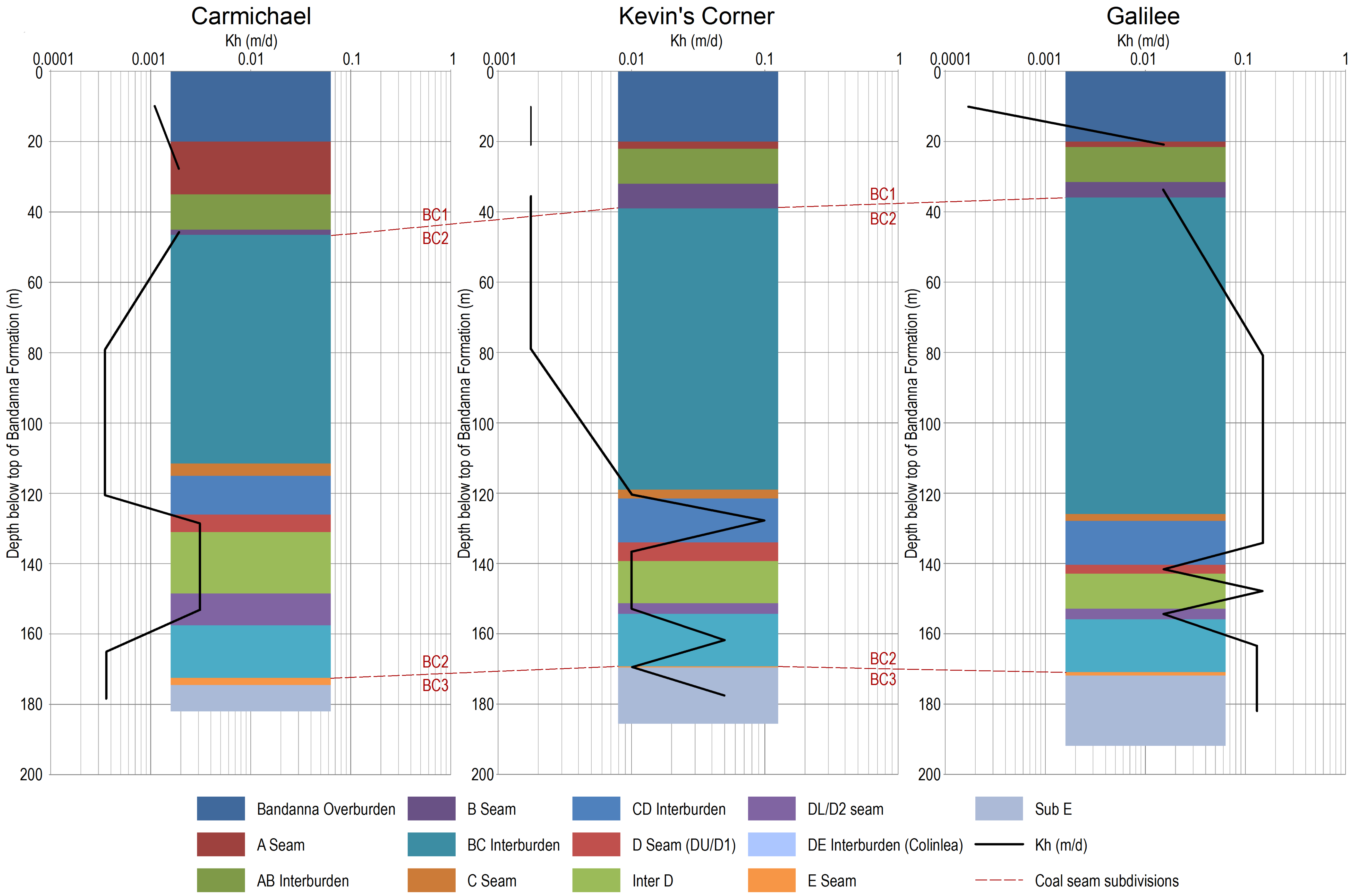


**Figure 64 Profiles of hydraulic conductivity in the upper Permian coal measures at Carmichael, Kevin's Corner and China First (Galilee) coal projects**

These coal mine developments are located along the eastern margin of the Galilee subregion. Carmichael coal project is the northern most of the three mentioned here, while China First (Galilee) is the southernmost of the three.
Data: Bleakley et al. (2014), Queensland Department of Employment, Economic Development and Innovation (Dataset 4)

This figure has been optimised for printing on A3 paper (420 mm x 297 mm).

The data points for Figure 65, Figure 66 and Figure 67 come from two distinctly different sources. Along the eastern margin the data points are water level measurements in boreholes drilled by the mining proponents. However, in the western areas the pressures were calculated from drill stem tests (DST) done in petroleum exploration wells. This was necessary because there are no bores deep enough to measure water levels of these units in the west. Although erroneous DSTs were culled during the rigorous QA/QC process carried out by the Assessment team, there still remains an element of uncertainty in the formation pressure estimates, even in the better tests; consequently this uncertainty is propagated to the interpreted potentiometric surfaces presented in Figure 65, Figure 66 and Figure 67.

The potentiometric surfaces (corrected for temperature and salinity) for BC1, BC2 and BC3 are shown in Figure 65, Figure 66 and Figure 67 respectively. The patterns are similar for all three. All show an easterly component of flow towards the Belyando River valley on the Galilee and northern part of the Jericho 1:250,000 sheets (Figure 10 in Section 2.1.2). Elsewhere the flow direction is largely westward. Based on the available data a major groundwater divide must exist for all three sub-units. Groundwater flow is directed away from this divide towards the eastern (against the regional west dip of bedding) and western margins of the Galilee Basin. Figure 65, Figure 66 and Figure 67 show that prominent north-trending groundwater mounding approximates a topographically elevated area situated between the Great Dividing Range and prominent ridge that defines the margin of the Eromanga Basin.

The genesis of the groundwater divides warrants investigation as it is not immediately obvious why such divides should exist. The upper Permian coal measures are confined by overlying sedimentary sequences (Rewan Group, Clematis Group, Moolayember Formation) in the vicinity of the groundwater divide; hence the groundwater divide cannot be due to direct recharge from the surface. One possible explanation is that the north-trending groundwater divide represents a northward extension of the west-south-west-trending recharge mound that is apparent to the east of Blackall. This explanation may be plausible for BC1 (Figure 65) but not really so for BC2 (Figure 66) and BC3 (Figure 67) or the underlying Joe Joe Group (see next subsection). Further discussion on the origin of the groundwater divide is provided in Section 2.3.2 of companion product 2.3 (Evans et al., 2018).

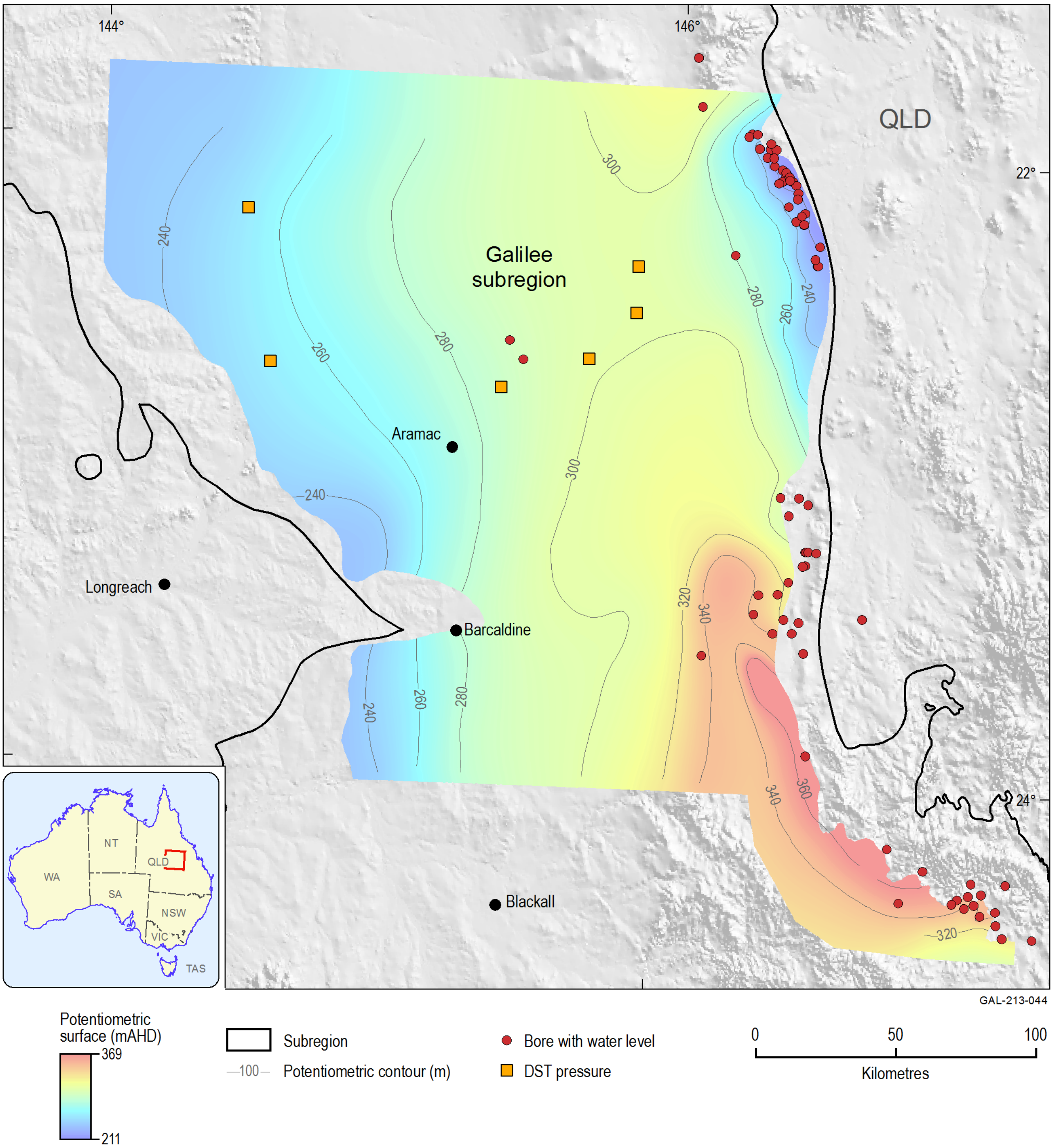


**Figure 65 Potentiometric surface of BC1, Galilee subregion**

Data points are adjusted to a datum of 25 ˚C and equivalent fresh water head
DST = drill stem tests
Data: Bioregional Assessment Programme (Dataset 15, Dataset 16, Dataset 17, Dataset 19)

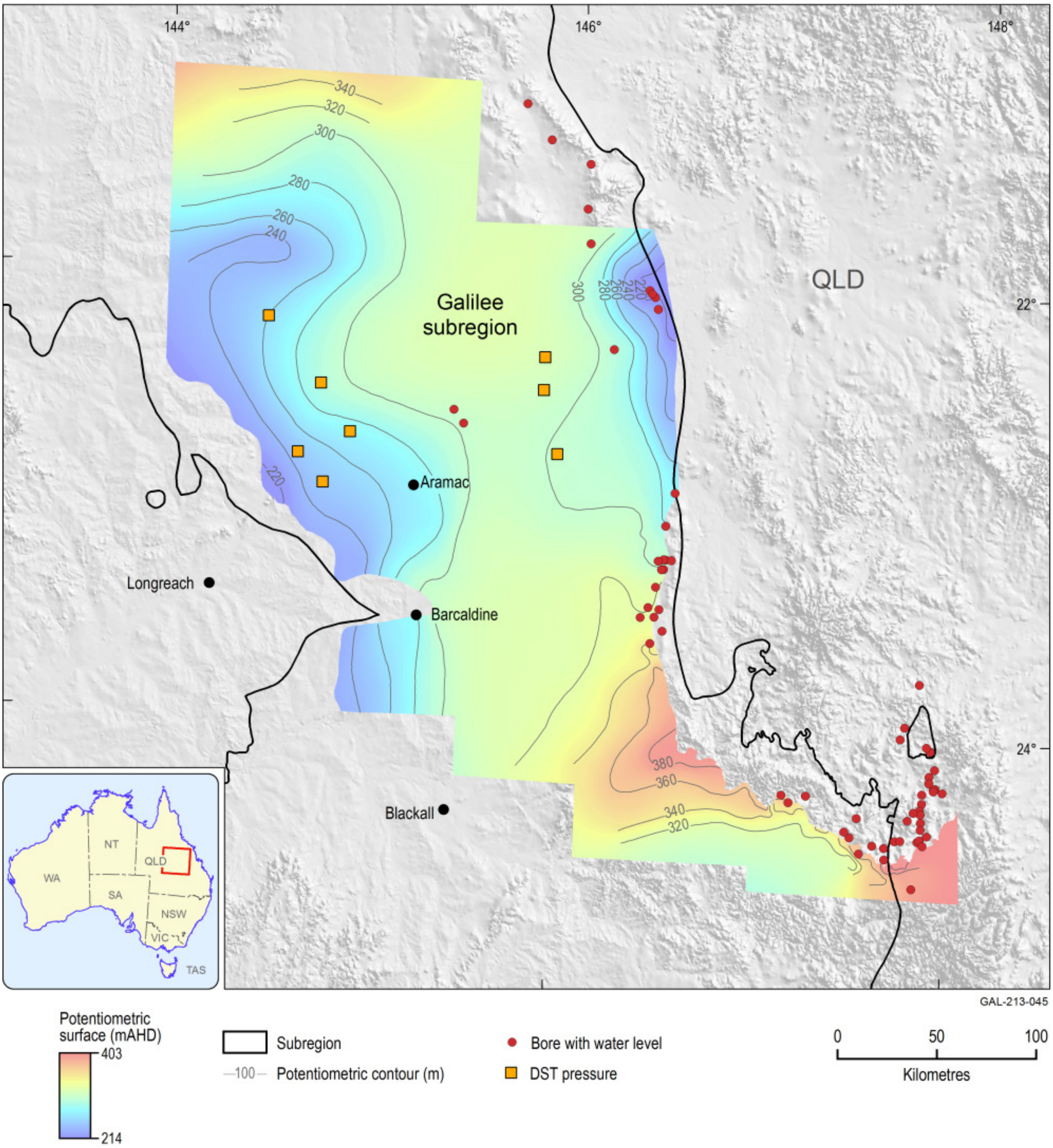


**Figure 66 Potentiometric surface of BC2, Galilee subregion**

Data points are adjusted to a datum of 25 ˚C and equivalent fresh water head
DST = drill stem tests
Data: Bioregional Assessment Programme (Dataset 15, Dataset 16, Dataset 17, Dataset 19)

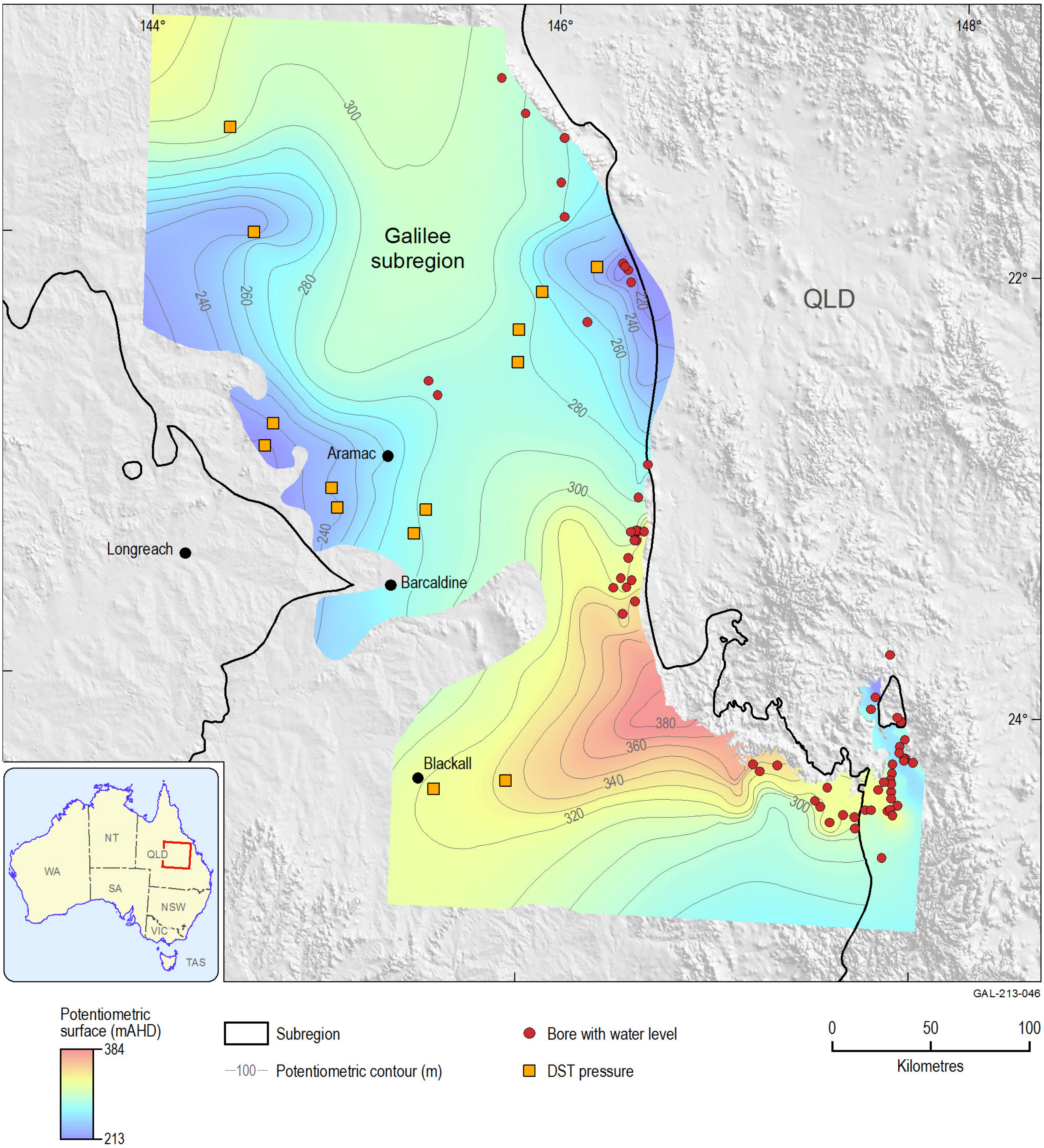


**Figure 67 Potentiometric surface of BC3, Galilee subregion**

Data points are adjusted to a datum of 25 ˚C and equivalent fresh water head
DST = drill stem tests
Data: Bioregional Assessment Programme (Dataset 15, Dataset 16, Dataset 17, Dataset 19)

### Joe Joe Group aquitard

Although the Joe Joe Group is regarded as a regional aquitard, the unit nevertheless has the capacity to store and transmit groundwater and supplies water to a few dozen stock and domestic bores in the southern areas. The (corrected) potentiometric surface for the Joe Joe Group is shown in Figure 68. Unfortunately data are sparse for this formation. Like the upper Permian coal measures data points, the eastern points are water level measurements from boreholes and the western points are pressures calculated from DSTs. Like the overlying upper Permian coal measures partial aquifer, the Joe Joe Group exhibits an easterly flow component towards the Belyando River valley (northern half of Jericho sheet) but elsewhere the flow direction is westward. In common with the upper Permian coal measures partial aquifer and the Clematis Group aquifer, a major groundwater divide must occur that segregates eastern- and western-directed flow components of the groundwater system. Further discussion on the origin of the groundwater divide is provided in Section 2.3.2 of companion product 2.3 (Evans et al., 2018). In general, heads in the Joe Joe Group are higher than the heads in BC3.

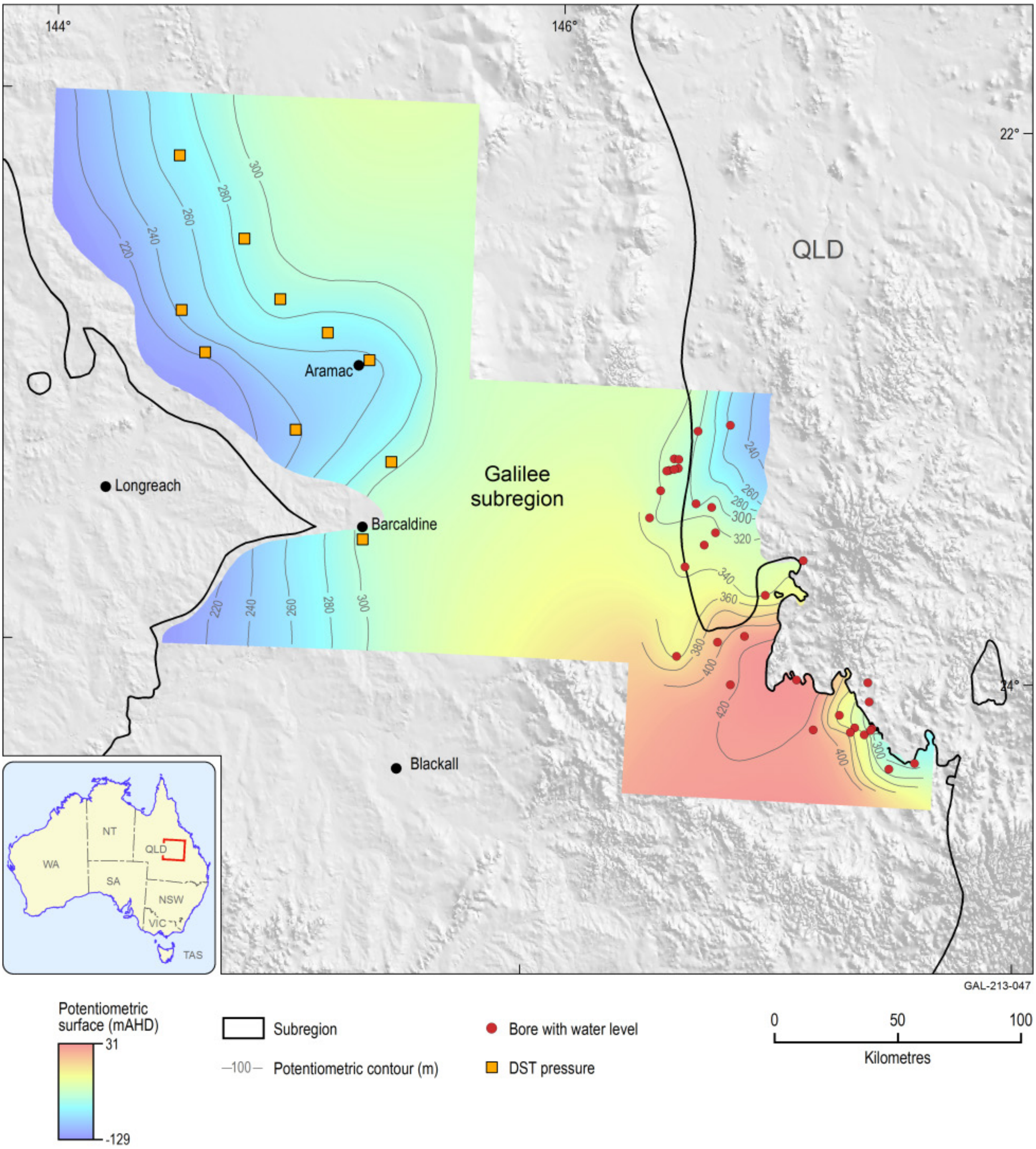


**Figure 68 Potentiometric surface of the Joe Joe Group aquitard, Galilee subregion**

Data points are adjusted to a datum of 25 ˚C and equivalent fresh water head
DST = drill stem tests
Data: Bioregional Assessment Programme (Dataset 15, Dataset 16, Dataset 17, Dataset 19)

### 2.1.3.2.3 Water level trends

Time series groundwater level data for 202 observation wells were obtained from the Queensland groundwater database (Queensland Department of Natural Resources and Mines, Dataset 2). However, not all available time series data were applicable for the purposes of the bioregional assessment. For instance, for some wells it was not possible to assign a hydrogeological unit to the time series water level data.

In descending stratigraphic order the stratigraphic units used in this section are:

- Cenozoic (Alluvium)
- Cenozoic (Paleogene–Neogene)
- Hooray Sandstone
- Adori Sandstone
- Hutton Sandstone
- Clematis Group
- Rewan Group
- upper Permian coal measures.

Time series data from all bores in the dataset (Dataset 20) were analysed using the Theil-Sen regression method (Singh and Singh, 2013) to identify whether there were statistically significant trends in the time series records of the observation bores. The Thiel-Sen method is preferable to a simple linear regression as it is insensitive to outliers and more likely to identify meaningful trends in datasets with a high level of variability.

Many bores had time series record lengths of less than two years. The GAB is a groundwater system where water can have residence times of tens or hundreds of thousands of years, and water levels at a given time are the product of numerous different influences, some of which may operate on very long time spans. It seems unlikely then that a record of only two years would be representative of the long-term trends in the system. Therefore bores with record lengths of less than two years will be discussed separately to bores with long records of water level. Similarly, a number of bores had only one or two observations of water level throughout their recording history. Obviously these were not sufficient data on which to draw conclusions about trends over time.

Figure 69 shows the distribution of observation bores in the Galilee subregion with time series water level monitoring records for a period of time greater than two years. Most of these bores are non-artesian. However, a number of bores monitoring Great Artesian Basin (GAB) aquifers under artesian conditions occur in the western part of the subregion. Most observation wells are in the east of the subregion, with clusters of bores around proposed coal resource developments. A smaller number of bores occur in the north-west and south-west.

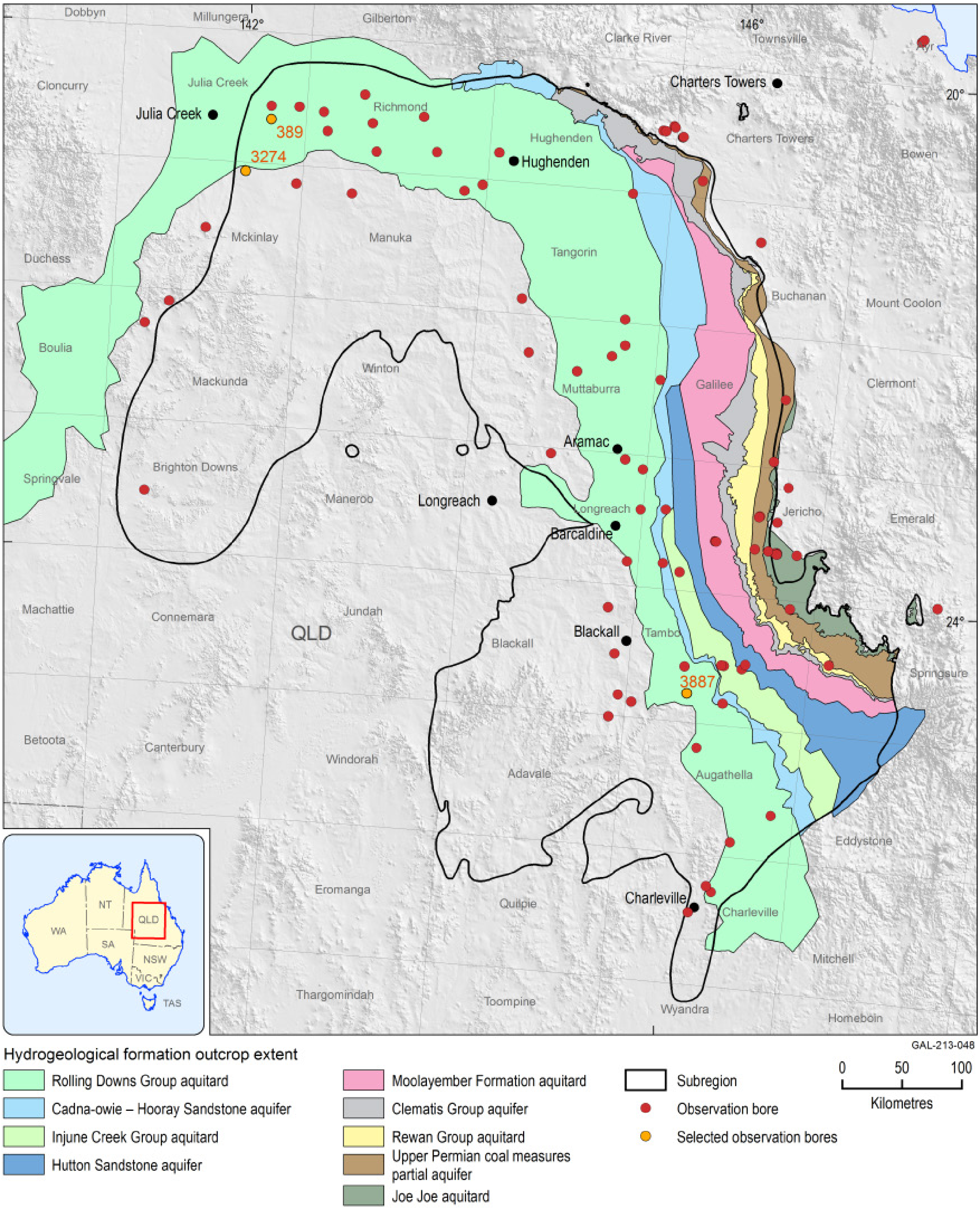


**Figure 69 Location of bores in the Galilee subregion with time series data record lengths greater than two years**

Refer to Figure 71, Figure 72 and Figure 73 for hydrographs of the selected observation bores.
Data: Bioregional Assessment Programme (Dataset 20, Dataset 21)

### *2.1.3.2.3.1 Bores with long recording periods*

Of the 129 bores with records longer than two years, 24 had records which finished before 1997 and cannot be assumed to represent the current state of the aquifer they are screened in. These bores were mostly screened in the Cenozoic or Alluvium, or had unknown hydrogeology for the screened interval so were of limited use for investigating the hydrogeology of the subregion even if they had modern measurements.

The number of observation bores screened in each hydrogeologic unit in the subregion can be seen in Table 19.

This left 105 bores with a record longer than two years, with the most recent water level measurement taken within the last 20 years. Of these, 50 bores did not show a statistically significant trend in the time series data, and 55 showed a statistically significant increase or decrease in water level over the period of measurement. Table 18 summarises the results of statistical analysis of the observation data.

**Table 18 Statistically significant trends in observation bores in the Galilee subregion**

| Record length | Number of bores with increasing trend | Number of bores with decreasing trend | Number of bores with no statistically significant trend |
|---|---|---|---|
| Less than two years | 9 | 47 | 11 |
| More than two years | 25 | 30 | 50 |

Data: Bioregional Assessment Programme (Dataset 20)

Of the 50 bores with records longer than two years with no statistically significant trend, 16 were screened in alluvial deposits or Paleogene-Neogene rocks, which typically show high variability in water level data (see Figure 70). It seems likely that the absence of a statistically significant trend is the result of rapid responses to rainfall in these bores due to their shallow screened interval.

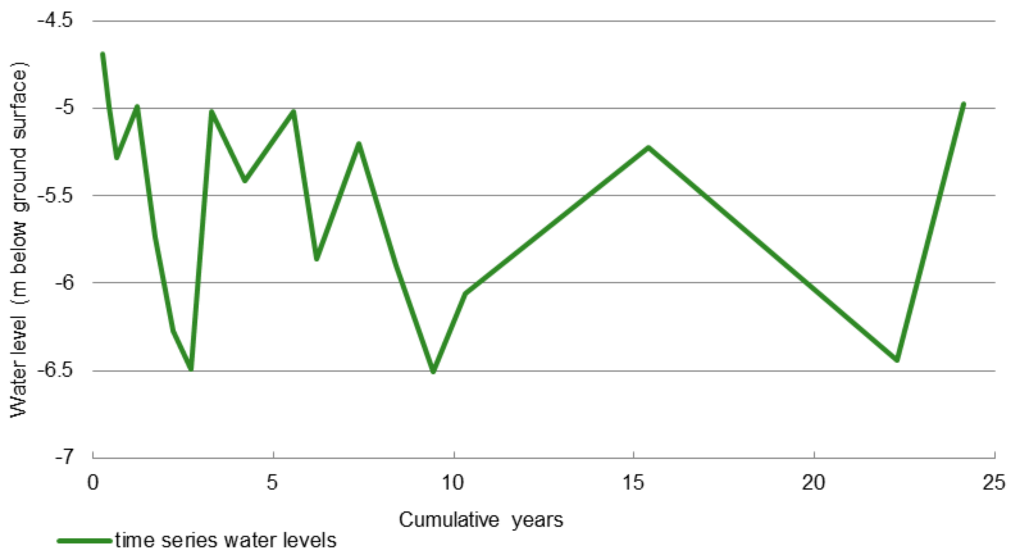


**Figure 70 Typical time series data response for an observation bore screened in alluvium (observation bore RN 12030001)**

On the “cumulative years” axis, year 0 = 1976, year 25 = 2001
Data: Bioregional Assessment Programme (Dataset 20)

The majority of non-artesian bores with a statistically significant trend and records longer than two years showed a decreasing trend in water levels over the recording period. The difference in water level recorded in bores with a decreasing trend ranged from 0.2 to 14 m over the recorded interval. The mean change was 2.5 m with a standard deviation of 3.03 m. The magnitude of decline in water level is strongly influenced by the length of the record. Some bores have measurements dating back to the 1950s and 1960s when it seems water levels were up to ten metres higher than observed today. Bores with recent (post 1990) records of only 10 to 20 years duration typically show declines in water level on the order of 10 cm to 3 m.

Non-artesian bores showing an increase in hydraulic head over the recording period showed changes in water level of 0.2 to 41 m with a mean change of 3.1 m and standard deviation of 9.2 m.

The majority of artesian bores did not show any statistically significant trend in the data. For some bores this is likely due to the small number of observations available for statistical analysis (only three or four points for some bores), but for many bores a change in the hydrological regime caused by the Great Artesian Basin Sustainability Initiative (GABSI) program may be the reason. The hydrographs of several bores in which a statistically significant trend could not be identified show stable water levels, or a decline in water levels, until sometime in the 1990s, after which water levels begin to rise sharply. Figure 71, Figure 72, and Figure 73 show examples of this hydrograph trend for three aquifers in the subregion. All three show a sharp increase in water levels in the early 1990s, when GABSI began. By 1995, 51 bores had been rehabilitated in just these three aquifers.

The change in trend caused by GABSI's influence makes a trend in water levels for these bores impossible to detect with linear analysis methods without pre-treatment of the data to separate observations from before and after the sealing of flowing artesian bores.

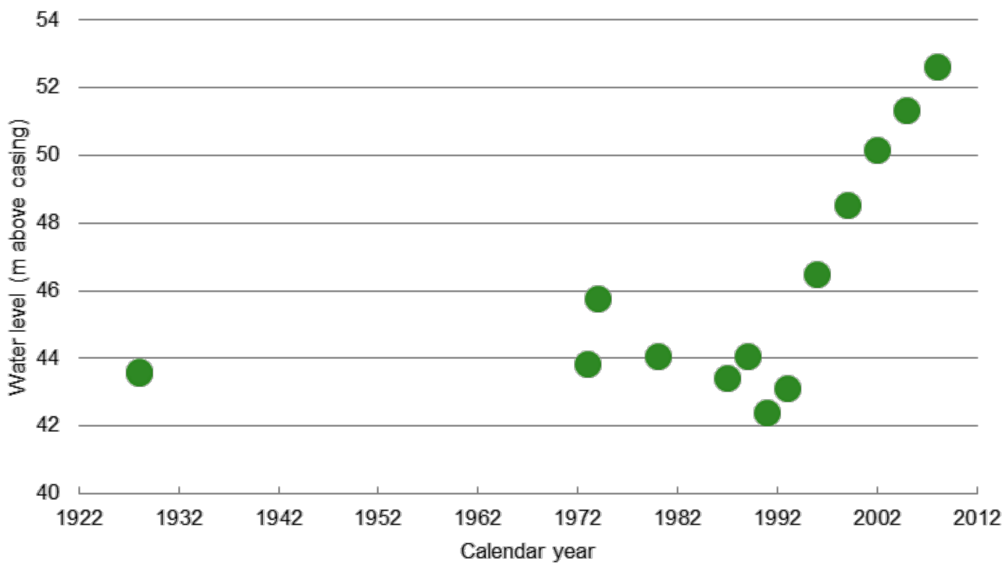


**Figure 71 Hydrograph data for artesian observation bore RN 389 in the Hooray Sandstone**

Refer to Figure 69 to see the location of RN 389.
Data: Bioregional Assessment Programme (Dataset 20)

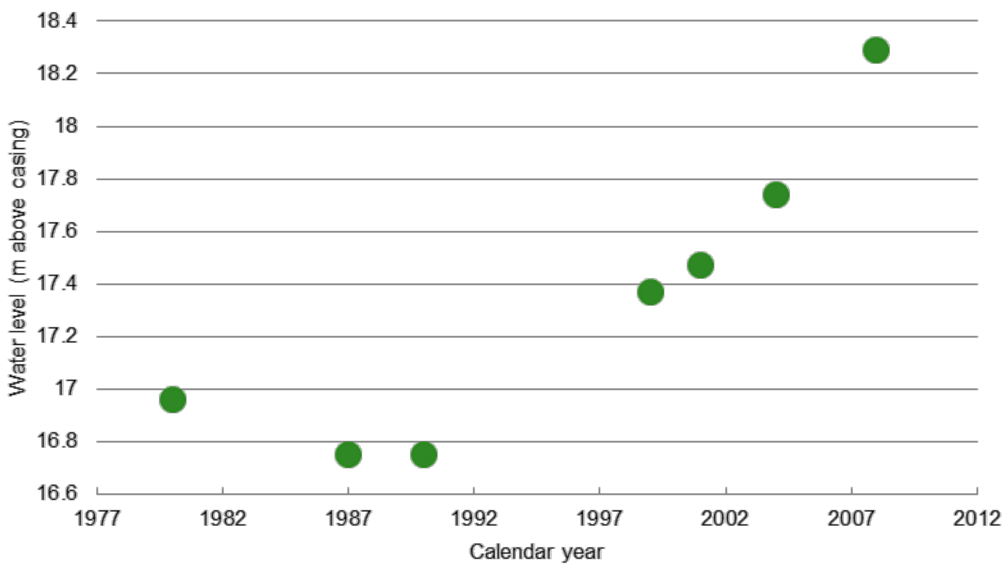


**Figure 72 Hydrograph data for artesian observation bore RN 3887 in the Hutton Sandstone**

Refer to Figure 69 to see the location of RN 3887.
Data: Bioregional Assessment Programme (Dataset 20)

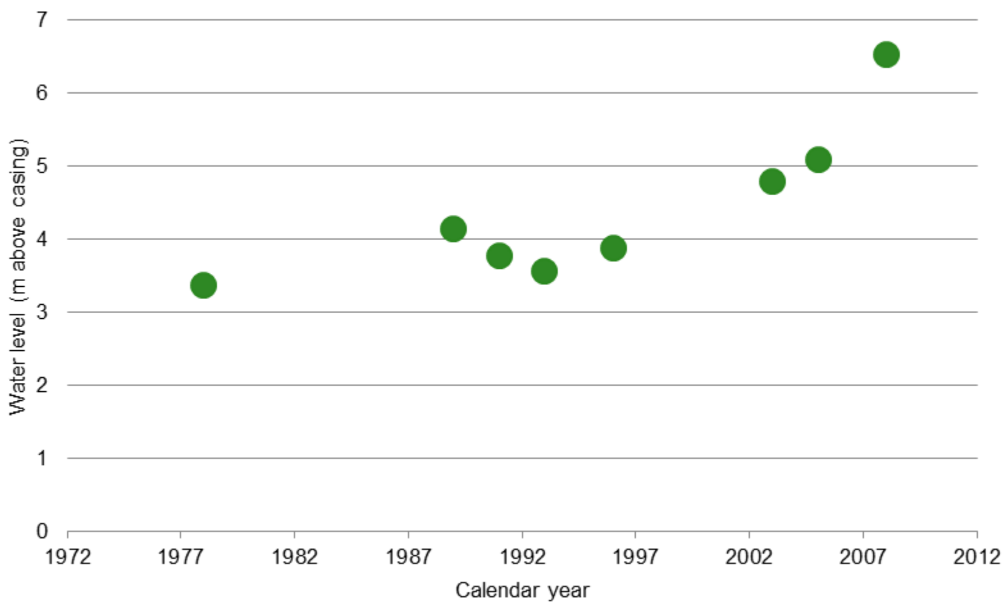


**Figure 73 Hydrograph data for artesian observation bore RN 3274 in the Cadna-owie – Hooray Sandstone**

Refer to Figure 69 to see the location of RN 3274.
Data: Bioregional Assessment Programme (Dataset 20)

Of the artesian bores which did show a statistically significant trend, all but one showed an increase in water levels over the recording period, also consistent with an expected increase in pressure resulting from capping and piping of flowing artesian bores.

Both increasing and decreasing trends in water level were seen in most hydrostratigraphic units. There were, however, some units which showed trends in only one direction. The trends observed in each hydrostratigraphic unit are summarised in Table 19 and discussed in detail below.

**Table 19 Statistically significant trends in water levels for bores with records longer than two years in the Galilee subregion**

| Lithostratigraphic unit | Total number of bores in the dataset after filtering | Number of non-artesian bores | Number of artesian bores | Number of records showing increase | Number of records showing decrease | Number of records with no statistically significant trend |
|---|---|---|---|---|---|---|
| Cenozoic (Alluvium) | 14 | 14 | 0 | 2 | 9 | 3 |
| Cenozoic (undefined) | 24 | 24 | 0 | 3 | 8 | 13 |
| Wallumbilla Formation | 1 | 0 | 1 | 0 | 0 | 1 |
| Hooray Sandstone | 18 | 4 | 14 | 4 | 3 | 11 |
| Adori Sandstone | 5 | 2 | 3 | 3 | 1 | 1 |
| Clematis Group | 5 | 5 | 0 | 1 | 0 | 4 |
| Hutton Sandstone | 25 | 9 | 16 | 4 | 8 | 13 |
| Rewan Group | 2 | 2 | 0 | 2 | 0 | 0 |
| Upper Permian coal measures | 2 | 2 | 0 | 1 | 1 | 0 |

Data: Bioregional Assessment Programme (Dataset 20)

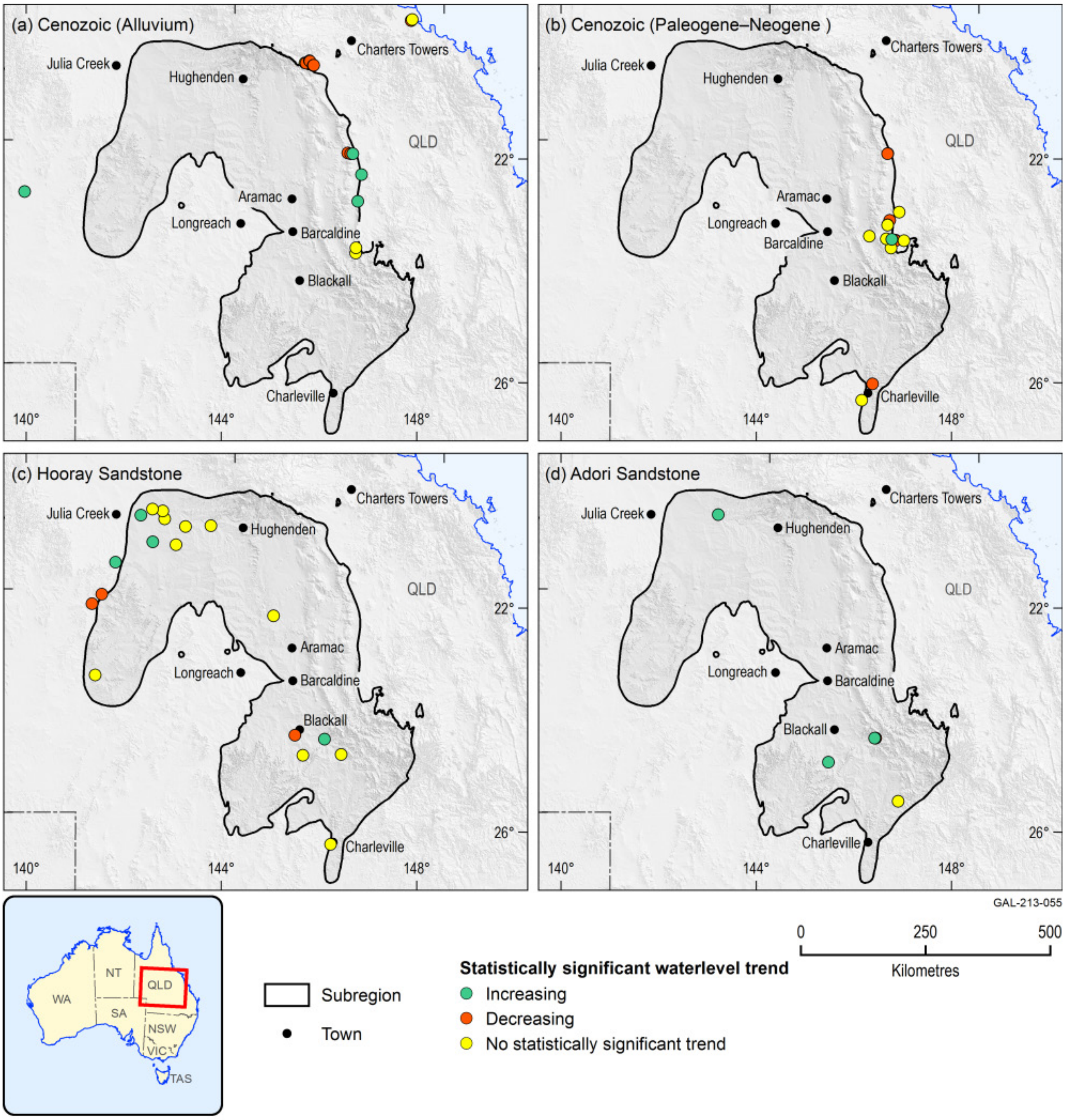


**Figure 74 Distribution and water level trends observed in bores screened in (a) Cenozoic (alluvium), (b) Cenozoic (Paleogene–Neogene), (c) Hooray Sandstone and (d) Adori Sandstone**

Data: Bioregional Assessment Programme (Dataset 22)

### Cenozoic (Alluvium)

All bores in the alluvium are non-artesian and monitor unconfined alluvial aquifers in the Belyando river basin. Many are clustered in the north of the subregion in the vicinity of Charters Towers (Figure 74a). Six of these bores show a decrease in water level with time, and the remaining two show no statistically significant trend. The remaining six bores in the alluvium are spread broadly across the subregion, and show both increasing and decreasing trends (Figure 74a). The variety of trends seen in bores screened in alluvial material is consistent with expectations that the alluvium is not a highly connected system, but contains a number of local flow systems which are unlikely to influence one another.

**Cenozoic (Paleogene–Neogene)**

Like the alluvium, bores screened in Cenozoic rocks and sediments are non-artesian and located in the eastern part of the subregion (Figure 74b), mostly in the Belyando river basin. These bores show both increasing and decreasing trends, as well as a large number of records in which there is no statistically significant trend. Water levels can be highly variable in these records, possibly due to rapid responses to rainfall due to the shallow screened intervals of the bores. Similar to bores in alluvial material, the different trends seen in bores screened in Cenozoic rocks may be an indication that flow systems in these rocks are relatively local and have little impact on one another.

**Hooray Sandstone**

There are 18 monitoring bores in the Hooray Sandstone in the filtered dataset. Four of these are sub-artesian and 14 are artesian.

Of the sub-artesian bores, one has no statistically significant trend, another has an increasing trend (greater than 40 m over 6 years), whilst the remaining two display a decreasing trend (of 10 m and 14 m). The magnitude of water level changes is greater in the Hooray Sandstone than in any other hydrogeological unit in any other GAB aquifer in the Galilee subregion. The increase of 40 m occurred in the early 2000s. Natural hydrogeologic processes would not cause such a large change over such a short time, and it is assumed that the rise in head is a result of the GABSI bore rehabilitation programme.

The two sub-artesian bores showing large decreases in water level are located in the north-west of the subregion and are within 30 km of each other.

Of the artesian bores, one shows a decrease in water levels whilst another three show a statistically significant increase. The other ten bores had no statistically significant trend. The increase in water levels (pressures) in some bores may again be due to the GABSI programme, with the capping and piping of a large number of uncontrolled flowing artesian bores in the Hooray Sandstone that commenced in the mid-1990s. Figure 74c shows the locations of observations bores screened in the Hooray Sandstone.

**Adori Sandstone**

Five bores in the filtered dataset were tapping into the Adori Sandstone aquifer. Two are sub-artesian and three are artesian.

Of the two sub-artesian bores, one was found to have a statistically significant increasing trend, while the other was found to have a decreasing trend. This is notable because the two bores are within 2 km of each other. Water levels in these bores are highly variable, which may be related to both bores being located in the recharge area of the Adori Sandstone; water levels observed here may be influenced by infiltrating recharge water. Both records show a sharp rise in water level at the end of the record.

Of the three artesian bores, two show a statistically significant increase in water levels. One of which shows a very large increase of greater than 11 m over the recording period.

All five monitoring bores screened in the Adori Sandstone show an increase in water levels from 1996. Figure 74d shows the locations of observation bores screened in the Adori Sandstone.

**Hutton Sandstone**

There were 22 bores in the filtered dataset in the Hutton Sandstone aquifer. Of these six are sub-artesian and 16 are artesian.

Of the six sub-artesian bores, five show a decrease in water level over the recording time, and one shows no statistically significant trend. The decrease occurs in all bores between 1993 and 2014, and is of a magnitude in the range 0.2 to 0.6 m. The distribution of these bores in the subregion is a roughly north–south transect covering most of the subregion (Figure 75c). This suggests that the reduction in water levels is occurring in the Hutton Sandstone aquifer throughout the Galilee Basin. The records of decreasing water levels in the Hutton Sandstone aquifer begin in the early 1990s and may be related to the abstraction of water from these units, as the Hutton Sandstone is an important water source in the region.

Of the artesian bores, four show an increase in water levels over the recording period, and eight show no statistically significant trend. Increases in water level are from 1 to 3 m over the recording period, and tend to be steepest after 1990. This may be related to the capping and piping of uncontrolled flowing artesian bores in the Hutton Sandstone during the GABSI project.

**Clematis Group**

There were five bores in the Clematis Group in the filtered dataset, clustered in two locations. All of these were sub-artesian. Only one showed a statistically significant trend, which was of increasing water levels. It is difficult to base any interpretation of water level trends in an aquifer on a single bore. The absence of a statistically significant trend in other bores screened in the Clematis Group may be due to their location in or close to the recharge area for the aquifer. This means the water level can be highly variable in response to rainwater entering the aquifer as recharge. Figure 75a shows the location of bores screened in the Clematis Group relative to the recharge zone.

**Rewan Group**

There are two bores in the Rewan Group in the filtered dataset. Both are sub-artesian. They both show an increasing trend in water levels. Both bores are located in or close to the recharge area for the Rewan Group.

**Upper Permian coal measures**

Two bores in the filtered dataset were present in the upper Permian coal measures (Figure 75b). Both of these are sub-artesian. One shows an increase in water levels over the recording period, while the other shows a decrease. Both of these bores are located in the outcrop area of the upper Permian coal measures. The bore showing an increase in water levels is located in the south-eastern part of the subregion, while the bore showing a decrease is located in the north.

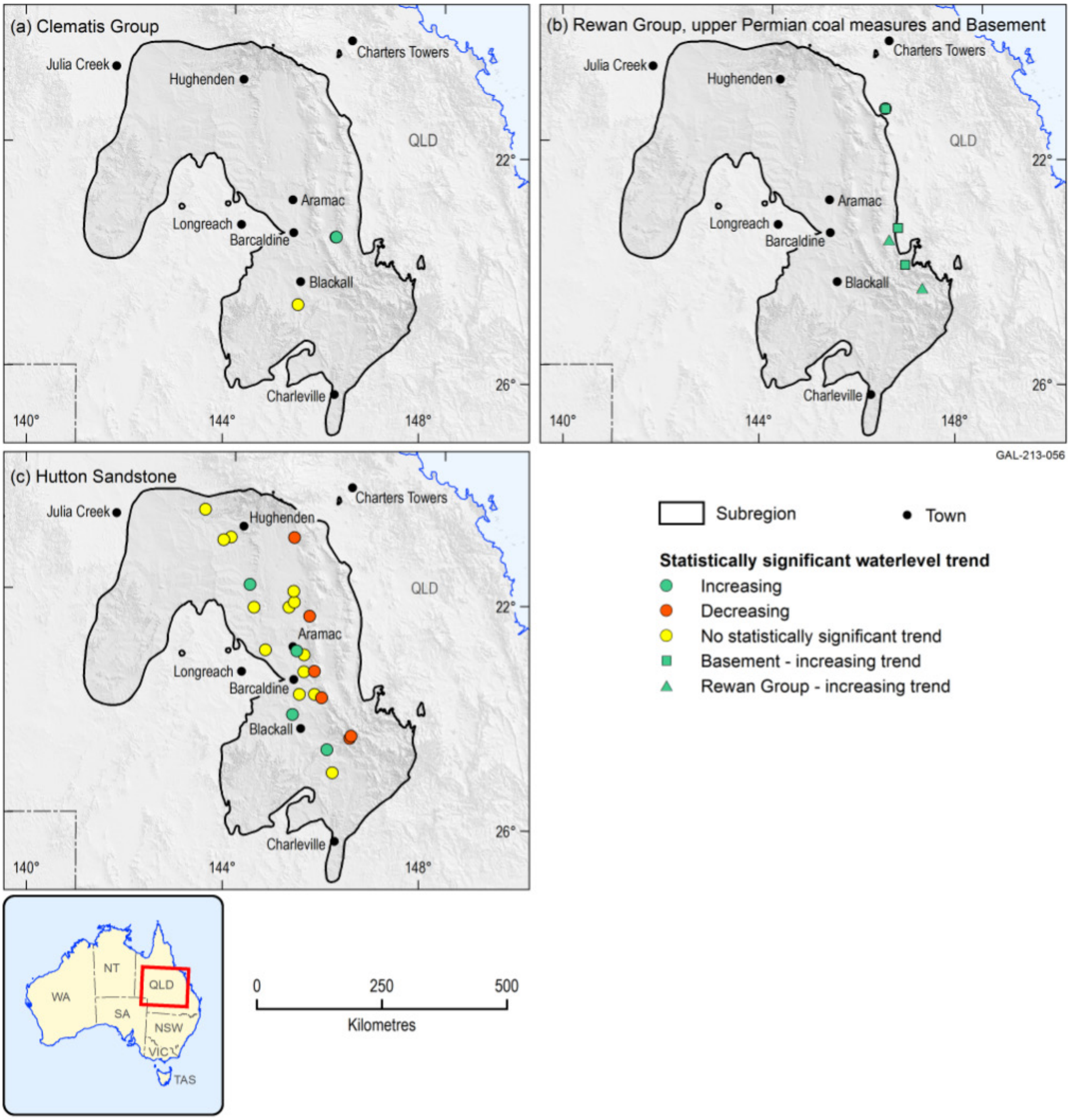


**Figure 75 Location of and water level trends observed in bores screened in the (a) Clematis Group, (b) Rewan Group, upper Permian coal measures and (c) Hutton Sandstone**

Data: Bioregional Assessment Programme (Dataset 22)

#### 2.1.3.2.3.2 Bores with short recording periods

All bores with recording periods of less than two years had data collected in 2012 or later. Therefore no further filtering of this dataset was required to ensure water levels representative of the modern system. Forty bores show a decreasing trend in water level. Nine bores show an increasing trend and 11 do not show any statistically significant trend. Most (45 of 67) are screened in the upper Permian coal measures. The majority of these bores were installed in association with proposed mining development in the Galilee Basin, in particular the Carmichael and Alpha coal projects. While piezometers have been installed, no mining operations have commenced, and the trends observed in these bores are a feature of the system pre-development rather than the result of any resource development.

While the declines in head show a statistically significant trend, the change in head is typically in the order of 5 or 10 cm and it is difficult to consider this trend as representative of the long-term behaviour of the aquifer due to the short duration of the record. Results of statistical analysis for each hydrogeologic unit are shown in Table 20.

**Table 20 Statistically significant trends in water levels for bores with records shorter than two years in the Galilee subregion**

| Lithostratigraphic unit | Number of bores in dataset | Number of records showing increase | Number of records showing decrease | Number of records with no statistically significant trend |
|---|---|---|---|---|
| Cenozoic (Alluvium) | 3 | 1 | 2 | 0 |
| Cenozoic sediments | 4 | 0 | 3 | 1 |
| Clematis Group | 1 | 0 | 1 | 0 |
| Dunda beds | 4 | 1 | 2 | 1 |
| Rewan Group | 8 | 7 | 0 | 1 |
| Upper Permian coal measures | 45 | 7 | 31 | 7 |
| Joe Joe Group | 2 | 0 | 1 | 1 |

Data: Bioregional Assessment Programme (Dataset 20)

#### 2.1.3.2.3.3 Nested bores

A small number of bores in the dataset were nested allowing comparison of water level changes in different aquifers at the same location. Time series data from nested bores indicates that deep and shallow aquifers are connected in some parts of the subregion, and disconnected in others. A pair of bores screened in the upper Permian coal measures and alluvium close to the proposed site for the Kevin’s Corner development show concurrent increases in water level in both aquifers (Figure 76). Bores screened in the upper Permian coal measures and Cenozoic sediments close to the proposed Alpha coal development site show a similar relationship between the upper Permian coal measures and the shallow aquifer (Figure 77).

In both cases the water level of the upper Permian coal measures is greater than in the alluvium, meaning a confining layer must separate the two aquifers. The similarity in water level trends could be due to minor leakage across a confining layer, allowing the upper Permian coal measures to influence the water level of overlying alluvium, or may be the result of mechanical loading of water in the alluvium causing water levels in the upper Permian coal measures to rise in response to increased downward pressure. Similar trends were observed in the Condamine Alluvium and Walloon Coal Measures, where mechanical loading was considered the most likely explanation due to the close correlation between rainfall events and water level rise in the alluvium (DNRM, 2015).

Examination of time series precipitation data in conjunction with water levels, and/or pump test data from both aquifers may be necessary to distinguish between mechanical loading and leakage across a confining layer as the cause of the trends observed.

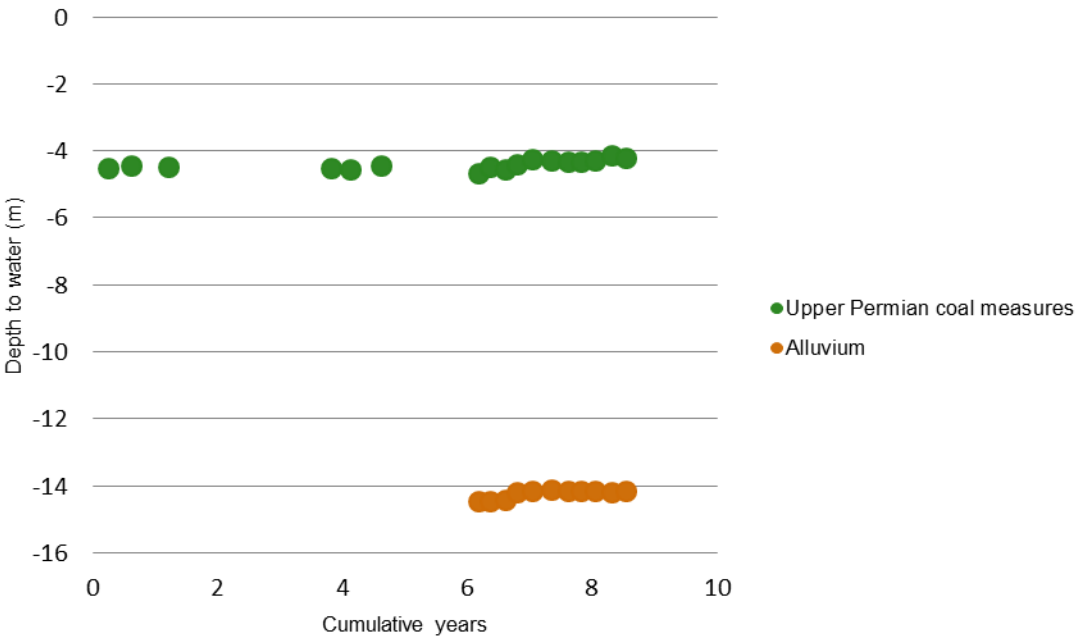


**Figure 76 Water level trends in both upper Permian coal measures (bore RN 12030099) and alluvium (bore RN 12030100) close to the proposed Kevin's Corner coal project**

On the "cumulative years" axis, year 0 = 2006, year 10 = 2016
Data: Bioregional Assessment Programme (Dataset 20)

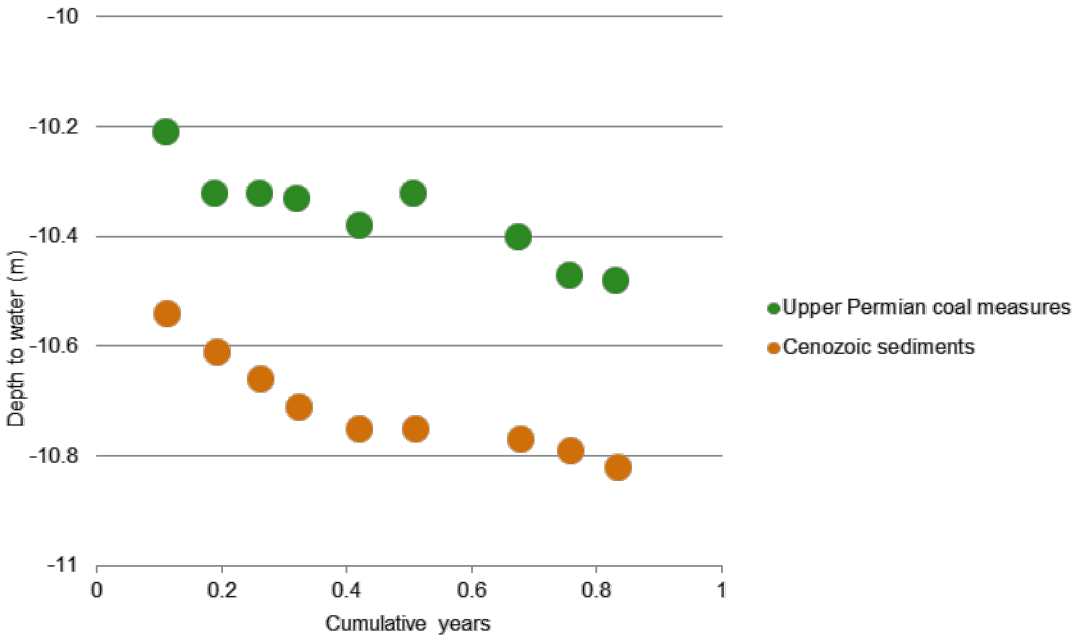


**Figure 77 Water level trend in the upper Permian coal measures (bore RN 132911) and Cenozoic sediments (bore RN 132903) close to the Alpha coal project**

On the “cumulative years” axis, year 0 = 2011, year 1 = 2012
Data: Bioregional Assessment Programme (Dataset 20)

## 2.1.3.2.4 Head differences between aquifers and seal characteristics of aquitards

It is instructive to examine head differences between aquifers to get a sense of potential direction of leakage (if pathways exist) and also to assess the seal characteristics of the intervening aquitard. In the following section the potentiometric surfaces of two aquifers are overlain, and one subtracted from the other. In areas where the head difference residual is less than ±10 m, the heads are assumed to be approximately equal (the 10 m buffer about zero is to allow for possible errors in contouring and data). This is a necessary, but not the only condition for an intervening aquitard to be considered to be leaking or to indicate the occurrence of inter-aquifer leakage. Conversely, where the head difference residual is larger than 10 m (i.e. a value less than –10 m or a value greater than +10 m), this indicates areas where significant pressure differences exist between the two aquifers. Such a condition is interpreted as indicating areas where the intervening aquitard may be acting as a tight seal or where inter-aquifer leakage is negligible.

### *2.1.3.2.4.1 Hutton Sandstone – Hooray Sandstone head difference*

Figure 78a shows the (corrected) head difference between the Hutton and Hooray sandstones. This can only be calculated where the Hooray Sandstone aquifer overlies the Hutton Sandstone aquifer and where data exists. Positive values are areas where the head in the Hutton Sandstone is higher than the head in the Hooray Sandstone. These positive areas occur near the intake beds in the eastern zone (where the outcrop of Hutton Sandstone is topographically higher than the Hooray Sandstone) and in the western artesian areas on the Winton and Mackunda 1:250,000 sheets. These are areas where it appears that the intervening aquitard, the Injune Creek Group, forms a tight seal. Elsewhere, in the central eastern, and in parts of the central western and western zones, the Injune Creek Group aquitard appears to be leaky (Figure 78b).

The Injune Creek Group aquitard comprises three units. At the top of this aquitard lies the Late Jurassic Westbourne Formation (carbonaceous siltstone and mudstone) overlying the Middle to Late Jurassic Adori Sandstone (labile sandstone). At the base of the Injune Creek Group lies the Middle Jurassic Birkhead Formation (labile sandstone, siltstone, minor coal). The Adori Sandstone is a GAB aquifer in its own right, though it is not as extensively utilised as the Hutton and Hooray sandstones. The Birkhead Formation is thought to be leakier and more permeable than the Westbourne Formation. In fact, in the Western Eromanga Basin oil and gas fields, the Birkhead Formation is regarded as a reservoir rock, being second only to the Hutton Sandstone in hydrocarbon production (Gravestock et al., 1998). Thus, in areas where it appears the Injune Creek Group forms a tight aquitard, the tightness is largely due to the impermeable nature of the Westbourne Formation.

According to Figure 78b, about 40% of the Injune Creek Group aquitard forms a tight seal and the remaining 60% is leaky. The notion of a significant component of the Injune Creek Group being leaky is supported by the hydrochemistry data. Like the Hutton and Hooray sandstones, groundwater in the Injune Creek Group is a Na-$HCO_3$-Cl type water. Table 21 shows the mean and ranges of TDS in the Hutton and Hooray sandstones and the Injune Creek Group.

**Table 21 Mean and range of TDS values in Hooray Sandstone, Injune Creek Group and Hutton Sandstone**

| Formation | Number of samples | Mean TDS (mg/L) | Range of TDS (mg/L) |
|---|---|---|---|
| Hooray Sandstone | 1302 | 834 | 180–7136 |
| Injune Creek Group | 146 | 597 | 133–2041 |
| Hutton Sandstone | 1269 | 482 | 55–3579 |

TDS = total dissolved solids
Data: Bioregional Assessment Programme (Dataset 1)

The mean TDS and TDS range in Table 21 indicates that chemically the Injune Creek Group is intermediate but with a TDS range that is closer to that of the Hutton Sandstone than the Hooray Sandstone. Therefore the dominant vertical flow direction through the leaky aquitard would be upwards from the Hutton Sandstone.

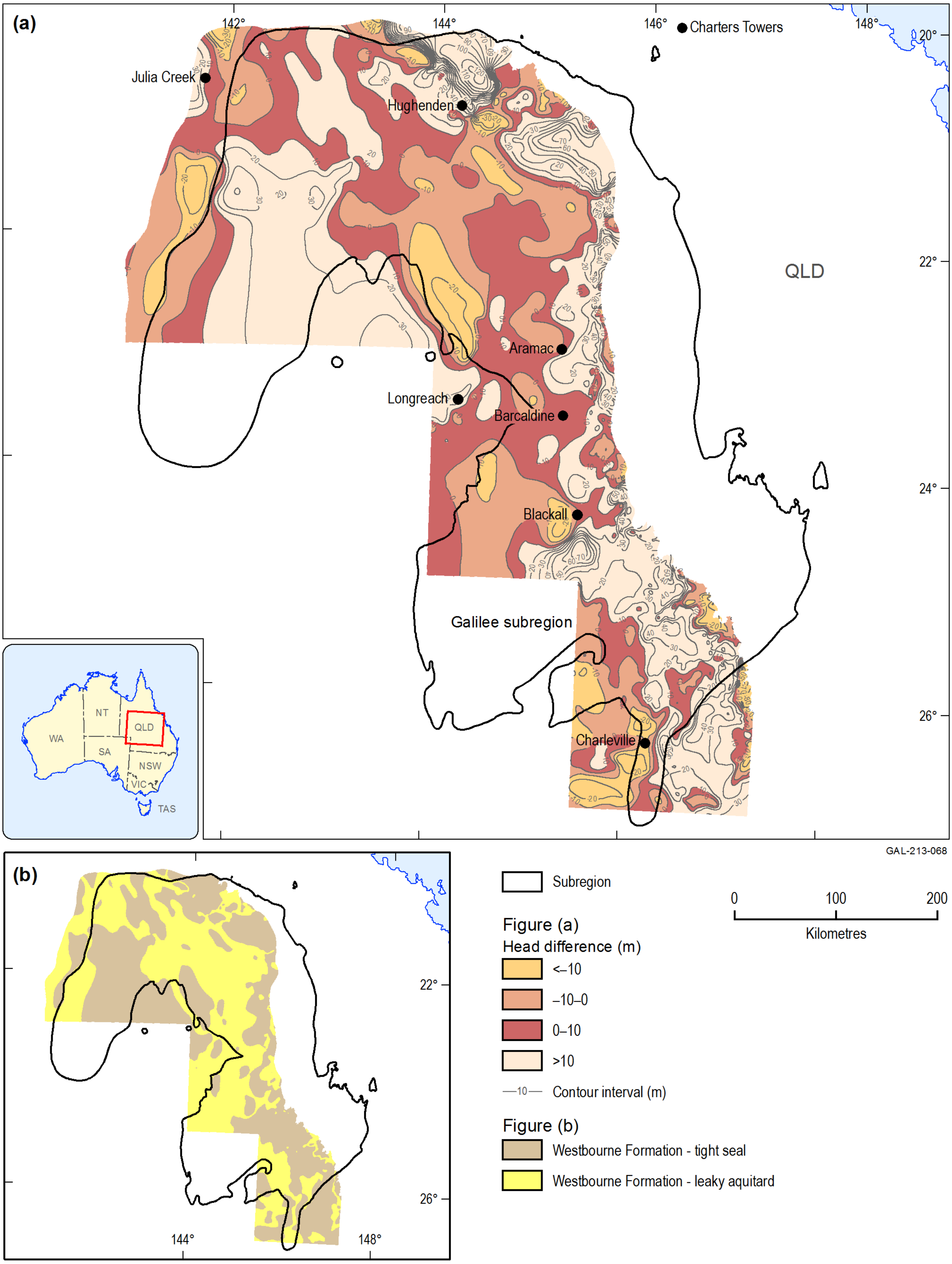


**Figure 78 (a) Head difference between Hutton Sandstone and Hooray Sandstone aquifers. Positive values indicate areas where the head in the Hutton Sandstone is higher than that in the Hooray Sandstone. (b) Seal characteristics of the Westbourne Formation aquitard**

Data: Bioregional Assessment Programme (Dataset 17)

#### *2.1.3.2.4.2 Hutton Sandstone – Clematis Group head difference*

Figure 79a shows the (corrected) head difference between the Hutton Sandstone and Clematis Group. This can only be calculated where Hutton Sandstone overlies the Clematis Group (central and western portions of the subregion) and where data exists. Positive values occur where the head in the Hutton Sandstone aquifer is higher than the head in the Clematis Group aquifer. These areas occur near the intake beds of the Hutton Sandstone and are also propagated down gradient into some parts of the central eastern zone. Such areas are interpreted as those where the intervening aquitard, the Moolayember Formation, forms a tight seal.

Heads in the Hutton Sandstone aquifer are higher than the heads in the Clematis Group aquifer everywhere except for a small area just south of Hughenden. Figure 79b indicates the Moolayember Formation forms a tight seal in the east but becomes leaky westward over the majority of the central eastern zone and for all of the Manuka 1:250,000 sheet in the central western zone.

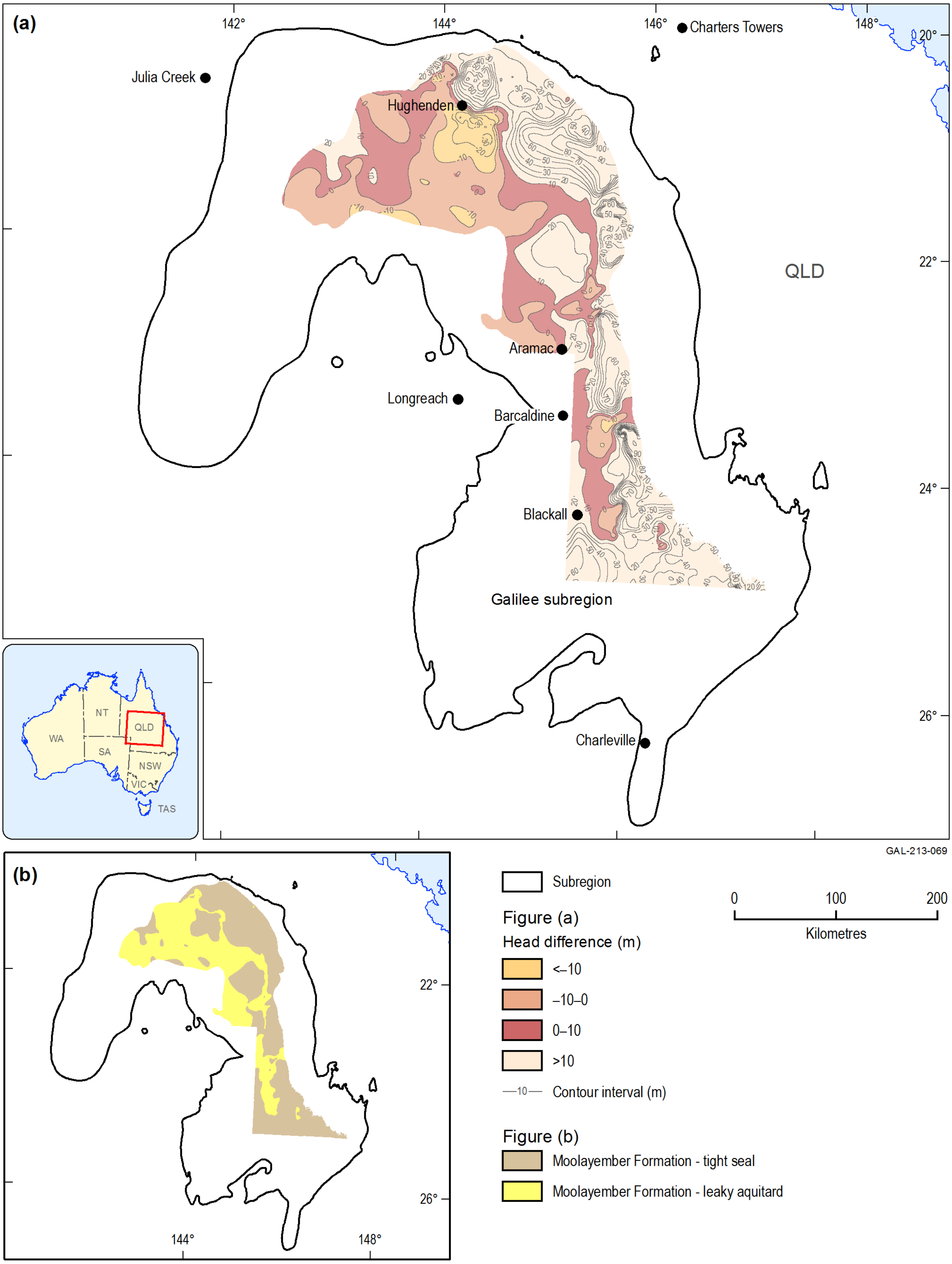


**Figure 79 (a) Head difference between Hutton Sandstone and Clematis Group aquifers. Positive values indicate areas where the head in the Hutton Sandstone is higher than that in the Clematis Group. (b) Seal characteristics of the Moolayember Formation aquitard**

Data: Bioregional Assessment Programme (Dataset 17)

#### *2.1.3.2.4.3 Clematis Group aquifer – BC1 partial aquifer head difference*

Figure 80a shows the (corrected) head difference between the Clematis Group aquifer and the BC1 partial aquifer. This can only be calculated where the Clematis Group aquifer overlies the BC1 partial aquifer and where data exists. Negative values indicate areas where the head in BC1 is higher than the head in the Clematis Group, and such values populate the majority of the mapped area (a small but important exception occurs on the Tambo 1:250,000 sheet where the heads in the Clematis Group aquifer are higher than those in the BC1 partial aquifer). These are areas where it appears that the intervening aquitard, the Rewan Group, forms a tight seal (Figure 80b).

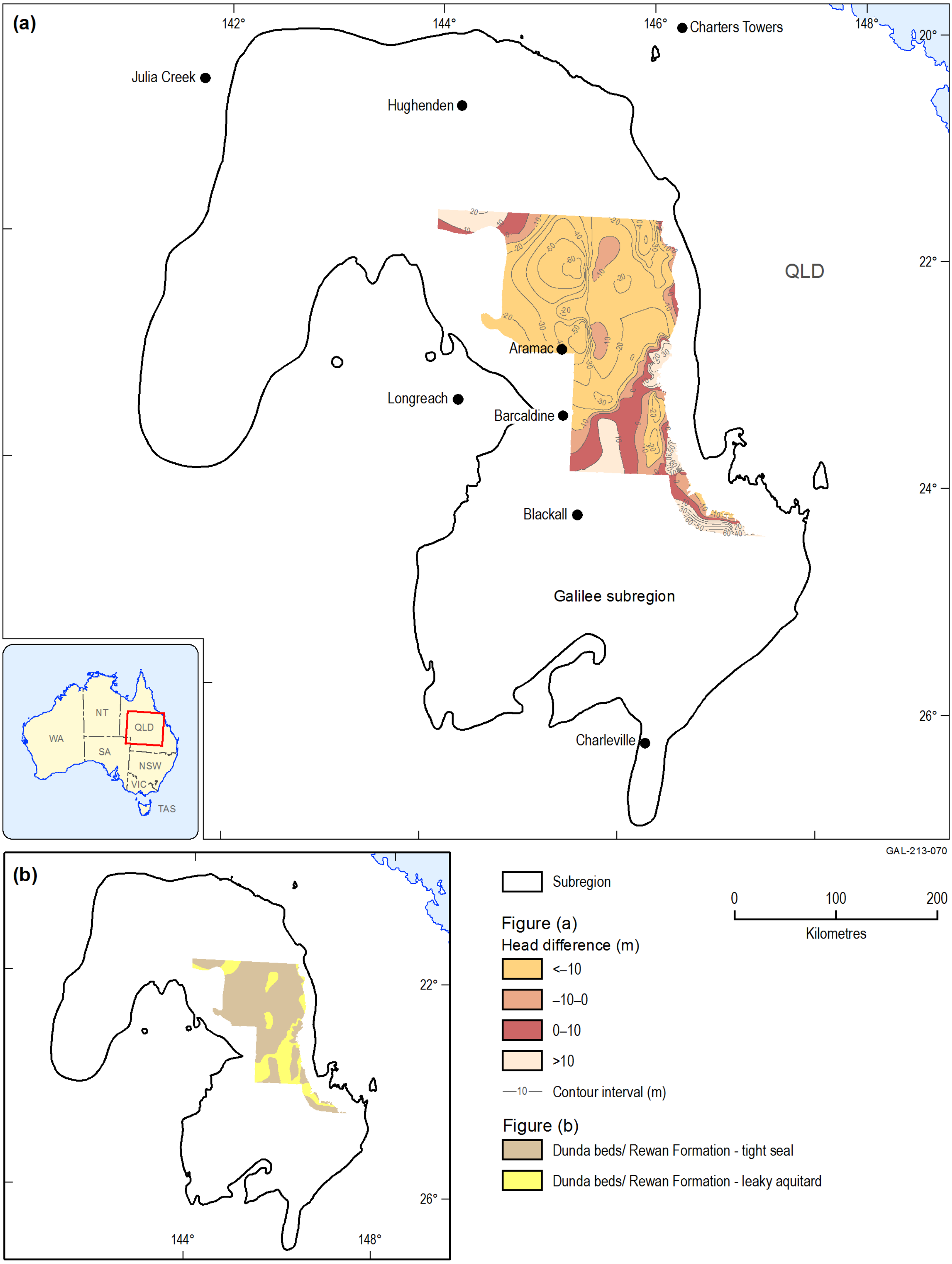


**Figure 80 (a) Head difference between Clematis Group aquifer and BC1 partial aquifer. Negative values indicate areas where the head in BC1 is higher than that in the Clematis Group. (b) Seal characteristics of the Dunda beds/Rewan Formation aquitard**

Data: Bioregional Assessment Programme (Dataset 17)

#### *2.1.3.2.4.4 BC1 – BC2 partial aquifer head difference*

Unlike the examples in previous subsections of Section 2.1.3.2.4, the BC1 and BC2 partial aquifers all occur within the one hydrostratigraphic unit (upper Permian coal measures). Lithologies within the upper Permian coal measures which can have aquitard properties include shale-rich sequences, coal or tight sandstone.

Figure 81a shows the (corrected) head difference between the BC1 and BC2 partial aquifers. This can only be calculated where the BC1 partial aquifer overlies the BC2 partial aquifer and where data exists. Negative values are areas where the head in BC2 is higher than the head in BC1, and such areas are to be found on the Muttaburra and Jericho 1:250,000 sheets. These are places where it appears that the aquitard at the top of BC2 (the BC interburden sandstone) forms a tight seal to exclude vertical hydraulic connection between BC1 and BC2 and is approximately collinear with the groundwater divide. The tight aquitard occurs across about 40% of the mapped area. A small but significant area where heads in BC1 are higher than BC2 (positive head difference values) occurs in the south-east corner of the Jericho 1:250,000 sheet. This area was mentioned previously as being the major recharge zone for the upper Permian coal measures and Figure 81a indicates the potential is for downward leakage from BC1 to BC2. The BC interburden sandstone aquitard is thought to be leaky over about 60% of the mapped area (Figure 81b).

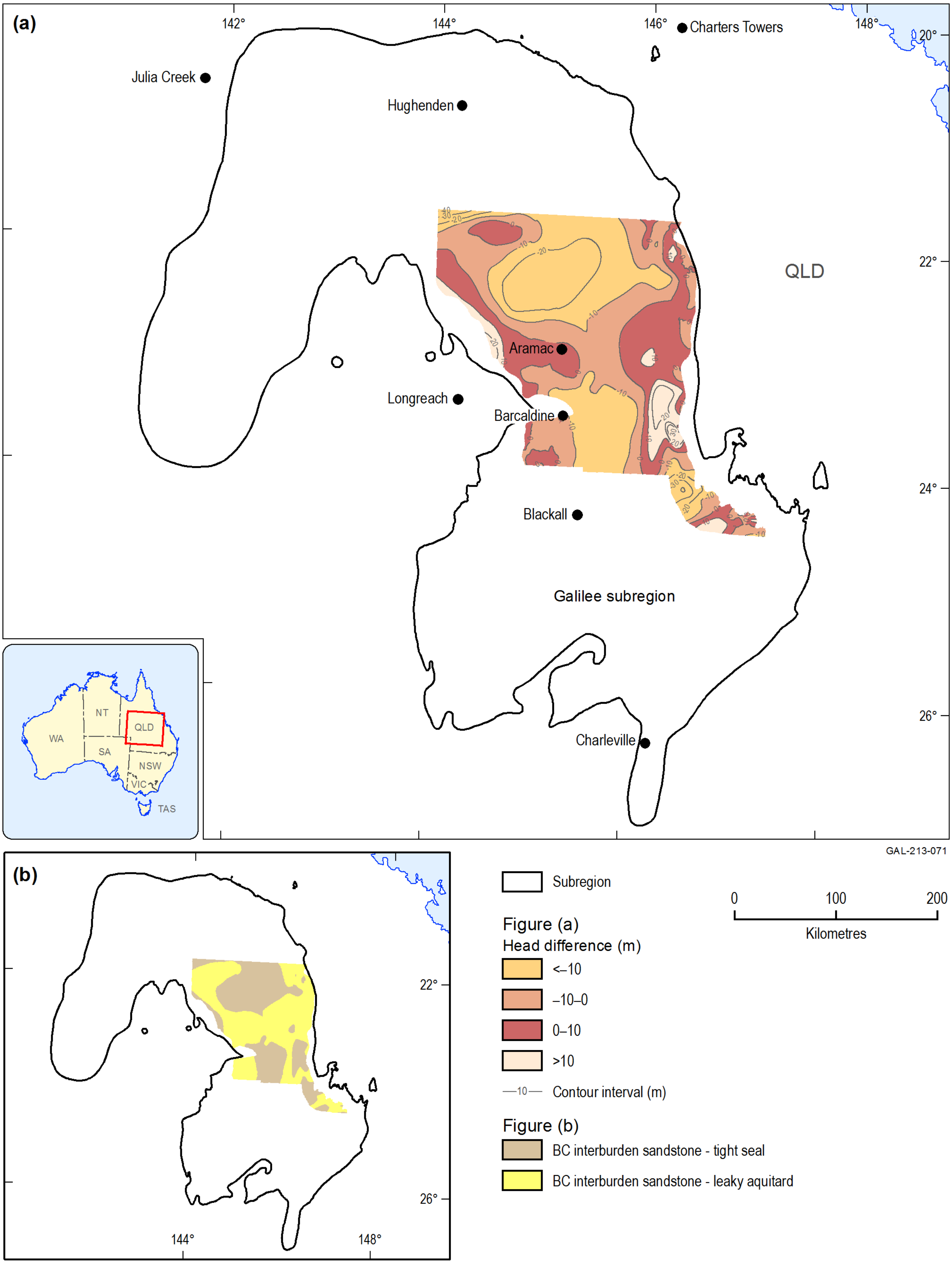


**Figure 81 (a) Head difference between BC1 and BC2 partial aquifer. Negative values indicate areas where the head in BC2 is higher than that in BC1. (b) Seal characteristics of the BC interburden sandstone aquitard**

Data: Bioregional Assessment Programme (Dataset 17)

#### *2.1.3.2.4.5 BC2 – BC3 partial aquifer head difference*

The BC2 and BC3 partial aquifers comprise parts of the upper Permian coal measures. Figure 82a shows the (corrected) head difference between the BC2 and BC3 partial aquifers. This can only be calculated where the BC2 partial aquifer overlies the BC3 partial aquifer and where data exists. Positive values are areas where the head in BC2 is higher than the head in BC3. Such areas occur on the Tangorin, Muttaburra, Galilee, Jericho and Springsure 1:250,000 sheets. These are places where it appears that the intervening aquitard (DE interburden sandstone) forms a tight seal. Elsewhere, on the eastern and western margins, the DE interburden sandstone aquitard appears to be leaky (Figure 82b).

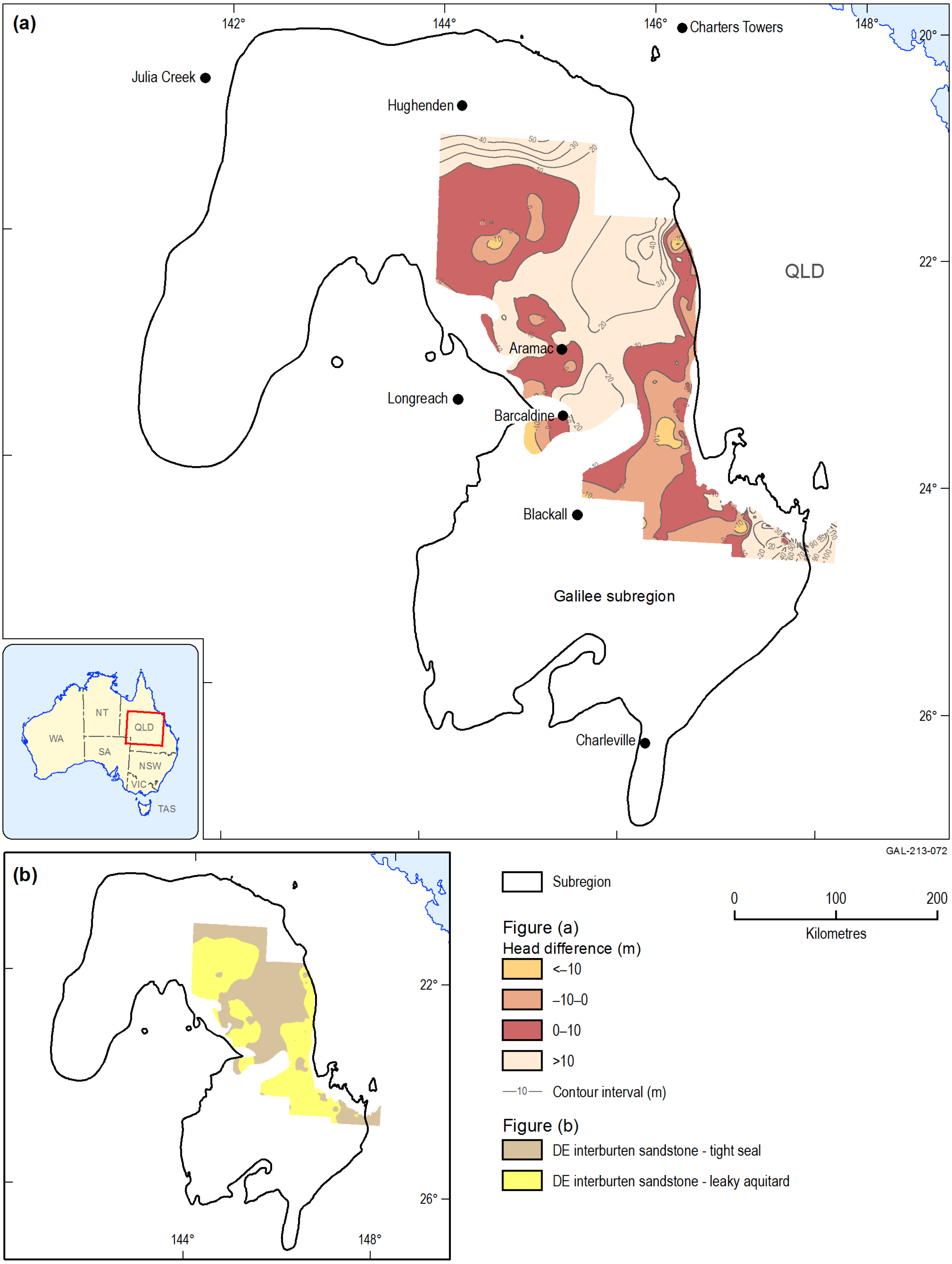


**Figure 82 (a) Head difference between BC2 and BC3 partial aquifer. Positive values indicate areas where the head in BC2 is higher than that in BC3. (b) Seal characteristics of the DE interburten sandstone aquitard**

Data: Bioregional Assessment Programme (Dataset 17)

#### *2.1.3.2.4.6 BC3 partial aquifer – Joe Joe Group aquitard head difference*

Figure 83a shows the (corrected) head difference between the BC3 partial aquifer of the upper Permian coal measures and the Joe Joe Group aquitard. This can only be calculated where the BC3 partial aquifer overlies the Joe Joe Group aquitard and where data exists. Negative values are areas where the head in the Joe Joe Group is higher than the head in BC3, and this condition applies over most of the mapped area. While there is a potential for vertical upwards flow, leakage is excluded by the tight seal afforded by the Joe Joe Group aquitard (Jochmus Formation).
Figure 83b shows an area on the western margin, and a smaller one on the eastern margin, where the Joe Joe Group aquitard appears to be leaky.

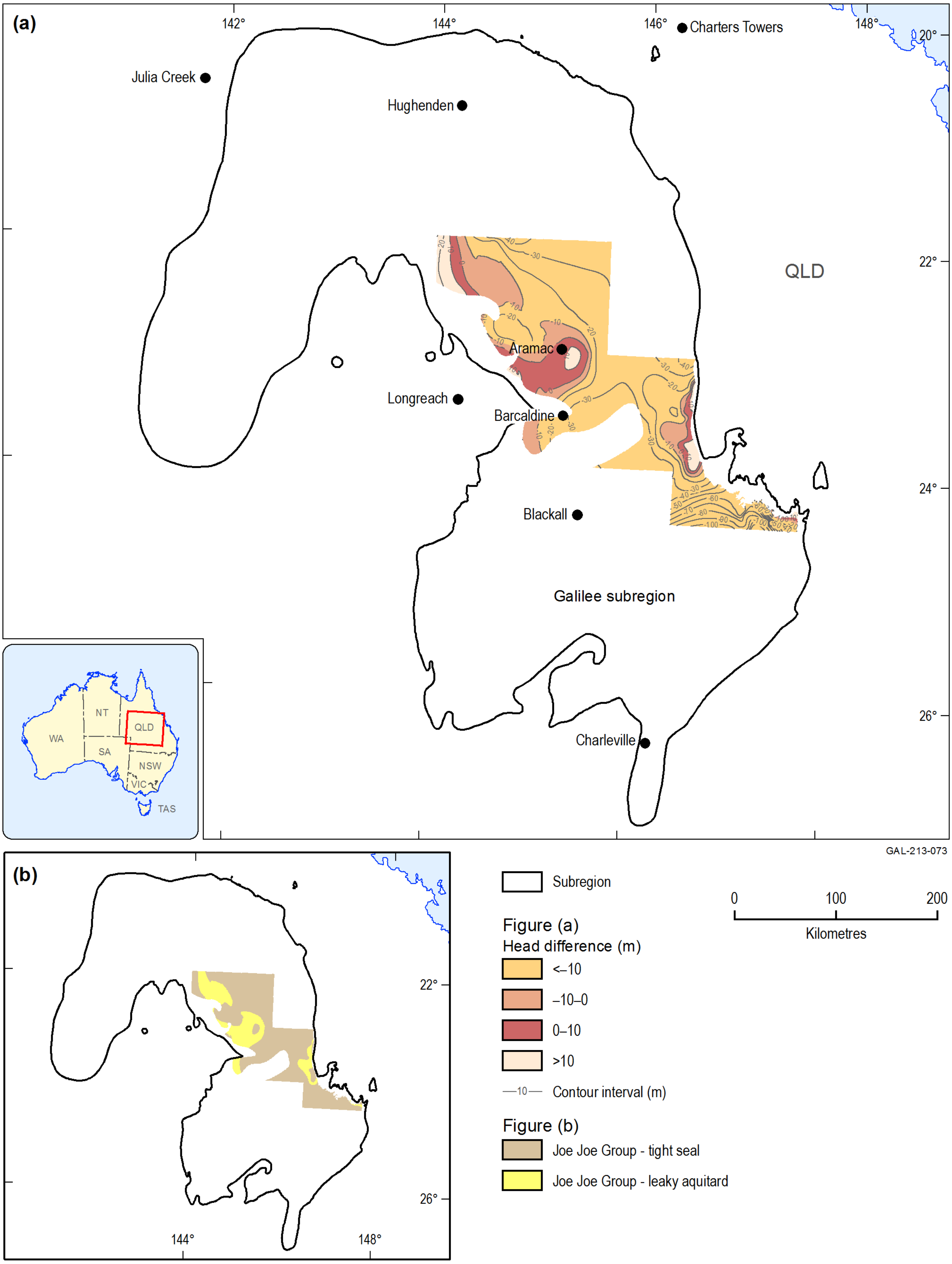


**Figure 83 (a) Head difference between BC3 partial aquifer and Joe Joe Group aquitard. Negative values indicate areas where the head in the Joe Joe Group is higher than that in BC3. (b) Seal characteristics of the Joe Joe Group aquitard**

Data: Bioregional Assessment Programme (Dataset 17)

## 2.1.3.2.5 Groundwater recharge and discharge

### ***2.1.3.2.5.1 Recharge***

**Cenozoic groundwater system**

Limited information is available to estimate recharge to the Cenozoic system. Bleakley et al. (2014) documents information available in environmental impact statements, which form the basis for the estimated *Kh* and recharge values, shown in Figure 84. The recharge rate in the Quaternary alluvium is thought to be an order of magnitude higher than that of the Cenozoic sediments and is likely to be in the order of 5 mm/year.

The low recharge rate of 0.2 mm/year in the Cenozoic unconsolidated sediments has been assigned based on the impedance to vertical infiltration by a dense, plastic, clay layer, 10 to 20 m thick, which is likely to be present throughout much of the area north of Barcaldine (A Bleakley, 2015, pers. comm.). This clay is well exposed in the Alpha test pit where its top lies 10 m below ground surface. At Alpha this layer has been mapped as a green clay, but its colour depends on whether the clay underwent pedogenesis under an oxidising or reducing environment. The clay texture is the critical hydrological property, not its colour. In places where the clay layer is absent, recharge rates for the Cenozoic unconsolidated sediments are considered to be similar to that of the underlying Eromanga Basin and Galilee Basin units (Figure 85). The saturated zone in the Cenozoic sediments may not be laterally continuous throughout the entire eastern zone, indicating poor intra-formational connectivity.

The same low recharge rate in the Cenozoic consolidated sediments is due to the tough silica cement which occurs as secondary infills in voids of the conglomerate and sandstone of the Glendower Formation (the brown areas apart from that on the Mackunda sheet in Figure 84). The latter (which has been incised by the Diamantina River) comprises sandstone of the Old Cork Beds and Mueller Sandstone. Though not of the same degree of silicification as the Glendower Formation, these rocks nonetheless are virtually impervious to water and have very low porosity, hence the very low recharge rate.

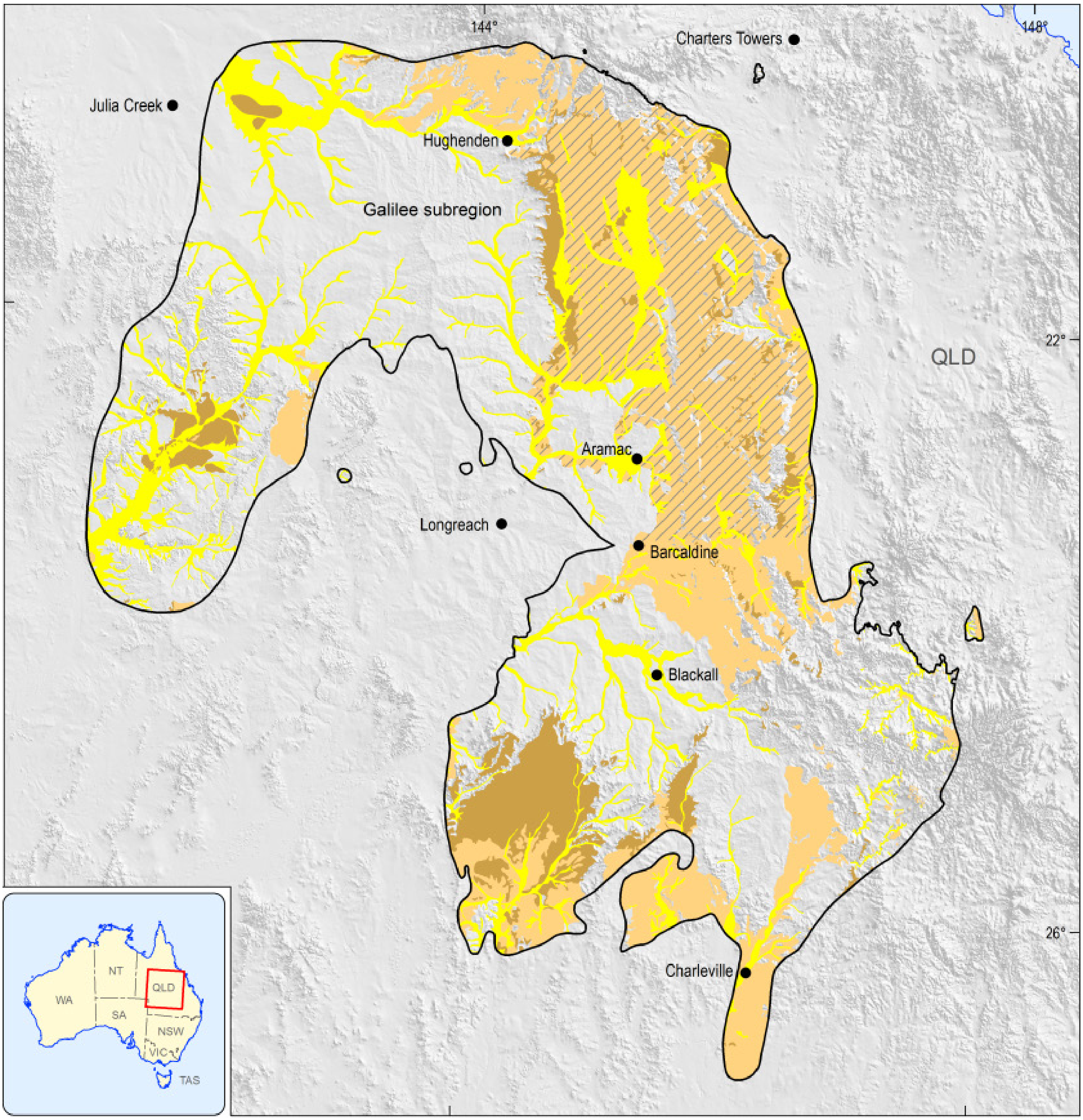


| Formation | Code | Hydraulic conductivity (m/day) | Infiltration rate (mm/year) |
|---|---|---|---|
| Quaternary alluvium | | 2.0 | 5.0 |
| Paleogene–Neogene unconsolidated sediments | | - | - |
| Paleogene–Neogene consolidated sediments | | 0.1 | 0.1 |
| Paleogene-Neogene clay | | 1.0 | 0.2 |

**Figure 84 Spatial distribution of Cenozoic sediments in the Galilee subregion with estimated horizontal hydraulic conductivities and recharge rates**

Areas where clay layer absent - horizontal hydraulic conductivity and recharge have not been estimated.
Data: Bioregional Assessment Programme (Dataset 23)

**Eromanga and Galilee groundwater systems**

Kellett et al. (2003) estimated total groundwater recharge of 21,360 ML/year in the Hooray Sandstone and 25,710 ML/year in the Hutton Sandstone intake beds in the eastern Galilee Basin. These authors used chloride mass balance to derive their recharge rates.

Importantly, the recharge areas used in the recharge flux calculations by Kellet et al. (2003) included both rock outcrop and sub-crop of the aquifers at the intake beds. In the BA programme only the rock outcrop areas of the aquifers have been used in the recharge estimates. The sub-crop areas are assumed to be blanketed by the Cenozoic clay described earlier in Section 2.1.3.2.5. This clay greatly impedes recharge and wherever it occurs, a recharge rate of 0.2 mm/year was applied irrespective of the substrate. Amended diffuse recharge rates in mm/year are shown for all formations in Figure 85. These recharge rates have been calculated using rainfall chloride accession rates outlined in Leaney et al. (2011) and groundwater chloride concentrations from Dataset 1.

Table 22 shows recharge fluxes by hydrogeological unit. As mentioned previously these recharge rates were calculated by chloride mass balance. These recharge estimates do not take into account episodic recharge from point sources such as leakage from river channels into underlying aquifers.

**Table 22 Estimated recharge fluxes by geologic formation for the Galilee subregion**

| Unit | Mean recharge rate (mm/y) | Recharge flux (ML/y) |
|---|---:|---:|
| Wallumbilla Formation | 0.2 | 19,094 |
| Winton-Mackunda formations | 0.17 | 18,685 |
| Hutton Sandstone | 2 | 18,672 |
| Cenozoic alluvium | 5 | 13,500 |
| Hooray Sandstone | 1.5 | 12,252 |
| Clematis Group | 2 | 10,940 |
| Moolayember Formation | 0.3 | 3,754 |
| Injune Creek Group | 0.5 | 2,850 |
| Upper Permian coal measures | 0.2 | 611 |
| Rewan Group | 0.1 | 316 |
| Joe Joe Group | 0.1 | 305 |
| Total | na | 100,979 |

na = not applicable
Data: Bioregional Assessment Programme (Dataset 26)

The surprising and comparatively high recharge flux for the Wallumbilla Formation is due to the large area of outcrop (97,624 km$^2$) and to the low chloride concentrations in bores on the Muttaburra, Longreach, Tangorin, Richmond and Julia Creek 1:250,000 sheets.

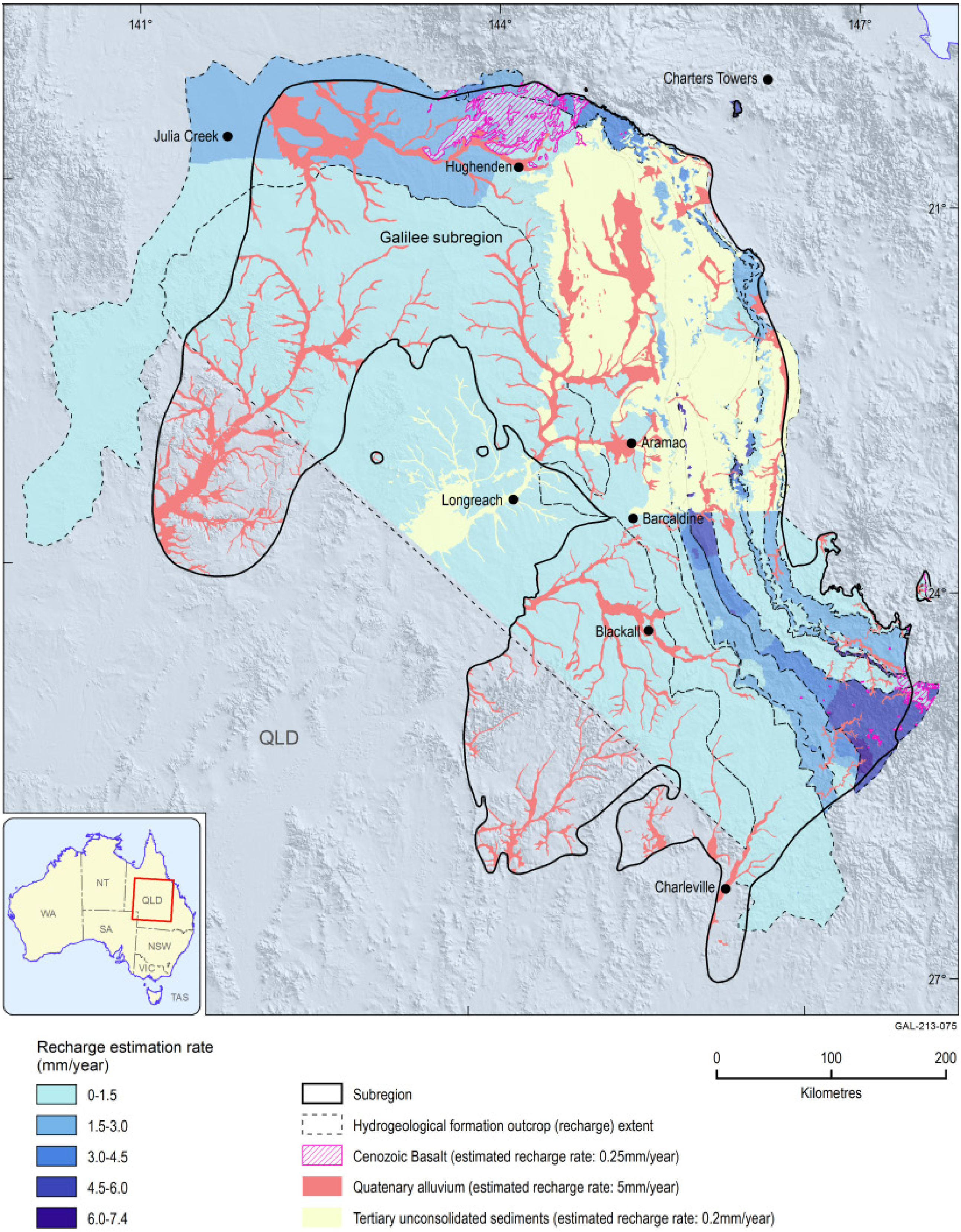


**Figure 85 Estimated recharge rates in the Galilee subregion by formation. Recharge rates estimated by chloride mass balance**

Data: Bioregional Assessment Programme (Dataset 23, Dataset 24)

Recharge to the Winton-Mackunda formations occurs over its entire area of outcrop, but the recharge rate is not uniform. In many places, the Winton-Mackunda formations are blanketed by a thick layer of saprolite and the lower horizon of the weathered profile greatly impedes downward infiltration of the wetting front and therefore also recharge. The Winton-Mackunda formations exhibit groundwater mounding in some areas, a characteristic more typical of a local flow system rather than a regional one. These mounds occur in those places where the saprolite has been eroded exposing relatively unweathered (fresh) rock. Recharge rates in such areas are about 1 mm/year, but in places where the saprolite cover has been preserved, recharge rates are considerably lower, of the order of 0.1 mm/year. Although the Winton-Mackunda formations have the largest area of occurrence (109,911 $km^2$), its recharge flux is only the second highest because of its low recharge rate.

The estimated recharge fluxes presented in Table 22 are lower than those estimated by Kellett et al. (2003) – only 73% of that estimated for the Hutton Sandstone and 57% for the Hooray Sandstone – for reasons explained earlier.

The recharge fluxes for the Rewan Group, upper Permian coal measures, and the Joe Joe Group, are particularly low.

**Discharge**

Artificial discharge includes groundwater pumping from bores, or discharge from free flowing artesian wells. For the Hooray and Hutton sandstones, flow from controlled or uncontrolled artesian water wells is by far the largest proportion of discharge from these aquifers (approximately 17,000 ML/year from the Hooray Sandstone aquifer and approximately 23,000 ML/year from the Hutton Sandstone (see companion product 1.5 for the Galilee subregion (Evans et al., 2015)). The remainder of the groundwater flux in these two aquifers, except for a minor component of flow to rejected recharge springs in the Barcaldine Springs complex (Figure 86), is ultimately naturally discharged in springs, salt lakes or vertical leakage in the south-west Eromanga Basin.

Natural groundwater discharge occurs from several spring supergroups in the Galilee subregion. Fensham et al. (2016) provides detail on spring supergroups and spring complexes that occur within the Galilee subregion (spring complexes are clumped together to define spring supergroups). The Barcaldine Springs complex (Figure 86) consists of over 300 individual springs (Fensham et al., 2016). The springs are concentrated in two lines along the flanks of the Eromanga Basin margin, which is where outcrop occurs of the Ronlow beds, Hooray Sandstone and Hutton Sandstone. The source aquifers for these springs are primarily the Hooray Sandstone aquifer, Hutton Sandstone aquifer and the Ronlow beds aquifer (which is mainly a Hooray Sandstone equivalent).

The Doongmabulla Springs complex (Figure 86) lies about 10 km west of the proposed Carmichael Coal Mine. The Doongmabulla Springs complex includes over 180 vents that feed some relatively large wetlands (Fensham et al., 2016). Some of the more well-known springs are called Joshua, Moses and Little Moses (the Moses springs includes more than 65 individual vents). The source aquifer is likely to be the Clematis Group aquifer. The Carmichael River receives outflow from the Doongmabulla Springs complex and baseflow from the Clematis Group aquifer.

Fensham et al. (2016) considers the upper Permian coal measures (specifically the Colinlea Sandstone) to be the likely source aquifer for the Mellaluka Springs complex, Lignum Springs and Albro Springs (Figure 86). Whilst the Dunda beds (part of the Rewan Group) is likely to be the source aquifer for Hector Springs, Greentree Springs and Hunter Springs (Fensham et al., 2016).

With the notable exception of the Clematis Group aquifer with groundwater pumping of about 1400 ML/year, artificial groundwater discharge by pumping from wells is negligible for the Galilee Basin units. However this is set to change when dewatering of the upper Permian coal measures begins due to the proposed coal resource development. Further information regarding artificial discharge is reported in companion product 2.6.2 (Peeters et al., 2018) and product 2.5 (Karim et al., 2018a) for the Galilee subregion.

As mentioned previously, a component of flow in the upper Permian coal measures partial aquifer and the Joe Joe Group aquitard discharges eastwards towards the Belyando River valley, but the majority of the groundwater flux in these formations is towards the west. It appears that the groundwater discharge from these formations is dominantly vertical upwards leakage into the overlying formations at the western margins of the Galilee Basin where the strata pinch out. This also appears to be the case for the Triassic formations of the Galilee Basin sequence.

Further discussion on types of discharge from groundwater systems and springs in the Galilee Basin is provided in Section 2.3.2 of companion product 2.3 (Evans et al., 2018). Companion Product 2.7 for the Galilee subregion (Ickowicz et al., 2018) and companion product 3-4 (Lewis et al., 2018) provide further detail on the hydrogeology and ecology of the Doongmabulla Springs complex, as well as other springs with source aquifers in the Galilee Basin.

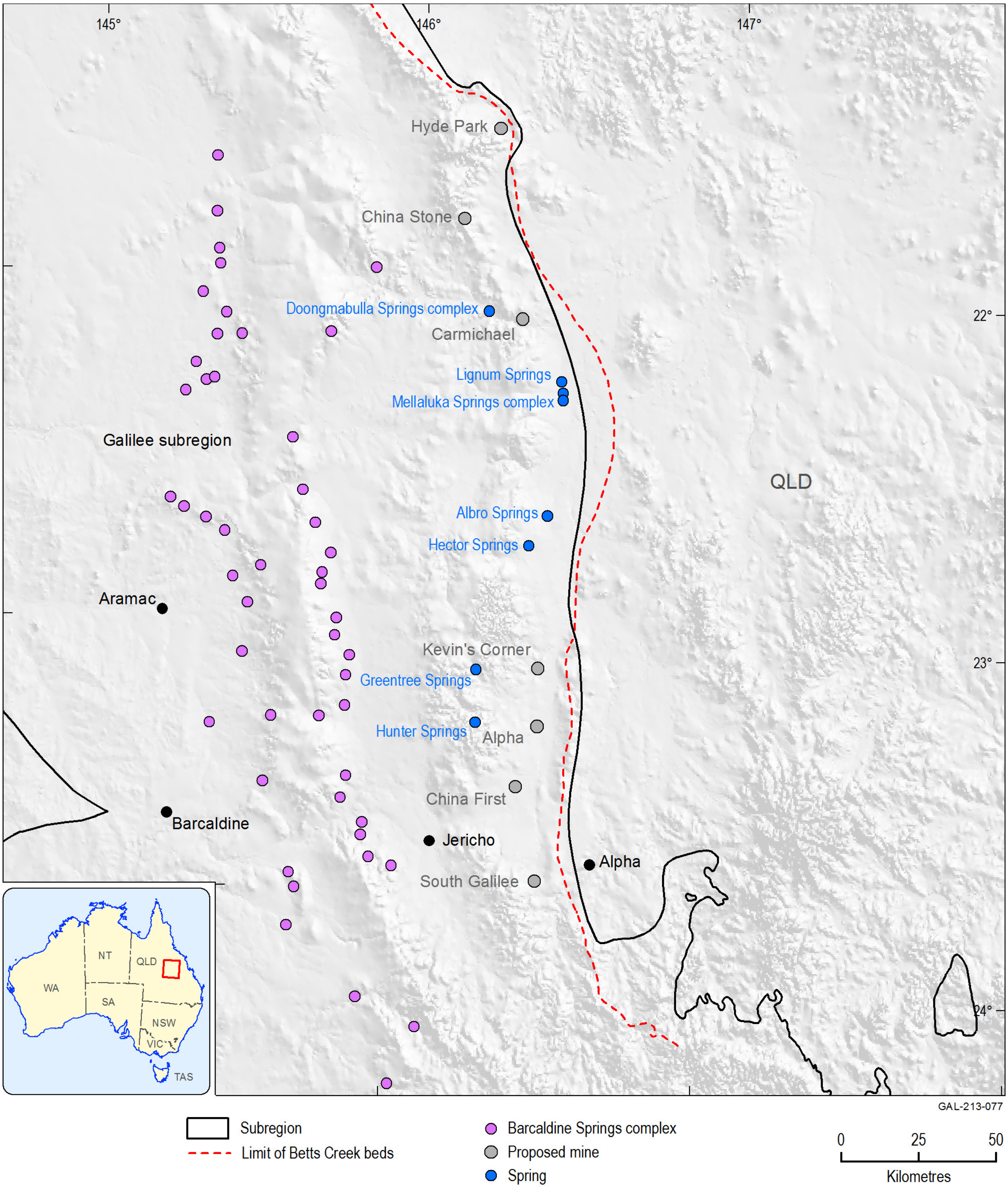


**Figure 86 Springs near the eastern margin of the Galilee subregion**

Data: Queensland Herbarium, Environmental Protection Agency (Dataset 27), Bioregional Assessment Programme (Dataset 28, Dataset 29), Geoscience Australia (Dataset 30)

### *2.1.3.3 Gaps*

A major data gap in the Galilee subregion is the lack of reliable bore screen information for determining the source aquifer. The majority of groundwater bores in the Galilee subregion do not have screen information to determine from which aquifer a particular bore is drawing water from. Therefore this analysis has been limited to only those bores that have sufficient information. Accurately determining a particular bores source aquifer is vital for interpreting both hydrochemistry and water level data.

#### 2.1.3.3.1 Hydrochemistry

The hydrochemistry data used in characterising the groundwater of the Galilee subregion are archival data collected over several decades and therefore there are considerable uncertainties associated with it. Many samples from the initial sample set had to be excluded from the analysis due to insufficient stratigraphic data. Without stratigraphic information, any other information associated with a groundwater sample is meaningless.

Additionally, the maximum uncertainty selected for use in filtering the data was relatively large: ± 10%. Commonly for regional hydrochemical studies ± 5% or better is considered best practice. An error of ± 10% was deemed acceptable to ensure a large number of samples were available for all stratigraphic units, and that there was sufficient spatial coverage in each unit to build a regional picture of hydrochemistry. However, it is possible that this level of uncertainty has obscured some relationships between different analytes in the dataset.

Trace element data are highly variable in the dataset, with no data for many important trace elements in several of the hydrogeologic units. Most trace elements are analysed in only a small number of hydrogeologic units, usually the Hutton-Precipice grouping and Westbourne-Birkhead grouping.

The GAB is a very large and complex groundwater system. A regional overview of the major aquifers in the Galilee subregion has been presented, but further targeted data collection and analysis would refine the conceptual understanding of groundwater hydrodynamics in the subregion, and assist in a more rigorous assessment of aquitard integrity. Further statistical analysis (e.g. cluster analysis of multiple hydrogeologic units) would assist in identifying where inter-aquifer mixing could be occurring, and differentiate regions based on the dominant chemical processes. Additional to major ion chemistry, groundwater isotopic data would greatly improve our understanding of hydrologic processes in the subregion.

In the case of aquifers with similar major ion chemistry, it is difficult to determine whether similarities are the result of aquifer connectivity, or similarities in aquifer composition or chemical processes. Isotopic analyses would help distinguish where similar chemical trends are the result of hydraulic connectivity, or similarities in aquifer material and/or recharge processes. Isotopic data may also help to identify water sources to aquifers or surface features (e.g. provide stronger evidence for which aquifer feeds a spring system), as well as further constrain residence times and flow rates. Potential isotopic systems are $^{87}Sr$:$^{86}Sr$, $_{2}H$ and $^{18}O$, $^{13}C$, $^{36}Cl$, and $_{4}He$:$_{3}He$. Currently, there are limited isotopic data available for the Eromanga Basin sequence (see Moya et al. (2015) for a summary), and almost none available for the Galilee Basin sequence. Samples have been collected from both Eromanga and Galilee Basin aquifers by Queensland University of Technology but remain unanalysed. Analysis of these samples is warranted, but is beyond the current scope of the BA Programme.

In addition to uncertainties in the major ion data, very limited information on reduction/oxidation (redox) conditions is available in the dataset. For this reason redox chemistry was omitted from this regional overview, however, a sound understanding of redox conditions is necessary to understand the chemical changes that may occur if different groundwater bodies mix, making it essential information to comment on the potential impacts of inter-aquifer leakage.

#### 2.1.3.3.2 Water level mapping

Uneven spatial distribution of measurement points across the subregion introduces uncertainty to the interpreted water level mapping. In some cases mapping has relied on sparsely distributed measurement points, particularly in the western, deeper portions of the Galilee and Eromanga units. In the case of the Betts Creek beds (upper Permian coal measures), water level mapping for the central and western portion of these units is based solely upon drill stem pressure tests which are inherently less reliable than actual water level measurements.

While the most recent available water level data were utilised to produce the water level maps, the extent of recent measurements (i.e. over the last ten years) is limited. In many cases historical water level measurements, which may have changed, have been used to approximate current levels.

#### 2.1.3.3.3 Water level trends

Some anomalous hydrographs introduce uncertainty to the data. One bore in the Hooray Sandstone showing a 40+ m rise over six years is not located nearby any bores sealed in the GABSI program, yet there seems no other explanation for the rapid increase in water level than nearby artesian bores being sealed. If there are sealed bores missing from the records available to us, interpretations of trends observed in other bores may be incorrect.

Record lengths are highly variable between bores, even after removing bores with less than two years of data and bores with records finishing before 1997. This makes it difficult to compare the trends observed in different bores; a trend which is statistically significant over a 5 year time frame may seem less clear over 20 years. The magnitude in change of water level is also affected by the length of the record. Bores with very long records (back to the 1950s or 1960s) tend to show changes in water levels of several metres, while records beginning in the last 20 years show much smaller changes.

There are only a small number of nested piezometers meaning comparisons of water level trends between different aquifers are limited. This is unfortunate as comparing time series data for different aquifers at the same location is one of the best ways to investigate potential connectivity between hydrostratigraphic units. Additionally, there are no nested bores in the artesian area of the subregion, meaning connectivity can only be investigated this way in the eastern part of the subregion.

## *References*


Appelo CAJ and Postma D (2005) Geochemistry, groundwater and pollution (2nd edition). AA Balkema Publishers, Leiden, Netherlands.

Bleakley A, Larsen D and McKay A (2014) Groundwater systems in the Eastern Galilee Basin. Background Paper – April 2014. Queensland Department of Natural Resources and Mines, Report, Brisbane

Burra A, Esterle JS and Golding SD (2014) Coal seam gas distribution and hydrodynamics of the Sydney Basin, NSW. Australia Australian Journal of Earth Sciences 61, 427–451.

DNRM (2013) Groundwater Database, Metadata, Data Dictionary & Standards Summary. Queensland Department of Natural Resources and Mines, Queensland Government, Brisbane.

DNRM (2015) Condamine alluvium connectivity with the Walloon coal measures. A hydrogeological investigation report. Queensland Department of Natural Resources and Mines, Queensland Government, Brisbane.

Draper JJ (2002) Geology of the Cooper and Eromanga Basins, Queensland. Queensland Minerals and Energy Review Series 1, 7–29.

Evans T, Tan KP, Magee J, Karim F, Sparrow A, Lewis S, Marshall S, Kellett J and Galinec V (2014) Context statement for the Galilee subregion. Product 1.1 from the Lake Eyre Basin Bioregional Assessment. Department of the Environment, Bureau of Meteorology, CSIRO and Geoscience Australia, Australia. Viewed 25 November 2015, http://data.bioregionalassessments.gov.au/product/LEB/GAL/1.1.

Evans T, Karim F, Cassel R and Harris-Pascal C (2015) Current water accounts and water quality for the Galilee subregion. Product 1.5 for the Galilee subregion from the Lake Eyre Basin Bioregional Assessment. Department of the Environment, Bureau of Meteorology, CSIRO and Geoscience Australia, Australia. Viewed 25 November 2015, http://data.bioregionalassessments.gov.au/product/LEB/GAL/1.5.

Evans T, Pavey C, Cassel R, Ransley T, Sparrow A, Kellett J, Galinec V, Dehelean A, Bell J, Caruana L and Kilgour P (2018) Conceptual modelling for the Galilee subregion. Product 2.3 for the Galilee subregion from the Lake Eyre Basin Bioregional Assessment. Department of the Environment and Energy, Bureau of Meteorology, CSIRO and Geoscience Australia, Australia. http://data.bioregionalassessments.gov.au/product/LEB/GAL/2.3.

Fensham RJ, Silcock JL, Laffineur, B and MacDermott HJ (2016) Lake Eyre Basin springs assessment project (LEBSA): hydrogeology, cultural history and biological values of springs in the Barcaldine, Springvale and Flinders River supergroups, Galilee Basin springs and Tertiary springs of western Queensland. Report to the Office of Water Science, Department of Science, Information Technology and Innovation, Brisbane. Viewed 13 September 2017, https://publications.qld.gov.au/dataset/lake-eyre/resource/c5d1813b-73a4-4e05-aa86-39a8ed3045fb.

Gravestock DI, Alexander EM, Morton JGG and Sun X (1998) Reservoirs and seals. In: Gravestock DI, Hibburt JE, Drexel JF (Eds) Petroleum Geology of South Australia. Cooper Basin, v4, Department of Primary Industry and Resources, South Australia, Report Book 98/9, 159–181.

Herczeg AL, Torgersen T, Chivas AR and Habermehl MA (1991) Geochemistry of ground waters from the Great Artesian Basin. Australia Journal of Hydrology 126, 225–245.

Hortle A, Otto C and Underschultz J (2013) A quality control system to reduce uncertainty in interpreting formation pressures for reservoir and basin pressure system analysis. Journal of Petroleum Geology 36(2), 163–178.

Ickowicz A, Hosack G, Dambacher J, Pavey C, Hayes K, O'Grady A, Evans T, Henderson BL and Holland KL (2018) Receptor impact modelling for the Galilee subregion. Product 2.7 for the Galilee subregion from the Lake Eyre Basin Bioregional Assessment. Department of the Environment and Energy, Bureau of Meteorology, CSIRO and Geoscience Australia, Australia. http://data.bioregionalassessments.gov.au/product/LEB/GAL/2.7.

Karim F, Hostetler S and Evans T (2018a) Water balance assessment for the Galilee subregion. Product 2.5 for the Galilee subregion from the Lake Eyre Basin Bioregional Assessment. Department of the Environment and Energy, Bureau of Meteorology, CSIRO and Geoscience Australia, Australia. http://data.bioregionalassessments.gov.au/product/LEB/GAL/2.5.

Karim F, Viney NR, Wang B, Peeters LJM, Zhang YQ, Marvanek SP, Shi X, Yang A and Buettikofer H (2018b) Surface water numerical modelling for the Galilee subregion. Product 2.6.1 for the Galilee subregion from the Lake Eyre Basin Bioregional Assessment. Department of the Environment and Energy, Bureau of Meteorology, CSIRO and Geoscience Australia, Australia. http://data.bioregionalassessments.gov.au/product/LEB/GAL/2.6.1.

Kellett JR, Ransley TR, Coram J, Jaycock J, Barclay DF, McMahon GA, Foster LM and Hillier JR (2003) Groundwater recharge in the Great Artesian Basin intake beds, Queensland. Department of Natural Resources and Mines (Queensland), Technical Report.

Leaney F, Crosbie R, O'Grady A, Jolly I, Gow L, Davies P, Wilford J and Kilgour P (2011) Recharge and discharge estimation in data poor areas: Scientific reference guide. CSIRO: Water for a Healthy Country National Research Flagship.

Lewis S, Evans T, Pavey C, Holland KL, Henderson BL, Kilgour P, Dehelean A, Karim F, Viney NR, Post DA, Schmidt RK, Sudholz C, Brandon C, Zhang YQ, Lymburner L, Dunn B, Mount R, Gonzales D, Peeters LJM, O' Grady A, Dunne R, Ickowicz A, Hosack G, Hayes KR, Dambacher J, Barry S (2018) Impact and risk analysis for the Galilee subregion. Product 3-4 for the Galilee subregion from the Lake Eyre Basin Bioregional Assessment. Department of the Environment and Energy, Bureau of Meteorology, CSIRO and Geoscience Australia, Australia. http://data.bioregionalassessments.gov.au/product/LEB/GAL/3-4.

Moya CE, Raiber M, Taulis M, and Cox ME (2015) Hydrochemical evolution and groundwater flow processes in the Galilee and Eromanga basins, Great Artesian Basin, Australia: A multivariate statistical approach. Science of the Total Environment 508, 411–426.

Peeters L, Ransley T, Turnadge C, Kellett J, Harris-Pascal C, Kilgour P and Evans T (2018) Groundwater numerical modelling for the Galilee subregion. Product 2.6.2 for the Galilee subregion from the Lake Eyre Basin Bioregional Assessment. Department of the Environment and Energy, Bureau of Meteorology, CSIRO and Geoscience Australia, Australia. http://data.bioregionalassessments.gov.au/product/LEB/GAL/2.6.2.

Post V, Kooi H and Simmons C (2007) Using hydraulic head measurements in variable-density groundwater flow analyses. Groundwater 45(6), 664–671.

Radke BM, Ferguson J, Cresswell RG, Ransley TR and Habermehl MA (2000) Hydrochemistry and implied hydrodynamics of the Cadna-owie – Hooray Aquifer, Great Artesian Basin, Australia. Bureau of Rural Sciences, Canberra.

Ransley TR and Smerdon BD (2012) Hydrostratigraphy, hydrogeology and system conceptualisation of the Great Artesian Basin. A report to the Australian Government from the CSIRO Great Artesian Basin Water Resource Assessment. CSIRO Water for a Healthy Country Flagship, Australia, Canberra. Viewed 12 April 2016, https://publications.csiro.au/rpr/download?pid=csiro:EP132693&dsid=DS5.

Singh A and Singh AK (2013) ProUCL Version 5.0.00 technical guide: statistical software for environmental applications for data sets with and without nondetect observations. U.S. Environmental Protection Agency office of research and development, USA Washington DC, dated September 2013. Viewed 12 April 2016, https://www.epa.gov/sites/production/files/2015-03/documents/proucl_v5.0_tech.pdf.

Vine RR and Doutch HF (1972) 1:250,000 Geological Series – Explanatory Notes; Galilee, Queensland. Sheet SF/55-10. Bureau of Mineral Resources, Canberra.

### *Datasets*

Dataset 1 Bioregional Assessment Programme (2016) Hydrochemistry analysis of the Galilee subregion. Bioregional Assessment Derived Dataset. Viewed 11 April 2016, http://data.bioregionalassessments.gov.au/dataset/fd944f9f-14f6-4e20-bb8a-61d1116412ec.

Dataset 2 Queensland Department of Natural Resources and Mines (2014) QLD Department of Natural Resources and Mines Groundwater Database Extract 20142808. Bioregional Assessment Source Dataset. Viewed 16 November 2016, http://data.bioregionalassessments.gov.au/dataset/a5c5cbdb-1152-43f7-9533-a123027b7ce1.

Dataset 3 Geological Survey of Queensland (2014) Queensland petroleum exploration data - QPED. Bioregional Assessment Source Dataset. Viewed 16 November 2016, http://data.bioregionalassessments.gov.au/dataset/cb357721-bf22-45c9-a82e-828807912dd4.

Dataset 4 Queensland Department of Employment, Economic Development and Innovation (2014) QDEX well completion reports (WCR) - Galilee v01. Bioregional Assessment Source Dataset. Viewed 16 November 2016, http://data.bioregionalassessments.gov.au/dataset/370a30da-54e3-4b58-a983-9c655b14ba3a.

Dataset 5 Queensland Department of State Development, Infrastructure and Planning (2014) Carmichael Coal Mine and Rail Project Environmental Impact Statement. Bioregional Assessment Source Dataset. Viewed 16 November 2016, http://data.bioregionalassessments.gov.au/dataset/2a595f74-aae6-4d83-9cd7-1459247d751a.

Dataset 6 Waratah Coal Pty Ltd (2014) China First Galilee Coal Project Environmental Impact Assessment. Bioregional Assessment Source Dataset. Viewed 11 April 2016, http://data.bioregionalassessments.gov.au/dataset/430086cc-9cc2-4cad-a21d-ca3eb920bee4.

Dataset 7 Queensland Department of State Development, Infrastructure and Planning (2014) Kevin's Corner Project Environmental Impact Statement. Bioregional Assessment Source Dataset. Viewed 16 November 2016, http://data.bioregionalassessments.gov.au/dataset/e8293ba3-f5bb-42ef-9704-be7beb19d5f0.

Dataset 8 AMCI (Alpha) Pty Ltd (2014) South Galilee Coal Project Environmental Impact Statement. Bioregional Assessment Source Dataset. Viewed 11 April 2016, http://data.bioregionalassessments.gov.au/dataset/683fa317-48ba-4a47-a0cc-2a1015708885d.

Dataset 9 Bioregional Assessment Programme (2014) QLD Dept of Natural Resources and Mines, Groundwater Entitlements linked to bores and NGIS v4 28072014. Bioregional Assessment Derived Dataset. Viewed 11 April 2016, http://data.bioregionalassessments.gov.au/dataset/b1ba5370-2c60-485f-9620-ddad39498999.

Dataset 10 Geoscience Australia (2011) Geoscience Australia, 1 second SRTM Digital Elevation Model (DEM). Bioregional Assessment Source Dataset. Viewed 11 April 2016, http://data.bioregionalassessments.gov.au/dataset/9a9284b6-eb45-4a13-97d0-91bf25f1187b.

Dataset 11 Bioregional Assessment Programme (2016) Galilee updated hydrochemistry xls. Bioregional Assessment Derived Dataset. Viewed 16 November 2016, http://data.bioregionalassessments.gov.au/dataset/bda25298-b4b6-465d-8cc4-0ff22dd538a4.

Dataset 12 Bioregional Assessment Programme (2016) Galilee hydrogeological formation subcrop extents. Bioregional Assessment Derived Dataset. Viewed 05 September 2016, http://data.bioregionalassessments.gov.au/dataset/0d96dcb9-a392-4d06-8705-08dde59b4d1e.

Dataset 13 Bioregional Assessment Programme (2016) Galilee updated hydrochemistry points. Bioregional Assessment Derived Dataset. Viewed 08 September 2016, http://data.bioregionalassessments.gov.au/dataset/5570fc4a-2f30-434f-b17d-8a2ad2b017b9.

Dataset 14 Geoscience Australia (2013) Great Artesian Basin major geological structural elements (GABWRA). Bioregional Assessment Source Dataset. Viewed 05 September 2016, http://data.bioregionalassessments.gov.au/dataset/8dbe0a37-408a-4458-b4cb-fb896b830cc5.

Dataset 15 Bioregional Assessment Programme (2015) GAL Group 2 contour data. Bioregional Assessment Derived Dataset. Viewed 11 April 2016, http://data.bioregionalassessments.gov.au/dataset/803b0f5c-acb8-4adf-9ae1-3cb385ed4061.

Dataset 16 Bioregional Assessment Programme (2015) Galilee bore water levels v01. Bioregional Assessment Derived Dataset. Viewed 17 November 2016, http://data.bioregionalassessments.gov.au/dataset/2f8fe7e6-021f-4070-9f63-aa996b77469d.

Dataset 17 Bioregional Assessment Programme (2015) Potentiometric head difference v01. Bioregional Assessment Derived Dataset. Viewed 11 April 2016, http://data.bioregionalassessments.gov.au/dataset/6c212a1a-658c-41de-92a7-6054349a848b.

Dataset 18 Bioregional Assessment Programme (2015) Ronlow beds partitioning. Bioregional Assessment Derived Dataset. Viewed 11 April 2016, http://data.bioregionalassessments.gov.au/dataset/d2f60560-eda7-417d-86ca-1d29ce994edd.

Dataset 19 Bioregional Assessment Programme (2015) Galilee groundwater bore and petroleum well data. Bioregional Assessment Derived Dataset. Viewed 17 November 2016, http://data.bioregionalassessments.gov.au/dataset/01130a0e-782a-4ec2-b8c8-ac6d9a2f5337.

Dataset 20 Bioregional Assessment Programme (2016) Galilee water level analysis. Bioregional Assessment Derived Dataset. Viewed 12 April 2016, http://data.bioregionalassessments.gov.au/dataset/5ced7ae4-1a3d-4d44-84cc-4238b42b7374.

Dataset 21 Bioregional Assessment Programme (2014) Galilee Groundwater Model, hydrogeological formation recharge (Outcrop) extents v01. Bioregional Assessment Derived Dataset. Viewed 17 November 2016, http://data.bioregionalassessments.gov.au/dataset/b0f0385e-c456-4fa4-9cdb-a5441cca407b.

Dataset 22 Bioregional Assessment Programme (2015) Galilee water level trend. Bioregional Assessment Derived Dataset. Viewed 12 April 2016, http://data.bioregionalassessments.gov.au/dataset/df5da9f1-afdd-4ec8-9c9a-0fc5a23526eb.

Dataset 23 Bioregional Assessment Programme (2014) Galilee - Alluvium and Cenozoic 1M surface Geology. Bioregional Assessment Derived Dataset. Viewed 12 April 2016, http://data.bioregionalassessments.gov.au/dataset/552d5323-bb28-43e9-b137-8dd2d81f7d3c.

Dataset 24 Bioregional Assessment Programme (2015) Merged Galilee model recharge estimates chloride mass balance v02. Bioregional Assessment Derived Dataset. Viewed 17 November 2016, http://data.bioregionalassessments.gov.au/dataset/b892b063-4df9-4199-80c8-2ed4a1077d5b.

Dataset 25 Bioregional Assessment Programme (2015) Galilee Recharge Cenozoic Alluvium Regions v01. Bioregional Assessment Derived Dataset. Viewed 06 September 2016, http://data.bioregionalassessments.gov.au/dataset/3c8e66e7-6a15-47ce-853b-bbe38435d28f.

Dataset 26 Bioregional Assessment Programme (2015) Galilee model recharge estimates: chloride mass balance v02. Bioregional Assessment Derived Dataset. Viewed 17 November 2016, http://data.bioregionalassessments.gov.au/dataset/d42a8497-9d67-42ad-9e7d-70a8d519875f.

Dataset 27 Queensland Herbarium, Environmental Protection Agency (2006) Springs of Queensland - Distribution and Assessment (Version 4.0). Bioregional Assessment Source Dataset. Viewed 12 April 2016, http://data.bioregionalassessments.gov.au/dataset/82749253-f555-47d9-ba76-7140c55b2a65.

Dataset 28 Bioregional Assessment Programme (2013) Asset list for Galilee - 20140605. Bioregional Assessment Derived Dataset. Viewed 12 April 2016, http://data.bioregionalassessments.gov.au/dataset/6968b11f-9912-42ca-8536-00cde75e75d9.

Dataset 29 Bioregional Assessment Programme (2014) Coal deposits and projects in the Galilee Basin. Bioregional Assessment Derived Dataset. Viewed 06 September 2016, http://data.bioregionalassessments.gov.au/dataset/784b7534-f2ae-426b-a60c-345d5dd08332.

Dataset 30 Geoscience Australia (2013) OZMIN Mineral Deposits Database. Bioregional Assessment Source Dataset. Viewed 06 September 2016, http://data.bioregionalassessments.gov.au/dataset/34247a24-d3cf-4a98-bb9d-81671ddb99de.

## 2.1.4 Surface water hydrology and water quality


### Summary

The Galilee subregion and its neighbouring areas contain 36 streamflow gauges as listed in companion product 1.1 for the Galilee subregion (Evans et al., 2014). This product describes data from 15 of them that were used for hydrological model calibration or assessment of impacts due to the coal resource development pathway (CRDP). The source of streamflow data, site information, data period and quality of the flow records are summarised in Section 2.1.4.1.

Analysis of the streamflow records was reported in the contextual information in companion product 1.1 for the Galilee subregion (Evans et al., 2014). The analyses included annual and monthly flow characteristics and baseflow component based on available flow records for each gauging station. No additional analyses have been undertaken in this product other than presenting a summary of the quality of the observed data. The period of record for some gauges is relatively short and may not represent the climate variability of the catchment well. Details of flow analyses are presented in companion product 1.1 (Evans et al., 2014) and companion product 2.6.1 for the Galilee subregion (Karim et al., 2018).

Water quality data for the surface water systems in the Galilee subregion is very limited in terms of data points and number of data. Therefore, no analysis on water quality data is performed other than reporting a summary of selected water quality parameters (e.g. electric conductivity, turbidity) as presented in companion product 1.5 for the Galilee subregion (Evans et al., 2015).


### *2.1.4.1 Observed data*

Daily streamflow data for the gauging stations within and adjacent to the Galilee subregion were obtained from the Department of Natural Resources and Mines (DNRM) of the Queensland Government. Out of 36 gauges, data from 15 gauges were used for hydrological model calibration and CRDP impact assessment (Figure 87). Location, catchment area and data period of the gauging stations are presented in Table 23. The first four (002105, 003204, 003205 and 003302) and last two (915011 and 915013) gauges in Table 23 are located within the Galilee subregion and the rest are in the Burdekin river basin where most of the proposed mining sites are located except one in the Fitzroy river basin (130210). Eight headwater gauges (002105, 003204, 003205, 003302, 120307, 130210, 915011 and 915013) were used for model calibration. Only gauges that have long-term measurements (>20 years from 1980), are currently not impacted by coal mining or coal seam gas or other major extractive industries, have no significant flow regulation (e.g. dams), are not nested, and are located within or close to the Galilee subregion, were selected for model calibration. Eight gauges (120301, 120302, 120303, 120304, 120305, 120307, 120309 and 120310), that were located within the surface water impact modelling domain, were used for model validation. The gauge 120307 (Pentland on Cape River) is common in both model calibration and validation. The majority of these gauges have about 40 years of observed data and the data show strong seasonal and inter-annual variability in streamflow (Figures 44 to 49 in companion product 1.1 for the Galilee subregion (Evans et al., 2014)).

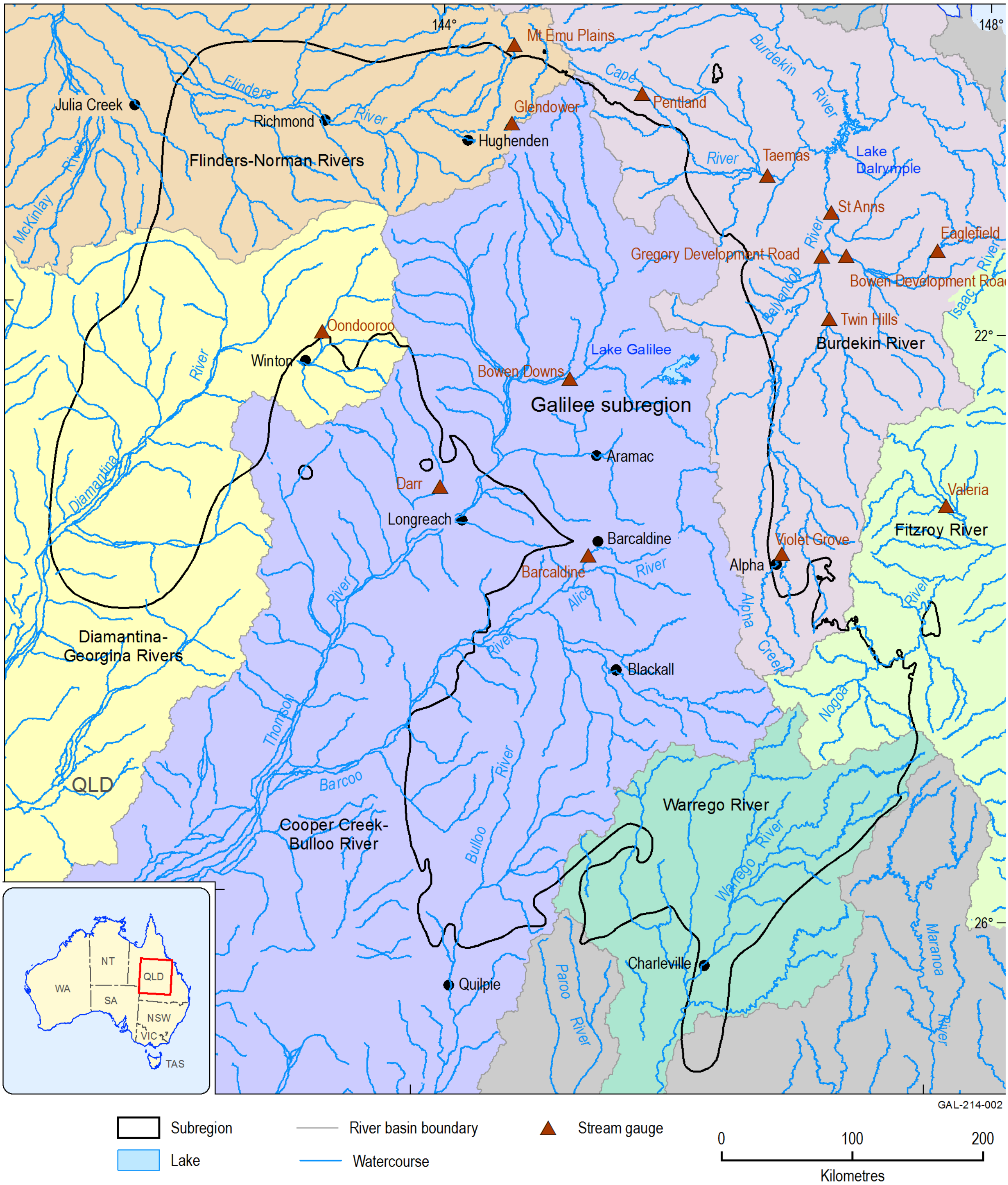


**Figure 87 Galilee subregion showing locations of stream gauges that were used for hydrological model calibration and assessment of impacts due to the coal resource development pathway (CRDP)**

Data: Bureau of Meteorology (Dataset 1)

**Table 23 Gauge information for streamflow data for the Galilee subregion**

| Gauge ID | Gauge name | Catchment area ($km^2$) | Latitude (degree) | Longitude (degree) | Data period |
|---|---|---|---|---|---|
| 002105 | Mills Creek at Oondooroo | 2,642 | –22.177 | 143.164 | 2007–present |
| 003204 | Cornish Creek at Bowen Downs | 22,825 | –22.449 | 145.024 | 1999–present |
| 003205 | Darr River at Darr | 2,700 | –23.216 | 144.081 | 1969–present |
| 003302 | Alice River at Barcaldine | 7,918 | –23.649 | 145.216 | 1967–present |
| 120301 | Belyando River at Gregory Development Road | 35,411 | –21.533 | 146.860 | 1976–present |
| 120302 | Cape River at Taemas | 16,074 | –21.000 | 146.427 | 1968–present |
| 120303 | Suttor River at St Anns | 50,291 | –21.229 | 146.913 | 1967–present |
| 120304 | Suttor River at Eaglefield | 1,915 | –21.450 | 147.714 | 1967–present |
| 120305 | Native Companion Creek at Violet Grove | 4,065 | –23.576 | 146.674 | 1967–present |
| 120307 | Cape River at Pentland | 775 | –20.476 | 145.475 | 1969–present |
| 120309 | Mistake Creek at Twin Hills | 8,048 | –21.957 | 146.942 | 1976–present |
| 120310 | Suttor River at Bowen Development Road | 10,758 | –21.537 | 147.042 | 2006–present |
| 130210 | Theresa Creek at Valeria | 4,421 | –23.186 | 147.895 | 1971–present |
| 915011 | Porcupine Creek at Mt Emu Plains | 540 | –20.178 | 144.523 | 1972–present |
| 915013 | Flinders River at Glendower | 1,958 | –20.710 | 144.527 | 1972–2012 |

Data: Queensland Department of Natural Resources and Mines (Dataset 2)

Streamflow records for all gauges listed in Table 23 were checked against the quality code used by the Queensland Government. The data were processed into unified six-class quality codes for each gauge (Zhang et al., 2013). The six unified quality categories against their quality codes are given in Table 24. The quality categories are defined as follows:

- good: data are an accurate representation of streamflow
- fair: data are a moderately accurate representation of streamflow
- poor: data are a poor representation of streamflow and may be unsuitable for some quantitative applications
- unverified: data quality is not known
- non-conforming: data are unsuitable for most applications requiring quantitative analysis, but may contain useful qualitative information
- missing: data are missing or unusable.

The streamflow data flagged as good, fair, poor and unverified were kept while the flow data flagged as non-conforming were excluded. The non-conforming and missing streamflow data are both labelled in the data set as –9999.

**Table 24 Quality codes for the Queensland gauging stations for the Galilee subregion**

| Numerical codes | Description |
|---|---|
| 1–18, 16 | Good |
| 20 | Fair |
| 30–69, 160 | Poor |
| 130–150 | Unverified |
| 79, 119, 160–200 | Non-conforming |
| 19, 151, 255 | Missing |

Data: Queensland Department of Natural Resources and Mines (Dataset 2)

Table 25 summarises the percentage of data under each quality code for the selected gauges. Most of the data fall into the good, fair and poor categories. Five gauges have more than 10% non-conforming data. The amount of missing data is relatively low (~2%) except for gauge 120304 (Suttor River at Eaglefield).

**Table 25 Percentage of streamflow data under different quality categories in the Galilee subregion**

| Gauge ID | Good (%) | Fair (%) | Poor (%) | Unverified (%) | Non-conforming (%) | Missing (%) |
|---|---|---|---|---|---|---|
| 002105 | 68.6% | 31.4% | 0.0% | 0.0% | 0.0% | 0.0% |
| 003204 | 86.2% | 13.8% | 0.0% | 0.0% | 0.0% | 0.0% |
| 003205 | 20.4% | 79.6% | 0.0% | 0.0% | 0.0% | 0.0% |
| 003302 | 90.3% | 9.7% | 0.0% | 0.0% | 0.0% | 0.0% |
| 120301 | 60.3% | 18.5% | 7.3% | 0.3% | 13.5% | 0.1% |
| 120302 | 45.1% | 24.4% | 10.5% | 0.7% | 16.8% | 2.4% |
| 120303 | 29.9% | 40.6% | 8.5% | 0.7% | 18.0% | 2.2% |
| 120304 | 64.8% | 9.3% | 7.4% | 0.3% | 2.1% | 16.1% |
| 120305 | 49.2% | 7.2% | 9.3% | 0.9% | 32.0% | 1.4% |
| 120307 | 93.8% | 6.2% | 0.0% | 0.0% | 0.0% | 0.0% |
| 120309 | 59.8% | 6.3% | 4.3% | 1.4% | 27.8% | 0.4% |
| 120310 | 17.3% | 40.9% | 37.7% | 4.1% | 0.0% | 0.0% |
| 130210 | 80.0% | 20.0% | 0.0% | 0.0% | 0.0% | 0.0% |
| 915011 | 89.0% | 11.0% | 0.0% | 0.0% | 0.0% | 0.0% |
| 915013 | 89.0% | 11.0% | 0.0% | 0.0% | 0.0% | 0.0% |

Data: Queensland Department of Natural Resources and Mines (Dataset 2)

### *2.1.4.2 Statistical analysis and interpolation*

No further analyses have been undertaken other than those reported in companion product 1.1 for the Galilee subregion (Evans et al., 2014).

### 2.1.4.3 Gaps

The stream gauges have relatively few missing records except one in Suttor River (120304). The missing data are particularly less for the headwater catchments. The period of record for some gauges is relatively short. These gauges may not represent the climate variability of the catchment well. More information on data gaps will be provided in later products, because the modelling and analysis contributes to identifying further gaps. Likewise, recommendations for monitoring will be reported in later products.

Water quality data for the surface water systems in the Galilee subregion is very limited in terms of water quality parameters measured, and spatial and temporal distribution of data points. Therefore, it is difficult to draw any conclusion on water quality based on available data. Further discussions on data gaps and potential opportunities for future work are outlined in companion product 3-4 for the Galilee subregion (Lewis et al., 2018).

## References

Evans T, Tan KP, Magee J, Karim F, Sparrow A, Lewis S, Marshall S, Kellett J and Galinec V (2014) Context statement for the Galilee subregion. Product 1.1 from the Lake Eyre Basin Bioregional Assessment. Department of the Environment, Bureau of Meteorology, CSIRO and Geoscience Australia, Australia. Viewed 12 April 2016, http://data.bioregionalassessments.gov.au/product/LEB/GAL/1.1.

Evans T, Karim F, Cassel R, and Harris-Pascal C (2015) Current water accounts and water quality for the Galilee subregion. Product 1.5 for the Galilee subregion from the Lake Eyre Basin Bioregional Assessment. Department of the Environment, Bureau of Meteorology, CSIRO and Geoscience Australia, Australia. Viewed 12 September 2016, http://data.bioregionalassessments.gov.au/product/LEB/GAL/1.5.

Karim F, Viney NR, Wang B, Peeters LJM, Zhang YQ, Marvanek SP, Shi X, Yang A and Buettikofer H (2018) Surface water numerical modelling for the Galilee subregion. Product 2.6.1 for the Galilee subregion from the Lake Eyre Basin Bioregional Assessment. Department of the Environment and Energy, Bureau of Meteorology, CSIRO and Geoscience Australia, Australia. http://data.bioregionalassessments.gov.au/product/LEB/GAL/2.6.1.

Lewis S, Evans T, Pavey C, Holland KL, Henderson BL, Kilgour P, Dehelean A, Karim F, Viney NR, Post DA, Schmidt RK, Sudholz C, Brandon C, Zhang YQ, Lymburner L, Dunn B, Mount R, Gonzales D, Peeters LJM, O' Grady A, Dunne R, Ickowicz A, Hosack G, Hayes KR, Dambacher J, Barry S (2018) Impact and risk analysis for the Galilee subregion. Product 3-4 for the Galilee subregion from the Lake Eyre Basin Bioregional Assessment. Department of the Environment and Energy, Bureau of Meteorology, CSIRO and Geoscience Australia, Australia. http://data.bioregionalassessments.gov.au/product/LEB/GAL/3-4.

Zhang YQ, Viney N, Frost A, Oke A, Brooks M, Chen Y and Campbell N (2013) Collation of Australian modeller's streamflow dataset for 780 unregulated Australian catchments. CSIRO: Water for a Healthy Country National Research Flagship, Canberra, Australia.

### *Datasets*

Dataset 1 Bureau of Meteorology (2013) National Surface Water sites Hydstra. Bioregional Assessment Source Dataset. Viewed 12 April 2016, http://data.bioregionalassessments.gov.au/dataset/f7edc5e5-93ee-4527-bed5-a118b4017623.

Dataset 2 Queensland Department of Natural Resources and Mines (2014) DNRM Water Measurement Information System Extract April 2014. Bioregional Assessment Source Dataset. Viewed 12 April 2016, http://data.bioregionalassessments.gov.au/dataset/c320a7f8-85c4-48b2-89cf-251d41b9d100.

## 2.1.5 Surface water – groundwater interactions


### *Summary*

Interaction between groundwater and surface water in the Galilee subregion manifests in various ways including: baseflow to rivers, discharge to springs and lakes, and groundwater-dependent ecosystems. Available streamflow gauge data for Belyando and Thomson rivers has allowed development of an approach to estimate the baseflow contribution to stream flow. A major assumption behind the approach is that all baseflow is derived via groundwater discharge from aquifers, which is currently untested in the Galilee subregion.

The Belyando River flows partly inside and partly outside of the Galilee subregion. Its flow is characterised by high discharges in response to large rainfall events followed by long periods of virtually no flow. The Belyando River hydrograph, however, exhibits significant baseflow recession which may persist for up to two months after a high-flow event. These high-flow events usually occur during the summer months. The calculated mean annual baseflow index for the Belyando River at Belyando Crossing (75 km downstream of the Galilee subregion) is 0.127, giving a mean annual baseflow of about 83,450 ML/year. The groundwater flux through the Cenozoic sediments into the Belyando River, computed using Darcy’s Law, is 7950 ML/year, which means that only 9.5% of the mean annual baseflow is generated within the subregion.

The Thomson River flows through Longreach and is the major stream draining the central part of the Galilee subregion. The Thomson River is not a single channel, but like the other major rivers of western Queensland, is strongly anastomosed with up to several parallel braided channels entrenched deeply in alluvial belts 3 to 5 km wide. The riverbed contains many elongated waterholes, some of which contain permanent water. The mean annual discharge based on 40 years (1970–2010) of records from the gauge at Longreach is 1,246,600 ML/year. The Thomson River is believed to be underlain by a paleochannel of Cenozoic age, which is incised into the Winton-Mackunda formations for a depth of up to 200 m. Like the Belyando River, flow in the Thomson River is characterised by high discharges in response to large rainfall events interspersed with long periods of virtually no flow. However, bed underflow in the paleochannel sediments continues indefinitely.

The annual baseflow index of the Thomson River at Longreach is 0.180, giving a mean annual baseflow of 224,390 ML/year. Lateral seepage to the Thomson River paleochannel and upwards leakage from the Winton-Mackunda formations is estimated to be 163,670 ML/year which comprises 73% of total baseflow.

Data that may improve the understanding of surface water—groundwater interactions includes: shallow groundwater and surface water chemistry and isotopic data; time-series of groundwater level measurements; a better understanding of degree of connectivity; geological variation in alluvial and Paleogene–Neogene sediments and variation in hydraulic properties of shallow aquifers; and an improved understanding of the water sources for the baseflow component of streamflow.

### 2.1.5.1 *Observed data*

Observed data are discussed in Section 2.1.3.2 and Section 2.1.4.

### 2.1.5.2 *Statistical analysis and interpolation*

Interaction between groundwater and surface water in the Galilee subregion is manifested in a variety of ways including:

- interactions between groundwater systems and streams. Streams that may be receiving groundwater discharge include the: Alice, Carmichael, Belyando and Thomson rivers. Surface water flow data are only available for the latter two rivers and these will be discussed in the next two sections. Adani Mining Pty Ltd are collecting information on groundwater discharge and baseflow in the Carmichael River but these data are not available for the bioregional assessment
- leakage of surface water to the Quaternary alluvium in losing streams such as Dunda, Tallarenha and Lagoon creeks. These leakages cannot be quantified due to the lack of data
- groundwater-dependent ecosystems and springs
- discharge to lakes, for example, Lake Galilee, Lake Buchanan and Lake Dunn.

Baseflow refers to the component of stream flow that isn't directly related to runoff from rainfall events. The baseflow component of streamflow can be derived from a number of sources including: stream bank storage effects due to a high surface water flow event, groundwater discharge from shallow alluvial aquifers, groundwater discharge from deep aquifers (if applicable), and interflow through the unsaturated zone to a river. The baseflow component of a hydrograph (Figure ) is a mathematical construct derived from streamflow data and can't necessarily be attributed to a particular source. However, for the purposes of the following discussion, the baseflow component of streamflow is assumed to be derived through fully saturated groundwater discharge from an aquifer to surface drainage. This may provide a theoretical upper estimate of the potential fluxes of groundwater that may occur between a particular river reach and nearby aquifers.

The following sections will focus on the estimation of potential groundwater flux that may occur to some major drainage lines, in particular the Belyando River and Thomson River. Source aquifers for the various spring groups are discussed in Section 2.1.3. No data were available to assess the degree of surface water – groundwater interactions for lakes in the subregion. Some conceptualised understandings for the lakes and springs are presented in Section 2.3.2 of companion product 2.3 for the Galilee subregion (Evans et al., 2018) and in companion product 3-4 for the Galilee subregion (Lewis et al., 2018).

#### 2.1.5.2.1 Estimate of groundwater flux to the Belyando River

The Belyando River is found near the eastern margin of the Galilee subregion, in the upper part of the eastward draining Burdekin river basin. Its flow is characterised by high discharges in response to large rainfall events followed by long periods of virtually no flow. The Belyando River hydrograph, however, exhibits significant baseflow recession as shown in Figure , and baseflow may persist for up to two months after a high-flow event. These high-flow events usually occur during the summer months.

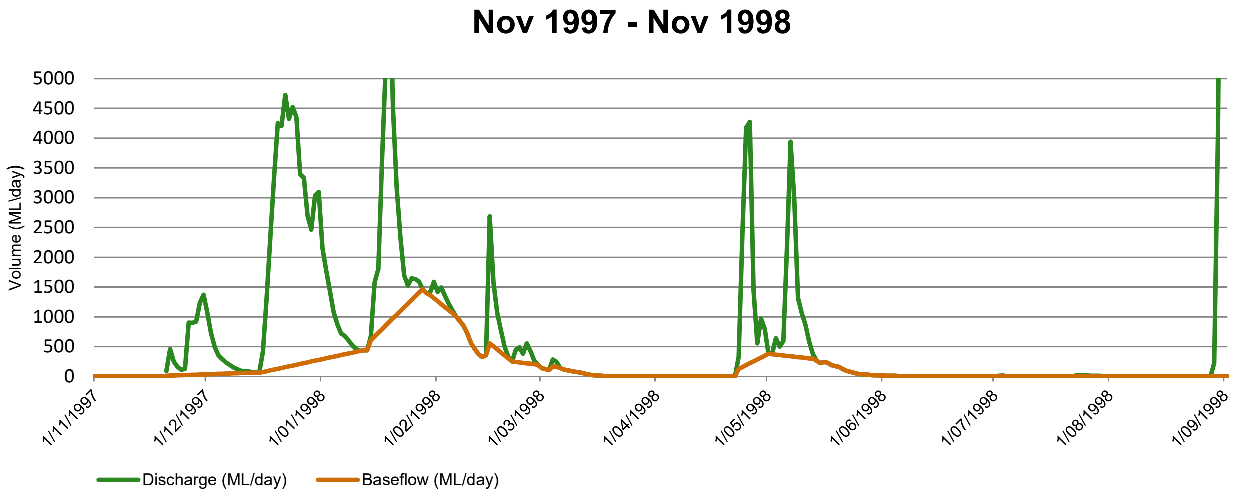


**Figure 88 Example hydrograph of Belyando River at Belyando Crossing showing baseflow recession**

Baseflow is calculated by the baseflow separation program developed by the Institute of Hydrology (Wallingford, UK) – Tallaksen and van Lanen (2004).

The baseflow component of a hydrograph can include surface water flow derived from a number of sources, including discharge of groundwater from an aquifer. For the purposes of Section 2.1.5 it is assumed that all baseflow equates to groundwater discharge from an aquifer.

Data: Queensland Department of Natural Resources and Mines (Dataset 1)

The hydrograph in Figure  is from the gauge at Belyando Crossing, 75 km downstream of the Galilee subregion, where the Gregory Development Road crosses the river. Flow records exist from 1976 to the present. The baseflow recession components shown in Figure  were calculated by the baseflow separation program developed by the Institute of Hydrology (Wallingford, UK) (Tallaksen and van Lanen, 2004). This method of determining baseflow estimates baseflow volumes by dividing a daily flow record into overlapping three day time steps, and making linear interpolations between observations of flow minima in each time step of the record. Flow minima are only used in determining the baseflow line on the hydrograph where 0.9 × the central daily flow value of the time step is less than both outer values of the time step. Additionally, if linear interpolation between two minima observed on the baseflow line would result in baseflow estimates greater than the total streamflow for a given day, the baseflow estimate for that day is adjusted to be equal to the total streamflow. This method does not require the assumption of coefficients used to calculate baseflow in other baseflow separation techniques. The Wallingford program also calculates the baseflow index (BFI) of the river on a seasonal or annual basis. Figure 89 shows the BFIs calculated on a (wet) seasonal and annual basis using flow data from 1976 to 2012.

A couple of features shown in Figure 89 deserve comment. Firstly, there is considerable variation from year to year in both the wet season and annual BFIs. Secondly, for about two-thirds of the years, the wet season BFI exceeds the yearly BFI. This must mean that low winter rainfall events generate little baseflow. According to the Wallingford program, the mean annual BFI for the 35 years of recording is 0.127. Given a mean annual flow of 657,060 ML/year for the Belyando River at Belyando Crossing (Prendegast and Davidson, 2014), this equates to a mean annual baseflow of about 83,450 ML/year.

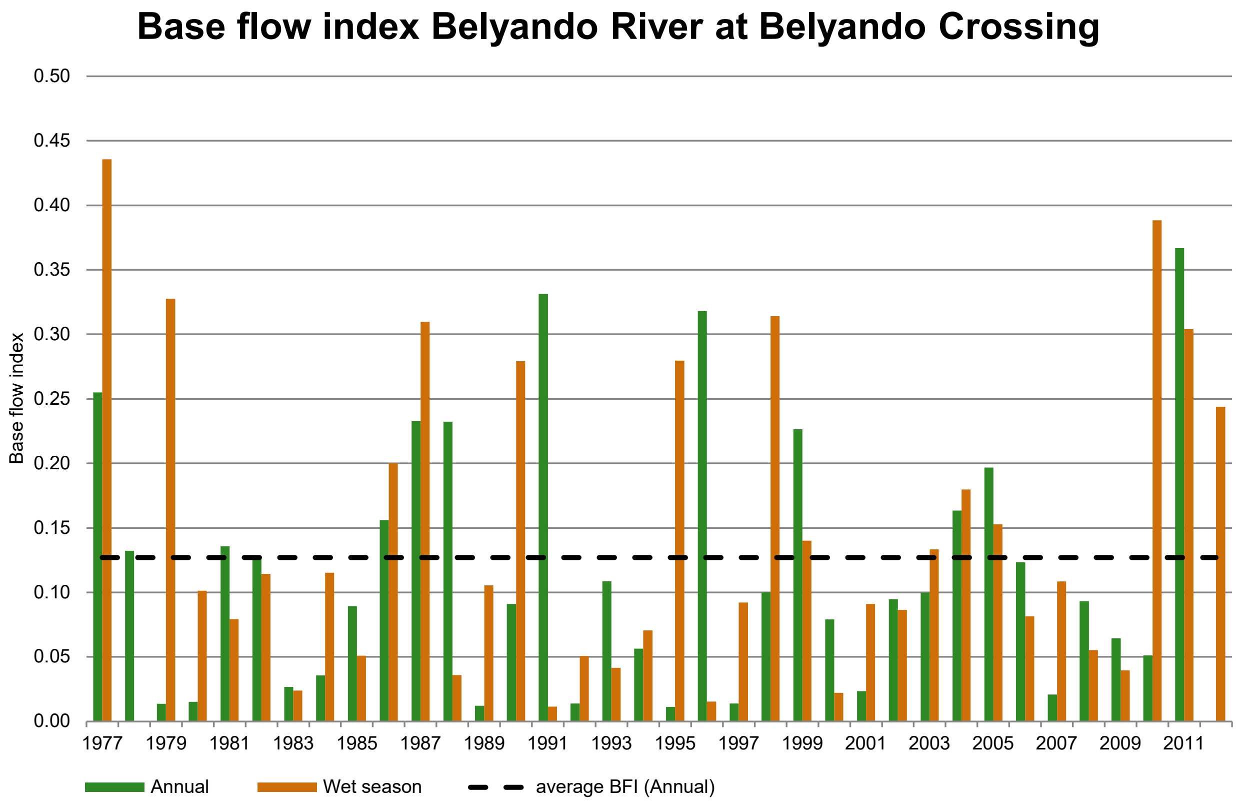


**Figure 89 Baseflow index (BFI) values for the Belyando River at Belyando Crossing for 35 years of recording; BFIs are shown on a wet seasonal and annual basis**

Wet season = November to February
The BFI is the ratio of baseflow to total river flow. The baseflow component of a hydrograph can include surface water flow derived from a number of sources, including discharge of groundwater from an aquifer. For the purposes of discussion in Section 2.1.5 it is assumed that all baseflow equates to groundwater discharge from an aquifer.
Data: Queensland Department of Natural Resources and Mines (Dataset 1)

A proportion of the baseflow measured at Belyando Crossing is generated within the Galilee subregion. It is necessary to determine the proportion of this flow that may be affected due to large-scale dewatering of the coal seams. A significant assumption here is that baseflow, as outlined in Figure  and Figure 89 is derived solely through the discharge of groundwater from aquifers.

Figure 90 is a subset of Figure 56 in Section 2.1.3.2.2 and shows the potentiometric surface of the combined Quaternary alluvium and unconsolidated Paleogene–Neogene sediments in the Belyando river basin. The flow lines define boundaries between flow elements, numbered from 1 to 19 in Figure 90. The groundwater flux through each element may be computed using Darcy's Law; in these calculations it is assumed the hydraulic conductivity of the Cenozoic sediments is 1.5 m/day (the mean *Kh* value of the Quaternary and Paleogene–Neogene sediments) and the saturated thickness is 70 m. Calculated groundwater fluxes for each element are shown Table . These data indicate that only 9.5% of the total baseflow measured at Belyando Crossing is generated within the Galilee subregion.

For the initial estimate of groundwater flux as outlined in Table  (and Table 27), a number of conservative assumptions were made. Assumptions and limitations on the calculations include that:

- the baseflow estimate at the Belyando River crossing is applicable to reaches of the Belyando River that are located some 75 km upstream from the stream gauge
- all baseflow occurs under fully saturated conditions (i.e. no interflow or bank storage) and that it only equates to groundwater flux between a river and an aquifer
- Quaternary alluvium and underlying Paleogene–Neogene sediments have unimpeded hydraulic connection
- there is connection between underlying upper Permian coal measures (Bandanna Formation or Colinlea Sandstone) and overlying Cenozoic sediments
- the mean saturated thickness of unconfined shallow aquifers in Cenozoic sediments is 70 m
- the mean horizontal hydraulic conductivity is 1.5 m/day
- the aquifer in the Cenozoic sediments is homogenous and isotropic in every flow element
- the hydraulic flux calculated for each flow element identified in Figure 90 fully discharges to the river. So for instance, there is no discharge via evapotranspiration from deep rooted vegetation (e.g. redgums, coolibah), or pumping of groundwater
- no groundwater underflow occurs in the flow element areas
- the river is always a gaining stream
- the effect of yearly climatic variations on groundwater levels in shallow aquifers are not taken into account
- potentiometric surfaces for Cenozoic aquifers (Figure 90, Figure 92) are not derived from measurements of groundwater levels at a specific point in time as very limited time series groundwater level data exists (see Section 2.1.3.3.3 for detail). Available water level measurements are often only a single measurement taken at different times of the year. Thus the potentiometric surfaces for the Cenozoic aquifers are more representative for potential flow trends. However, as outlined in Section 2.1.3.3.3, yearly fluctuations and trends are well within the 10 m contour intervals shown on the potentiometric surfaces.

Not all of the assumptions outlined above are likely to be met in the Belyando river basin. For instance, pumping bores do occur in these areas and there is significant seasonal climatic variation. Also, it is highly likely that over such a large area, there would be significant variation in hydraulic parameters, for example, hydraulic conductivity, which in turn will affect calculations for groundwater flux and localised distribution of flow potentials and hydraulic gradients. Consequently, these results represent a first pass estimate only and due to all the assumptions should be considered to be conservative. Essentially more site-specific data and other approaches would be required to crosscheck the estimate and the validity of the assumptions. Other data that would be of use include groundwater and surface water chemistry and isotopic data with samples acquired as part of one field visit.

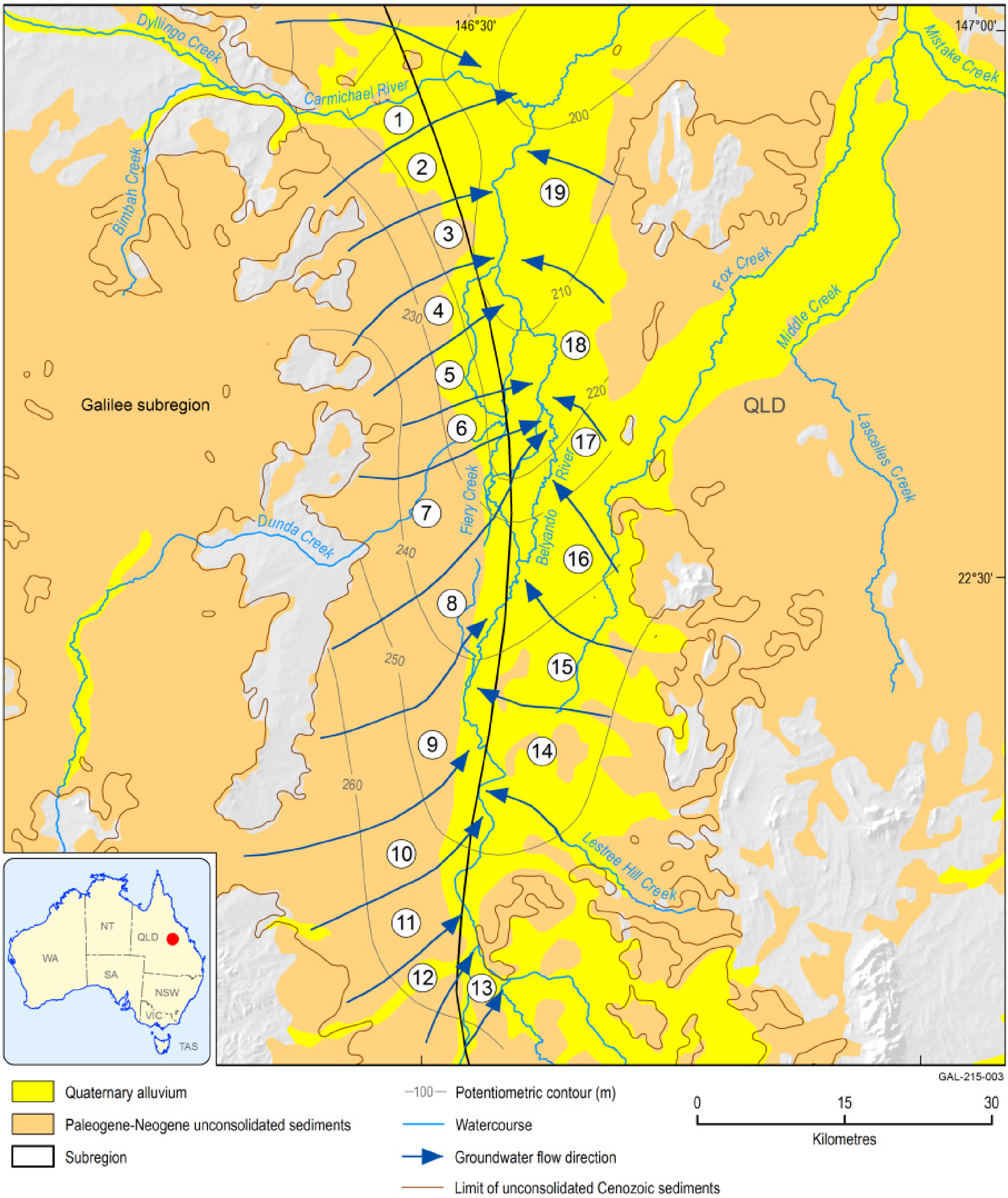


**Figure 90 Potentiometric surface of Cenozoic sediments in the Belyando river basin; numbered groundwater flux elements shown**

Data: Bioregional Assessment Programme (Dataset 2, Dataset 3)

**Table 26 Groundwater fluxes in Cenozoic sediments which contribute to Belyando River baseflow**

| Element number (Figure 90) | Groundwater flux (ML/y) |
|---:|---:|
| 1 | 657.0 |
| 2 | 447.1 |
| 3 | 670.7 |
| 4 | 574.9 |
| 5 | 511.0 |
| 6 | 383.3 |
| 7 | 718.6 |
| 8 | 359.3 |
| 9 | 547.5 |
| 10 | 298.1 |
| 11 | 184.0 |
| 12 | 119.8 |
| 13 | 383.3 |
| 14 | 165.5 |
| 15 | 364.1 |
| 16 | 328.5 |
| 17 | 511.0 |
| 18 | 404.5 |
| 19 | 321.9 |
| **Total** | **7950.1** |

Data: Bioregional Assessment (Dataset 2)

Large drawdowns will need to be generated in the upper Permian coal measures in order to develop the proposed coal mines. It is conceptually possible that to some degree downwards leakage from the Cenozoic sediments will be induced into the upper Permian coal measures, which could result in a reduction to baseflow. The current best estimate of baseflow to the Belyando River in the subregion is 7950 ML/year, which represents less than 10% of the total streamflow at the Belyando Crossing gauge.

### 2.1.5.2.2 Baseflow to the Thomson River

The Thomson River lies in the Cooper Creek-Bulloo river basin. The Thomson River flows through Longreach and is the major stream draining the central part of the Galilee subregion. The Thomson River is not a single channel, but like the other major rivers of western Queensland, is strongly anastomosed with up to several parallel braided channels entrenched deeply in alluvial belts 3 to 5 km wide. The riverbed contains many elongated waterholes, some of which contain permanent water. The mean annual discharge based on 40 years (1970–2010) of records from the gauge at Longreach is 1,246,600 ML/year. The Thomson River is believed to be underlain by a paleochannel of Cenozoic age (Ransley and Smerdon, 2012) which is incised into the underlying Winton-

Mackunda formations to a depth of up to 200 m. Like the Belyando River, flow in the Thomson River is characterised by high discharges in response to large rainfall events interspersed with long periods of virtually no flow. However, bed underflow in the paleochannel sediments is likely to continue indefinitely.

The annual BFI (Figure 91) estimated from the Wallingford program is 0.180 giving a mean annual baseflow estimate of 224,390 ML/year.

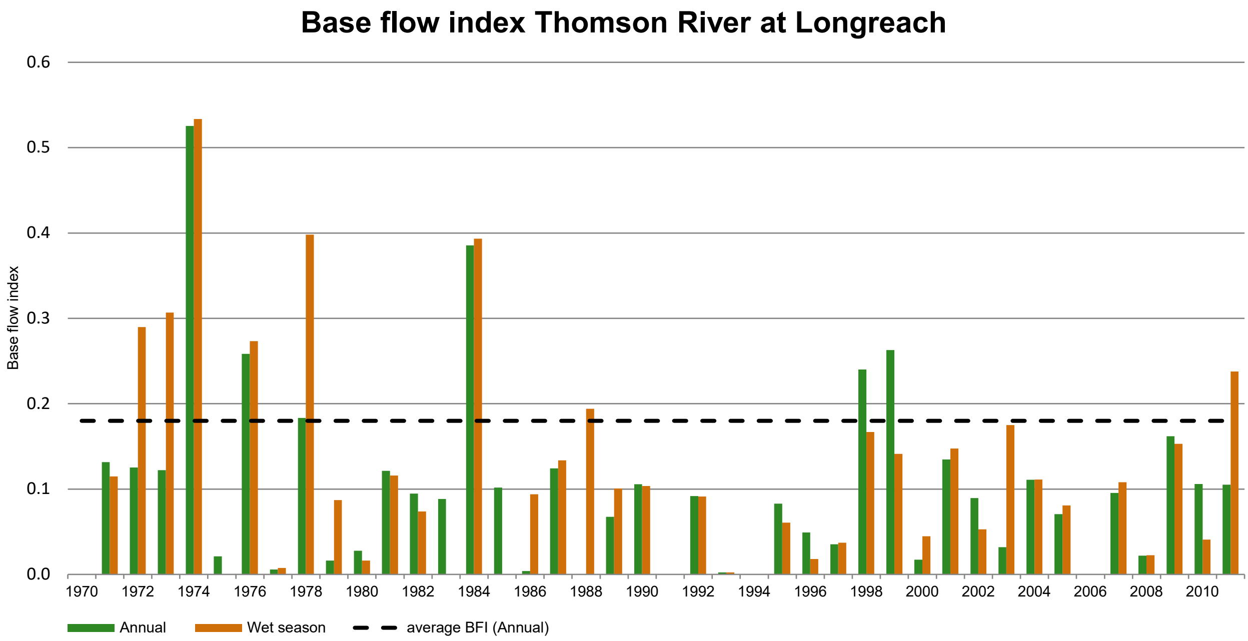


**Figure 91 Baseflow index (BFI) values for the Thomson River at Longreach for 40 years of records**

Wet season = November to February
The BFI is the ratio of baseflow to total river flow. The baseflow component of a hydrograph can include surface water flow derived from a number of sources, including discharge of groundwater from an aquifer. For the purposes of discussion in Section 2.1.5 it is assumed that all baseflow equates to groundwater discharge from an aquifer.
Data: Queensland Department of Natural Resources and Mines (Dataset 1)

Like the Belyando River BFIs, the Thomson River BFIs display considerable year-to-year variation, the years 1974 and 1984 in particular. Figure 92 is a subset of Figure 57 in Section 2.1.3.2.2 and shows the watertable in the Winton-Mackunda formations on the Longreach and Muttaburra 1:250 000 map sheets. The flow lines shown in Figure 92 define boundaries between flow elements numbered from 1 to 16, which shows the potentiometric surface for the Winton-Mackunda aquifer. Using the same assumptions and approach as undertaken for the Belyando River analysis (Section 2.1.5.2.1), the groundwater flux through each numbered flow element in Figure 92 is computed using Darcy's Law; in these calculations it is assumed the hydraulic conductivity of the Winton-Mackunda formations is 1 m/day and the aquifer's saturated thickness is 469 m. The same assumptions that were applied to the Belyando River example, apply to the Thomson River example. It should be stressed that this is an estimate only based on idealised conditions. Estimated groundwater fluxes for each element are shown in Table 27. These results represent a first pass estimate only and due to all the assumptions is likely to be highly conservative.

These data indicate that 72.9% of the total baseflow in the Thomson River at Longreach is generated by upward leakage and lateral seepage from the Winton-Mackunda formations aquifer between Longreach and Muttaburra. The dominant mechanism is possibly lateral seepage to the paleochannel alluvium since formation of the paleochannel would have eroded through the weathered sections of the Winton-Mackunda formations. The erosion may have resulted in direct unimpeded hydraulic connection between the alluvium and fresh rock.

Moya et al. (2014) reinterpreted some seismic and borehole data for central portions of the Galilee Basin, and discovered a previously unknown major fault that runs parallel with the Thomson River in the vicinity of Longreach. These authors named this structure the Thomson River Fault and measured a vertical displacement of up to 650 m along the fault plane (uplifted on the eastern side). They further speculated that the Thomson River Fault may act as a conduit for vertical upwards transmission of groundwater from the Cadna-owie—Hooray aquifer to discharge into the Thomson River alluvium.

Conceptually, baseflow to the Thomson River could be comprised of:

- upward leakage from the Hooray Sandstone upstream of Muttaburra (along Landsborough, Towerhill and Cornish Creeks)
- upward leakage from the Hooray Sandstone along the lower Aramac Creek
- upward leakage from the Hutton Sandstone along the Thomson River Fault, and along Aramac, Landsborough and Cornish Creeks (not as large as the upward leakage from the Hooray Sandstone)
- lateral seepage from the Cenozoic sediments of the alluvial belts
- a combination of upward leakage along the Thomson River Fault and lateral seepage into the alluvium of the Thomson River paleochannel from the Winton-Mackunda formations.

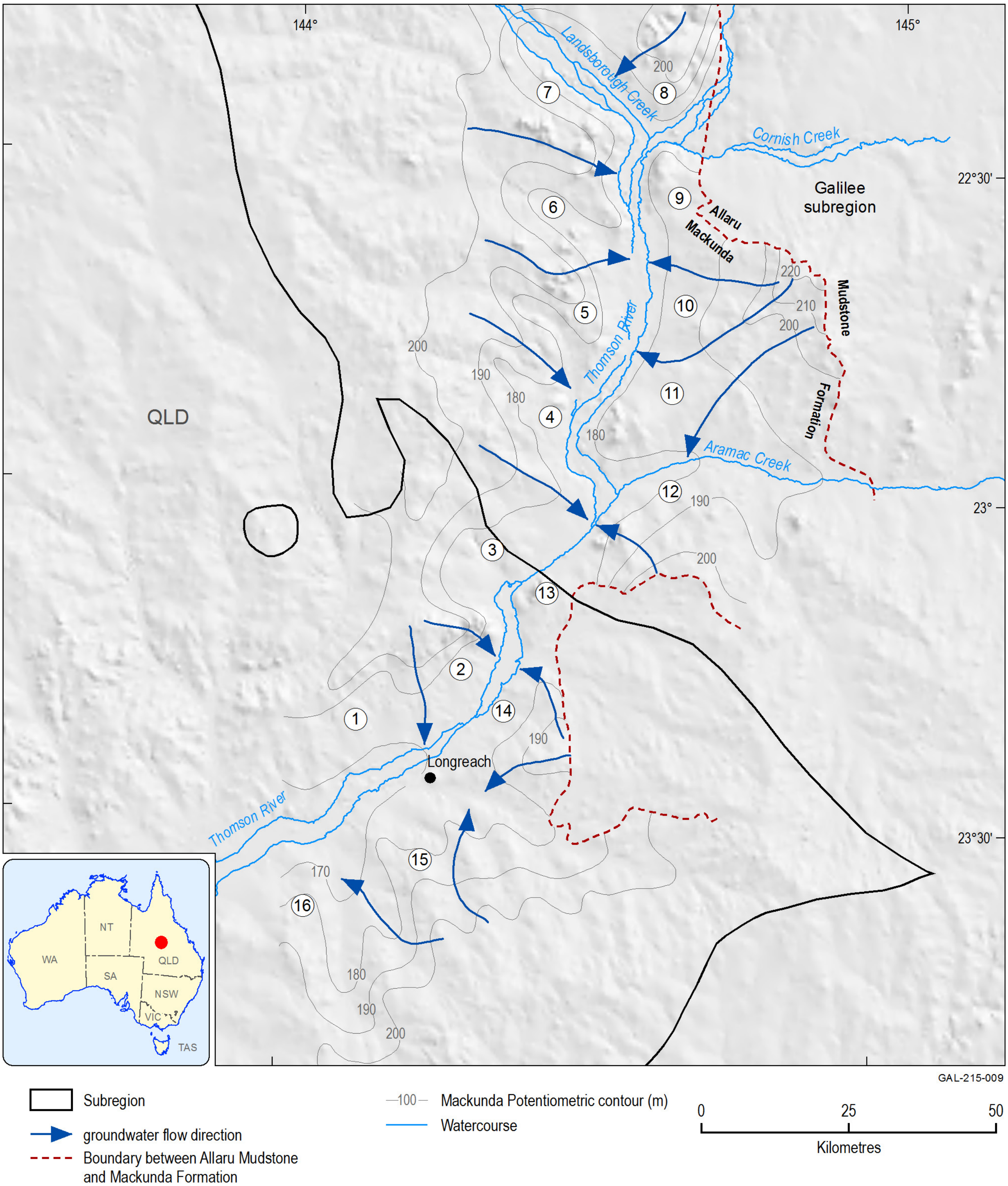


**Figure 92 Potentiometric surface and flow directions of the Winton-Mackunda formations partial aquifer in the vicinity of the Thomson River; numbered groundwater flux elements shown**

Data: Bioregional Assessment Programme (Dataset 2, Dataset 3)

**Table 27 Groundwater fluxes in the Winton-Mackunda formations partial aquifer which contribute to Thomson River baseflow**

| Element number (Figure 92) | Groundwater flux (ML/y) |
|---:|---:|
| 1 | 7,395.2 |
| 2 | 4,061.8 |
| 3 | 8,114.2 |
| 4 | 1,1983.0 |
| 5 | 22,254.1 |
| 6 | 14,721.9 |
| 7 | 29,101.5 |
| 8 | 21,303.0 |
| 9 | 5,135.6 |
| 10 | 3,043.3 |
| 11 | 2,366.4 |
| 12 | 5,792.0 |
| 13 | 5,477.9 |
| 14 | 6,536.2 |
| 15 | 7,395.2 |
| 16 | 8,987.2 |
| **Total** | **163,668.5** |

Data: Bioregional Assessment Programme (Dataset 2)

### *2.1.5.3 Gaps*

There have been limited studies of surface water – groundwater interactions in the Belyando and Thomson river basins. A number of assumptions were required in order to make the computations outlined in this section and discussions on data gaps are outlined in companion product 3-4 for the Galilee subregion (Lewis et al., 2018). However, information that would assist in gaining a better understanding of the surface water – groundwater interactions includes:

- streamflow gauge data acquired by coal mining proponents, in particular for the Carmichael River
- thickness maps for alluvium and Paleogene–Neogene sediments
- more hydraulic parameter measurements, in particular in the vicinity of river reaches of interest such as the Thomson River. For example, hydraulic conductivity
- time-series bore hydrograph data covering more than a couple of years

- access to at least some company coal bore data would greatly improve the accuracy of geological models in the vicinity of coal exploration areas and proposed coal development. Not all bore data would be required. Primarily well location data, stratigraphic picks and if possible some geophysical well logs. Data from near-surface portion of the well logs would be useful for more detailed characterisation of lithological variation of the alluvium, Paleogene–Neogene sediments and their relationship to underlying geological units
- river bed profiles for river reaches of interest
- improved understanding of distribution of buried paleochannels
- monitoring bores in alluvium and Paleogene–Neogene sediments near major drainage channels and particularly near streamflow gauges if located in the Galilee subregion
- hydrochemistry and isotopic data from shallow groundwater systems in alluvium and Paleogene–Neogene sediments and surface water
- investigations utilising remote sensing data e.g. Landsat. These data could be used to delineate GDEs or fluxes of water in landscape with time
- knowledge of the thickness, structure and lithological variations within Cenozoic sequences is very limited across the Galilee subregion. One option that would improve understanding of the Cenozoic sediments would be acquisition of airborne electromagnetic (AEM) data in the subregion. If required, the AEM survey could be complemented by a shallow drilling programme or use of existing company-supplied drilling data (if applicable), to provide stratigraphic control for modelling the thickness and characteristics of the near-surface cover. The AEM data would also provide information on shallow groundwater systems, and potentially identify areas of connectivity between Cenozoic cover and underlying regional GAB aquifers.

## *References*


Evans T, Pavey C, Cassel R, Ransley T, Sparrow A, Kellett J, Galinec V, Dehelean A, Caruana L and Kilgour P (2018) Conceptual modelling for the Galilee subregion. Product 2.3 for the Galilee subregion from the Lake Eyre Basin Bioregional Assessment. Department of the Environment and Energy, Bureau of Meteorology, CSIRO and Geoscience Australia, Australia. http://data.bioregionalassessments.gov.au/product/LEB/GAL/2.3.

Lewis S, Evans T, Pavey C, Holland KL, Henderson BL, Kilgour P, Dehelean A, Karim F, Viney NR, Post DA, Schmidt RK, Sudholz C, Brandon C, Zhang YQ, Lymburner L, Dunn B, Mount R, Gonzales D, Peeters LJM, O' Grady A, Dunne R, Ickowicz A, Hosack G, Hayes KR, Dambacher J, Barry S (2018) Impact and risk analysis for the Galilee subregion. Product 3-4 for the Galilee subregion from the Lake Eyre Basin Bioregional Assessment. Department of the Environment and Energy, Bureau of Meteorology, CSIRO and Geoscience Australia, Australia. http://data.bioregionalassessments.gov.au/product/LEB/GAL/3-4.

Moya CE, Raiber M and Cox ME (2014) Three-dimensional geological modelling of the Galilee and central Eromanga basins, Australia: new insights into aquifer/aquitard geometry and potential influence of faults on inter-connectivity. Journal of Hydrology: Regional studies 2 (2014) 119–139.

Prendegast JB and Davidson KJ (2014) Galilee Basin Groundwater - Preliminary Assessment of Recharge, Long Term Extraction Limit and Cumulative Mining Impacts (draft). Queensland Department of Natural Resources and Mines, Brisbane.

Ransley TR and Smerdon BD (eds) (2012) Hydrostratigraphy, hydrogeology and system conceptualisation of the Great Artesian Basin. A technical report to the Australian Government from the CSIRO Great Artesian Basin Water Resource Assessment. CSIRO Water for a Healthy Country Flagship, Australia, Canberra. Viewed 12 April 2016, https://publications.csiro.au/rpr/download?pid=csiro:EP132693&dsid=DS5.

Tallaksen LM and van Lanen HAJ (eds) (2004). Hydrological drought. Processes and estimation methods for streamflow and groundwater. Developments in Water Science, 48, Elsevier Science B.V.

## *Datasets*

Dataset 1 Queensland Department of Natural Resources and Mines (2014) DNRM Water Measurement Information System Extract April 2014. Bioregional Assessment Source Dataset. Viewed 12 April 2016, http://data.bioregionalassessments.gov.au/dataset/c320a7f8-85c4-48b2-89cf-251d41b9d100.

Dataset 2 Bioregional Assessment Programme (2015) GAL Group 2 contour data. Bioregional Assessment Derived Dataset. Viewed 12 April 2016, http://data.bioregionalassessments.gov.au/dataset/803b0f5c-acb8-4adf-9ae1-3cb385ed4061.

Dataset 3 Bioregional Assessment Programme (2015) GAL230 Flow directions. Bioregional Assessment Derived Dataset. Viewed 12 April 2016, http://data.bioregionalassessments.gov.au/dataset/38b5f525-373b-409b-8934-7274b19b1f96.

## 2.1.6 Water management for coal resource developments


### Summary

The baseline development for the Galilee subregion contains no active coal mining or coal seam gas (CSG) operations. Only the water management systems for coal mines in the modelled coal resource development pathway (CRDP) are discussed below as there was insufficient information on water management available for the other coal mines and CSG projects in the Galilee subregion CRDP.

As of September 2016 no coal mine projects had commenced operations and because of this there are some data gaps common to all publicly available water management plans. They include: finalisation of sources for external water; external water offtake volumes and off site discharge conditions (e.g. when and where an operation can discharge) and water quality.


Some of the issues related to water management processes for coal mining operations that need to be considered include:

- water produced through groundwater inflows to mine areas or on-site rainfall
- diversion of water around the mine areas
- water required for on-site processes (e.g. coal washing and processing, dust suppression)
- excess water disposal (if required) in accordance with regulation and project approval conditions
- water supply from sources external to mine site (if required)
- clean water supply (e.g. drinking water)
- water treatment strategies for mine contaminated water
- separate water storages for water from various sources.

In general, water management plans that consider in detail the aspects mentioned previously are developed when a coal or CSG project reaches an advanced stage (environmental impact statement (EIS) stage) of the approval process. Coal resource projects at that stage are detailed in the modelled coal resource development pathway (modelled CRDP), which is detailed in Section 2.3.4 of companion product 2.3 for the Galilee subregion (Evans et al., 2018). These projects are: Alpha Coal Project, Carmichael Coal Project, China First Coal Project, China Stone Coal Project, Hyde Park Coal Project (although no EIS documentation is available yet), Kevin's Corner Coal Project and South Galilee Coal Project.

This section provides qualitative detail from water management plans for the coal mine projects included in the Galilee subregion modelled CRDP. Information on external water requirements, changes in mine footprint area with time and expected groundwater inflows are detailed in the following companion products for the Galilee subregion: product 2.5 (water balance assessment) (Karim et al., 2018a), product 2.6.1 (surface water numerical modelling) (Karim et al., 2018b), and product 2.6.2 (groundwater numerical modelling) (Peeters et al., 2018).

As of September 2016 none of these coal mine projects mentioned previously had commenced operations and because of this there are some data gaps common to all publicly available water management plans. These gaps include: finalisation of sources for external water and water offtake volumes, off site discharge conditions (e.g. when and where an operation can discharge) and water quality.

Table 28 outlines some common abbreviations used in describing water management systems in the following sections.

**Table 28 Common abbreviations used in water management plans**

| Abbreviation | Meaning |
|---|---|
| CHPP | coal handling and preparation plant |
| MIA | mine infrastructure area |
| MAW | mine affected water |
| ROM | run-of-mine |
| TSF | tailings storage facility |

### *2.1.6.1 Alpha Coal Project*

The information below is from the Supplementary Environmental Impact Statement (EIS) for the Alpha Coal Project (Parsons Brinckerhoff, 2011).

The proposed water management system for the Alpha Coal Project classifies water into five types, each with a management system:

1. process water management system – managing process water that has been used in the coal handling and preparation plant (CHPP). This includes the tailings storage facility (TSF), decant dam and return water system
2. clean water system – separating clean runoff from undisturbed areas, from runoff from the open-cut mine pits and other contaminated dirty water management systems, and diverting it to Sandy Creek and Spring Creek. This type of water has low turbidity and low salinity
3. contaminated water management system – managing runoff from the open-cut pits and other areas that could contribute contaminants such as the mine infrastructure area (MIA), CHPP, coal stockpiles and dump stations
4. dirty water management system – treating runoff from overburden dumps and other areas that could contain sediment
5. groundwater management system.

The systems are discussed in more detail below.

#### 2.1.6.1.1 Process water management system

Wet tailings slurry will be transferred by pipe and pump to the TSF. Excess water in the TSF will be decanted to a separate dam and a pump and pipeline system returns the water to the CHPP for reuse as required.

#### 2.1.6.1.2 Clean water system

The purpose of this system is to minimise the site water inventory and maintain pre-development discharges into Lagoon Creek and Sandy Creek. Lagoon, Sandy and Spring creeks will be diverted around or through the mine site. Levees will be used to prevent waters entering the pit. Dams, levees and additional intermediate diversion drains west of the pit will capture and divert water from undisturbed catchments found up slope (west) of the mine area. Water will only be imported onto site if there is not sufficient water in the contaminated water management system or if high quality water is required for on-site processes. Imported water will be stored in the raw water dam and a pump and pipeline system will deliver this water to where it will be used on site.

#### 2.1.6.1.3 Contaminated water management system

Small sumps in the pit floor will collect and contain local surface water runoff from the pit floor, highwall, low wall and end walls. Pit dewatering pumps and pipelines will transfer pit water to the nearest pit dewatering dam (via a small staging dam if required). A drainage system will convey runoff from disturbed areas to the nearest environmental dam. The environmental and pit dewatering dams have been designed to minimise the areas draining to them which minimises the storage requirements in order to reduce the risk of uncontrolled spilling during rainfall events. A pump and pipeline system will deliver water from these dams to where it will be used on site.

A borefield will be used to minimise groundwater seepage into the pit and this will provide water for use in mine processes.

During extended wet periods, if one of the dewatering and environmental water storage dams reach their active storage capacity then the pits will provide temporary storage for surplus contaminated water.

#### 2.1.6.1.4 Dirty water management system

Dirty water runoff from disturbed areas, such as overburden dumps, will be captured in sediment dams to encourage suspended solids to settle. Once settled, water will be transferred to environmental dams for reuse on site or if the storages have reached capacity it will be discharged to Lagoon Creek subject to water quality and release conditions. It is expected that during dry and median rainfall periods, sediment dam water will be reused on site and only released to the creek during prolonged wet periods. Water from the sediment dams will be moved around site (either for reuse or release) via a pump and pipeline system.

#### 2.1.6.1.5 Groundwater management system

Groundwater will be extracted from the upper Permian coal measures using a borefield to minimise seepage into the pit. Bore water will be stored in environmental dams for reuse in various on-site processes. Bore water is expected to be of reasonable quality.

### *2.1.6.2 Carmichael Coal Project*

The information below is taken from the Supplementary EIS for the Carmichael Coal Project (GHD Pty Ltd, 2013).

Water is considered to belong to one of five categories:

1. raw water – received from an external water supply as an input. Raw water is considered clean and has not been used in a task
2. mine affected water (MAW) – has been through a task and is potentially contaminated by mining activities
3. sediment affected water – contains higher sediment load but is not contaminated by mining activities
4. clean water – runoff from undisturbed areas of catchment. This will be diverted around the project and is not part of the project water balance
5. treated water – has been treated on site to achieve a particular water quality objective. MAW and raw water can be treated to allow for further use or released as a controlled discharge
6. process water – used on site to complete a task.

### 2.1.6.2.1 Raw water

Raw water will be delivered and temporarily stored in a raw water dam.

### 2.1.6.2.2 Mine affected water

MAW water is generated from areas of active mining. This includes: dewatering of six open-cut pits; dewatering of five underground mines; dewatering three box cut areas of underground mines; dewatering two highwall access areas; the coal handling and preparation plant (CHPP) tailings decant dam and runoff from industrial working areas (such as MIA, ROM coal area, CHPP and the train load out facility).

MAW will be retained on site and stored in MAW dams. When necessary MAW will be discharged to receiving waterways under the mine’s approval conditions. The aim is to only discharge during extreme climatic events that exceed the design parameters.

### 2.1.6.2.3 Sediment affected water

Sediment affected water is generated from disturbed areas not contaminated with coal or other mining contaminates (such as areas disturbed due to vehicle movements or overburden areas). Sediment affected water will be treated to achieve minimum reductions in key pollutants before being reused or released to the natural environment.

### 2.1.6.2.4 Clean water

Clean water is diverted around mine workings or disturbed areas and released downstream into the same waterway. Mine workings are protected from local stormwater and regional flooding.

### 2.1.6.2.5 Treated water

Acid mine drainage water will be treated in through a neutralisation process in sediment basins or MAW dams.

### 2.1.6.3 China First Coal Project

The information below is taken from the Commonwealth EIS for the China First Coal Project (Engeny Water Management, 2013).

Water has been classified into four types:

1. contaminated water – surface runoff from the CHPP, ROM and stockpile areas and water contained within open-cut pits. This water is likely to be saline and may be of low pH and may also contain hydrocarbons or other contaminants such as trace metals. This water will be managed to prevent discharge to waterways and to meet on-site water requirements
2. dirty water – surface runoff from spoil dumps and rehabilitated areas that could contain sediments but typically not elevated levels of contaminants. This water will be directed to sedimentation dams for settling of suspended solids and reuse on site. This water would only be discharged to receiving waters during significant rainfall events
3. clean water – surface runoff from natural catchments. This will not be contained on site and will pass through the site via creek diversions and bunding walls around open-cut pits
4. groundwater – water produced through dewatering of underground mine working and aquifer pre-drainage. This is expected to be low salinity (<1500 µS/cm). This water will be reused for underground mining processes, additional supply for raw water requirements and treated as necessary for potable water supply.

The components of the water management system are:

- box cut spoil sediment dams
- pit spoil sediment dams
- environmental dams
- pit dewatering dams
- underground dewatering dams
- clean water dams
- return water dam.

#### 2.1.6.3.1 Box cut spoil sediment dams

These dams will be provided in the box cut spoil areas prior to year 1 of operations. They will retain stormwater runoff to maximise settling of suspended solids and provide water for construction related purposes such as dust suppression. Once the mine commences these areas will be progressively rehabilitated and the sediment load to the catchments will decrease significantly. The good quality water is intended for reuse in underground mining operations.

#### 2.1.6.3.2 Pit spoil sediment dams

These dams will be constructed in-pit for open-cut mining operations. The number of dams required will increase with the progression of the open-cut highwall. The assumption is that spoil areas will be progressively rehabilitated which will improve the runoff water quality. Water in the spoil dams will be used for dust suppression operations. The size of the spoil dams is based on the assumption that the spoil will be non-acid forming and low salinity, the size may need to be adjusted if this is not the case. The dams will be designed to allow removal of suspended sediments through natural sedimentation.

#### 2.1.6.3.3 Environmental dams

Environmental dams will manage contaminated runoff from run-of-mine (ROM) stockpiles, product stockpiles and industrial areas. It is expected that runoff from these areas has the potential to be saline and contain contaminants such as metals and hydrocarbons. Water captured in the environmental dams will be transferred to the pit dewatering dams via the return water dam. Two environmental dams are proposed, one located adjacent to the CHPP and the other adjacent to the second ROM stockpile in the infrastructure corridor.

#### 2.1.6.3.4 Pit dewatering dams

Pit dewatering dams will provide primary storage for water pumped from the open-cut pits. Up until ten years of operations the pit dewatering dams will be located to the west of highwall side of the pits. At approximately 15 years of operations the pit dewatering dams will be progressively relocated to within the spoil dumps to allow progression of mining. It is proposed that there will be four pit dewatering dams. These dams will be ‘turkey’s nest’ design to prevent inflows from the catchment and reduce the risk of overflow.

#### 2.1.6.3.5 Underground dewatering dams

Two underground dewatering dams are proposed. They will store groundwater from aquifer pre-drainage (to reduce groundwater inflows to underground and open-cut mines) as well as dewatering of underground operations. The underground dewatering dams will be used to supply underground mining operations and raw water requirements. These dams will be ‘turkey’s nest’ construction or with catchment diversion to prevent external catchment inflow and contamination.

#### 2.1.6.3.6 Clean water dams

There will be two 120 ML clean water dams. One will be located next to the coal handling and preparation plant (CHPP) and the other near the underground portals. The dams will hold enough raw water for two weeks of operation of the CHPP and underground mining in the event of pipeline or pump failure. The dams will be ‘turkey’s nest’ construction to prevent contamination from inflows and will be lined to prevent seepage losses.

#### 2.1.6.3.7 Return water dam

The return water dam will manage excess water from the CHPP. The return water dam will be a ‘turkey’s nest’ construction to prevent inflow of catchment water which will reduce the chances of it overflowing.

### *2.1.6.4 China Stone Coal Project*

The information below is taken from the draft EIS for the China Stone Coal Project (Hansen Bailey Environmental Consultants and MacMines, 2015).

There are six types of water in the water management system (WMS):

1. underground mine pit water – comprised of groundwater inflow to underground workings and water recycled from underground operations
2. open-cut mine pit water – comprised of groundwater inflow to the open-cut pit and runoff from the pit catchment
3. return water from tailings storage facility (TSF) – comprised of water recovered from tailings slurry afters the solids have settled out of the mixture in the storage facility, rainfall and runoff from the contained TSF catchment and runoff from the power station waste storage area
4. runoff from disturbed areas – also includes overburden emplacement areas and mine infrastructure areas
5. runoff from areas affected by mine subsidence
6. runoff from areas unaffected by project activities.

### 2.1.6.4.1 Underground mine pit water

Modelling has estimated peak groundwater inflows to the Northern Underground to be 1410 ML/year at year 16 and the Southern Underground 1520 ML/year at year 13. The actual amount of dewatering will be reduced due to evaporation and infiltration to the pit walls and floor. It has been estimated that up to 250 ML/year of underground supply water will be recycled from each operating longwall. This will be collected in sumps along with groundwater inflow.

Underground pit water will be pumped to the surface and stored on site for reuse. Both the Northern and Southern underground will have pit water dams in their respective mine infrastructure areas (MIAs). Water from the pit water dams will be pumped to a dedicated Mine Water Dam for storage and reuse as mine water supply. The pit water dams will have nil catchment and will be operated to ensure nil overflow.

### 2.1.6.4.2 Open-cut mine pit water

Modelling has estimated peak groundwater inflow rates to the open pit to be 4070 ML/year. Evaporation, surface wetting and infiltration to the pit walls and floor will reduce the volume of dewatering.

The pit catchment area includes the active pit area as well as any areas of overburden emplacement and areas above the highwall that cannot be diverted around or away from the pit. The pit catchment will progressively increase as the mine develops. A series of temporary and permanent diversions and drains will be constructed to minimise the generation of mine affected water from rainfall-runoff.

Open-cut pit water will collect in sumps in the floor of the active pit. It will be pumped to a series of four open-cut pit water dams located along the length of the open-cut mining area. Water from these dams will then be transferred to the Mine Water Dam for storage and reuse. The pit water dams will have nil catchment and will be operated to ensure nil overflow.

During high rainfall events the open-cut pit will collect significant volumes of water. To allow for continued operation of the mine this water will be discharged under controlled conditions.

#### 2.1.6.4.3 Return water from tailings storage facility and power station waste storage facility

The TSF will develop progressively over the 50 year project life and will cover 603 ha when complete. The TSF catchment area will be isolated first by temporary diversion drains and then by an embankment around the perimeter. The power station waste storage facility (PSWSF) will also develop progressively over the first ten years of the project and will cover 80 ha when complete. The PSWSF catchment will also be isolated with perimeter diversion drains.

Tailings slurry will be pumped from the CHPP to the TSF. Tailings solids will settle out within the TSF and supernatant will collect in a decant pond within the TSF. Rainfall-runoff will also collect within the decant pond.

The PSWSF will be developed by trucks placing dry power station waste, similar to an out-of-pit overburden emplacement. Surface runoff from the PSWSF will drain to internal sumps and then be pumped to the adjacent TSF.

A perimeter seepage collection drain will collect any seepage from the TSF and PSWSF. This will be pumped to the TSF decant pond.

Water from the TSF decant pond will be pumped to the return water dam. The return water dam will be a primary water supply for the CHPP.

#### 2.1.6.4.4 Runoff from disturbed areas

Diversion drains will be installed upstream to divert overland flow away from overburden areas. Based on the overburden leach test results overburden leach in rainfall-runoff will be suitable for passive drainage from the site. As runoff from rehabilitated overburden areas is likely to have high sediment load, runoff from these areas will be directed through sediment dams prior to discharge from the site. Rehabilitated overburden areas will generate clean runoff which will be allowed to drain passively from the site.

In the MIA runoff will be isolated by diversion drains and/or bunding. Runoff from these areas will be directed through sediment traps (and oil separators where hydrocarbons are potentially present) and collected in a catch dam. Water from catch dams will be transferred to the Industrial Area Dam and used as mine water supply.

#### 2.1.6.4.5 Runoff from areas affected by mine subsidence

Subsidence may cause localised alteration to drainage paths and ponding in shallow surface depressions. This will be mitigated by the installation of minor remedial drainage earthworks.

#### 2.1.6.4.6 Runoff from areas unaffected by project activities

Where possible runoff from undisturbed areas will be diverted around disturbed areas and allowed to drain from site.

Permanent highwall dams and drains will be constructed and these will remain in place after mine closure. Clean runoff from the northern and southern drainage corridors will flow to the headwaters of Tomahawk Creek and North Creek respectively.

The permanent highwall dams will create temporary isolated undisturbed catchments during the operations phase. Temporary diversion drains will be put in place and water collected will be used for dust suppression.

#### *2.1.6.5 Hyde Park Coal Project*

No information on water management is available as the Hyde Park coal project is not at an EIS stage. The Hyde Park Coal Project will be included in the modelled CRDP (for further detail see Section 2.3.4 in companion product 2.3 for the Galilee subregion (Evans et al., 2018)).

Resolve Coal Pty Ltd (2015) presents a conceptual mine plan of the Hyde Park Coal Project. It outlines some of the following features:

- buffers between natural drainage lines and proposed open-pit areas, to preserve the existing drainage through the mine area
- a series of water storage dams situated away from natural drainage lines in the mine area.

Hyde Park Coal Project will be an open-cut mining operation. It is possible that the Hyde Park Coal Project water management system could have similar components and processes to those envisaged for the Alpha Coal Project mine water management system (see Section 2.1.6.1).

#### *2.1.6.6 Kevin's Corner Coal Project*

The information below is taken from the Supplementary EIS for the Kevin's Corner Coal Project (URS, 2012).

There are seven components to the water management system:

1. mine water dams (MWDs) – dams to store mine affected water (MAW)
2. spoil runoff system – surface runoff from all active (un-rehabilitated) spoil and overburden dumps will be diverted and contained in a series of spoil dams and transferred to one of the MWDs
3. open-cut pit dewatering system – this water is the result of either runoff or direct rainfall. A borefield will reduce groundwater seepage into the open pit to a negligible level. Water will be pumped into collection dams and then transferred to the MWDs
4. process area runoff system – runoff from run-of-mine (ROM) pads and dump, train load out/product stockpile and central mine industrial area and immediate haul roads will be contained at each source and transferred to the MWDs
5. CHPP and TSF process water system – water decanted from the tailings storage facility (TSF) will be reused within the coal handling and preparation plant (CHPP)/tailings pumping system. During high rainfall events, decant water may need to be transferred to MWD2 for subsequent reuse
6. raw water system – supply of water for when there is insufficient quantity of water available or when the use of MAW is unsuitable

7. water transfer system – the mechanical means to move water around the site.

In addition to these systems dewatering is required to allow for underground mining operations. The water will be extracted via the proposed borefield or via the underground mines. Water extracted from the underground mines as part of the mine 'water make' also includes the unused portion of the water demand required to sustain mining operations. All groundwater will be pumped into collection dams and then transferred to the MWDs.

#### 2.1.6.6.1 Mine water dams

There will be two large mine water dams (MWDs) to store the MAW generated over the life of the mine. Water will be contained and collected in various smaller dams around the site and then transferred to a MWD based on proximity. The MWDs will be the source of most of the water used on site and water may be transferred between the two to meet demand or capacity requirements.

#### 2.1.6.6.2 Spoil runoff system

All stormwater runoff originating from each spoil or overburden dump is collected by the spoil runoff system and diverted by gravity flows to one of four spoil dams. Clean runoff originating outside the spoil and overburden dumps will be passively diverted by catch drains and diversion channels to reduce the volume of water requiring containment. Water in the spoil dams will be transferred to the MWDs for reuse.

#### 2.1.6.6.3 Open-cut pit dewatering system

It is assumed groundwater seepage into each pit will be negligible due to the operation of the borefield. Water collected by the open-cut pit dewatering system includes water entering a pit as rainfall, rainfall-runoff originating from pit ramps, temporary spoil dumps and other disturbed areas inside the pit shell. Pit dewatering inflows will be directed to a common location in the pit and pumped to a pit dewatering dam.

#### 2.1.6.6.4 Process area runoff system

Runoff from each underground mine ROM pad will be contained in the respective adit/ROM dam and runoff from the ROM dump will be directed to the ROM dump dam. Runoff from the product stockpile pad will be collected in the train load out/product stockpile dam.

The central mine industrial area (CMIA) has too many potential sources of mine affected water (MAW) to have a separate dam for each source so all runoff from the CMIA will be treated as MAW and stored in the CMIA dam. In order to have the required capacity there will be a secondary overflow basin in the CMIA to receive overflows from the CMIA dam as required and then pump back into the CMIA dam as it is drawn down.

#### 2.1.6.6.5 Coal handling and preparation plant and tailings storage facility process water system

The CHPP is the largest individual demand for water within the project. Process water for the CHPP and TSF will be sourced from the stored MAW except when there is insufficient water stored or additional conditioning (such as dilution) is required. In such cases raw water will be used.

Tailings will be stored out-of-pit (TSF1) and in-pit (TSF2). Water from the CHPP and TSF process water system will be stored in the process water decant dam (PWDD).

##### 2.1.6.6.6 Raw water system

Raw water will be used when there is insufficient MAW to meet project water demands and to supply water for demands that MAW is unsuitable for. The project will source raw water through an external pipeline. Raw water will be stored in the raw water dam. Raw water will be used to supply the water treatment plant to produce potable water as well as some process demands. Raw water may also be used to make-up supply for all processes that are normally supplied by MAW.

##### 2.1.6.6.7 Water transfer system

The water transfer system is the mechanical means to move water from points of collection to points of storage and from points of storage to point of use. The water transfer system will consist of a series of pumps, pipes and storages (tanks).

#### *2.1.6.7 South Galilee Coal Project*

The information below is taken from the Additional EIS (AEIS) for the South Galilee Coal Project (WRM Water + Environment, 2014).

The AEIS contains a conceptual design for the water management system with the details to be finalised later. The water management system will have three subsystems according to water quality. The layout of the water management system will change over the life of the mine. All the dams except the south sediment dam (which will be adjacent to Sapling Creek) will be in the Tallarenha Creek catchment. The south pit water dam will be on the boundary between the Sapling Creek and Tallarenha Creek catchments.

The subsystems of the water management system are:

- saline water system
- waste rock runoff water system
- raw water system.

##### 2.1.6.7.1 Saline water system

The saline water system manages water which is potentially coal-affected. It is expected that water captured by this system will have high salinity and has the potential to be contaminated by metals. Water in this system will be pumped to pit water dams to be later reused on site. Dams in the saline water system are: pit water dams N and S; ROM dump dams N and S; MIA dams N and S; ROM stockpile dams N and S; product stockpile dams; dam A and dam B.

##### 2.1.6.7.2 Waste rock runoff water system

The waste rock runoff system manages water from waste rock areas which is expected to have high turbidity, moderate risk of high salinity and a lower risk of metals contamination.

### 2.1.6.7.3 Raw water system

The raw water system will manage externally supplied raw water. This water is expected to be low salinity and will be stored in the raw water dam.

## *References*

Engeny Water Management (2013) China First / Galilee Coal Project Commonwealth Environmental Impact Statement, Volume 4, Appendix 19 Mine Site Water Management. Viewed 15 October 2015, http://waratahcoal.com/publications/.

Evans T, Pavey C, Cassel R, Ransley T, Sparrow A, Kellett J, Galinec V, Dehelean A, Caruana L and Kilgour P (2018) Conceptual modelling for the Galilee subregion. Product 2.3 for the Galilee subregion from the Lake Eyre Basin Bioregional Assessment. Department of the Environment and Energy, Bureau of Meteorology, CSIRO and Geoscience Australia, Australia. http://data.bioregionalassessments.gov.au/product/LEB/GAL/2.3.

GHD Pty Ltd (2013) Carmichael Coal Mine and Rail Project Supplementary Environmental Impact Statement (SEIS), Appendix K2 Water Balance Report. Report dated 22 October 2013. Viewed 15 October 2015, http://eisdocs.dsdip.qld.gov.au/Carmichael%20Coal%20Mine%20and%20Rail/SEIS/Appendices/Appendix%20K/Appendix-K2-Water-Balance-Report.pdf.

Hansen Bailey Environmental Consultants and MacMines (2015) Project China Stone Draft Environmental Impact Statement: Chapter 13 Surface Water. Viewed 15 October 2015, http://eisdocs.dsdip.qld.gov.au/China%20Stone%20Coal/DEIS/Draft%20EIS%20-%20Volume%201A/china-stone-chapter-13-surface-water.pdf.

Karim F, Hostetler S and Evans T (2018a) Water balance assessment for the Galilee subregion. Product 2.5 for the Galilee subregion from the Lake Eyre Basin Bioregional Assessment. Department of the Environment and Energy, Bureau of Meteorology, CSIRO and Geoscience Australia, Australia. http://data.bioregionalassessments.gov.au/product/LEB/GAL/2.5.

Karim F, Viney NR, Wang B, Peeters LJM, Zhang YQ, Marvanek SP, Shi X, Yang A and Buettikofer H (2018b) Surface water numerical modelling for the Galilee subregion. Product 2.6.1 for the Galilee subregion from the Lake Eyre Basin Bioregional Assessment. Department of the Environment and Energy, Bureau of Meteorology, CSIRO and Geoscience Australia, Australia. http://data.bioregionalassessments.gov.au/product/LEB/GAL/2.6.1.

Peeters L, Ransley T, Turnadge C, Kellett J, Harris-Pascal C, Kilgour P and Evans T (2018) Groundwater numerical modelling for the Galilee subregion. Product 2.6.2 for the Galilee subregion from the Lake Eyre Basin Bioregional Assessment. Department of the Environment and Energy, Bureau of Meteorology, CSIRO and Geoscience Australia, Australia. http://data.bioregionalassessments.gov.au/product/LEB/GAL/2.6.2.

Parsons Brinckerhoff (2011) Alpha Coal Project Supplementary Environmental Impact Statement, Volume 2, Appendix L Site Water Management System and Water Balance technical report. Report dated 11 April 2011. Prepared for Hancock Coal Pty Ltd by PB Pty Ltd. Viewed 15 October 2015, http://gvkhancockcoal.com/documents/Publications/EIS/ACPSEIS2011/Volume2/Volume%202%20Appendix%20%20L%20Site%20Water%20Management%20System%20and%20Water%20Balance%20Technical%20Report%20Issue%203%20Final.pdf.

Resolve Coal Pty Ltd (2015) Hyde Park Coal Project Presentation, dated October 2015. Viewed 12 September 2016, http://www.queenslandexploration.com.au/wp-content/uploads/2012/02/HPCP-Galilee-Resolve-Coal-October-2015.pdf.

URS (2012) Kevin's Corner Supplementary Environmental Impact Statement, Volume 2 appendix M Site Water management (Basis of Design) Report. Dated 3 October 2012. Prepared for Hancock Galilee Pty Ltd by URS Australia. Viewed 15 October, http://gvkhancockcoal.com/documents/Publications/EIS/KevinsCornerSEIS2012/Volume2/Volume%202%20-%20App%20M%20Site%20Water%20Management%20(BoD)%20Report.pdf.

WRM Water and Environment (2014) Additional Environmental Impact Statement South Galilee Coal Project, Volume 1, Chapter 9.3.3 Surface Water Model / Management System. Dated March 2014. Viewed 15 October 2015, http://eisdocs.dsdip.qld.gov.au/South%20Galilee%20Coal/AEIS/Volume%201.pdf.

# Glossary

The register of terms and definitions used in the Bioregional Assessment Programme is available online at http://environment.data.gov.au/def/ba/glossary (note that terms and definitions are respectively listed under the 'Name' and 'Description' columns in this register). This register is a list of terms, which are the preferred descriptors for concepts. Other properties are included for each term, including licence information, source of definition and date of approval. Semantic relationships (such as hierarchical relationships) are formalised for some terms, as well as linkages to other terms in related vocabularies.

activity: for the purposes of Impact Modes and Effects Analysis (IMEA), a planned event associated with a coal seam gas (CSG) operation or coal mine. For example, activities during the production life-cycle stage in a CSG operation include drilling and coring, ground-based geophysics and surface core testing. Activities are grouped into components, which are grouped into life-cycle stages.

analytic element model: a groundwater model in which the groundwater flow equations are solved based on the representation of internal boundary conditions, points, lines or polygons where constant groundwater level, constant flux or flux dependence on groundwater level is imposed (Bakker, 2013). The resulting groundwater flow equations can be evaluated at arbitrary points in space and time. The solution is therefore independent of a spatial discretisation of the model domain into grids, and a temporal discretisation into time steps, as is necessary for finite element or finite difference groundwater models.

annual flow: the volume of water that discharges past a specific point in a stream in a year, commonly measured in GL/year. This is typically reported as the maximum change due to additional coal resource development over the 90-year period (from 2013 to 2102).

aquifer: rock or sediment in a formation, group of formations, or part of a formation that is saturated and sufficiently permeable to transmit quantities of water to bores and springs

aquitard: a saturated geological unit that is less permeable than an aquifer, and incapable of transmitting useful quantities of water. Aquitards often form a confining layer over an artesian aquifer.

artesian aquifer: an aquifer that has enough natural pressure to allow water in a bore to rise to the ground surface

asset: an entity that has value to the community and, for bioregional assessment purposes, is associated with a subregion or bioregion. Technically, an asset is a store of value and may be managed and/or used to maintain and/or produce further value. Each asset will have many values associated with it and they can be measured from a range of perspectives; for example, the values of a wetland can be measured from ecological, sociocultural and economic perspectives.

baseflow: the portion of streamflow that comes from shallow and deep subsurface flow, and is an important part of the groundwater system

baseflow index: the ratio of baseflow to total streamflow over a long period of time (years) basement: the crust below the rocks of interest. In hydrogeology it means non-prospective rocks below accessible groundwater. Commonly refers to igneous and metamorphic rocks which are unconformably overlain by sedimentary beds or cover material, and sometimes used to indicate 'bedrock' (i.e. underlying or encasing palaeovalley sediments).

bioregion: a geographic land area within which coal seam gas (CSG) and/or coal mining developments are taking place, or could take place, and for which bioregional assessments (BAs) are conducted

bioregional assessment: a scientific analysis of the ecology, hydrology, geology and hydrogeology of a bioregion, with explicit assessment of the potential direct, indirect and cumulative impacts of coal seam gas and coal mining development on water resources. The central purpose of bioregional assessments is to analyse the impacts and risks associated with changes to water-dependent assets that arise in response to current and future pathways of coal seam gas and coal mining development.

bore: a narrow, artificially constructed hole or cavity used to intercept, collect or store water from an aquifer, or to passively observe or collect groundwater information. Also known as a borehole or piezometer.

coal deposit: an early stage exploration development category whereby a coal deposit is known to exist in the tenement, although there is insufficient knowledge of the critical deposit characteristics to determine if it is economic or subeconomic to develop into an operating mine at some stage in the future

coal resource development pathway: a future that includes all coal mines and coal seam gas (CSG) fields that are in the baseline as well as those that are expected to begin commercial production after December 2012

component: for the purposes of Impact Modes and Effects Analysis (IMEA), a group of activities associated with a coal seam gas (CSG) operation or coal mine. For example, components during the development life-cycle stage of a coal mine include developing the mine infrastructure, the open pit, surface facilities and underground facilities. Components are grouped into life-cycle stages.

conceptual model: abstraction or simplification of reality

connectivity: a descriptive measure of the interaction between water bodies (groundwater and/or surface water)

consequence: synonym of impact

context: the circumstances that form the setting for an event, statement or idea

dataset: a collection of data in files, in databases or delivered by services that comprise a related set of information. Datasets may be spatial (e.g. a shape file or geodatabase or a Web Feature Service) or aspatial (e.g. an Access database, a list of people or a model configuration file).

derived dataset: a dataset that has been created by the Bioregional Assessment Programme dewatering: the process of controlling groundwater flow within and around mining operations that occur below the watertable. In such operations, mine dewatering plans are important to provide more efficient work conditions, improve stability and safety, and enhance economic viability of operations. There are various dewatering methods, such as direct pumping of water from within a mine, installation of dewatering wells around the mine perimeter, and pit slope drains.

discharge: water that moves from a groundwater body to the ground surface or surface water body (e.g. a river or lake)

drawdown: a lowering of the groundwater level (caused, for example, by pumping). In the bioregional assessment (BA) context this is reported as the difference in groundwater level between two potential futures considered in BAs: baseline coal resource development (baseline) and the coal resource development pathway (CRDP). The difference in drawdown between CRDP and baseline is due to the additional coal resource development (ACRD). Drawdown under the baseline is relative to drawdown with no coal resource development; likewise, drawdown under the CRDP is relative to drawdown with no coal resource development.

ecosystem: a dynamic complex of plant, animal, and micro-organism communities and their non-living environment interacting as a functional unit. Note: ecosystems include those that are human-influenced such as rural and urban ecosystems.

effect: for the purposes of Impact Modes and Effects Analysis (IMEA), change in the quantity and/or quality of surface water or groundwater. An effect is a specific type of an impact (any change resulting from prior events).

fairway: a term used in geology to describe a regional trend along which a particular geological feature is likely to occur, such as a hydrocarbon fairway. Understanding and predicting fairways can help geologists explore for various types of resources, such as minerals, oil and gas.

formation: rock layers that have common physical characteristics (lithology) deposited during a specific period of geological time

Galilee subregion: The Galilee subregion is part of the Lake Eyre Basin bioregion and is entirely within Queensland. It extends westwards across the Great Dividing Range and into the Lake Eyre drainage basin. The subregion is sparsely populated, with most people living in towns and localities including Charleville, Barcaldine, Blackall and Hughenden. The subregion encompasses the headwaters of several major waterways including the Cooper Creek and the Diamantina, Belyando, Cape, Thomson, Barcoo, Flinders, Bulloo, and Warrego rivers. In addition to the river systems, the subregion has numerous wetlands, springs, waterholes and lakes, including the nationally important lakes Buchanan and Galilee. Some of these are home to diverse and unique plants and animals, many of which are listed as rare or threatened under Queensland and Commonwealth legislation. Native vegetation consists largely of grasslands in the west and open eucalyptus woodlands in the east. Cattle and sheep grazing on native pasture is the main land use and groundwater is of great importance.

geological formation: stratigraphic unit with distinct rock types, which is able to mapped at surface or in the subsurface, and which formed at a specific period of geological time groundwater: water occurring naturally below ground level (whether stored in or flowing through aquifers or within low-permeability aquitards), or water occurring at a place below ground that has been pumped, diverted or released to that place for storage there. This does not include water held in underground tanks, pipes or other works.

groundwater-dependent ecosystem: ecosystems that rely on groundwater - typically the natural discharge of groundwater - for their existence and health

groundwater recharge: replenishment of groundwater by natural infiltration of surface water (precipitation, runoff), or artificially via infiltration lakes or injection

groundwater system: see water system

hydrogeology: the study of groundwater, including flow in aquifers, groundwater resource evaluation, and the chemistry of interactions between water and rock

impact: a change resulting from prior events, at any stage in a chain of events or a causal pathway. An impact might be equivalent to an effect (change in the quality and/or quantity of surface water or groundwater), or it might be a change resulting from those effects (for example, ecological changes that result from hydrological changes).

impact mode: the manner in which a hazardous chain of events (initiated by an impact cause) could result in an effect (change in the quality and/or quantity of surface water or groundwater). There might be multiple impact modes for each activity or chain of events.

inflow: surface water runoff and deep drainage to groundwater (groundwater recharge) and transfers into the water system (both surface water and groundwater) for a defined area

likelihood: probability that something might happen

lithic: sediment or sedimentary rock that contains a significant proportion of detrital rock fragments (10 to 50%) derived by erosion from older, pre-existing rock outcrop

marine transgression: the landward spreading of the sea over a large area within relatively short space of geological time (a few million years or less). The reverse of transgression is regression.

percentile: a specific type of quantile where the range of a distribution or set of runs is divided into 100 contiguous intervals, each with probability 0.01. An individual percentile may be used to indicate the value below which a given percentage or proportion of observations in a group of observations fall. For example, the 95th percentile is the value below which 95% of the observations may be found.

permeability: the measure of the ability of a rock, soil or sediment to yield or transmit a fluid. The magnitude of permeability depends largely on the porosity and the interconnectivity of pores and spaces in the ground.

porosity: the proportion of the volume of rock consisting of pores, usually expressed as a percentage of the total rock or soil mass

preliminary assessment extent: the geographic area associated with a subregion or bioregion in which the potential water-related impact of coal resource development on assets is assessed recharge: see groundwater recharge

risk: the effect of uncertainty on objectives

runoff: rainfall that does not infiltrate the ground or evaporate to the atmosphere. This water flows down a slope and enters surface water systems.

saturated zone: the part of the ground in which all the voids in the rocks or soil are filled with water. The watertable is the top of the saturated zone in an unconfined aquifer.

source dataset: a pre-existing dataset sourced from outside the Bioregional Assessment Programme (including from Programme partner organisations) or a dataset created by the Programme based on analyses conducted by the Programme for use in the bioregional assessments (BAs)

spring: a naturally occurring discharge of groundwater flowing out of the ground, often forming a small stream or pool of water. Typically, it represents the point at which the watertable intersects ground level.

stratigraphy: stratified (layered) rocks

subcrop: 1 - A subsurface outcrop, e.g. where a formation intersects a subsurface plane such as an unconformity. 2 - In mining, any near-surface development of a rock or orebody, usually beneath superficial material.

subregion: an identified area wholly contained within a bioregion that enables convenient presentation of outputs of a bioregional assessment (BA)

subsidence: localised lowering of the land surface. It occurs when underground voids or cavities collapse, or when soil or geological formations (including coal seams, sandstone and other sedimentary strata) compact due to reduction in moisture content and pressure within the ground.

surface water: water that flows over land and in watercourses or artificial channels and can be captured, stored and supplemented from dams and reservoirs

tmax: year of maximum change

uncertainty: the state, even partial, of deficiency of information related to understanding or knowledge of an event, its consequence, or likelihood. For the purposes of bioregional assessments, uncertainty includes: the variation caused by natural fluctuations or heterogeneity; the incomplete knowledge or understanding of the system under consideration; and the simplification or abstraction of the system in the conceptual and numerical models.

water-dependent asset: an asset potentially impacted, either positively or negatively, by changes in the groundwater and/or surface water regime due to coal resource development

water make: the groundwater extracted for dewatering mines water system: a system that is hydrologically connected and described at the level desired for management purposes (e.g. subcatchment, catchment, basin or drainage division, or groundwater management unit, subaquifer, aquifer, groundwater basin)

water use: the volume of water diverted from a stream, extracted from groundwater, or transferred to another area for use. It is not representative of 'on-farm' or 'town' use; rather it represents the volume taken from the environment.

watertable: the upper surface of a body of groundwater occurring in an unconfined aquifer. At the watertable, pore water pressure equals atmospheric pressure.

well: typically a narrow diameter hole drilled into the earth for the purposes of exploring, evaluating or recovering various natural resources, such as hydrocarbons (oil and gas) or water. As part of the drilling and construction process the well can be encased by materials such as steel and cement, or it may be uncased. Wells are sometimes known as a ‘wellbore’.

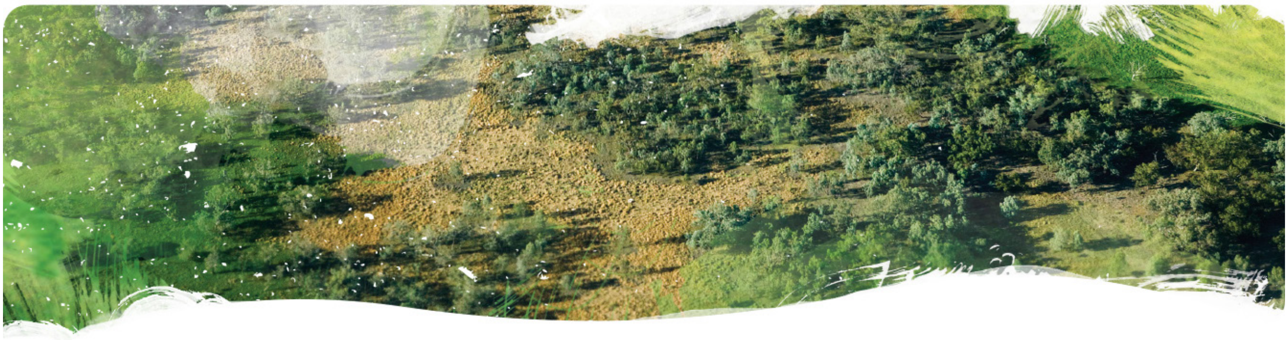

# 2.2 Statistical analysis and interpolation

Originally the statistical analysis and interpolation was intended to be reported independently of the observations analysis. Instead it has been combined with the observations analysis as product 2.1-2.2 to improve readability. For statistical analysis and interpolation see Section 2.1 of this product.

www.bioregionalassessments.gov.au

Australian Government

Department of the Environment and Energy

Bureau of Meteorology

Geoscience Australia

CSIRO